

# **Assessing the feasibility of constructing a groundwater contaminant fate and transport model for an LNAPL affected fractured rock aquifer**

By

**Samuel Möhr**

A dissertation submitted to meet the requirements for the degree of

**Magister Scientiae**

in the

**Institute of Groundwater Studies  
Faculty of Natural and Agricultural Sciences**

at the

**University of the Free State**

Supervisor: Dr Ingrid Dennis

## Acknowledgments

Sincere words of thanks must be extended to all the staff at the Institute for Groundwater Studies, in particular my academic supervisor Dr. Ingrid Dennis for all the reviews and helpful conversations. Thanks must also be extended to Prof. Gideon Steyl, Dr. Danie Vermeulen and Prof. Gerrit van Tonder for many stimulating conversations and insightful ideas during my times spent at the IGS. Special words of thanks to Mr Modreck Gomo and Ms Jamie Bothwell for the access to their field data and to the IGS-WRC LNAPL Project Team at large for the free flow of information between themselves and the Author.

Thank you to Dr Jennifer Pretorius who, on one of the few rainy days in Beaufort West, initially suggested the idea of completing an MSc to me. A special word of gratitude to Willem van Biljon of GPT Cape, who supported and encouraged me during the completion of my MSc and whom I consider to be a great mentor and one from whom I have learned far more than I ever expected.

Thanks to my family and friends for the support, prayers and encouragement during these last two years. And most importantly, my utmost thanks, love and gratitude to my wife Bridg ette M ohr who effectively lost her husband to a dusty town in the Karoo for the last two years, and has supported and loved me continuously throughout the whole time - I'm all yours from now on.

*“The teaching of the wise is a fountain of life, turning a man from the desert of destruction” –  
Proverbs 13:14 The Bible NLT Version*

## Plagiarism Declaration

I, Samuel Möhr declare that; this thesis hereby submitted by me for the Master of Science Geohydrology degree in the Faculty of Natural and Agricultural Sciences, Institute of Groundwater Studies at the University of the Free State is my own independent work. The work has not been previously submitted by me or anyone at another university and that all external data sources have been properly referenced as such. I furthermore cede the copyright of the thesis in favour of the University of the Free State.

---

Date: 1 May 2011

## Abstract

Groundwater contamination as a result of Light Non Aqueous Phase Liquid (LNAPL) releases into the subsurface is a widespread occurrence across South Africa which threatens current and future water resources within the country. Groundwater contaminant fate and transport modelling are common elements of hydrogeological investigations and remedial design methodologies in many developed countries where the models are used as management and decision making tools. In South Africa this is not the case, with contaminant flow and transport modelling rarely being employed as part of LNAPL contamination investigations.

Over the last 3 years the Beaufort West study area has had extensive investigative work carried out with regards to the determination and delineation of LNAPL related groundwater contaminant plumes which are present underneath a significant portion of the town. As a result an extensive data set has been generated with regards to aquifer geometry, fracture network distribution, aquifer parameters and contaminant plume concentrations and extent. The dataset should in theory provide an opportunity to construct a groundwater contaminant fate and transport model for the area as a remedial management tool. By means of collating previously existing data through a comprehensive desktop study, and supplementing this data with a toolkit of field investigations techniques such as diamond barrel core drilling, percussion drilling, electrical conductivity profiling, fluid electrical conductivity profiling, aquifer pump testing, and low flow inorganic and organic groundwater sampling, the conceptual model of the study area was updated and refined to a point where feasibility of constructing a groundwater contaminant fate and transport model could be assessed.

Based upon the conceptual understanding of the study area as defined in the conceptual model developed in the study, a groundwater contaminant fate and transport model is not considered feasible for the study area with the body of data currently available. This is attributed mainly to the high level of complexity of the observed natural environment and the challenges in acquiring acceptable quality field data such as aquifer parameters given the uncontrolled pumping environment which is present due to the high number of private groundwater users. Potentially an even greater detractor to the construction of a model, is that considering the conceptual understanding of the study area, there are very few questions of significance whose answers could be provided by a model, and this would indicate that a model would not be an effective remedial management or decision making tool in the current scenario.



## Opsomming

Grondwaterbesoedeling as 'n gevolg van Ligte Nie-Waterige Fase Vloeistowwe (Light Non Aqueous Phase Liquids - LNAPL) vrystelling in die ondergrond is 'n wydverspreide voorkoms regoor Suid-Afrika, wat huidige en toekomstige waterhulpbronne in die land bedreig. Grondwaterbesoedeling eindpunt- en vervoer modelle is algemene elemente van geohidrologiese ondersoeke en regstellende ontwerpsmetodes in baie ontwikkelde lande waar die modelle gebruik word as bestuurs- en besluitnemings middels. In Suid-Afrika is dit egter nie die geval nie, waar besoedelingsvloei- en vervoer modellering selde ingespan word as deel van LNAPL besoedeling ondersoeke.

Oor die laaste drie jaar is daar uitgestrekte navorsing in die Beaufort-Wes studie area gedoen met 'n klem op die bepaling en afbakening van LNAPL-verwante grondwater besoedelingspluime wat teenwoordig is onder 'n beduidende gedeelte van die dorp. As gevolg hiervan is 'n uitgebreide datastel beskikbaar wat die geometrie, naatnetwerk verspreiding, akwifere parameters en besoedelingspluim konsentrasies omvat. Die data bied in teorie die geleentheid om 'n grondwaterbesoedeling eindpunt- en vervoer model vir die area op te stel as 'n remediërende bestuursmiddel. Die konseptuele model vir die studiegebied is opgedateer en verfyn tot 'n punt waar die haalbaarheid van die model geassesseer kon word met behulp van die samestelling van bestaande data, 'n omvattende literatuurstudie, en aangevul deur veldondersoek tegnieke soos diamantkern boorwerk, druklug- boorwerk, elektriese geleidingsvermoë profilering, elektriese vloeistofgeleidingsvermoë profilering, akwifere pomptoetse, en lae-vloei anorganiese en organiese grondwater monitering.

Gebaseer op die konseptuele begrip van die studiegebied soos omskryf in die konseptuele model, is 'n grondwaterbesoedeling eindpunt en vervoer model as onuitvoerbaar beskou met die data wat huidiglik beskikbaar is. Dit word hoofsaaklik toegeskryf aan die hoë vlake van ingewikkeldheid van die waargenome natuurlike omgewing en die uitdagings in die verkryging van aanvaarbare gehalte velddata soos akwifere parameters, toegeskryf die onbeheerde vloeitoestande as gevolg van die hoë aantal private grondwaterverbruikers. 'n Moontlik selfs groter uitdaging vir die samestelling van 'n model, is dat met betrekking tot die konseptuele begrip van die studie area, daar min betekenisvolle vrae is wat deur 'n model beantwoord kan word, wat daarop dui dat 'n model huidiglik nie die mees effektiewe remediërende bestuursmiddel of besluitnemingsmiddel in die huidige scenario is nie.

# Keywords

Light Non Aqueous Phase Liquids

Contaminant Fate and Transport Model

Conceptual Site Model

Fractured Rock Aquifer

Karoo Aquifer

Physical Characterisation

Chemical Characterisation

Aquifer Parameter Estimation

Hydrocensus

Electrical Conductivity Profiling

Fluid Electrical Conductivity Profiling

Low Flow Sampling

# Table of Contents

List of Figures .....	iv
List of Tables .....	vii
List of Terms and Acronyms .....	viii
1 Introduction.....	1-1
1.1 Basis for the Study .....	1-1
1.2 Study Objectives .....	1-2
1.3 Data Collection Strategy .....	1-3
1.3.1 Desktop Study .....	1-3
1.3.2 Fieldwork Activities.....	1-4
1.3.3 Groundwater Model Objectives .....	1-6
2 Literature Study .....	2-1
2.1 Groundwater Resource Prospecting and Aquifer Characterisation.....	2-1
2.2 Chemical Characterisation .....	2-3
2.2.1 Hydrocarbon Fate and Transport in Groundwater .....	2-5
2.3 Field Characterisation Techniques.....	2-6
2.3.1 Numerical flow modelling in fractured rock aquifers.....	2-9
3 The Hydrogeology of Hydrocarbons in the Subsurface.....	3-1
3.1 Physical Fluid Properties of Hydrocarbons.....	3-1
3.1.1 Fluid Density.....	3-1
3.1.2 Wettability.....	3-1
3.1.3 Interfacial and Surface Tension .....	3-2
3.1.4 Viscosity .....	3-2
3.1.5 Capillary Pressure .....	3-3
3.1.6 Relative Permeability.....	3-3
3.1.7 Residual Saturation .....	3-4
3.2 The Behaviour of LNAPL in Fractured Rocks .....	3-4
3.3 The Hydro-geochemistry of Hydrocarbons in Groundwater .....	3-10
3.3.1 Petroleum Product Composition .....	3-10
3.3.2 Solubility & Volatility .....	3-11
3.3.3 Advection and Dispersion.....	3-14
3.3.4 Sorption.....	3-14
4 Description of Study Area .....	4-1

4.1	Location .....	4-1
4.2	Climate .....	4-1
4.3	Topography .....	4-6
4.4	Geology .....	4-6
4.5	Structural Geology .....	4-10
4.6	Hydrogeology .....	4-11
4.6.1	A Brief description of Karoo Aquifers.....	4-11
4.7	High Level Conceptual Model.....	4-13
5	Summary of Work Done to Date .....	5-1
5.1	Historical Overview .....	5-1
5.2	WRC LNAPL Project .....	5-3
5.2.1	Drilling.....	5-3
5.2.2	Borehole Geophysics .....	5-4
5.2.3	Aquifer Parameter Estimation.....	5-6
5.2.4	Hydro-geochemical Characterisation.....	5-8
6	Hydrocensus.....	6-1
7	Physical Characterisation.....	7-1
7.1	Intrusive Investigations .....	7-1
7.1.1	Core Drilling .....	7-4
7.1.2	Percussion Drilling.....	7-8
7.2	Electrical Conductivity Profiling .....	7-12
7.2.1	Ambient EC Profiling .....	7-14
7.2.2	Electrical Conductivity Profiles of Private Boreholes .....	7-22
7.2.3	Fluid EC Profiling (FEC Profiling).....	7-27
7.3	Physical Characterisation Summary .....	7-35
8	Aquifer Parameter Estimation.....	8-1
8.1	Water Level Measurements .....	8-1
8.2	Constant Rate Discharge Tests .....	8-4
8.2.1	Nico Brummer Pump Test – March 2009 .....	8-7
8.2.2	PW12 Constant Rate Discharge Test .....	8-19
8.2.3	PW49 Constant Rate Discharge Test – December 2009.....	8-20
8.2.4	PW2 Constant Rate Discharge Test – December 2009.....	8-23
8.2.5	PW17 Constant Rate Discharge Test – December 2009.....	8-25
8.2.6	MW12 Pump Test –December 2009.....	8-30
8.3	Non Aqueous Phase Liquid Recover Tests.....	8-32
8.4	Aquifer Parameter Estimation Summary .....	8-39

9	Chemical Characterisation .....	9-1
9.1	Solute Forming Processes .....	9-1
9.2	Inorganic Sampling .....	9-2
9.2.1	Recharge Calculation – The Chloride Method.....	9-4
9.3	Organic Sampling .....	9-4
9.3.1	March 2009 Sampling Event.....	9-5
9.3.2	July 2009 Sampling Event .....	9-9
9.3.3	December 2009 Sampling.....	9-21
9.4	Monitored Natural Attenuation.....	9-24
10	Site Conceptual Model.....	10-1
10.1.1	Physical Characteristics .....	10-1
10.1.2	Flow and Transport.....	10-2
10.1.3	Chemical Characteristics.....	10-3
11	Conclusion .....	11-5
11.1	A Review of Data Requirements for a Model.....	11-5
11.2	Concluding remarks .....	11-7
12	References.....	12-1

## List of Figures

Figure 2-1 $\delta D$ vs $\delta^{18}O$ compositional facies (from Conrad & Rose, 2008) .....	2-4
Figure 3-1 Idealised LNAPL fracture flow scenario (Part 1) .....	3-7
Figure 3-2 Idealised LNAPL fracture flow scenario (Part 2) .....	3-7
Figure 3-3 Idealised LNAPL fracture flow scenario (Part 3) .....	3-8
Figure 3-4 Pure Phase Solubility of Selected Hydrocarbon Compounds (From API, 2004).....	3-11
Figure 3-5 Concentrations of MTBE, benzene and toluene over time (From API, 2004).....	3-13
Figure 4-1 Climatic data from 1973 to 2008 for the Beaufort West Area. ....	4-2
Figure 4-2 Total Yearly Rainfall for the Beaufort West Area .....	4-2
Figure 4-3 Topographic map of the study area .....	4-3
Figure 4-4 Aerial photograph of the study area .....	4-4
Figure 4-5 Closer view of the Study Area within the town of Beaufort West. ....	4-5
Figure 4-6 Generalised stratigraphy of the Karoo Supergroup with reference to the formations observed in the study area .....	4-7
Figure 4-7 Looking south, a view of the transgressive Beaufort West sill (outlined by dotted red line) .....	4-8
Figure 4-8 A cross cut section of the Beaufort West sill, dipping to the north.....	4-8
Figure 4-9 Weathered mudstone on the footwall of the Beaufort West sill.....	4-9
Figure 4-10: Models of sediment deposition in a.) a braided stream and b.) a meandering stream environment [Taken from Botha et al (1998)] .....	4-10
Figure 4-11 Rose diagram of joint set orientations within a 30km radius of Beaufort West (Campbell, 1980).....	4-11
Figure 4-12: Regional conceptual model for the Study Area. (Figure adapted from Rose and Conrad, 2008).....	4-15
Figure 4-13 Regional geological and hydrogeological features .....	4-16
Figure 5-1 EC tracer breakthrough measurements the abstraction/observation hole MW8 (From Gomo, 2009) .....	5-7
Figure 5-2 Piper Diagram of IGS sampled wells along with wells sampled by GPT in 2009 (from Gomo, 2009) .....	5-10
Figure 5-3 Dissolved phase compositions from the April 2008 sampling event depicting the differing dissolved phase compositions across the study area.....	5-11
Figure 5-4 Locations of boreholes/monitoring wells investigated during the activities described in Section 5. ....	5-12
Figure 6-1 Pie chart breakdown of boreholes identified in hydrocensus.....	6-2
Figure 6-2 Pie chart of usage from boreholes with known uses .....	6-2

Figure 6-3 Orthophoto displaying all hydrocensus wells and their uses across the study area .....	6-4
Figure 7-1 Monitoring wells installed during the various groundwater investigations which have taken place over the years.....	7-3
Figure 7-2 Core log of MW3 drilled at Donkin Motors.....	7-5
Figure 7-3 Core log of MW10 at Beaufort West Service Station .....	7-7
Figure 7-4 Percussion Drill Log of MW9 at Beaufort West Service Station.....	7-9
Figure 7-5 Percussion Drill Log of MW11 at Beaufort West Service Station.....	7-10
Figure 7-6 Percussion Drill of MW12 at Beaufort West Service Station .....	7-11
Figure 7-7 Boreholes and monitoring wells which were used for ambient flow electrical conductivity (EC) profiling.....	7-13
Figure 7-8: EC and basic geology log for MW3, MW4 and PW5 (MW4 & PW5 data courtesy of M. Gomo, IGS).....	7-17
Figure 7-9: EC log and basic geology of MW5 and MW6.....	7-18
Figure 7-10: EC log and basic geology of MW7 (percussion) and MW8 (core hole).....	7-19
Figure 7-11: EC Log and basic geology of MW9 and MW10.....	7-20
Figure 7-12: EC log and basic geology of MW11 and MW12 .....	7-21
Figure 7-13: Electrical conductivity profiles of PW6, PW12 and PW49. ....	7-23
Figure 7-14: EC profiles of private wells PW16, PW20 and PW35 .....	7-25
Figure 7-15: EC profiles of NB1 (primary school), MS02 (municipal well) and HS2 (high school).....	7-25
Figure 7-16 Borehole which were used for fluid flowing electrical conductivity profiling .....	7-26
Figure 7-17: Flowing FEC Profile of PW9.....	7-31
Figure 7-18: Flowing FEC and Ambient FEC Profiles of PW17 .....	7-32
Figure 7-19: Flowing FEC Profile of PW18 .....	7-33
Figure 7-20: Flowing FEC Profile of PW16.....	7-34
Figure 8-1 Monthly rainfall data and water level measurements from NB1 .....	8-2
Figure 8-2 Static water level gradient map .....	8-3
Figure 8-3: Site layout of boreholes and monitoring wells used in constant rate discharge test. ....	8-6
Figure 8-4: Pump test data for the entire 72 hours.....	8-12
Figure 8-5: Drawdown data from Monday 14:00 to Tuesday 14:00.....	8-13
Figure 8-6: Drawdown data from Tuesday 07:00 until Tuesday 21:30 .....	8-14
Figure 8-7: Drawdown data from Tuesday 21:30 until Wednesday 14:00 .....	8-15
Figure 8-8: Drawdown data from Wednesday 14:30 until Thursday 12:00 .....	8-16
Figure 8-9. Water level data plotted on different scale axes. PW20 is plotted on the axis on the right.....	8-17
Figure 8-10 Water level data of MS02 and NB1 after pump test completion whilst HS2 was pumping .....	8-18
Figure 8-11: Drawdown - recovery curve of PW12.....	8-19

Figure 8-12: PW12 water level recovery data used to calculate transmissivity in FC Method .....	8-20
Figure 8-13: Drawdown & recovery data from PW49 constant rate discharge test .....	8-21
Figure 8-14: PW49 water level recovery data used to calculate transmissivity in FC Method .....	8-22
Figure 8-15: Drawdown & recovery data from PW2 constant rate discharge test .....	8-23
Figure 8-16: Early time data on the Drawdown vs Log (t) for PW2 .....	8-24
Figure 8-17: Drawdown & recovery data from PW17 constant rate discharge test .....	8-25
Figure 8-18: Sustainable yield Cooper Jacob method for PW17 .....	8-26
Figure 8-19 Recovery of water level vs t' .....	8-28
Figure 8-20 Theis (log-log) plot of drawdown vs time.....	8-28
Figure 8-21 Fourth root of time vs drawdown for PW17 .....	8-29
Figure 8-22: Drawdown & recovery data from MW12 constant discharge test .....	8-30
Figure 8-23 Drawdown derivative plot of MW12 .....	8-31
Figure 8-24: Sustainable yield Cooper Jacob method for MW12.....	8-32
Figure 8-25 LNAPL recovery data for PW12.....	8-34
Figure 8-26 s/Q vs Log t plot for PW12 .....	8-35
Figure 8-27 LNAPL recovery data for PW49.....	8-36
Figure 8-28 s/Q vs Log t plot for PW49 .....	8-36
Figure 8-29 PW12 LNAPL thickness vs time .....	8-38
Figure 8-30 PW49 LNAPL thickness vs time .....	8-38
Figure 9-1 Piper diagram of major cation/anion chemistry of sampled wells (Total M Alkalinity plotted a CO <sub>3</sub> on diagram) .....	9-3
Figure 9-2 BTEX Compositions from March 2009 Sampling.....	9-8
Figure 9-3 BTEX, TMB, TAME Compositions from July 2009 Sampling.....	9-11
Figure 9-4 FFEC profiles and sampling points for PW9 & PW17 .....	9-15
Figure 9-5 FFEC profiles and sampling points for PW16 & PW18 .....	9-16
Figure 9-6 3 Dimensional Classed Post Diagram of Benzene Concentrations from July 2009 Sampling Event.....	9-19
Figure 9-7 An idealised conceptualisation of contaminant transfer between PW17 and PW9.....	9-20
Figure 9-8 BTEX, TMB, TAME Compositions from December 2009 Sampling.....	9-23
Figure 9-9 Radial Diagrams Displaying ORP, Fe(II), Mn(II), SO <sub>4</sub> & NO <sub>3</sub> .....	9-26



## List of Tables

Table 2-1 Key parameters which should be determined during a fractured rock LNAPL investigation (from Hardisty et al, 2004).....	2-7
Table 2-2 Characterisation methods in fractured rock aquifer systems (from Hardisty et al, 2004) ...	2-8
Table 5-1 Significant depth intervals in IGS wells where flow zones were identified and the method of identification. ....	5-5
Table 5-2 Selected aquifer parameter values from the Beaufort West study area (Gomo, 2009).....	5-8
Table 6-1 Summary of Borehole Usage in the Study Area.....	6-3
Table 7-1 Flow zone locations in monitoring wells which were installed within the study area. ....	7-35
Table 7-2 Flow zone locations in private boreholes in Bird Street and De Villiers Street .....	7-36
Table 7-3 Flow zone locations in the municipal supply borehole and school boreholes.....	7-36
Table 8-1 Aquifer parameter estimation summary .....	8-39
Table 9-1 Field measurements and inorganic chemistry data from samples collected in March 2009 (Total M Alkalinity expressed as mg/l CO <sub>3</sub> ).....	9-2
Table 9-2 Field measurements and inorganic chemistry data from samples collected in March 2009 (Total M Alkalinity expressed as mg/l CO <sub>3</sub> ).....	9-3
Table 9-3 Dissolved phase hydrocarbon concentrations from boreholes and monitoring wells sampled during March 2009.....	9-7
Table 9-4 Conventional sampling results from the July 2009 sampling event .....	9-10
Table 9-5 Depth discrete low flow results for PW12, PW16, PW17 and PW18 .....	9-17
Table 9-6 Depth discrete low flow results for PW6, PW9 and PW49.....	9-18
Table 9-7 Dissolved phase hydrocarbon concentrations from boreholes and monitoring wells sampled during December 2009.....	9-22
Table 9-8 Monitored natural attenuation parameters and analytes .....	9-25

## List of Terms and Acronyms

LNAPL	Light Non - Aqueous Phase Liquid
DNAPL	Dense Non - Aqueous Phase Liquid
UST	Underground Storage Tank
VOC	Volatile Organic Carbon
MNA	Monitored Natural Attenuation
TPH	Total Petroleum Hydrocarbon
DRO	Diesel Range Organics
GRO	Gasoline Range Organics
BTEX	Benzene Toluene Ethylbenzene Xylene
MTBE	Methyl Tert – Butyl Ether
TAME	Tertiary Amyl Methyl Ether
PAH	Polycyclic Aromatic Hydrocarbons
TMB	Trimethylbenzene
FWS	Full Wave Sonic
AV	Acoustic Viewer
SP	Spontaneous Potential
GPT	Geo Pollution Technology Cape
ORP	Oxidation Reduction Potential
TDS	Total Dissolved Solids
EC	Electrical Conductivity
FEC	Fluid Electrical Conductivity
FFEC	Flowing Fluid Electrical Conductivity
GPS	Global Positioning System
DGPS	Differential Global Positioning System
MW	Monitoring Well (designated as boring installed to monitor groundwater quality)
PW	Private Well (designated as private residential boreholes)
WRC	Water Research Commission of South Africa
m bgl	meters below ground level
m amsl	meters above mean seal level

# 1 Introduction

## 1.1 *Basis for the Study*

The contamination of groundwater resources by LNAPL products and associated compounds is one of the most widespread groundwater challenges faced globally to date (Dobson et al, 2007). A significant portion of South Africa's groundwater resources exist within fractured rock aquifers, and yet the remediation of LNAPL affected fractured rock aquifers is often limited by a poor understanding of the fracture networks within the aquifer, along which the contaminants migrate. This may often result in an incorrect remedial approach due to an incomplete conceptual model related to a poor understanding of the site's characteristics. With regards to sources of hydrocarbon contamination, petrol and diesel filling stations are by far the most widespread and numerous potential sources of hydrocarbon contamination, with approximately 5000 filling stations being present across South Africa.

The majority of these filling stations have been present in excess of 20 years, and for the most part have ageing and outdated fuel storage equipment. The potential for hydrocarbon release events is therefore very likely and can have far reaching effects on South Africa's groundwater resources. Considering that South Africa is a water stressed country, and that the one most viable large scale future water resources will be groundwater, the importance of understanding the fate and transport of LNAPL contaminants, particularly in fractured rock aquifers, is of great importance.

The town of Beaufort West is located in the arid Karoo region of the Western Cape in South Africa, and has been the focus of extensive hydrogeological investigations in recent years due to several LNAPL releases which have occurred from leaking UST installations at the various filling stations in the town. The town residents rely heavily on groundwater for the irrigation and upkeep of their gardens in this water stressed area, and so the impacts of the contamination have been acutely felt by the residents of the town, with boreholes having been decommissioned due to the contamination and lush gardens being reduced to dry bare ground. This has negatively affected property prices in the area, and coupled with the potential health risks imposed by the contaminated groundwater, has resulted in extensive site characterisation work having been conducted by the private oil industry.

Groundwater contaminant fate and transport models are considered to be a common element of many hydrogeological contaminant investigations in developed parts of the world such as the USA and Europe, and are used as decision making tools in the effective remediation management of contaminated sites. Yet their use in South Africa is infrequent and rare. This is quite often due to the perceived lack of value which models are considered to provide given their perceived high costs, and also due to the costs involved in acquiring sufficient data to construct a robust model. When models are constructed, it is often the case that insufficient data has been collected to construct a robust model and so the results of the model are of little value, thereby perpetuating the perception of the apparent lack of value provided by models. The Beaufort West investigations have yielded an extensive amount of data beyond that which is normally available for a regular site investigation and therefore in theory, should provide an opportunity to construct a groundwater contaminant fate and transport model to assist in the management of remediation and/or the identification.

## ***1.2 Study Objectives***

The overall objective of the study is to assess the feasibility of a contaminant fate and transport model in an LNAPL affected fractured rock aquifer. The critical steps taken in order to achieve this are listed below:

- The definition of the model objectives;
- The collation of available existing data from previous studies conducted in the area and from available literature sources;
- Carrying out of fieldwork in the Beaufort West area in order to provide outstanding information where possible and to provide data on the nature, severity and extent of the LNAPL contamination problem in Beaufort West;
- The development of a site conceptual model which includes an understanding of the governing physical, chemical, and flow conditions in the aquifer on which the feasibility of a contaminant fate and transport model can be assessed.

It must be noted that the study objectives did not include the construction of the fate and transport model, but rather to develop the conceptual understanding of the site to a point where a model's feasibility and applicability could be assessed.

### ***1.3 Data Collection Strategy***

The following sections provide a brief overview of the manner in which data was assimilated for the study and largely reflects the layout of the thesis. The desktop study phase of the study included the literature study, description of the study area and summary of work done to date whilst the fieldwork phase included the physical characterisation, aquifer parameter estimation and chemical characterisation of the aquifer.

#### **1.3.1 Desktop Study**

##### ***1.3.1.1 Literature Study***

The literature study (Section 2) conducted for this thesis involved researching and collating the available body of data which is present regarding the hydrogeology of Beaufort West, with the objective of providing a platform from which the current study could embark. The literature study included Geological Survey reports dating back as far as the late 1940's, progressing through to private consultancy reports related to groundwater abstraction management and regional conceptual site model development, which ranged from late 1995 through to 2008. Additional studies, papers and journals were consulted regarding the various site characterisation techniques which were employed during the study, citing their applicability to fractured rock environments as is the case in the current study.

##### ***1.3.1.2 Description of Study Area***

The description of the study area (Section 3) is aimed at developing a high level regional conceptual model which will act as a framework within which the local, more detailed site conceptual model will be placed. Information regarding climate, topography, geology, structural geology and hydrogeology was sourced and collated from cartographic data, various reports and publications to develop the high level conceptual model.

### ***1.3.1.3 Summary of Work Done to Date***

As mentioned previously, extensive investigations had occurred prior to the current study being initiated. Where available, the data from previous investigations pertaining directly to the hydrocarbon contamination in Beaufort West was reviewed, with the most pertinent data being summarised in Section 5. This data was largely sourced from private consultancy reports, previous IGS student's dissertations reports and deliverable reports completed by the IGS as part of the WRC funded LNAPL project.

## **1.3.2 Fieldwork Activities**

### ***1.3.2.1 Hydrocensus***

An extensive hydrocensus (Section 6) was carried in the town of Beaufort West in March 2009 in order to identify groundwater users which are present in the study. The object of the hydrocensus was firstly to identify all groundwater users. Secondly, to investigate any potential hydrocarbon contamination impacts which may be occurring on the private boreholes and thirdly, to obtain an estimate of the groundwater usage in the area with regards to the volumes abstracted and purpose of abstraction.

### ***1.3.2.2 Physical Characterisation***

Physical characterisation (Section 7) was conducted during site visits throughout the course of 2009 with the objective of improving the understanding of the physical geometry of the aquifer with regards to the location of preferred flow paths such as fractures and joint systems. This was carried out by means of rotary air percussion drilling and diamond core barrelling drilling, with all borings being logged with reference to the dominant geology, water strikes and fracture locations. Ambient EC profiling was also conducted on selected wells to identify significant flow zones whilst FFEC and FEC profiling was also conducted to identify preferential flow zones in selected boreholes.

### ***1.3.2.3 Aquifer Parameter Estimation***

Aquifer parameter estimation (Section 8) was conducted by means of constant rate discharge tests which were carried out in March and December 2009, with aim of determining transmissivity and storativity values for selected boreholes and monitoring wells across the study area. Pump tests lasted between 15 minutes and 72 hours with selected data being inputted into the FC Programme developed by the IGS in order to calculate aquifer parameters. Product recovery tests were also performed on boreholes which had significant free phase LNAPL present in order to assess the effective conductivities of the observed product.

### ***1.3.2.4 Chemical Characterisation***

Chemical characterisation (Section 9) was conducted by means of groundwater sampling for organic and inorganic analyses. Boreholes with installed pumps were generally sampled by means of the installed pump, whilst low flow sampling using bladder pumps was also conducted. Inorganic samples were analysed for the major water chemistry cations and anions, along with Mn(II) and Fe(II) in order to assess the potential for microbial degradation within the plume areas. Organic samples were analysed for BTEXN, TAME, MTBE compounds and TPH C<sub>10</sub>-C<sub>40</sub> compounds in selected cases. Low flow discrete depth organic sampling was also conducted in selected wells.

### 1.3.3 Groundwater Model Objectives

Groundwater models are used as management tools which are built on a sound understanding of the prevailing hydrogeological conditions on a site. The most common uses for groundwater models are:

- To identify data gaps in the current hydrogeological conceptual model;
- To aide in the design of monitoring networks
- To aide in the determination of contaminated ground water on nearby supply wells and receptors
- To aid in the selection, design and management of remedial actions at contaminated sites.

(Belluomini *et al*, 1995)

Specific to contamination investigations, there are several applications which are considered the most common, these are:

- The evaluation/design of hydraulic containment systems;
- The evaluation of physical containment systems;
- The analysis of “no action” alternatives;
- Assessment of attenuation/transformation processes;
- The evaluation of LNAPL on remediation activities.

(From Bear *et al*, 1992)

With respect to the current investigation, the application of hydraulic containment of the observed contaminant plumes to prevent impacts to local private groundwater users has historically been considered the most feasible remedial management option. In light of this, the model objective has been formulated as follows:

“Is it feasible to employ hydraulic containment within the identified source zones and if so, what would the effects of source pumping at different rates and locations have on the observed contaminant plume in light of the observed groundwater abstraction within the town?”

Consequently, the site conceptual model needs to be developed adequately in order to assess the feasibility of this modelling objective. The site conceptual model should attempt to constrain the following information:



- The aquifer type and geometry with respect to hydraulic barriers and zones of preferential flow
- The model boundary conditions
- The mode of flow
- The governing aquifer parameters such as transmissivity and storativity
- The initial conditions within the aquifer
- Field observation data to calibrate the flow model
- Relevant groundwater sources (such as recharge) and sinks (such as abstraction)

(From Bear *et al*, 1992)

## 2 Literature Study

### 2.1 *Groundwater Resource Prospecting and Aquifer Characterisation*

A moderate body of data and literature is available with regards to hydrogeological investigations within the Beaufort West area (hereafter referred to as the “study area”). The relative scarcity of available sources of potable water has necessitated the investigation of groundwater resources in the area from the late 1940’s and early 1950’s. This (scarcity) has also led to the majority of the literature being focused on groundwater supply. Initial drilling reports by Pike (1948) and more specifically, Kent (1949) were the first to document the presence and attitude of the inclined dolerite sill (hereafter referred to as the “Beaufort West sill”) directly to the north of the town and several of their drilling locations were based upon the attitude of the sill. Geophysical surveys such as electrical resistivity depth profiles and magnetometer surveys were conducted by Schumann and Mellet (1959) which commented on the relative lack of large scale structures within the Adelaide sub-group sediments in the study area.

A study made by Enslin (1961) of the municipal boreholes along the Gamka River concluded that the transgressive Beaufort West sill was an impervious structure in the study area due to the differences in water level elevations to the north and the south of the sill. One of the more extensive hydrogeological investigations carried out in the area was conducted by Campbell from 1975 to 1977. The primary driver of the investigation carried out by Campbell was to provide a broad quantification of the quality and occurrence of groundwater resources in the areas which fell within a 30km radius of Beaufort West. The investigation entailed large scale structure identification by aerial maps followed by geophysical investigations, field reconnaissance trips, exploratory boreholes and aquifer parameter estimation tests (pump tests). In excess of 580 boreholes were drilled during the two year investigation along with 130 geophysical soundings during the initial stages and in excess of 60 pumping tests were conducted during the aquifer parameter estimation phase. Groundwater occurrence was found to be strongest along structures such as dykes, along river courses or in areas near to recharge zones (Nuweveld Mountains). Drilling generally observed a high frequency of groundwater strikes within the first 30m of the geological profile (the weathered zone of the aquifer) whilst the highest yielding fractures were generally found between 50m-60m depth, but at a lower frequency. Parameter estimation found a wide range of transmissivity values ranging from  $10\text{m}^2/\text{day}$  to  $1500\text{m}^2/\text{day}$  whilst storage co-efficient values ranged from  $10^{-2}$  to  $10^{-7}$  with a mean value of  $5 \times 10^{-4}$ .

At the same time as Campbell was conducting the abovementioned investigation, Vandoolaeghe (1978) conducted further geophysical work in the study area which included electrical resistivity and

magnetic surveys. The most pertinent finding with regards to the current study was the improvements made in describing the nature and attitude of the inclined Beaufort West sill. Magnetic surveys conducted during these studies indicated the Beaufort West sill to be dipping in a northerly (upstream) direction with an approximate angle of 35°, however further tracing of the sill to the north found it to increase in dip angle. Vandoolaeghe concluded that the sill was a regional barrier to flow, but that localised leakage through the sill may be occurring at areas such as where the Gamka and Kuils Rivers cut through the sill in the town. This regional flow barrier with localised leakage points is consistent with observations made during drilling along the sill by the Beaufort West Municipality which found wells drilled directly to the south of the sill to be very poor yielding or “dry” with the exception of wells located within the town in the channel cut out of the sill by the two abovementioned rivers (L. Smit, *pers. comm.*)

Private consultancy investigations were conducted by Kotze et al (1997) for the Beaufort West Municipality with the aim of assessing supply status of the Brandwag and Lemoenfontein wellfields which were located in the Brandwag aquifer to the north east of the town. Water balance calculations carried during a modelling phase confirmed an annual recharge of 2% of precipitation infiltrating into the aquifer. The investigation concluded that the aquifer was under stress due to increased abstraction between 1987 and 1997. Further work by Kotze et al (2000) investigated the possibility of increased groundwater supply to Beaufort West by prospecting for groundwater along the Tweeling-Brandwag-Renosterkop (TBR) dyke which strikes in a west to east direction to the north of the town. Drilling of several boreholes along the dyke intersected strong yielding fractures with borehole blow yields in excess of 15 l/s. A key finding of the study was the prevalence for strong yielding boreholes to be located along the chilled/weathered zones of the dolerite dyke. The abovementioned drilling also confirmed the previous observations of Campbell which found the greatest frequency of groundwater bearing fractures to be located in the first 30m of the geological profile, but the highest yielding fractures were found at greater depths down to 60m.

Further aquifer characterisation and flow regime determination was carried out by Rose and Conrad (2008) compiled a range of transmissivity and storativity values for Beaufort West and surrounding areas with transmissivities in the town generally ranging from 40-400m<sup>2</sup>/day and storativity values ranging from 1x10<sup>-3</sup> to 1x10<sup>-5</sup>. No clear correlations between geology and observed transmissivity values were visible however the findings were consistent with Kotze et al, in that higher yielding wells were often found along dolerite dykes.

## ***2.2 Chemical Characterisation***

The most significant body of data collected with regards to groundwater quality in the Beaufort West area was conducted by Campbell during the 1970's with over 1200 electrical conductivity readings being taken and 600 groundwater samples being submitted for analysis from boreholes within a 30 km radius of Beaufort West. Electrical conductivity readings were found to be a reliable indicator of groundwater quality, and the general trend which was observed was that electrical conductivity readings were low nearer the Nuweveld Mountains where recharge occurred, and water quality progressively degraded as one moved further south. Water qualities were found to be the best directly to the north of the town of Beaufort West and began to degrade to the south east of the town. Predominant water chemistries were observed to range across the area from Ca-Na-HCO<sub>3</sub>-SO<sub>4</sub>-Cl, to Ca-Na-Mg-SO<sub>4</sub>-Cl to Na-Mg-SO<sub>4</sub>-Cl. Elevated nitrate levels (61mg/l - 93mg/l) were also observed from boreholes within the town, and this was interpreted to be due to potentially leaking sewerage systems in the town.

Significant geochemical characterisation of the aquifers in the Beaufort West area has been carried by Rose & Conrad (2008) as part of consultancy services rendered to the Beaufort West Municipality. During studies performed for the municipality, data from sampling events from 1997, 2006 and 2008 was collated with regards to water chemistry information and stable isotope chemistry data was also obtained. The results indicated that the majority of the waters plotted between the Ca-Mg-HCO<sub>3</sub> and Ca-Mg-SO<sub>4</sub>-Cl end members, with a progressive evolution from the former towards the latter as one moved away from the zones of recharge (Nuweveld Mountains) towards the south and east. The Ca-Mg-HCO<sub>3</sub> end member was thus considered to represent recently recharged waters whilst the Ca-Mg-SO<sub>4</sub>-Cl end member represented water which has undergone alteration by means of host rock interaction within the aquifer. A good correlation was observed between electrical conductivity, water chemistry and distance from the recharge zones, with low EC values (<1500µS/cm) being related to the recent recharged waters whilst higher EC values (>1500 µS/cm) were observed in the more distal areas relative to the recharge zones where the Ca-Mg-SO<sub>4</sub>-Cl facies was more dominant. As observed previous by Campbell, the best groundwater qualities (using EC as an indicator) were observed in the Town Well Field directly to the north of the town.

Stable isotope analysis carried out by Rose and Conrad identified three distinct δO<sup>18</sup> compositional facies (See Figure 2-1). The first group were characterised by a relatively light isotopic composition

( $\delta^{18}\text{O} < 5\text{‰}$ ) and included most of the wells sampled from the Town Well Field to the north of the town. The lighter isotopic compositions plotted close to the Global Meteoric Water Line (GMWL) and were interpreted to represent recent recharge along the Nuweveld Mountains. The second facies related to water sampled from the Beaufort West Spring yielded a relatively heavier isotopic composition ( $\delta^{18}\text{O} = 0.07\text{‰}$ ). This heavier isotopic composition was interpreted to represent more stagnant flow, possibly associated with paleo-water ( $\delta^{18}\text{O} = 0.0\text{‰}$  and  $\delta\text{D} = 0.0\text{‰}$ ) of the deeper regional groundwater flow systems. The shallow occurrence isotopically heavier groundwater is attributed to presence of the inclined Beaufort West Sill which is interpreted to have forced the groundwater from deeper levels up along the sill. The third facies included wells from the southern portion of the Town Well Field (to the north of the Beaufort West Sill) and private wells at Beaufort Manor (to the south of the Beaufort West Sill). These wells yielded intermediate isotopic compositions ( $0.5\text{‰} > \delta^{18}\text{O} > -2.5\text{‰}$ ) but were more closely linked with the heavier isotopic compositional facies. This “zone of mixing” was interpreted to represent upwards leakage along the sill, and in the case of the wells to the south of the sill, leakage across the sill. The conclusion to this being that the Beaufort West Sill was considered to not be an impervious barrier to flow (as was previously thought by Enslin and Campbell) and that leakage through the sill does occur as was alluded to by Vandoolaeghe.

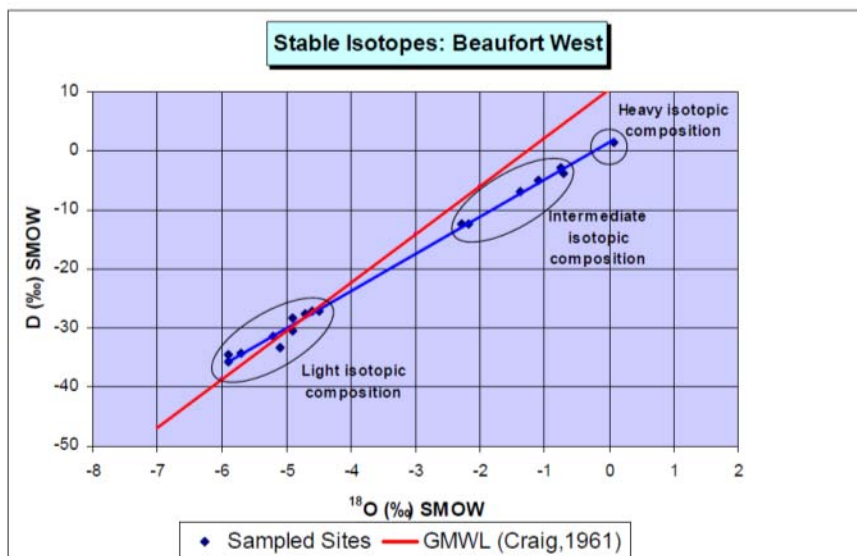


Figure 2-1  $\delta\text{D}$  vs  $\delta^{18}\text{O}$  compositional facies (from Conrad & Rose, 2008)

## 2.2.1 Hydrocarbon Fate and Transport in Groundwater

The body of literature related to the fate, transport and biodegradation of hydrocarbon carbon compounds is widespread and extensive. Specific factors pertaining directly to the fate and transport of hydrocarbons in groundwater will be discussed in Section 3. Studies by Small and Weaver (2001) compared the fate and transport of benzene and MTBE in groundwater with the aim of updating the conceptual understanding of the two respective compounds behaviour in groundwater. MTBE contaminant plumes were found to be significantly larger than benzene plumes, due to MTBE's comparatively higher solubility, lower susceptibility to degradation and low affinity for retardation. In certain cases complete detachment of MTBE plumes has been observed, and whilst benzene is considered to be attenuated more rapidly due to its affinity for biodegradation, detachment of the centre of mass of benzene plumes from the original source zones has been observed in scenarios where high groundwater flow velocities are present.

The degradation of hydrocarbon compounds by microbial processes is well documented with many studies having been conducted to assess monitored natural attenuation since it is often a preferred and cost effective remedial option for hydrocarbon impacted sites. Farhadian *et al* (2008) provide a review of the various microbial organisms which commonly assist in biodegrading hydrocarbon plumes. Farhadian *et al* go on to summarise the various enhancements which can be made to the bioremediation process, such as the addition of sulphates and other rate limiting components which enhance the microbial activity and rate of contaminant biodegradation. Biodegradation of dissolved phase hydrocarbon plumes has been documented in aerobic and anaerobic conditions, even in sub-arctic aquifer conditions where the analysis of benzene isotopes and metabolites has indicated that biodegradation can occur even under relatively extreme environmental conditions (McKelvie *et al*, 2005)

Studies conducted by Rubin *et al* (2007) provided insights into the parameters which govern the remediation of dual porosity aquifers. The most significant parameters to be noted which control the dissolution of contaminants into the aquifer were the rate of mass transfer between the LNAPL and the water phase, the ratio of flow taking place within the matrix to flow taking in fracture networks. In addition to this, constitutive relationships which also affected the remediation of dual porosity aquifers were identified as being 1.) the relationship between the saturation of entrapped LNAPL within the aquifer and the porosity of the matrix and 2.) the relationship between matrix groundwater flow velocities and entrapped LNAPL saturations with regards to the rate of mass transfer from the affected matrix back into the groundwater. This notion of "back diffusion" will be discussed in chapters to follow.

### ***2.3 Field Characterisation Techniques***

Field characterisation techniques within fractured rock aquifers are numerous and varied. Most contamination investigations within a South African context will usually employ the most basic of these techniques, which would usually entail the drilling of rotary air percussion boreholes, sampling of the boreholes and in selected cases, aquifer parameter estimation tests such as pumping tests (See Kruseman & De Ridder, 1999). This section of the literature survey focuses less commonly used and (in the author's opinion) slightly more innovative investigation techniques which have been used in the current study.

Whilst LNAPL contamination within fractured rock aquifers is key point of concern with the groundwater industry, the majority of available body of data regarding the nature and behaviour of LNAPL within aquifer systems has been largely focused on porous primary aquifer scenarios with relatively little being available regarding the specific factors governing LNAPL distribution, migration, and behaviour in fractured rock aquifers. Work conducted by Hardisty et al (2004) provides one of the more complete summaries regarding the abovementioned points, as well as detailing the various methods currently available to assess these parameters within fracture rock aquifers. Some of the key points raised by Hardisty et al were that relatively small volumes of LNAPL within vertical or sub-vertical fractures could penetrate to significant depths below the static water level due to the significant pressure heads which arise from having a continuous column of LNAPL within the fracture from the source zone down to the water level. Furthermore, the rising and falling of water levels can acts as a pumping mechanism which injects LNAPL deeper into the aquifer and laterally along bedding plane fractures. The mechanisms governing LNAPL migration, distribution and behaviour will be dealt with in more detail in Section 4. Hardisty et al suggested several important parameters which need to be ascertained in order to provide and these are indicated in Table 2-1 below.

**Table 2-1 Key parameters which should be determined during a fractured rock LNAPL investigation (from Hardisty et al, 2004)**

Category	Parameters
LNAPL Properties	density, viscosity, interfacial tension
	chemical composition
Fracture Network	location of major fracture sets
	orientation of fracture sets
	fracture apertures and length estimates
	fracture network connectivity
	fracture density
Rock Matrix	permeability. Porosity
	capillary pressure characteristics
	LNAPL presence in rock matrix
LNAPL occurrence	fractures containing LNAPL
	depth range of LNAPL
	areal distribution of LNAPL
Hydrogeology	groundwater flow regime
	system transients
	hydraulic parameters (K, T & S)
	groundwater chemistry

In addition to this Hardisty et al goes on to suggest field techniques which could be employed in order to assess and characterise the LNAPL affected fractured rock aquifer. A summary of these techniques is given in Table 2-2 overleaf.



**Table 2-2 Characterisation methods in fractured rock aquifer systems (from Hardisty et al, 2004)**

<b>Method</b>	<b>Data Provided</b>
Aerial-photo and remote sensing fracture lineament studies;	Regional fracture trends
Fracture mapping at outcrop	Local fracture data and statistics
Surface geophysical techniques: high resolution seismic, electrical resistance tomography	Identification of major vertical fractures
Rock coring	Site fracture data and statistics,
Lab analysis of rock matrix plug samples from core	Rock matrix properties
Digital borehole imaging; other wellbore geophysical logging;	Fracture data and statistics, fracture aperture data; presence of fractures and fracture zones
Hydraulic packer testing	Fracture aperture, bulk and fracture conductivity estimates
Sleeved coring with field analysis of fluorescence, sponge coring and laboratory analysis	LNAPL occurrence and distribution, identification of LNAPL-bearing fractures, matrix Pc and LNAPL saturation measurements
Depth-specific short-screened monitoring wells, aqueous phase sampling and monitoring	Mobile LNAPL presence and temporal behaviour in individual or groups of fractures; aqueous phase plume position and migration; inferred presence of residual LNAPL
Flexible absorbent borehole liners	System fracture-specific LNAPL identification
Laboratory analysis of LNAPL fluid samples	LNAPL density, viscosity, interfacial tension properties, chemical composition
Single hole and multi-well tracer tests	Identification of flowing fractures, network connectivity
LNAPL bail-down tests	LNAPL flow potential and volume

Doughty & Tsang (2005) conducted extensive research in the area of Fluid Electrical Conductivity (FEC) profiling as an alternative to packer testing or spinner flow meters in order to investigate fracture locations and to provide estimations of individual fracture transmissivities. The method entails altering the EC in a borehole (either by circulating de-ionised water or water with increased salinity), pumping the borehole at low abstraction rates and measuring the time evolution of dilution across borehole interval as formation water enters the borehole in response to the head differential

induced by the abstraction. The method was found to be more accurate than spinner flow meters, which can be very sensitive to variations in well bore radius, and less costly than inflatable packer testing, which is labour and time intensive. The method allows for the identification of points of inflow (fractures) and further work conducted by Doughty & Tsang resulted in the construction of the simulation program BORE II which is able to model fracture inflow and outflow points (under ambient flow conditions) as well as to calculate individual fracture transmissivities. This method has been found to be extremely effective at various test sites across the world including the Honorobe Underground Research Laboratory in Japan (Kurikami et al, 2008).

### 2.3.1 Numerical flow modelling in fractured rock aquifers

Whilst papers relating to numerical flow and transport models are in abundance, the majority of models are conducted as porous medium finite difference models, even when the natural environment being modelled is a fractured rock aquifer. This approximation is commonplace and relies on the scale of the model being large enough to account for, and override the small scale variations within the fractured medium. This approximation of fractured media to porous media, and avoidance of flow modelling in fracture rock is often the result of the increased complexity and difficulty in constructing and running flow models in fractured rock settings. Selroos *et al* (2002) provides a comparative study where groundwater flow and contaminant transport in a fractured rock aquifer was modelled using three alternative modelling approaches. The approaches were:

- Stochastic continuum modelling - whereby the assumption exists that over some representative elementary volume, the fracture rock may be represented as an equivalent homogenous porous medium which is governed by Darcy's Law. This is considered to be the most common approach to fractured rock groundwater modelling;
- Discrete fracture network modelling – this approach is based on the premise that groundwater flow in fracture rock settings occurs primarily within fractures. The model then solves for flow and transport in the interconnected fracture network. Whilst stochastic fracture networks can be generated based upon the properties of the site reference set, this approach generally requires a high level of detail in order to generate the reference set.
- Channel network modelling – this approach conceptualises the fracture surfaces as being uneven and mineralised such that flow is irregular and is distributed non-uniformly across the fracture in preferential flow paths which are termed channels. These channels may intersect in 3 dimensional space, forming a network of channels through which flow and transport may occur.

The results of the comparison indicated that whilst the modelling approached did yield small scale variation in the results, the predominant conceptual model specifications such as boundary conditions and gross hydrogeology played the most significant roles in limiting conceptual uncertainty within the modelled domain.

## **3 The Hydrogeology of Hydrocarbons in the Subsurface**

A clear understanding of the subsurface flow and transport of hydrocarbons and water in the presence of each other is of key importance in order to construct a robust conceptual model which will account for the movement of these two fluids within the aquifer. A system where both water and LNAPL are present is known as a multiphase system with the movement of the one fluid being dependent upon various characteristics of the second fluid. Both the physical and chemical properties of hydrocarbons should be considered when assessing the potential fate and transport of LNAPL and its associated dissolved phase within an aquifer. The following sub sections provide a summary of the most important physical and chemical properties of hydrocarbons which are relevant to contaminant investigations.

### ***3.1 Physical Fluid Properties of Hydrocarbons***

#### **3.1.1 Fluid Density**

Fluid density is defined as the mass of fluid per unit volume ( $\text{g/cm}^3$  or  $\text{g/ml}$ ). Density is influenced by temperature; as temperatures increase, density decreases. A liquid's specific gravity (SG) is defined as the ratio of the weight of a given volume of the liquid at a specified temperature to the weight of the same volume of water at a given temperature. The specific gravity is the critical indicator that determines whether the LNAPL will float ( $\text{SG} < 1.0$ ) or sink beneath the water table ( $\text{SG} > 1.0$ ). LNAPLs by definition will have an SG of less than 1.0 whilst DNAPLs will have an SG greater than 1.0. In general leaded petrol has an approximate density of 0.73, unleaded petrol an approximate density of 0.75-0.85 and diesel has an approximate density of 0.83 (API, 2004). These densities are specified for a temperature of 15°C.

#### **3.1.2 Wettability**

Wettability is the relative affinity of a porous medium for a given fluid and in the current context, is a measure of water, air, or LNAPL to preferentially spread over the medium's surface. The concept is used to describe the fluid distribution at pore scale and in a multiphase system the wetting fluid will

preferentially coat the porous media's surfaces and will occupy the smallest pores. The non-wetting fluid will generally be restricted to larger pores spaces. In most unsaturated soils, where air, water, and LNAPL are present, water is the primary wetting phase, followed by LNAPL, and then air. In the saturated zone, with only water and LNAPL present, water will generally be the wetting phase and displace LNAPL from pore spaces. Factors influencing wettability relations in immiscible fluid systems include mineralogy of the aquifer, chemistry of the groundwater and the petroleum hydrocarbon, presence of organic matter or surfactants, and the saturation history of the media (API, 2004).

### **3.1.3 Interfacial and Surface Tension**

Interfacial energy between two immiscible fluids is due to differences between the inward attraction of the molecules in the interior of the respective fluids and those near the surface of contact. The greater the interfacial energy between the two fluids, the greater the potential for immiscibility and the less likely emulsions will form. In the subsurface, interfacial tension occurs between the water phase and LNAPL phase. The interfacial tension between a liquid (water or LNAPL) and its own vapour is the surface tension. Interfacial tension is the primary factor controlling wettability. The interfacial tension for completely miscible liquids is 0 dyne/cm. Water (at 25°C) has a surface tension of 72 dynes/cm. Interfacial tension values for petroleum hydrocarbon-water systems range between these two extremes. The interfacial tension between these fluids may change due to pH, temperature, gases within the fluids, and surfactants. In general, increasing temperature decreases the interfacial tension

### **3.1.4 Viscosity**

A fluid's viscosity is a measure of its resistance to flow and results from molecular cohesion. The lower the viscosity of a fluid, the more easily it flows and the more readily it will penetrate a porous media. In general, as temperature increases in a liquid, the cohesive forces decrease and the absolute viscosity decreases. Viscosity is commonly defined in two general forms, dynamic viscosity and kinematic viscosity. These forms are related as follows:

$$\text{Dynamic Viscosity} = \text{shear stress} / \text{shear rate}$$

$$\text{Kinematic Viscosity} = \text{dynamic viscosity} / \text{density}$$

The unit of dynamic viscosity is the millipascal-second (mPa/s) or the centipoises (cP). The unit for kinematic viscosity is the centistokes (cSt).

### 3.1.5 Capillary Pressure

The pressure that is exerted across a fluid interface between a wetting and non wetting phase fluid is termed the capillary pressure. The term is usually expressed as the height of equivalent water column. In any small pore, capillary forces usually play a dominant role with regards to the distribution of multiple phases in that pore space. Capillary forces are the result of the attraction of a surface of a liquid to the surface of a solid, which elevates or depresses depending on the molecular surface forces. The capillary pressure ( $P_c$ ) for a water system is defined as:

$$P_c = \frac{2\sigma_{aw}}{r} \quad (1)$$

where  $\sigma_{aw}$  is the air-water interfacial tension and  $r$  is the radius of the capillary tube (approximated to the average pore throat radius in the aquifer sediment). Capillary head or height of the water rise in the capillary tube / sediment pore network is the capillary pressure divided by the unit weight of water ( $\gamma_w$ ) and is defined as:

$$H_c = \frac{2\sigma_{aw}}{r\gamma_w} \quad (2)$$

From equation 2 it can be seen that the capillary head is directly proportional to the interfacial tension of the fluid and inversely proportional to the pore throat radius. The practical implications of this is that LNAPL tends to have a larger capillary fringe due to its increased interfacial tension and finer grained soils tend to have larger capillary fringes due to decreased pore throat sizes.

### 3.1.6 Relative Permeability

Relative permeability is a factor that reflects the ability of a particular fluid to move through the pore space when it is partially occupied by other fluids. The ratio of the permeability of a fluid at a given saturation relative to the permeability of the fluid at 100% saturation is termed relative permeability. When a fluid completely fills the pore space, the relative permeability for the phase is one, and when no mobile phase is present the relative permeability is zero. In the context of an LNAPL-water

system, when the LNAPL saturations are high, the LNAPL relative permeability will approach one whilst the water relative permeability will approach zero. Conversely, if water dominates the saturation profile, the relative permeability of the LNAPL will approach zero whilst the water relative permeability will approach one.

### **3.1.7 Residual Saturation**

Saturation refers to the relative fraction of total pore space which is occupied by the non wetting phase fluid (LNAPL). LNAPL saturations vary across the depth profile of the LNAPL plume, but vary from 0 at the plume edges to a maximum of approximately 0.8 within the mass centre of the plume (API, 2004). Complete LNAPL saturation of the pores is not observed since not all water is displaced from the pore spaces. Upon removal of the LNAPL from the system, water will re-flood the pore spaces but will not displace all of the LNAPL, resulting in entrapped residual LNAPL. Residual saturation is term which defines the irreducible saturation of a fluid within a porous media beyond which hydraulic recovery is not possible. The entrapment of the LNAPL occurs when continuous pore pathways of LNAPL get cut off due LNAPL saturation falling below a certain threshold value. Residual saturations will tend to be higher in fine grained sediments and can be as high as 60 percent of the overall saturation. This has significant implication for remediation since it may result in significant volumes of LNAPL becoming trapped in the aquifer, forming long term secondary sources of contamination.

### **3.2 *The Behaviour of LNAPL in Fractured Rocks***

Hardisty et al (1998 & 2004) has provided an idealised conceptual model of LNAPL behaviour within a fractured rock aquifer, and the following paragraphs are a summary of this conceptualisation along with selected governing equations which describe the behaviour.

Upon entering the subsurface from leaking infrastructures (UST's, pipelines, dispenser pumps) LNAPL will migrate vertically by means of a continual wetting front through the unconsolidated unsaturated zone until the bedrock topographic profile is reached. LNAPL will then tend to pool in depressions within the bedrock and flow along the surface of the bedrock topography until a vertical or sub-vertical fracture is intersected at which point the LNAPL will migrate down the fracture as a

single phase fluid flow. Flow through the fracture will increase as the viscosity of the fluid decreases and as the fracture aperture increases.

Visualising the LNAPL within the fracture as an idealised “plate”, the unit plate width viz. the fracture aperture width ( $b$ ) and plate length ( $L$ ) will induce a hydrostatic driving pressure head which is dependent on the dip angle of the fracture ( $\Psi$ ). Vertical migration of LNAPL through the unsaturated zone in fractured rock occurs most effectively in fractures with a steep dip angle and/or in fractures with a wide aperture. The connected vertical height of the NAPL column (pressure head) can thus be expressed as:

$$h_L = L \sin \Psi \quad (3)$$

As the connected vertical height increases, so too will the LNAPL pressure head ( $h_L$ ). Upon reaching the static water level, LNAPL will begin to accumulate on top of the water, gradually depressing the water level within the fracture. In order for LNAPL to enter a fracture that is occupied by water (in a water wet system), the LNAPL-water capillary pressure ( $P_c$ ) must exceed the fracture entry pressure ( $P_e$ ). In an idealised parallel plate scenario, the fracture entry pressure can be described as (Kueper and McWhorter, 1991):

$$P_e = \frac{2\sigma \cos \phi}{b} \quad (4)$$

where  $\sigma$  is the LNAPL-water interfacial tension and  $\phi$  is the interface contact angle through the wetting phase. At the water level, the capillary pressure within the fracture is equal to the LNAPL fluid pressure at the LNAPL/water interface which is in turn dependant on the vertical column height of the LNAPL within the fracture ( $h_L$ ). Under equilibrium conditions, the pressure system is balanced by the buoyancy of the LNAPL (as a result of its penetration below the water level) and the fracture entry pressure. This equilibrium is described by the following equation (Hardisty et al, 1998):

$$h_L \rho_L g = h_p \rho_w g + \left( \frac{2\sigma \cos \phi}{b} \right) \quad (5)$$

where  $\rho_L$  is the LNAPL density,  $\rho_w$  is the density of water,  $g$  is gravity,  $h_p$  is the LNAPL penetration depth below the water level and  $b$  is the fracture aperture width. Re-arranging the equation to:

$$h_p = \frac{h_L \rho_L g}{\rho_w g} - \left( \frac{2\sigma \cos \phi}{b} \right) \quad (6)$$

It can be observed that (keeping all fluid properties constant) the depth of LNAPL penetration is largely dependent on the LNAPL pressure head and the fracture aperture width. Another consideration is that fractures which intersect the LNAPL bearing fracture beneath the water level can also be invaded by the LNAPL depending on their aperture width and dip angle. Penetration of



LNAPL to significant depths beneath the water may result in instances where LNAPL becomes trapped within fractures beneath the water level due to sudden perturbations within the pressure system (ie. a sudden rise in water levels), resulting in the fracture entry pressure exceeding the LNAPL-water capillary pressure.

It is possible for trapped LNAPL to remobilise when a decrease in water levels occurs, thereby reducing the hydrostatic pressure at the LNAPL/water interface. The introduction of additional LNAPL or lateral redistribution of existing LNAPL within the system may reconnect trapped LNAPL with LNAPL in vertical and sub-vertical fractures. This can potentially lead to significant increases in the overall LNAPL column height and pressure head, resulting in remobilisation of LNAPL along fractures and into observation wells. This model would explain the “pulse like” appearance and disappearance of LNAPL and varying LNAPL thicknesses that are often observed in monitoring wells.

The fluctuation of groundwater levels may have a significant effect on the migration, entrapment and distribution of LNAPL within a fractured aquifer. In a scenario where groundwater levels fall, the LNAPL within the (sub) vertical fractures will migrate downward under the influence of gravity and then migrate laterally along newly unsaturated horizontal / less steeply dipping fractures. Upon a water level rise, the LNAPL within the vertical fractures will be most able to follow, entering into previously water filled fractures. Entrapment of LNAPL in less steeply dipping fractures may occur which may then be remobilised when water levels drop again. In such a manner the rising and falling of water levels can actually “pump” LNAPL laterally along the fracture network. These phenomena are displayed graphically in the following figures.

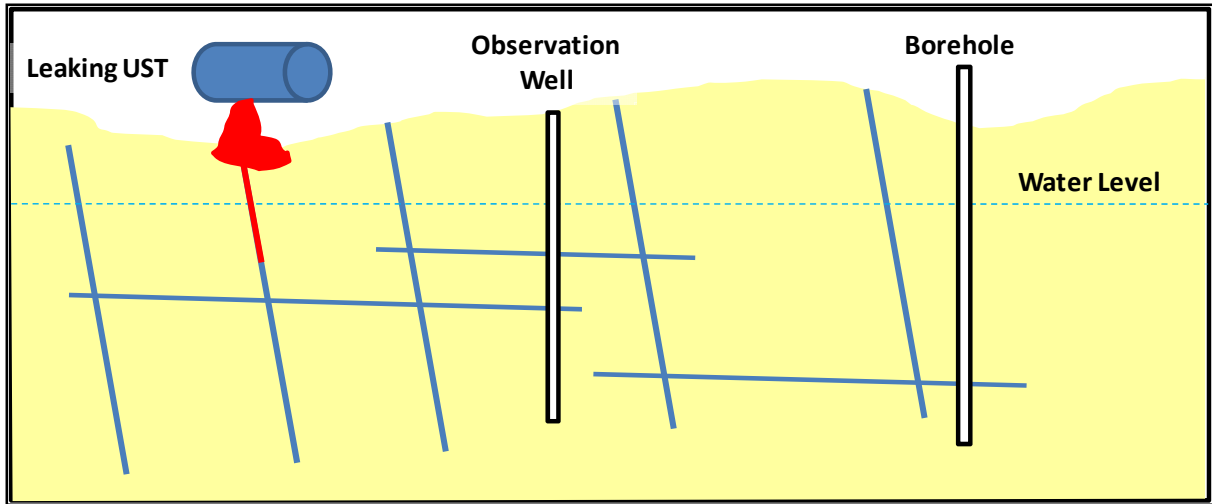


**Figure 3-1 Idealised LNAPL fracture flow scenario (Part 1)**

In Figure 3-1, the LNAPL enters the fracture network via a sub vertical fracture and penetrates to a given depth where the LNAPL-water capillary pressure and fracture entry pressure are in equilibrium. No LNAPL is observed in the observation well.

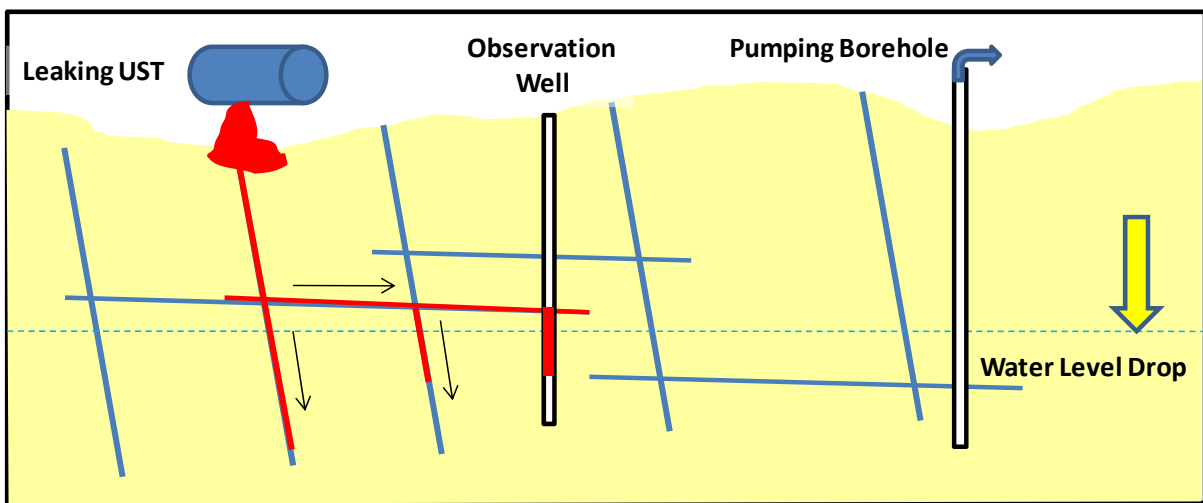


**Figure 3-2 Idealised LNAPL fracture flow scenario (Part 2)**

In Figure 3-2, a water level drop is experienced from a nearby pumping well. The LNAPL travels down the sub-vertical fracture, but also along sub-horizontal fractures, intersecting new sub-vertical fractures and the observation well. LNAPL is observed in the well.

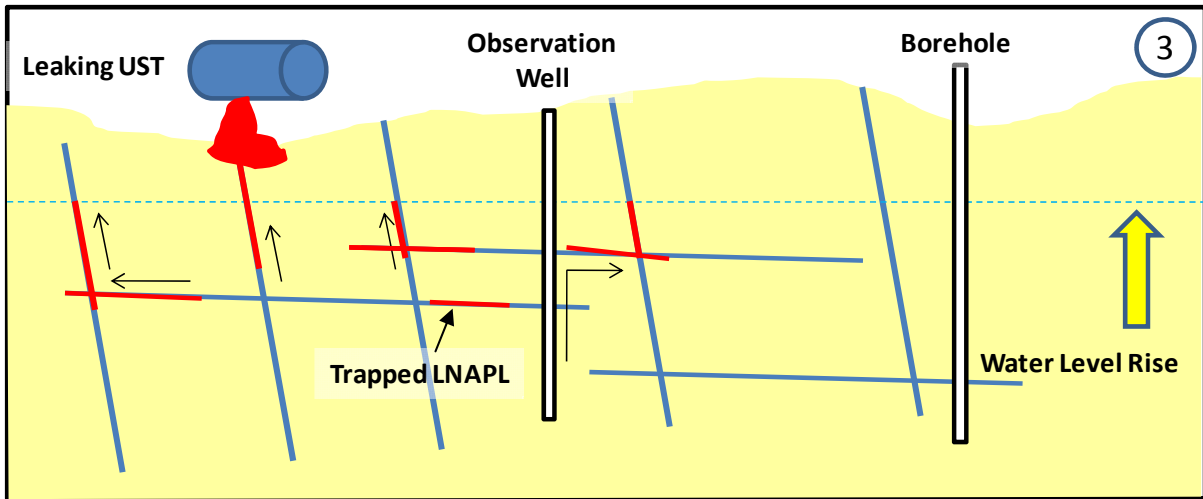


**Figure 3-3 Idealised LNAPL fracture flow scenario (Part 3)**

In Figure 3-3, the water level rises after the abstracting well is disengaged. The LNAPL in sub-vertical fractures rises with the water level mobilising along previously water filled fractures, whilst some of the LNAPL is trapped beneath the water level. LNAPL within the observation well rises and begins to migrate along another unsaturated sub-horizontal fracture. As a result, the LNAPL thickness within the well decreases significantly or disappears altogether, displaying the pulse like nature of LNAPL appearance (and disappearance) often observed within observation wells.

In order to illustrate the point that significant penetration below the water level is possible, a hypothetical scenario is presented similar to the scenario depicted in figure. In the a situation where the source release is at 3m below ground level (average depth of UST bottom) and the water level is at 12m (an average water level in the study area), the LNAPL head would be 9m. Assuming the following factors and referring to equations 4 and 6:

Fracture aperture,  $b = 1\text{mm}$  (0.1cm)

LNAPL head,  $h_L = 9\text{m}$  (900cm)

LNAPL-water interfacial tension,  $\sigma = 50$  dynes/cm

Contact angle through the wetting phase,  $\phi = 80^\circ$

LNAPL density  $\rho_L = 0.73 \text{ g/cm}^3$

Water density  $\rho_w = 1.00 \text{ g/cm}^3$

Based upon equation 4, the fracture entry pressure  $P_e$  is equal to 1.7m (174cm). Using the abovementioned information with equation 6, the depth of penetration beneath the water level in a 1mm fracture was calculated to be 4.8m.

### ***3.3 The Hydro-geochemistry of Hydrocarbons in Groundwater***

#### **3.3.1 Petroleum Product Composition**

Petroleum products (ie. unleaded and leaded petrol) are generally composed of a mixture of low molecular weight hydrocarbons (C<sub>4</sub>-C<sub>10</sub>) and non hydrocarbon additives such as methyl tertiary-butyl ether (MTBE), TAME, and ethanol. Isoalkanes and n-alkanes are the dominant molecules in petrol, followed by cycloalkanes and aromatic compounds. During the petroleum distillation process, the light aromatic compounds are preferentially enriched, resulting in relatively elevated concentrations of benzene, toluene, ethylbenzene and xylenes (BTEX). Toluene is generally the dominant compound with regards to relative composition. Petrol generally consists of approximately 20 percent BTEX compounds. Polycyclic aromatic hydrocarbon (PAH) compounds are also present within petroleum, but due to their high molecular weight and elevated boiling points, they generally only occur in very small percentages within petrol.

Since petrol is composed mainly of light fraction hydrocarbons, it tends to be more mobile, volatile and soluble than other LNAPL hydrocarbon products. The relatively BTEX enriched composition of petrol results in a readily volatile and soluble product which, when introduced into the subsurface environment, can produce significant dissolved phase plumes along with associated vapour phase plumes in the vadose zone above the affected saturated zone. Over time, the BTEX compounds are preferentially leached out of the product, and “degraded” gasoline may contain less than 5% BTEX compounds (API, 2004).

Diesel, which is termed a middle distillate fuel (includes kerosene, jet fuel, and lighter fuel oils) generally consists of C<sub>10</sub>-C<sub>20</sub> hydrocarbons compounds and tends to have higher concentrations of cycloalkanes and PAH compounds. BTEX concentrations generally range between 1 to 3 percent (API, 2004). As a result, middle distillate products tend to be more dense, less volatile and soluble, and less mobile than gasoline.

### 3.3.2 Solubility & Volatility

When an LNAPL hydrocarbon release occurs and the product comes into contact with the air in the vadose zone and groundwater, various compounds will begin to dissolve from within the LNAPL into the abovementioned fluids. Mass transfer from the LNAPL phase into the water (or vapour) phase is dependent upon the composition of the LNAPL, the chemical and physical characteristics of the aqueous phase, and the physical contact surface area between the different fluids. The pure phase solubility of a compound is the maximum concentration that a specific compound in its pure phase can be dissolved into water at a specific temperature and pressure. Pure phase solubility concentrations of selected hydrocarbon compounds are shown in Figure 3-4.

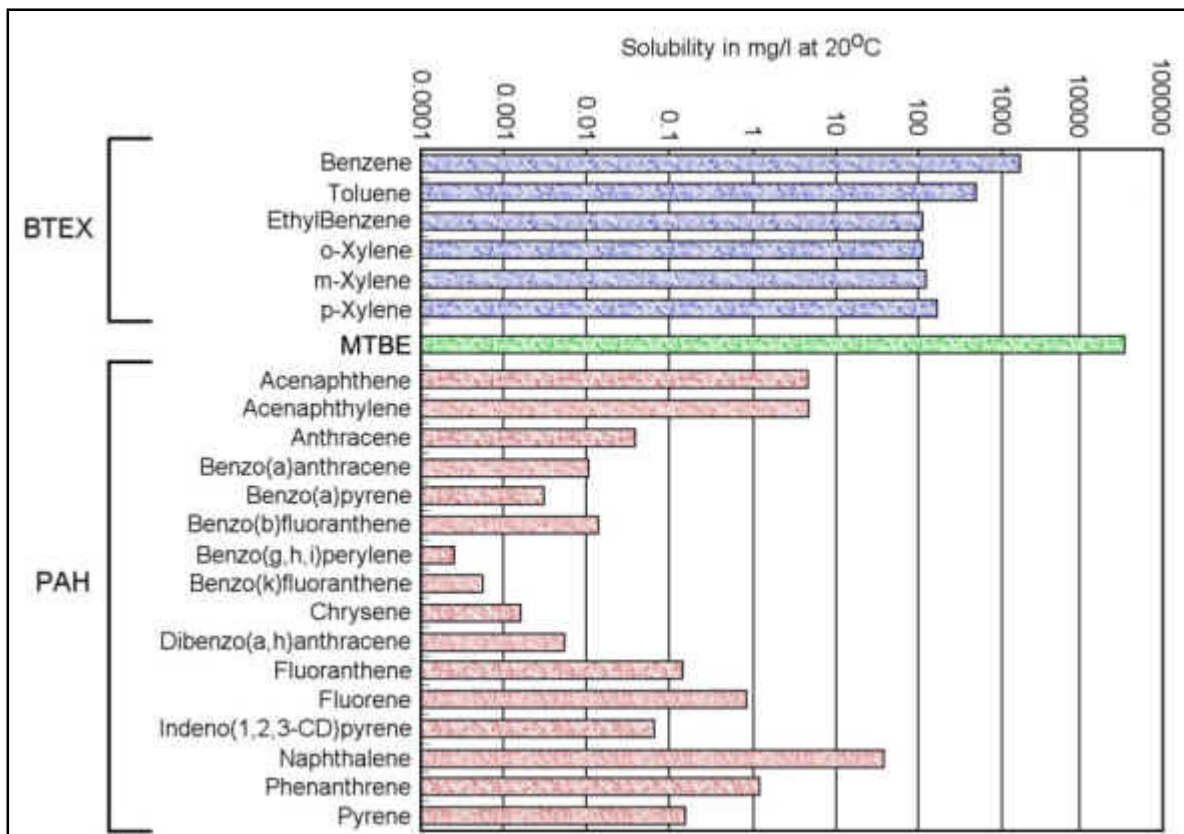


Figure 3-4 Pure Phase Solubility of Selected Hydrocarbon Compounds (From API, 2004)

Given that hydrocarbon products consist of a wide variety of compounds, the equilibrium concentration, or “effective solubility” for a specific compound within the product will be significantly lower than its pure phase solubility. Effective solubility can be estimated using Raoult’s Law, which states that the concentration of specific compound in the aqueous phase is proportional to the mole fraction of that specific compound in the parent LNAPL phase. Raoult’s Law can be described mathematically as:

$$C_i^{eq} = S_i MF_i \quad (7)$$

Where  $C_i^{eq}$  is the equilibrium aqueous concentration of hydrocarbon constituent  $i$ ,  $S_i$  is the pure phase solubility of hydrocarbon constituent  $i$ , and  $MF_i$  is the mole fraction of hydrocarbon compound  $i$  in the LNAPL product. The mole fraction of a specific compound within the LNAPL product is approximately equal to the mass fraction of the compound in the LNAPL (API, 2004). Given that various compounds within the LNAPL will have different effective solubilities, the rate of dissolution of the various compounds from the LNAPL into the groundwater will also vary between compounds. As a result the mole fractions of the various compounds within the LNAPL will change over time, with the resulting aqueous solubilities of the compounds varying accordingly. A consequence of this is that compounds with higher effective solubilities will tend to more readily leach out from the parent LNAPL product and over time their relative mole fractions will become depleted. As this occurs, the relative mole fractions of less soluble compounds will increase.

Figure 3-5 illustrates the differing dissolution behaviours of MTBE, benzene and toluene by tracking the concentrations of the abovementioned compounds in a hypothetical well located downgradient of a petrol spill. As shown in Figure 3-4, the solubility of MTBE is orders of magnitude greater than the majority of BTEX compounds and this results in a rapid transfer of MTBE from the LNAPL into the aqueous phase (as shown in Figure 3-5). Benzene, due to its lower effective solubility produces lower dissolved concentrations, and as benzene and MTBE are progressively leached and depleted from the LNAPL, toluene becomes the more dominant species. With a solubility of 515 mg/l (515,000µg/l) and an average mole fraction of 5%, toluene will tend leach from the LNAPL for a considerable period of time (API, 2004).

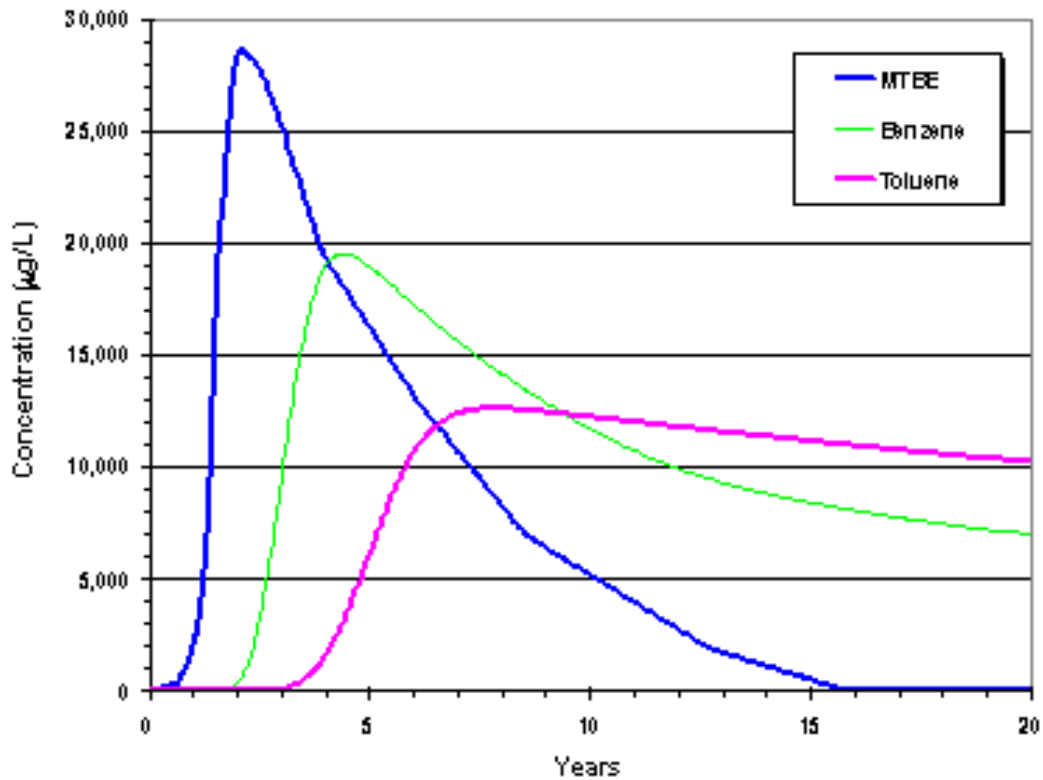


Figure 3-5 Concentrations of MTBE, benzene and toluene over time (From API, 2004)

Although effective solubilities can be estimated using Raoult's Law, these "true" effective solubilities are generally not observed in practice and provides evidence that the partitioning between LNAPL and water is not an efficient process. By means of an example, the pure phase solubility of benzene is approximately 1,780mg/l, whilst the average mole fraction of benzene in fresh petrol is 2 percent. Raoult's Law would predict a true effective solubility concentration of approximately 36mg/l and notwithstanding process such as dilution, dispersion and degradation which may decrease the concentration, rarely are concentrations above 10mg/l observed (API, 2004). The rate of mass transfer of a specific compound from the LNAPL product into groundwater is dependent upon the existing dissolved phase concentrations in the groundwater viz. the concentration gradient, the groundwater velocity, the surface area of the LNAPL-water contact zone and the molecular diffusivity of the LNAPL components in water. The transfer rate can be described by the following equation:

$$T_i = k_o q (C_i^{eq} - C_i^W) \quad (8)$$

where  $T_i$  is the transfer rate within the LNAPL-water system for the compound  $i$ ,  $k_o$  is a dimensionless LNAPL-water mass transfer coefficient,  $q$  is the groundwater velocity,  $C_i^{eq}$  is the



effective solubility of compound  $i$  in groundwater and  $C_i^W$  is the observed concentration of compound  $i$  in the groundwater directly adjacent to the LNAPL-water interface. From the mass transfer equation it can be observed that the greater the groundwater velocity, the greater the potential rate of transfer. The concentration gradient will also control the rate of dissolution. As a result, dissolution will take place more readily on the upgradient boundary of a plume as opposed to the downgradient boundary since the concentration gradients will be greatest at the upgradient boundary.

### **3.3.3 Advection and Dispersion**

Advection is generally the dominant transport mechanism of dissolved phase contaminants, particularly within a fractured rock aquifer setting, and describes the movement of dissolved compounds in response to an induced pressure gradient which results in the observed groundwater flow system. Dispersion is scale dependant, and although more dominant in porous media aquifers, must also be considered in fractured aquifers, particularly when large scale areas are being considered. Dispersion relates to the fluid mixing which results from heterogeneities within the aquifer and diffusion which is the migration of molecular compounds in response to concentrations gradients. This migrations related to concentration gradients is a significant factor in double porosity fracture aquifers since dissolved phase compounds will tend to diffuse into the bedrock matrix under concentration gradients between the water in the fractures and the water in the matrix. Diffusion is time dependent and is significant at low velocities. In general, dispersion acts to attenuate the contaminant concentrations whilst increasing the size and rate of transport of the dissolved hydrocarbon plume when compare to plume migration by advective transport alone.

### **3.3.4 Sorption**

Sorption describes the interaction of dissolved compounds with solids. Sorption is further sub classified into adsorption, which describes the process of dissolved phase compounds binding to the surface of a solid, and absorption which the process where the dissolved compound physically penetrates the solid. In contrast to advection, sorption tends to attenuate plume movement with the difference in the velocity (relative to purely advective velocity) of the dissolved phase due to sorption, is termed retardation (R) and is expressed as:

$$R = \frac{v}{v_c} \quad (9)$$

where  $v$  is the velocity of the groundwater and  $v_c$  is the velocity of the dissolved hydrocarbon.

Retardation is a function of the partition coefficient ( $K_d$ ), which describes ratio between the dissolved phase compound the soil, including factors such as soil bulk density ( $\rho_b$ ), and the soil porosity ( $\phi$ ).

The abovementioned parameters can be expressed in the equation:

$$R = 1 + K_d \left( \frac{\rho_b}{\phi} \right) \quad (10)$$

The partition coefficient ( $K_d$ ), is related to the fraction organic content ( $f_{oc}$ ) of the aquifer substrate.

$K_d$  can be estimated for each individual hydrocarbon compound as the product of  $f_{oc}$  and the organic carbon partition coefficient ( $K_{oc}$ ) of the compound.

$$K_d = K_{oc} f_{oc} \quad (11)$$

Sediments with more organic carbon (high  $f_{oc}$ ), such as clays, peats and shale, will increase the potential for sorption and increase retardation. Conversely, sediments with small amounts of organic carbon, such as clean sands and gravels, will decrease the potential for sorption and decrease retardation. Similarly, compounds with a high  $K_{oc}$  will sorb more readily than those with a low  $K_{oc}$ . As a simplified example, on average, the majority of benzene plumes generally do not extend more than 70m downgradient of their source zones (API, 2004), whilst MTBE plumes have been observed to extend in excess of 1.8km downgradient from their source zones (Ellis, 2000). This is largely due to the increased solubility and low retardation factor of MTBE (relative to benzene). Referring to equations 10 and 11, keeping soil bulk density, porosity, and the organic carbon fraction constant (ie. both compounds in the same aquifer and from the same release), the retardation becomes a function of the carbon partition coefficient. The  $K_{oc}$  of benzene is 98 whilst that of MTBE is 11, indicating that MTBE does not readily undergo sorption whilst benzene will do so to a moderate degree. Despite sorption reducing the migration and the concentration of a dissolved hydrocarbon plume, most sorption processes are reversible. Consequently, sorption may potentially inhibit the remediation of a dissolved plume as mass may potentially be re-released from the aquifer substrate back into the groundwater.

## 4 Description of Study Area

### 4.1 Location

Beaufort West is located approximately 450km to the north west of Cape Town within the semi arid area known as the Great Karoo, and forms the halfway point between Cape Town and Bloemfontein. The town has approximately 37 000 inhabitants and falls within the co-ordinate grid 32° 21' 48.91'' S, 22° 34' 02.71'' E to 32° 20' 00.33'' S, 22° 36' 15.94'' E. The overall area of study falls within the town limits of Beaufort West and extends out towards the eastern boundary of the town as is shown in Figure 4-3, with the majority of the detailed investigations conducted as part of this study being carried out in a smaller sub-area from Donkin Rd in the west towards the eastern boundary of the Kuils River, with Voortrekker Rd being the boundary to the north as indicated in Figure 4-4. The potential hydrocarbon source zones, which will be discussed in following sections have been indicated in Figure 4-5.

### 4.2 Climate

The mean rainfall in the Beaufort West area is approximately 300mm per year, with hot wet summers and cold dry winters (IGS, 2009). Temperatures can rise above 40° Celsius in summer and can drop to below freezing in the winter months. The bulk of the rainfall occurs throughout the summer months with most of the precipitation taking the form of sudden, violent thunderstorms with associated downpours. Potential evapotranspiration rates are expected in the order of 2000mm/annum. As can be observed in Figure 4-1, March on average is the wettest month of the year whilst June and July are the driest months. Figure 4-2 displays the total yearly rainfall for three rainfall stations in the Beaufort West area (Beaufort West town, Beaufort West water tank on the western part of Beaufort West sill and De Hoop farm 30km north east of the town), with data extending back to 1973. From the figure it can be seen that 2008 had a below average rainfall as did 2009 (L. Smit, *pers comm.*) for which there is no data available at present. In communication with the Beaufort West Municipality it was confirmed that the area has been experiencing below average rainfall since 2008 up until the present.

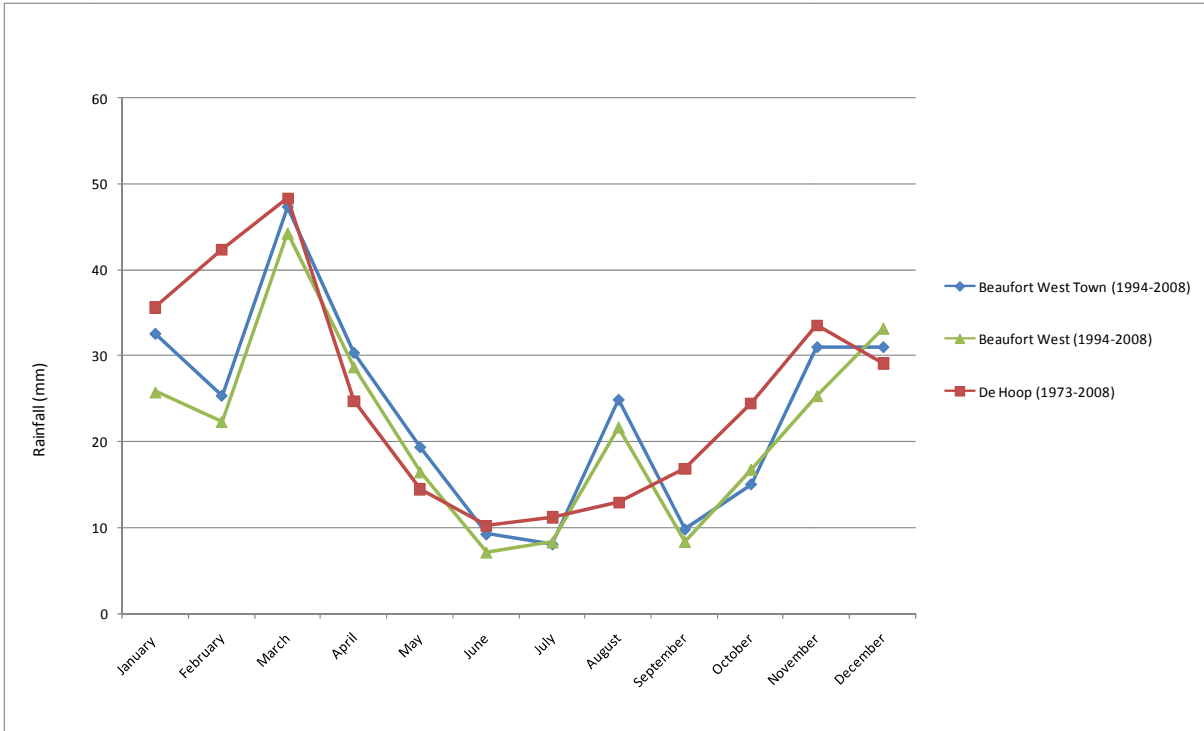


Figure 4-1 Climatic data from 1973 to 2008 for the Beaufort West Area.

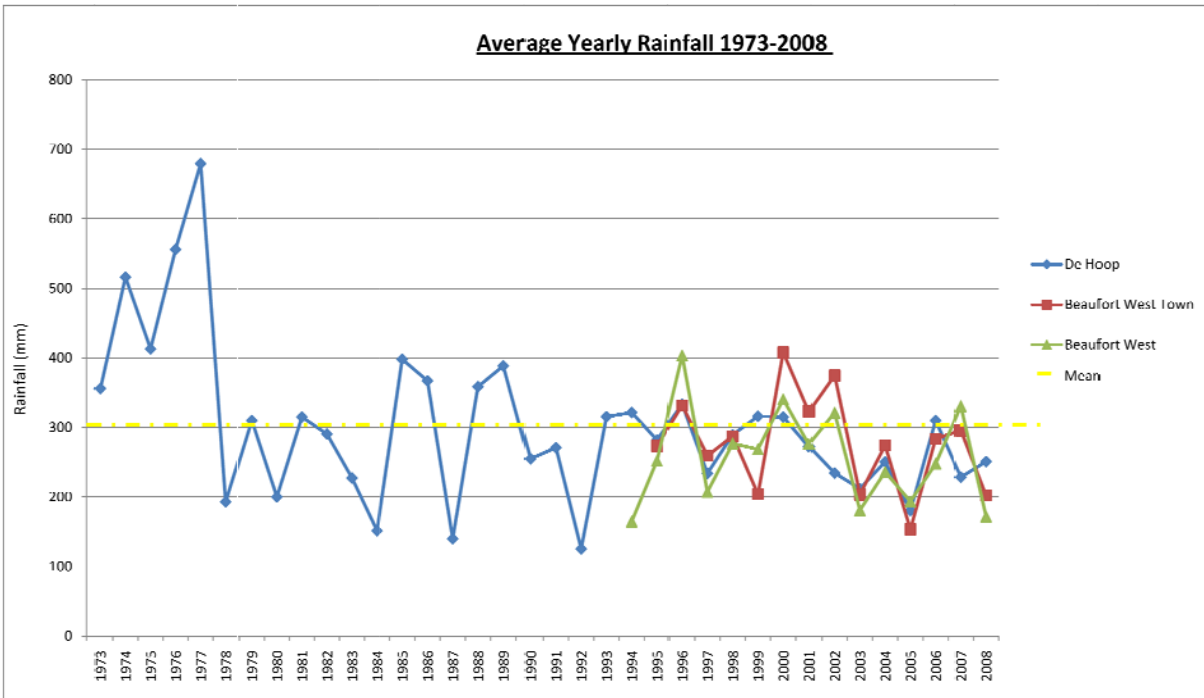


Figure 4-2 Total Yearly Rainfall for the Beaufort West Area

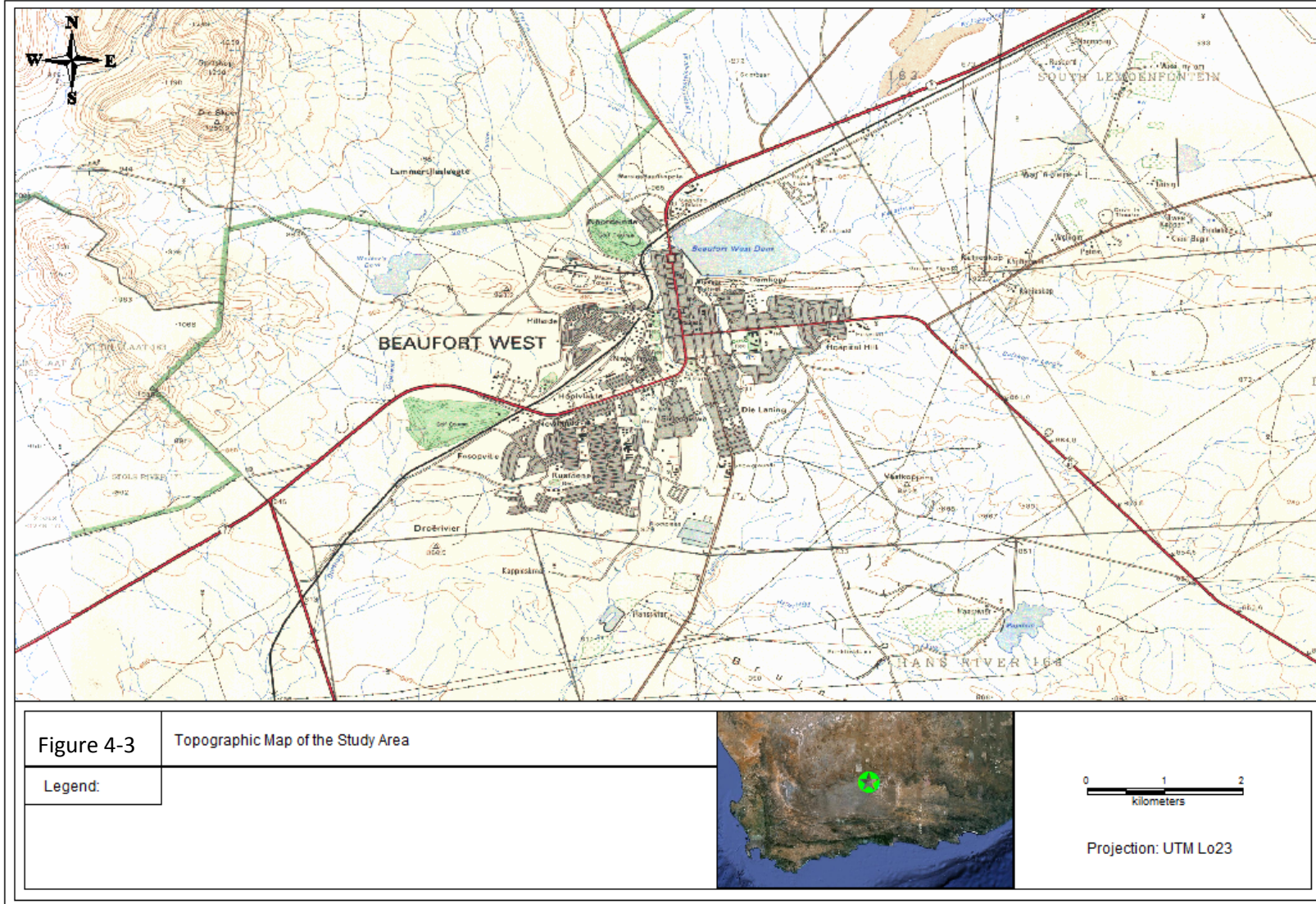


Figure 4-3 Topographic map of the study area





Figure 4-4 Aerial photograph of the study area





**Figure 4-5 Closer view of the Study Area within the town of Beaufort West.**

### ***4.3 Topography***

The topography of the study area is generally flat, with a very slight regional topographic gradient of approximately 0.006 (based on NASA 90m contour data) towards the south. The study area is at an average altitude of 840m but the land elevation rises rapidly to the north as one approaches the piedmont of the Nuweveld Mountains (6km to the north of the town), which rise to an altitude of between 1100m-1300m. A large inclined dolerite sill crosses the northern region of the town and forms a topographic high within this area.

### ***4.4 Geology***

According to the 1:250 000 Geological Map of the Beaufort West Area, the town is underlain by the Teekloof Formation, which forms part of the Adelaide Subgroup which in turn forms part of the Beaufort Group. The Beaufort Group was deposited in a foreland basin environment with two fluvial processes, namely braided and meandering streams being responsible for the deposition of the sediments (Davis, 1983). The Teekloof formation consists of mainly of green to bluish grey to maroon mudstones and siltstones with intermittent fine to coarse grained sandstones (Campbell, 1980) and is considered to have been deposited in the meandering stream depositional environment. Underlying the Teekloof formation is the Abrahamskraal formation, which tends to have a greater percentage of sandstone than the Teekloof formation (Campbell, 1980) and is related more to a braided river depositional environment. In the meandering river depositional environment the mudstone, siltstone and sandstone beds were deposited in a horizontal fashion on top of each other, whilst in the braided depositional environment the mudstones and sandstones were deposited in a more sheet like, wedge shaped manner (Tankard et al, 1982). Intrusive investigations in the study area have confirmed the geology to be dominated by the alternating mudstones and siltstones of the Teekloof Formation. The Beaufort Group is considered to be highly indurated with significant amounts of calcite, quartz, chlorite and sericite (Tankard et al, 1982).



<b>Karoo Supergroup</b>	<b>Stormberg Group</b>	<i>Sandstone &amp; mudstone</i>		
	<b>Beaufort Group</b>	Tarkastad Subgroup	<i>Mudstone &amp; subordinate sandstone</i>	
		Adelaide Subgroup	Teekloof Formation	Mudstone, siltstone and subordinate fine to coarse grained sandstone
			Abrahamskraal Formation	Mudstone, siltstone and more predominant sandstone
	<b>Ecca Group</b>	<i>Shales &amp; mudstone</i>		
<b>Dwyka Group</b>	<i>Diamictite</i>			

**Figure 4-6 Generalised stratigraphy of the Karoo Supergroup with reference to the formations observed in the study area**

Figure 4-10 depicts the two differing depositional situations. What is important to note is that these depositional processes have generally caused the more coarse grained sediments (sandstones) to be deposited as lens shaped bodies which are not laterally continuous and often pinch out (Botha et al, 1998). Sandstones can occur in layers up to 15m in thickness whilst siltstones vary in thickness from a few centimetres up to 4m. The mudstones occur in units up to 50m in thickness and form approximately 50% of the stratigraphic interval, whilst siltstones contribute approximately 30% and the sandstones approximately 20% (Campbell, 1980). Jurassic dolerites in the form of linear dolerite dykes and transgressive sills are also present in the area with a large east-west striking dolerite inclined sill (termed the Beaufort West sill) crossing the northern portion of the town and another northwest-southeast striking dyke being present to the south of the town. A walkover survey of the quarry at the Springfontein Dam wall in the town found the sill to be dipping at an angle of approximately 30 degrees to the north, with an average outcrop thickness of 4m. Highly weathered mudstones were observed to exist within the chill margin of the sill.



Figure 4-7 Looking south, a view of the transgressive Beaufort West sill (outlined by dotted red line)

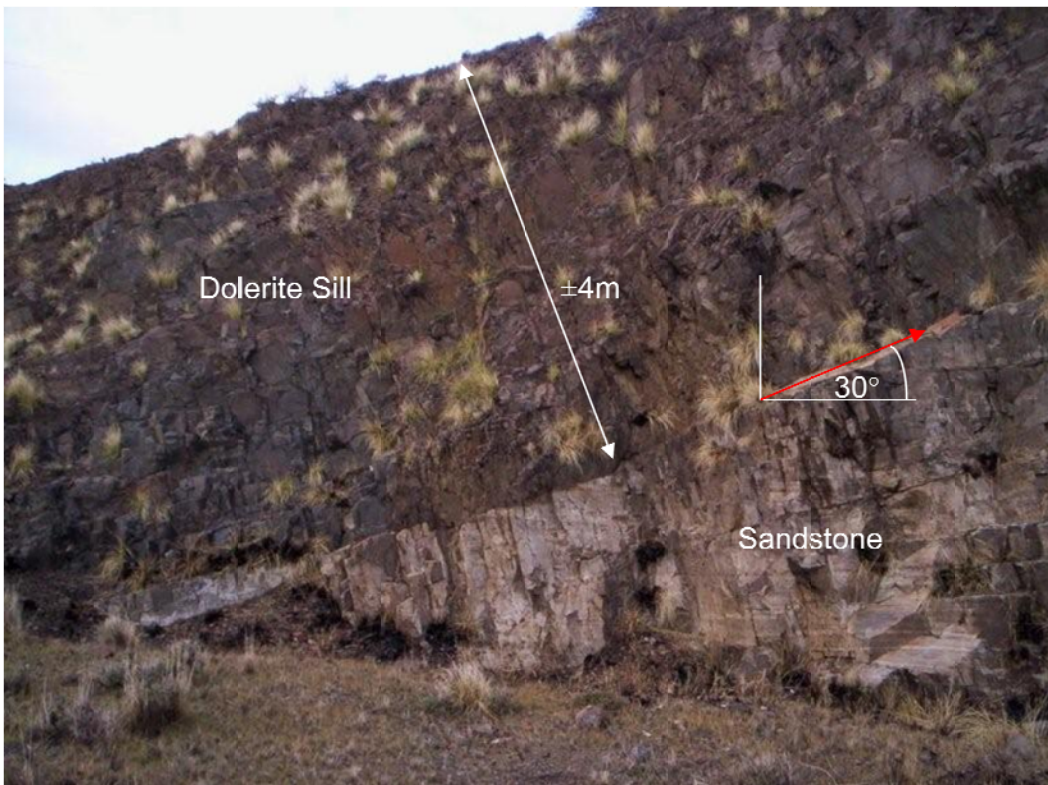


Figure 4-8 A cross cut section of the Beaufort West sill, dipping to the north



**Figure 4-9 Weathered mudstone on the footwall of the Beaufort West sill**

Quaternary deposits along dominant river courses have been observed to be major feature in the Karoo Basin (Woodford & Chavelier, 2002) and drilling work in the study area has confirmed that unconsolidated river sediments and boulder terraces underlie the study area ranging from depths of 4m to 7m, at which point the weathered bedrock profile is intercepted. Calcrete cemented layers have also been observed to be present within the river course areas.



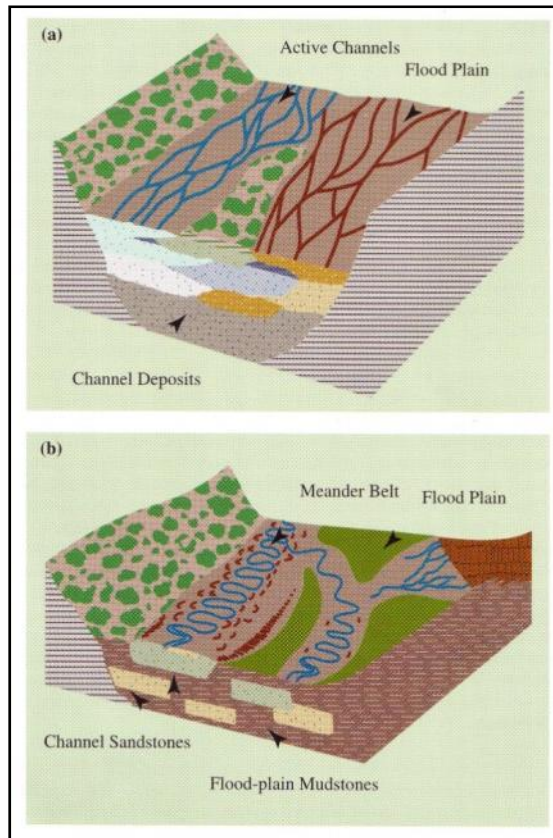


**Figure 4-10: Models of sediment deposition in a.) a braided stream and b.) a meandering stream environment [Taken from Botha et al (1998)]**

## 4.5 Structural Geology

Structural geology refers to the study of the structural deformation of geologic units by compressional (and dilational) forces. These forces will give rise to jointing, fracturing and folding within the bedrock, all which have significant control over the flow of groundwater in a fractured aquifer. Campbell (1980) has by far conducted the most extensive fieldwork in the Beaufort West area during hydrogeological investigations in the mid 1970's in which over 500 boreholes were drilled with a total length exceeding 45km. The 1980 investigation has identified several structural features that are present over the study area.

Several vertical to sub-vertical joint sets are present in the study area with two tension joint sets striking in an east to west and north to south direction, and two conjugate joint sets striking in a north-west to south-east direction and a north-east to south-west direction (Campbell, 1980). The north-west/south-east conjugate joint set and the east/west tension joint set have been observed to be the

most developed in the area (Campbell, 1980). Campbell goes on to note that in almost all cases the vertical/sub-vertical joint sets are continuous in the sandstone and siltstone facies, but are discontinuous, displaced or absent in the mudstone facies. Horizontal fractures and joints are most commonly found near bedding planes where deformational forces have caused the differing lithologies to “slide” over each other, usually along the bedding planes which are preferential zones of weakness (Campbell, 1980). From a weathering perspective, the investigations in the 1970’s have identified that the first 30m of the stratigraphic profile is usually highly weathered with the bedrock below 30m usually being in an unweathered condition (Campbell, 1980).

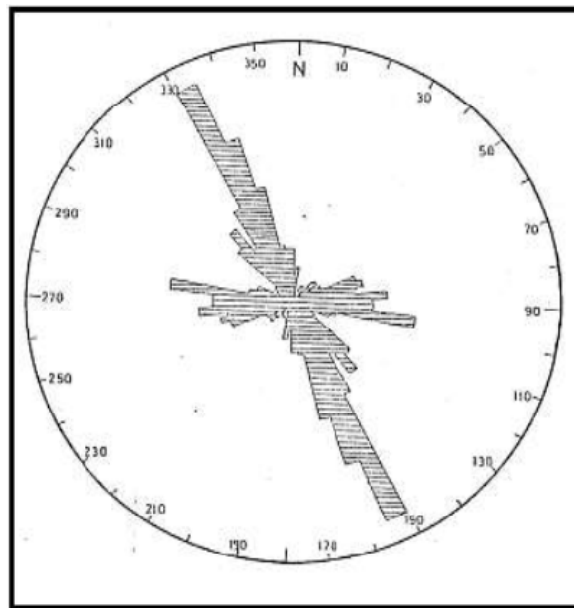


Figure 4-11 Rose diagram of joint set orientations within a 30km radius of Beaufort West (Campbell, 1980)

## 4.6 Hydrogeology

### 4.6.1 A Brief description of Karoo Aquifers

Karoo aquifers have been classified as multi-layered, multi-porous aquifers with the main fluid transport pathway being identified as the bedding plane parallel fractures, however fluid flow is inferred to occur in two fashions: Fluid flow through the fractures and fluid flow from bedrock matrix into the fractures (Botha et al, 1998). The horizontal bedding plane fractures are generally observed to be sparsely distributed (vertically) and the apparent lack of vertical fractures in case studies done to date has given rise to the inference that horizontal bedding parallel fracture networks are poorly connected in a vertical sense (Botha et al, 1998). Botha et al goes on to state that boreholes in Karoo aquifers only have significant yields if they intersect a bedding parallel fracture. This has implications

for contamination investigations since monitoring wells would need to intersect the bedding plane fractures in order to effectively observe the contaminant status in these predominant transport pathways in the aquifer. If no fracture is intersected then the well will be monitoring the groundwater quality of the matrix at that position which may or may not detect contamination depending on the proximity of the well to a fracture and the extent of diffusion of the contaminants into the matrix. Another possibility is that even if a fracture is intersected, it might belong to a set that is not linked to those that are contaminated.

The aquifers are generally thought of as dual porosity aquifers with the bedrock matrix having one porosity value and the fracture possessing another porosity value and whilst it may seem at first that the fracture networks would store the majority of the water, this is not the case with bedrock matrix storing the majority of the water and the fractures simply being the predominant flow pathways (Botha et al, 1998). Despite this, storativity values are generally low, ranging from  $1 \times 10^{-2}$  to  $1 \times 10^{-7}$  with a mean value of  $1 \times 10^{-4}$ , whilst transmissivity values range from  $10 \text{m}^2/\text{day}$  to  $1500 \text{m}^2/\text{day}$  (Campbell, 1980). Boreholes with high transmissivities were generally found in preferentially weathered zones such as along the chill margins of intrusive dolerite dykes. Studies done at the IGS of the University of the Free State (UFS) have shown that the Karoo aquifers are extremely susceptible to matrix diffusion, which is the diffusion of fluid base compounds from groundwater in the fractures into the matrix. This coupled with the generally low permeabilities of the bedrock matrix result in it being extremely difficult to remediate a contaminated Karoo aquifer, since the contaminants, which diffuse into the matrix, form long term contamination sources which back-diffuse into the fractures for an extended period of time even after all primary contaminant sources have been removed. This effect has been observed in the holes surrounding Donkin Motors where long term monitoring data is available (Van Biljon and Swanepoel, 2007). Recharge across the study area is considered to be in the region of 2% of annual rainfall (Kotze et al, 1997).

## ***4.7 High Level Conceptual Model***

According to the Department of Water Affairs and Forestry's (DWA) 1:500 000 hydrogeological series map of Beaufort West, a fractured rock aquifer occurs below the site with a median borehole yield in excess of 5.0 L/s. This would be considered a high yielding area. According to the abovementioned map, the groundwater quality is fair to moderate with electrical conductivities for the region measuring 700 – 3000  $\mu\text{S}/\text{cm}$ . This is consistent with historical field observations which have measured EC values ranging from 800 – 1500  $\mu\text{S}/\text{cm}$ .

Figure 4-13 depicts the regional geological and hydrogeological factors which influence the study area. From Figure 4-13 it can be seen that a drainage divide is present to the east and the north of the site in the form of the Nuweveld Mountains. The Gamka and Kuils rivers bound the central part of the town on its western and eastern sides with both rivers joining at a confluence to south of the town. These non-perennial rivers are seen as major recharge zones during the rainy season. The majority of the rainfall in the Beaufort West area takes place in the form of thunderstorms which are characterised by heavy rainfall over a fairly short period. Surface flow within the river usually takes place after heavy thunderstorms have occurred in the river's catchment areas to the north. A characteristic of many Karoo non-perennial rivers is that when the rivers do flow, a large amount of water moves down the river in short space of time in a flood like fashion.

On a regional scale, groundwater is expected to flow in a southerly direction from the Nuweveld mountains in the north. Recent work done by GEOSS on the town well field to the north of the town has identified that two aquifer systems are present in the area: A shallow aquifer system which is recharged by rainfall on the Nuweveld Mountains, and a deeper regional aquifer system which flows beneath and consists predominantly of connate groundwater (Rose and Conrad, 2008). The large inclined dolerite sill which runs through the town of Beaufort West has been interpreted to be a partial barrier to the southerly regional flow, as isotopic compositions of groundwater from springs along the northern side of the dyke indicate that the deeper regional waters are being forced upwards along the dyke and the springs are manifestations of the regional discharge points (Rose and Conrad, 2008). This has implications for the study area which is to south of the sill with regards to whether or not the area to the south of the dyke is influenced by the southerly regional flow direction which manifests on the north side of the dyke. Isotope data (Rose and Conrad, 2008) from boreholes directly to the south of the sill indicate that some mixing of deeper regional waters and recently recharged water is occurring and this would support the notion that the sill is only a partial barrier to flow, with leakage across the sill occurring. From a purely topographical perspective the regional flow on the south side of the dyke would also be in a southerly direction.

As mentioned previously the hydrogeological investigation carried out by Campbell in the 1970's drilled over 500 boreholes in the Beaufort West area and found the first 30m of the stratigraphic profile to be highly weathered with a large amount of fracturing and jointing occurring in this depth range. The drilling observations found that most of the water strikes (interception of water bearing fractures) occurred between 10m and 30m (the weathered zone) with the strongest yielding fractures in this zone occurring from 25m to 30m. The highest yielding boreholes were found in the depth range 45m to 70m with the strongest fractures being found between 55m to 60m (Campbell, 1980). The implication of this is that many fractures are present within the first 30m, but the strongest fractures are present at deeper levels. Several deep (>200m), high yielding wells have been drilled in the well field north of Beaufort West where the boreholes are observed to have punctured the Teekloof formation and gone into the Abrahamskraal formation. These wells were inferred to have punctured the confined aquifers within the channel sandstone units in the Abrahamskraal formation, which are considered to be the most water bearing of all sedimentary facies in the south western Karoo (Campbell, 1980). The weathered zone of the aquifer is interpreted to be unconfined whilst the unweathered, deeper levels are considered to be semi-confined (Botha et al, 1998). Pump tests data from Campbell (1980) indicated that extensive pumping of the semi-confined aquifer (below 30m) induced leakage or draining from the shallower, unconfined weathered zone aquifer into the deeper semi-confined zone and would suggest that the vertical jointing observed does allow for the inter-formational movement of groundwater from shallower to intermediate levels, but most likely not to the extremely deep levels (>100m) (Campbell, 1980).

Groundwater usage in the town is widespread and the volumes abstracted are significant however this will be discussed in more detail in Section 4. Groundwater levels in town are usually found between 7 and 12 meters below ground surface with most boreholes extended to a depth of between 50m and 60m (which is consistent with the high yielding fractures zones noted by Campbell). Significant seasonal fluctuation has been observed over the years, with the water levels reacting fairly quickly to recharge events. The past summer has been fairly dry with less than normal rainfall reported. In general groundwater levels have also dropped significantly for those holes where it has been tracked.



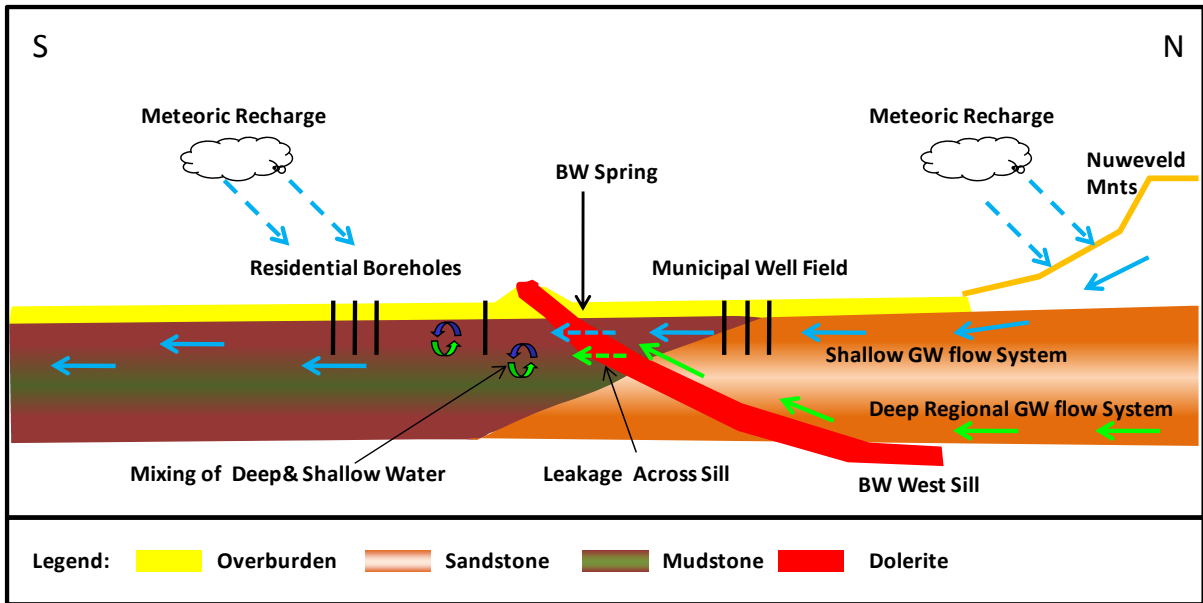
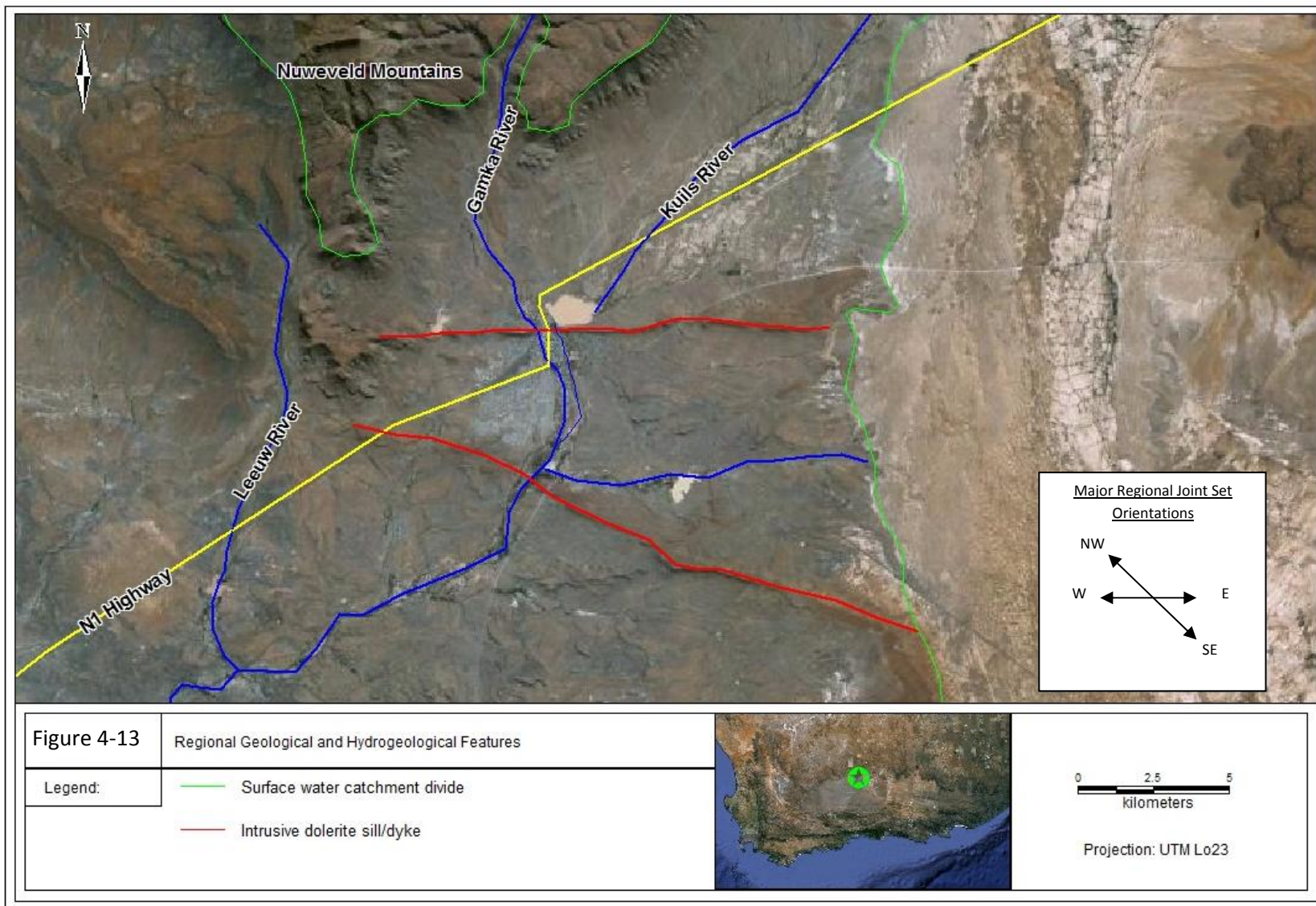


Figure 4-12: Regional conceptual model for the Study Area. (Figure adapted from Rose and Conrad, 2008)

Figure 4-13 Regional geological and hydrogeological features



## **5 Summary of Work Done to Date**

Whilst much investigative work has been done in the Beaufort West area since the 1940's as detailed in Section 2, several investigations have been conducted in the recent past by various consultancies under the employ of the oil industry. In addition to this, the WRC funded LNAPL Project was conducted during the same period in which this project's fieldwork was being conducted at the study area and a certain amount of overlap and information transfer has occurred between the author and the IGS team involved in the LNAPL project. What follows is a brief historical overview of the various contaminant investigations conducted in the study area, followed by a summary of the more salient points of LNAPL project as it pertains to this project and the construction and refinement of the site conceptual model. Figure 5-4 located at the end of this chapter displays the relevant boreholes mentioned the following paragraphs.

### ***5.1 Historical Overview***

Below follows a discussion on the history of fuel storage in Beaufort West. Most of this information was gathered during conversations with locals and much of it has not been verified. As far as possible the certainty in dates and statements has been indicated in the discussion.

The current fuel dispensing stations within the town of Beaufort West have all been present since the 1960's (approximately). Some sites in the main road have been closed for quite some time and these are not included in this discussion. The BKB filling station has been present since the late 1960's when the site acted as a fuel depot. Some tanks were apparently removed in 1976 but it is not known how many were removed (Burgers & Rosewarne, 2009). Marren Motors has been present since approximately 1954. The tanks were most likely replaced in the 1970's although this cannot be confirmed, and another tank was installed in 1986. All pipelines and fillers were replaced at Marren Motors in 1990's but the tanks have been on site since the abovementioned approximate dates. Beaufort West Service Station has been present since at least since the early 1980's however the site was revamped in 2001. Donkin Motors has been present since the 1960's. A revamp of the site occurred in 2002. It is not known what the age of the underground tank (paraffin) at Gordon's Camp and Gas is.

Further away from the affected area are several other potential sources. There is a decommissioned Engen station to the north along the main road as well as an Engen and Caltex at the circle on the northern side of the town to the north of the Beaufort West sill. A large abandoned fuel depot is present on the south west border of the town and according to local residents it functioned as a strategic fuel reserve and was operated by Total, although this is unconfirmed at present. The depot was decommissioned in the 1970's and upon visiting the site it was found to be totally abandoned. In the industrial area also to the south west of the town there are at least two other underground installations; one at the municipal depot and another at the railway yard. Further away south westwards at the edge of the town there are several truck stop sites.

Local resident knowledge in the town of Beaufort West indicates that groundwater contamination has been known to be present for approximately two decades, with local residents first allegedly discovering free phase LNAPL in a borehole of the NG Church residence in Bird Street (PW2) in the late 1980's at which time a leak was apparently discovered at Donkin Motors. In 2002, a leak was reported at Donkin Motors after residents at the NG Church residence again reported free phase LNAPL in the borehole. Further investigation found the LNAPL plume to have affected several other residents to the north east of Donkin Motors. In response to this, a pump and treat system was put in place at Donkin Motors (along with a Monitored Natural Attenuation monitoring program) and was seen to be containing the plume until April 2008 at which point the contaminant plume seemed to be expanding. Analytical data from the sampling runs suggested that multiple sources may have been present due to the variation in dissolved phase compositions observed in the newly affected areas when compared to those known to have been affected by the leak at Donkin Motors in 2002 (See Figure 5-3).

A hydrogeological contamination investigation was carried out at Marren Motors in February 2007 and the results indicated that dissolved phase BTEX compounds were present in the groundwater beneath the site and at least one well on the site has free phase LNAPL present to date. Some wells were too shallow and although free phase was present, the water level dropped below the bottom of the holes. The Institute for Groundwater Studies began conducting a hydrogeological investigation in Beaufort West in September 2008 and this forms part of the WRC funded "LNAPL Project" being conducted by the IGS at present. The IGS conducted a core drilling program in October 2008, with an additional core hole being drilled at Donkin Motors during this time. During this field visit, nearly 5m of LNAPL was observed in a private well at Young's Restrooms in Donkin Street (PW12). The IGS conducted further core drilling and percussion drilling in November 2008 and during this time the LNAPL thickness in PW12 was observed to have increased to 6m.

In February 2009, a groundwater contamination investigation was carried out at the BKB and found low levels of dissolved phase BTEX and GRO compounds present in the groundwater beneath the site. Further drilling was also carried out at Marren Motors and a free phase LNAPL plume was found to be present. During the same time a groundwater contamination investigation was carried out at Beaufort West Service Station with field and analytical observations indicating that a free phase LNAPL plume and an associated dissolved phase plume were present underneath the site. Whilst drilling at Beaufort West Service Station another private borehole directly to the south of the site was identified (PW49) with approximately 2.4m of free phase LNAPL present. The LNAPL thickness in PW12 was observed to have increased to in excess of 7m during this time.

## **5.2 WRC LNAPL Project**

Significant work has been conducted under the auspices of the IGS in the Beaufort West area over the last 18 months. This work has formed part of the Water Research Commission LNAPL Project which has several overarching objectives ranging from the evaluation of site assessment techniques for plume delineation, to the development of reliable predictions for the fate and transport of LNAPL within South African flow systems, to the development of appropriate guidelines for the remediation of LNAPLs within a South African context. The majority of the fieldwork was carried from October 2008 through to February 2009, with the findings being published in the LNAPL project document Deliverable 3: Initial Field Results, and unpublished MSc Theses (Gomo, 2009). The following sections provide a brief summary of the work conducted by the IGS, and are provided to substantiate the final conceptual model.

### **5.2.1 Drilling**

Intrusive investigations were carried out by the IGS in two separate site visits to Beaufort West with first visit being in October 2008, where MW4 was installed by core drilling, whilst the second site visit occurred in February 2009 where monitoring wells MW6 and MW8 were installed by core drilling whilst MW5 and MW7 were installed by percussion drilling. MW5 was drilled 4m away from MW6, whilst MW7 was drilled approximately 4m away from MW8. In addition to performing tracer tests and point dilution tests between the two sets of wells (MW5 & MW6 and MW7 & MW8), the

core holes and percussion holes were drilled next to each other in order to compare the variations in geological description and fracture positions/water strike locations. MW4 which was drilled in Bird St between PW2 and PW5 was found to have a fracture zone between 13m to 18.5m below ground level. MW5 intersected a significant water strike at 29m-30m depth whilst the core log of MW6 confirmed the fracture zone in at this depth interval. MW7 encountered a water strike at a depth of 28m but the core from MW8 did not encounter a fracture at 28m. This would suggest that the bedding plane fractures are laterally discontinuous. There was a generally poor correlation between the core logs and the percussion drill cuttings and considering that the geology would not be expected to vary significantly over a distance of four meters, would suggest that the method of drilling significantly affects the description of the geological profile.

## **5.2.2 Borehole Geophysics**

Several geophysical investigative techniques were employed by the IGS during the LNAPL investigation. These included ambient flow EC profiling and downhole geophysical tools such as Acoustic Televiewer (AV), Fill Wave Sonic (FWS), Gamma Logging, Resistivity (Res) and Spontaneous Potential (SP). Whilst EC profiling has been employed within this thesis project, and will be elaborated upon in further sections, it is not the scope of this study to discuss the technical details of the downhole geophysics methods but rather to provide a summary of the more pertinent findings of the aforementioned methods. For further clarity regarding these methods the author refers the reader to the original study documentation (Field investigations to study the fate and transport of light non-aqueous phase liquids (LNAPLs) in groundwater: Deliverable 3: Initial Field Results)

### **5.2.2.1 EC Profiling**

Ambient flow electrical conductivity profiling was conducted on PW2, PW5, MW5, MW6, MW7 and MW8. Flow zones were identified within PW2 and PW5 at approximately 23m-24m below ground level. In MW5 a flow zone was observed at 29m, which is agreeable with the drilling observations which encountered a water strike at approximately 29m. In MW6 a flow zone was encountered in MW6 at 30m which is agreeable with the observations of the core log which identified a fracture zone at this depth. MW7 and MW8 were both found to have flow zones at approximately 24m and 34m below ground level.

### 5.2.2.2 Combined Downhole Geophysics

The geophysical toolkit was conducted on MW5, MW7 and MW8. With reference to MW5, both the gamma and resistivity tools detected a significant change of geology from a mudstone to sandstone at approximately 19m whilst the FWS and AV detected the presence of a bedding plane fracture at this depth. The FWS and Gamma tools detected a fracture at 30m and this is consistent with the water strike which was encountered at this approximate depth. With reference to MW7, FWS and AV detected bedding plane fractures at 15m, 24.5m and 34m whilst the gamma tool detected a change in geology from mudstone to sandstones at 24.5m. This corresponds well with the EC profiling which was conducted on the well. Finally with reference to MW8, the FWS and AV detected the 24.5m fracture observed in MW7 and this was agreeable with EC profiling conducted on MW8

**Table 5-1 Significant depth intervals in IGS wells where flow zones were identified and the method of identification.**

Depth	MW4	MW5	MW6	MW7	MW8
13m - 18m	Core Log			FWS, AV (15m)	
19m		Gamma, FWS, AV			
24m				EC, FWS, AV, Gamma	EC, FWS, AV
28m				Water Strike	
29m-30m		Water Strike, EC, FWS	Core Log, EC		
34m				FWS, AV, EC	

From this table it can be seen that no one single method was successful in describing all potential flow zones, and that the strength of the toolbox approach is displayed in that various methods will detect particular flow zones dependant on the conditions within the well.

### **5.2.3 Aquifer Parameter Estimation**

Several aquifer parameter estimation exercises were carried out by IGS between October 2008 and February 2009. These included constant discharge pump tests, point dilution tests, radial convergent tests and tracer tests.

#### **5.2.3.1 Constant Discharge Pump Tests**

During October 2008, a constant discharge test was carried out on RW1 with RW2, PW2 and PW5 serving as observation wells. The test was run for approximately 8 hours at an abstraction rate of 0.78l/s. Drawdown responses were observed in all three observation wells and a transmissivity of 3.5m<sup>2</sup>/day was calculated using the Flow Characteristic Method (Van Tonder et. al, 1998). RPTSOLV (Verwy, 1996) was used to provide an alternative value and yielded a T value of 5.8m<sup>2</sup>/day, with a matrix storativity value of 3x10<sup>-4</sup>. Drawdown response lag times of approximately 70 minutes and 120 minutes were observed in RW2 and PW2 respectively. Drawdown derivative plots indicated that a potential recharge boundary may have been reached during late time pumping stages and the presence of the Gamka River (160m to the west) and Kuils River (560m to the east) was alluded to as potential recharge boundaries.

The second constant discharge test was carried out on RW2 as part of a previous MSc Thesis (Gomo, 2009) with RW2 being pumped at a constant rate of 0.78l/s and PW2, PW5 and PW12 being used as observation wells. Using RPTSOLV, a transmissivity of 5.8m<sup>2</sup>/day was calculated for RW2. A third pump test was carried out in the core hole MW8, with the nearby MW7 being used as an observation well. The FC Programme was used to fit the drawdown data and a transmissivity of 15.4m<sup>2</sup> was calculated.

#### **5.2.3.2 Tracer Tests**

Several tracer tests were conducted during the IGS study however the majority of the tests did not yield an acceptable quality of data due to field related constraints. One successful tracer experiment was conducted between MW8 and MW7. The tracers (chloride and bromide tracers were used) were injected at a depth of 24m in MW7 whilst the pump was placed at a depth of 34m in MW8. This depth



corresponds to the inferred flow zones as identified by the EC profiling, although it is of importance to note that the combined geophysical tools did not detect the 34m flow zone in MW8, whilst the 24.5m flow zone was identified in both holes. The test was performed at an abstraction rate of 0.08l/s and an average seepage velocity of 23m/day was calculated from the test, with an effective porosity of 0.02 and a dispersion factor of 0.6m.

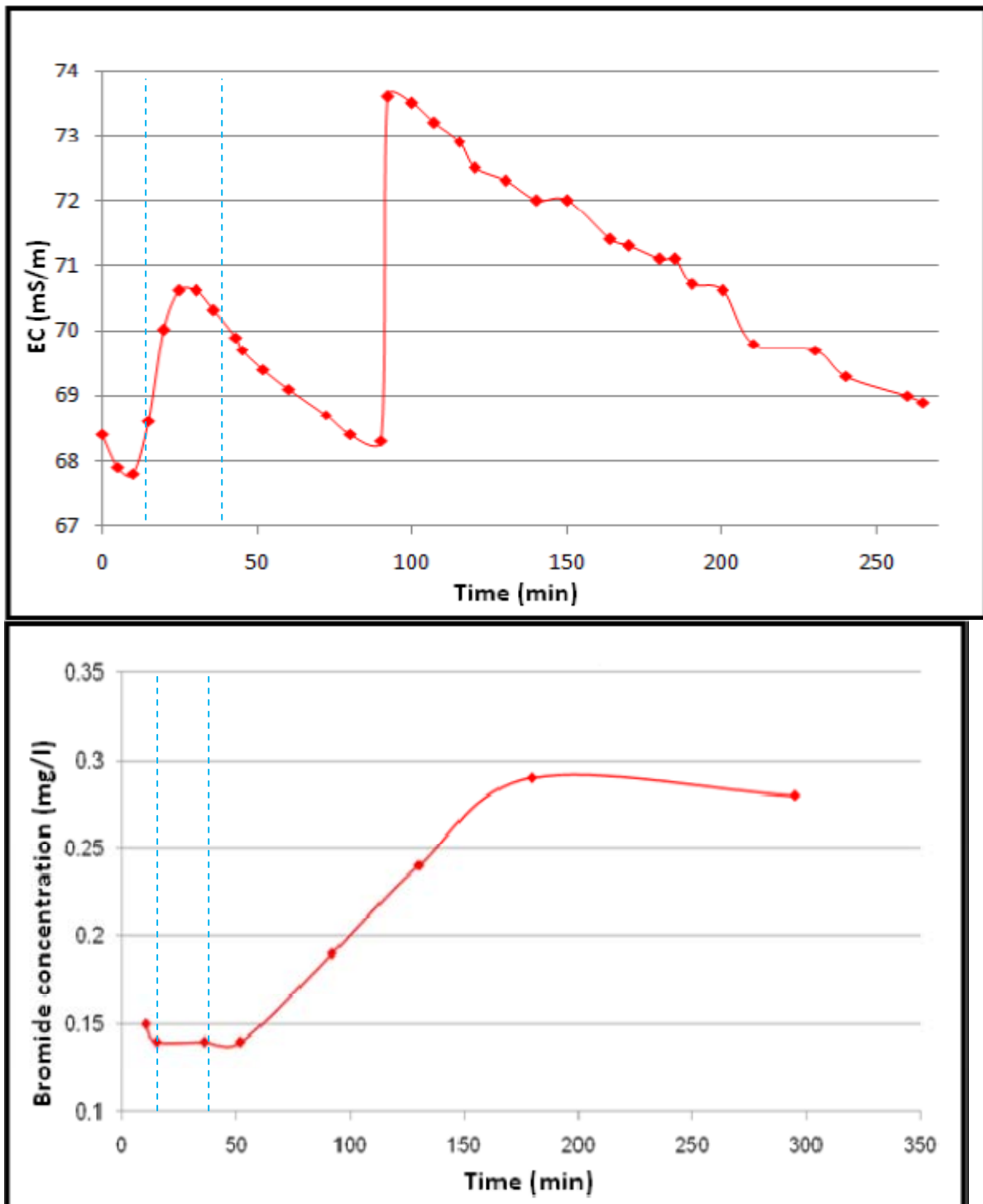


Figure 5-1 EC tracer breakthrough measurements the abstraction/observation hole MW8 (From Gomo, 2009)

The seepage velocity is regarded to be high in the context of a double porosity fractured rock aquifer and is interpreted to be due to preferential fracture/flow zones such as those identified at 24.5m, and not due to matrix flow. The double peak in the EC data was interpreted to be due to two fracture zones being present, with the 34m zone at the injection and pump depth, and the possibly more developed (based on combined the geophysics data) fracture zones at 24.5m. Two observations have been made by the author with regards to the tracer test data, firstly the absence of the first peak in the bromide measurements could be a function of the sampling frequency since the EC peak occurred predominantly over a period (indicated between the blue dotted lines) when no bromide sample was collected. Secondly, considering that the larger, delayed second EC peak may be related to tracer mass moving via the 24.5m fracture, 10m above the injection and abstraction points (as suggested in by Gomo), the calculated velocities (using the bromide tracer) may be an underestimation since the calculated velocities were based on a transport length of 4.7m, and did not take into account the potential vertical intra well transport which may have occurred along the tracer path.

**Table 5-2 Selected aquifer parameter values from the Beaufort West study area (Gomo, 2009)**

<b>Parameter</b>	<b>Unit</b>	<b>Value</b>	<b>Method</b>
Transmissivity (RW1)	m <sup>2</sup> /day	3.5	FC Programme (Cooper Jacob)
Transmissivity (RW1)	m <sup>2</sup> /day	5.8	RPTSOLV
Transmissivity (RW2)	m <sup>2</sup> /day	5.8	RPTSOLV
Transmissivity (MW8)	m <sup>2</sup> /day	15.4	FC Programme (Cooper Jacob)
Storativity	-	3x10 <sup>-4</sup>	RPTSOLV
Effective Porosity n <sub>eff</sub>	-	0.02	TRACER
Seepage Velocity v	m/day	23	TRACER
Dispersion	-	0.6	TRACER

## **5.2.4 Hydro-geochemical Characterisation**

Selected wells were sampled by the IGS during the October 2008 site visit. Whilst forthcoming sections of this thesis will discuss hydro-geochemical characterisation, the following paragraphs provide a brief summary of the additional information which the IGS field work added to the overall body of data already present at the end of 2008.

#### **5.2.4.1 Organic sampling**

Sampling for hydrocarbon related dissolved phase compounds such as BTEXN, TAME, MTBE, GRO (C<sub>6</sub>-C<sub>10</sub>) and DRO (C<sub>10</sub>-C<sub>40</sub>) was conducted within the network of wells that was being monitored by GPT with only MS02 and PW35 being new wells which had not been sampled before. The sample results of the existing network yielded concentrations which were consistent with previous monitoring data. MS02 yielded trace concentrations of benzene (48µg/l) and MTBE (6.7µg/l) whilst PW35 showed trace amounts of benzene (40 µg/l), toluene (2.5µg/l) and xylenes (13µg/l). MS02 is approximately 400m to the north east of the nearest source zones and these results indicated two important points. Firstly that the plume extent was much greater than originally thought, and secondly, that the plume had crossed to eastern side the Kuils River, which was originally thought to be a recharge boundary / no flow boundary.

#### **5.2.4.2 Inorganic Sampling**

Selected wells identified during the IGS's hydrocensus were sampled for major cation/anion chemistry (Ca, Mg, K, Na, Cl, HCO<sub>3</sub>, SO<sub>4</sub>) and were plotted on Piper Diagrams along with data previously obtained during biannual monitoring by GPT. The significant majority of the wells indicated a (C+Mg)-(Na+K)-(CO<sub>3</sub>+HCO<sub>3</sub>) chemistry, which evolved along two primary lines, one moving from Ca/Mg towards Na<sup>+</sup> and the other moving from CO<sub>3</sub>/HCO<sub>3</sub> towards SO<sub>4</sub>. An exception to this was MS01 which was found to have a more chloride dominated composition and was interpreted to represent older water which may be sourced from the deeper underlying regional aquifer system. Two key observations yielded from the sampling are the presence of Ca and HCO<sub>3</sub> suggest the presence of plagioclase weathering by recently recharged waters viz. the upper aquifer receives direct recharge and, the ranging sodium concentrations are attributed to cation exchange with calcium and magnesium ion on exchange sites, most likely on clay particles within shale/mudstone horizons within the aquifer system.

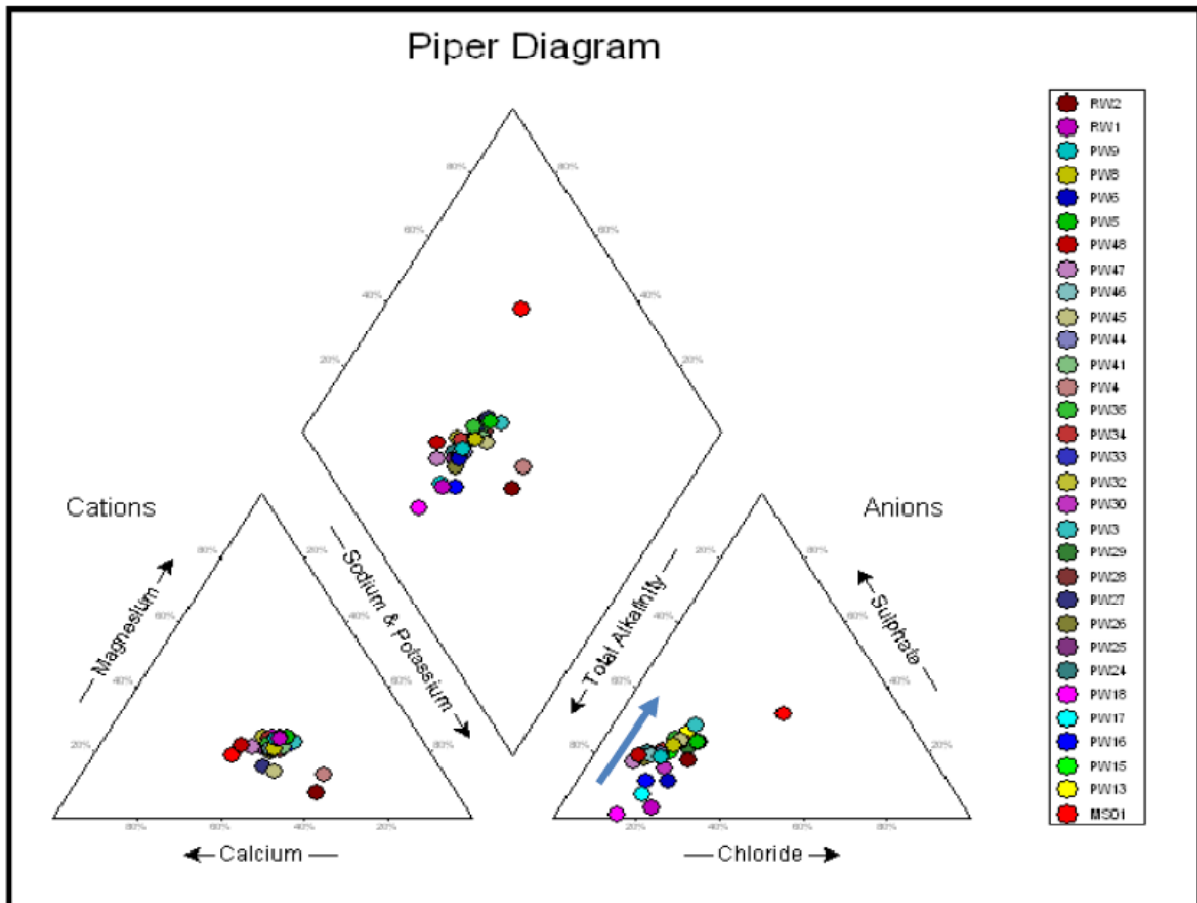


Figure 5-2 Piper Diagram of IGS sampled wells along with wells sampled by GPT in 2009 (from Gomo, 2009)

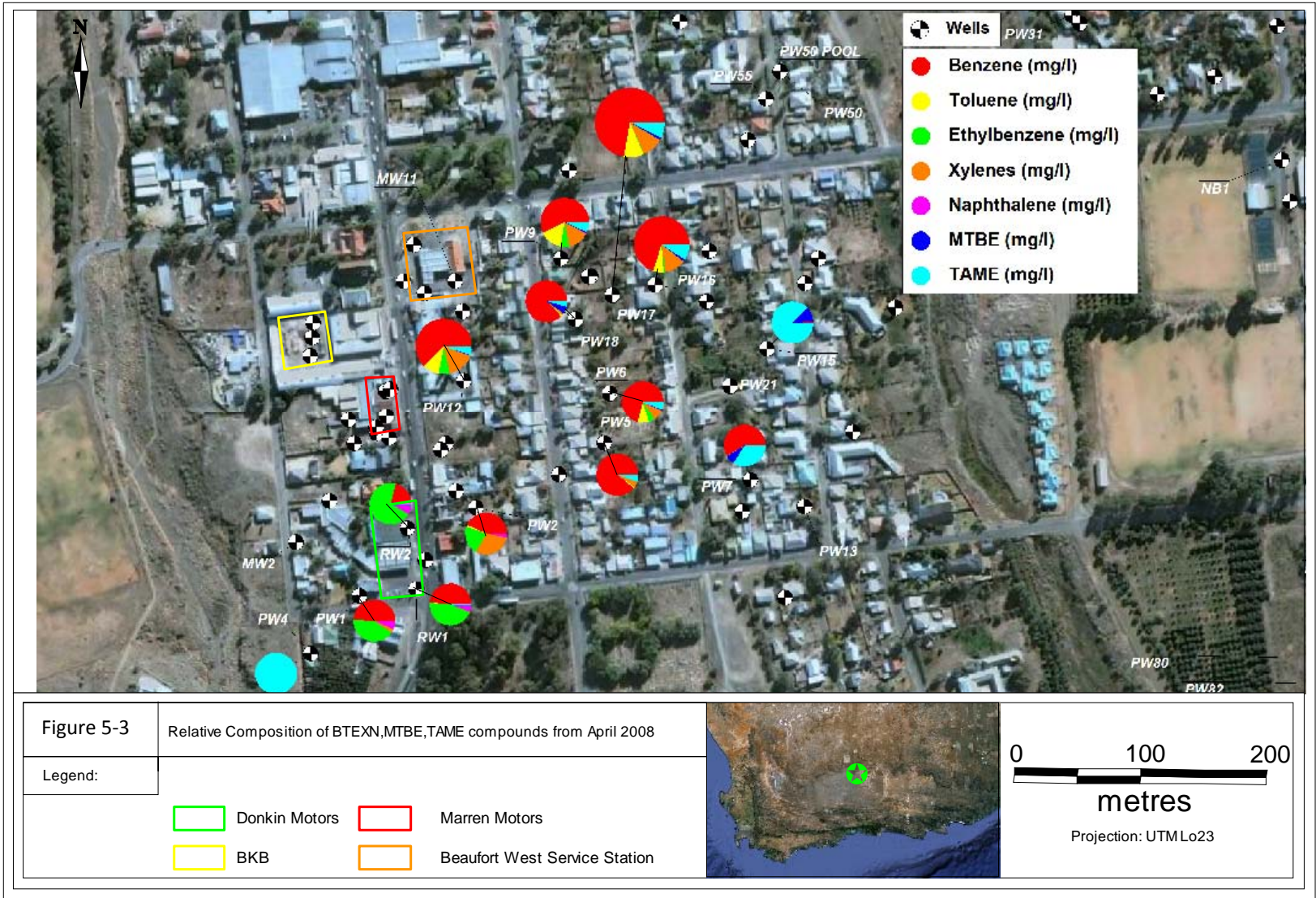


Figure 5-3 Dissolved phase compositions from the April 2008 sampling event depicting the differing dissolved phase compositions across the study area





Figure 5-4 Locations of boreholes/monitoring wells investigated during the activities described in Section 5.

## 6 Hydrocensus

The greater Karoo region and Beaufort West in particular are water scarce areas. The result being that a heavy reliance on groundwater resources is prevalent within the study area. Given this groundwater reliance, groundwater users are the key receptors with regards to potential groundwater contamination and as such, the quantification and verification of groundwater use within the study area is of key importance in understanding the nature and magnitude of any impact on the groundwater resource, as well as in understanding the nature and behaviour of contaminant migration within the aquifer.

Previous hydrocensus work carried out by private consultancies in the past had identified a significant amount of private groundwater users in the residential area to the east of Donkin Street and to the south of Voortrekker Street. In October 2008 the IGS expanded the hydrocensus and identified several new private boreholes to the north of Voortrekker Street in Bird Street, De Villiers Street and Brand Street however it was noted at the time that more boreholes could be present at properties where nobody was present at the time of the IGS's hydrocensus. The hydrocensus carried out as part of this study therefore attempted to complete the data set during the fieldwork phase carried out between the 16<sup>th</sup> and 19<sup>th</sup> of March 2008. The results are represented visually in Figure 6-3.

A second sweep of Brand Street, De Villiers Street and Bird Street identified several new boreholes in the area to the north of Voortrekker Street. Municipal plans were used to indicate which properties had boreholes, which properties did not have boreholes and which properties were unconfirmed due to nobody being present to verify if a borehole was present. The hydrocensus was generally conducted in the early morning, later afternoon and early evening when the likelihood of residents being at home was greatest. In addition to this, the hydrocensus was extended to the residential area to the east of the Kuils River and to the north of Nico Brummer primary school, with several boreholes from this area added to the current data set. In December 2009 a differential GPS survey was conducted which surveyed all known boreholes with regards to their x,y,z co-ordinates (lat, long, m amsl). This was done so that accurate height and position data could be available in order to survey water levels and fracture depths as will be discussed in Section 7.

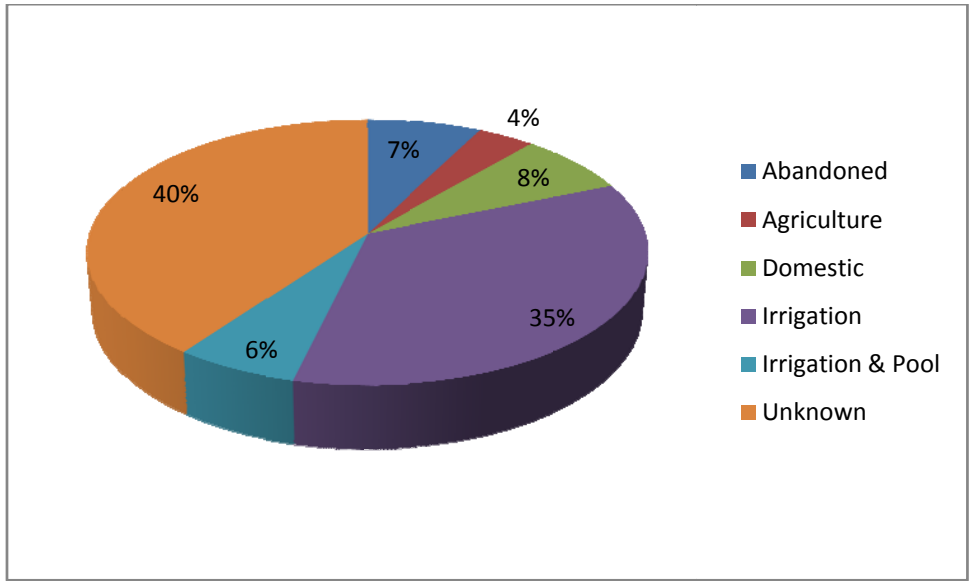


**Figure 6-1 Pie chart breakdown of boreholes identified in hydrocensus**

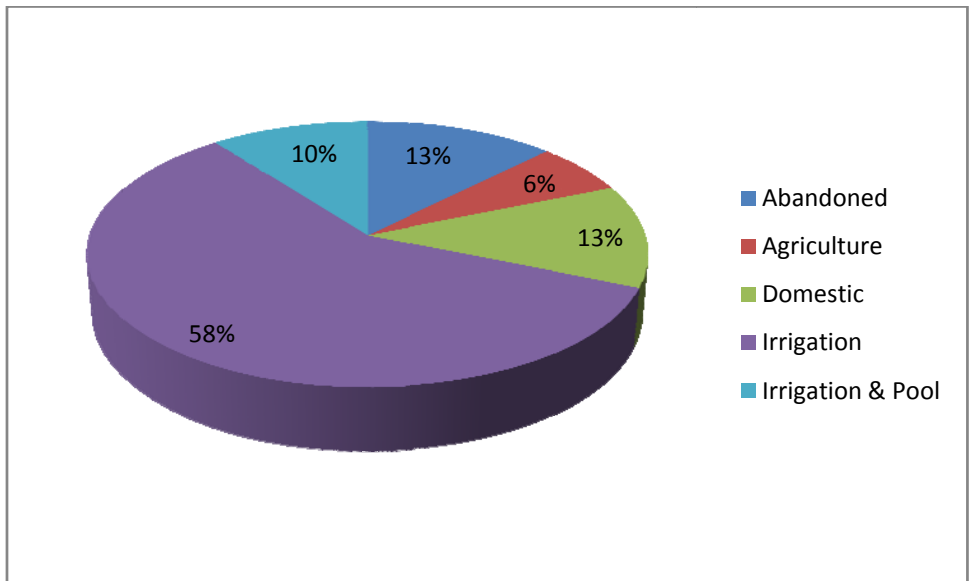


**Figure 6-2 Groundwater usage breakdown for the subset of private wells where groundwater use is known**

The combined results of all hydrocensus data to date are contained in Appendix A, whilst a summary of the results is contained in Table 6-1 and are displayed in Figure 6-1 and Figure 6-2. From this data it can be seen that the usage for 40% of the known boreholes (especially in the north of the town) is unknown. The unknown portion generally constitutes three types of unknowns. Firstly, properties which could be identified as having a borehole, but nobody was present to supply information. Secondly, properties where the residents would confirm the presence of a borehole, but were not



willing to supply any other information regarding the borehole and thirdly, where information was sourced from previous hydrocensus studies carried out where no information was available regarding borehole use. Figure 6-3 at the end of the chapter depicts the locations and uses of the known boreholes in the study area. Figure 6-2 indicates that of the boreholes where the groundwater use is known, close to 60% of groundwater users irrigate their gardens, followed by abandoned wells (13%). Wells used for domestic and drinking water purposes made up approximately 13% of the overall data set followed by those who irrigate but also top up their swimming pools (10%). Only a small percentage of groundwater users (6%) use the water for agricultural purposes such as irrigation of vegetables / orchards and this portion also includes the primary and high schools' irrigation of their olive groves. Domestic groundwater users generally only use the groundwater for domestic use occasionally, as all properties do have municipal supplied drinking water. Usage varies from property to property, but during the dry season most residents will pump their boreholes on daily basis for approximately one to two hours, generally in the early morning or in the evening. In the wet season the usage drops to an average of one or two pumping events a week. In conversation with the residents and by general observation, the average pumping rate of boreholes appears to be in the region of 0.75-1 l/s. Based upon these figures, the daily total abstraction within the study area (excluding the school's boreholes) is estimated to be between 300m<sup>3</sup> and 400m<sup>3</sup> per day in the dry season, and between 40m<sup>3</sup> and 60m<sup>3</sup> per day during the wet season. This is based on an assumption that 75% of the boreholes will be in use any given day.

**Table 6-1 Summary of Borehole Usage in the Study Area**

Borehole Usage in Beaufort West Study Area		
Use	Number of Wells	Percentage
Abandoned	6	8%
Agriculture	3	4%
Domestic	6	8%
Irrigation	28	35%
Irrigation & Pool	5	6%
Unknown	32	40%
Total	80	

The primary and high schools are by far the largest groundwater users in the central part of the town, with the combined water usage during the dry season of both schools being calculated to be in the region of 500m<sup>3</sup> per day. In the dry season, it is therefore plausible that a total approaching 900m<sup>3</sup> per day is being abstracted from the aquifer within the study area.

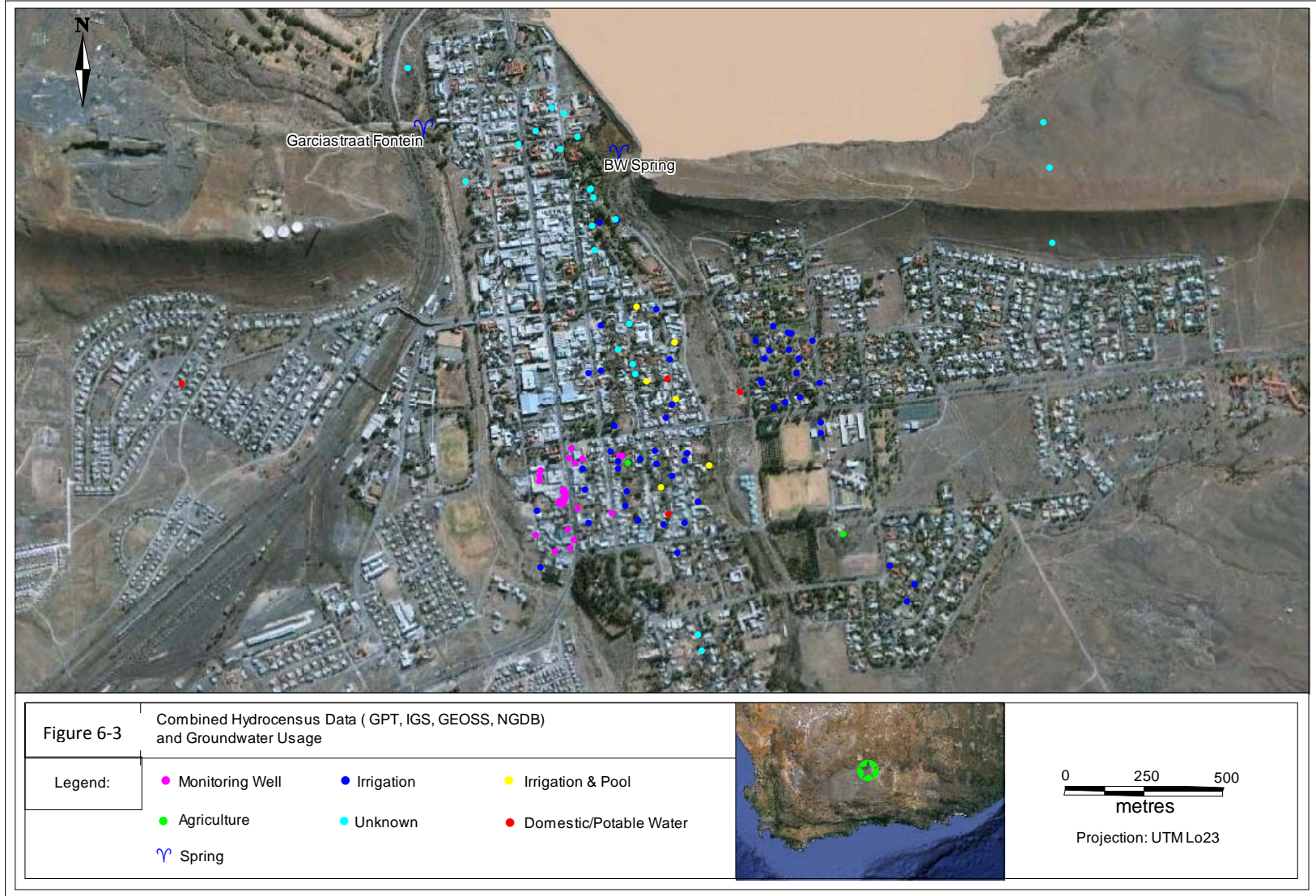


Figure 6-3 Orthophoto displaying all hydrocensus wells and their uses across the study area

## **7 Physical Characterisation**

Desktop studies, literature surveys and walkover hydrocensus surveys assist in providing the broad set of constraints within which a hydrogeological investigation takes place and provide the foundation of the conceptual understanding of a site. Physical characterisation forms the next level on which the conceptual model of the site is built upon and care must be taken to ensure that the scale and scope of the physical characterisation is consistent with the scale and objectives of the investigation. For example, it would not be effective or practical to conduct a detailed fracture mapping exercise over a site that is tens or hundreds of square kilometres in size, nor would it be advisable to generalise the physical properties of a small area on regional data such as joint orientation or regional groundwater flow. Thus it is imperative that the level of characterisation match the scale of the investigation. In the current study, the area under investigation is small to moderate, being approximately 500m by 500m in size. In addition to this, multiple source zones and a high number of groundwater users are present in the area. As a result the level of characterisation in certain areas was relatively detailed and involved a combination of intrusive investigations and downhole investigative techniques to provide information on the physical nature of the aquifer with regards to the distribution, frequency and orientation of potential fracture networks. The aim of the physical characterisation was to gain a better understanding of the nature of the preferential flow paths along which contaminants may migrate along within the aquifer.

### ***7.1 Intrusive Investigations***

Intrusive investigation by means of drilling is one of the dominant methods by which site characterisation is carried out as it provides the figurative “keyhole” through which the subsurface environment is characterised and quantified in its various forms. A common drawback of most fractured rock contamination investigations in South Africa is that percussion drilling is commonly the only drilling method employed. This is often done due to cost effectiveness and the primary aim of the drilling operation often being to simply install a monitoring well network to assess groundwater quality on the site in question. The drawback of this approach is that valuable structural and geological information is often lost from the site characterisation process since the drill cuttings are the only geological output of the process. The method and very nature of rotary air percussion drilling introduces a significant level of uncertainty in determining the location of a cutting sample’s provenance in the

subsurface due to factors such as drill cutting bridging in the well annulus and washout in weathered zones. Factors such as the field staff's experience and geological knowledge can add significantly to variations within the descriptions of the drill logs. Core drilling provides the opportunity to detail the subsurface environment at a much greater level of detail since physical rock cores can be removed and inspected in detail during or after drilling. Core drilling can provide information on fracture positions and the nature and orientations (when coupled with downhole geophysical techniques) of fractures at varying scales. Whilst percussion drilling can identify major flow zones by means of water strikes, the ability to detect small scale flow pathways by core drilling is a significant advantage since the most highly transmissive zones do not necessarily equate to the zones of greatest contamination. Neither of the drilling methods provide suitable sample media on which volatile organic carbon (VOC) vapour readings can be measured, and this screening technique is often forgone in these instances. Whilst on site VOC screening may not be possible, the coring technique does provide sample material to conduct laboratory analysis for hydrocarbon compounds by means of crushing the core, and performing a solvent extraction analysis on the material. Extensive intrusive drilling work has been done in the study area over the last 2 years by various parties and is depicted in Figure 7-1.

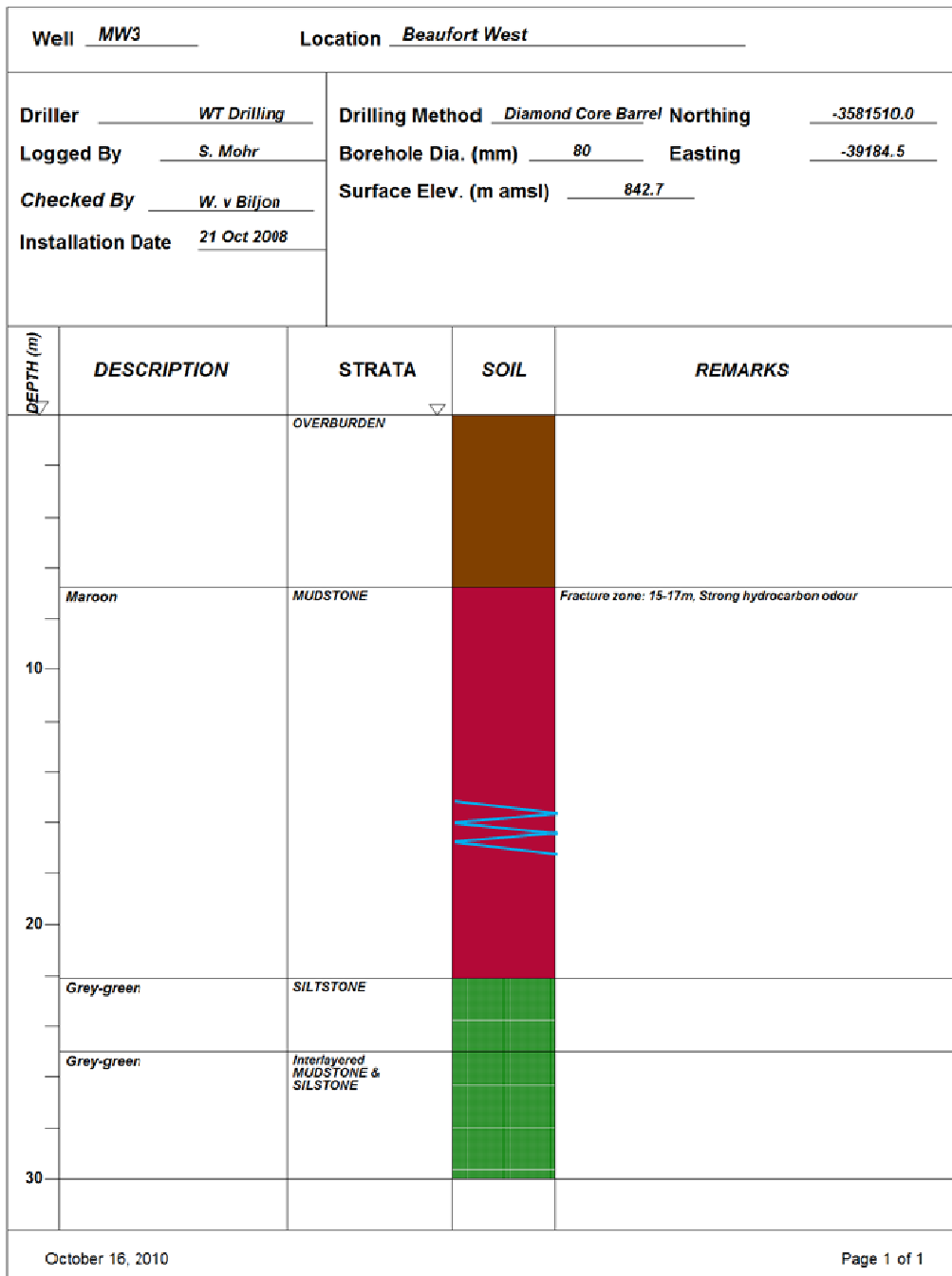




Figure 7-1 Monitoring wells installed during the various groundwater investigations which have taken place over the years

### **7.1.1 Core Drilling**

In addition to the core drilling done during the LNAPL study, one core hole was drilled at Donkin Motors (MW3) in October 2008 and was positioned approximately mid way between RW1 and RW2 whilst a second core hole, MW10 was installed at Beaufort West Service Station during monitoring well installation activities at the latter site in February 2009. The core drilling was carried out by WT Drilling of Beaufort West with a 6 inch barrel being used to penetrate the overburden layers. Once bedrock was reached a steel casing was inserted down to bedrock and coring was continued with a 4 inch core barrel. In both cases drilling was terminated at a depth of 30m. Drilling of MW3 indicated the geological profile to be dominated by overburden for the first 7.5m at which point maroon mudrock was present to a depth of 23m. This was underlain by a siltstone layer to a depth of 26m which in turn was underlain interlayered siltstone and mudstone to the well termination depth of 30m. A fracture zone was encountered at 15m depth with the removed core emitting a hydrocarbon odour at this depth. A weathered zone was encountered between 15m-17m below ground level. The degree of weathering in this zone was so great that the well collapsed at a depth of 17m the following day. The log of MW3 is depicted in Figure 7-2.



**Figure 7-2 Core log of MW3 drilled at Donkin Motors**

Drilling of MW10 at Beaufort West Service Station (approximately 400m to the north of MW3) yielded a generally similar pattern with a sandstone and dolerite boulder overburden being present to a depth of 7m at which point a weathered mudstone was present to a depth of 12.5m. Thinly interlayered beds of mudstone, silty sandstone and siltstone are present to a depth of 17m at which point slightly thicker layers (2m-4m thick) of siltstone, mudstone, silty sandstone and sandstone were present to the well termination depth of 32m. Of more

importance was the large amount of fractures, both horizontal and inclined, which were detected in the core. Sub-vertical fractures intersected the core log between 8m-10m below ground level and a 45° inclined fracture was observed at 17.6m below ground level. Major fracture zones were detected at 11.8m, 15m and 18m whilst additional horizontal fractures with apertures up to 2mm were found at 14.7m and 23m. A total of 38 fractures were observed between 7.6m and 24m with apertures ranging from less than 1mm to weathered zones which extended up to lengths of 20cm. The high frequency of fractures is agreeable with literature observations which suggest that the highest frequency of fractures is found within the weathered zone of the geological profile down to a depth of approximately 30m (Campbell, 1980). The core log description of MW10 is depicted in Figure 7-3



Well <u>MW10</u>		Location <u>Beaufort West</u>	
Driller <u>WT Drilling</u>		Drilling Method <u>Diamond Core Barrel Northing</u> <u>-3581263.4</u>	
Logged By <u>S. Mohr</u>		Borehole Dia. (mm) <u>80</u> Easting <u>-39179.9</u>	
Checked By <u>W. v Bijon</u>		Surface Elev. (m amsl) <u>343.5</u>	
Installation Date <u>15 Feb 2009</u>			

DEPTH (m)	DESCRIPTION	STRATA	SOIL	REMARKS
	Sandstone & Dolerite Boulders	OVERBURDEN		
	Maroon, weathered	MUDSTONE		Fractures: 1.68m, 7.36m, 8.35m
	Grey-green	SILTSTONE		Sub Vertical Fractures: 8.47-8.62m, 8.83-9.22m
10	Maroon	MUDSTONE		
	Grey-green	Silty SANDSTONE		Sub Vertical Fractures: 9.87 - 10.07m
	Maroon	MUDSTONE		Weathered Fracture Zone
	Maroon	MUDSTONE		Fractures 10.4m, 10.5m, 10.61m, 11.1m, 11.29 - 11.35m
	Grey-green	SILTSTONE		Fracture zone: 11.77 - 11.9m, 12.05m, Sub Vertical Fracture: 12.8 - 13.0m
	Grey-green	Silty SANDSTONE		
	Maroon	MUDSTONE		
	Grey-green	Silty SANDSTONE		Fractures: 13.4m
	Maroon	MUDSTONE		Fractures: 13.74m
	Grey-green	Silty SANDSTONE		
	Maroon	MUDSTONE		Fractures: 14.53m, 14.58m, 14.75m (2mm aperture), 14.87m
	Grey-green	SILTSTONE		Fracture Zone: 15.01-15.24m
	Grey-green	MUDSTONE		Fractures: 15.59m
	Maroon	Interlayered MUDSTONE & siltstone		Fractures: 16.4m
20	Grey-green	SILTSTONE		Fractures: 16.98m, 17.15m
	Maroon	MUDSTONE		Inclined 45 deg Fracture: 17.51m, Fracture zone: 18.00 - 18.08m, 18.18m, 18.1 - 18.36m
	Grey-green	Silty SANDSTONE		Fractures: 20.46m
	Maroon	MUDSTONE		Subvertical Fracture: 21.05-21.45m
				Fractures: 22.6m, 21.6m, 22m, 24.1m
	Grey-green	SANDSTONE		
	Grey-green	SILTSTONE		
30	Grey	Silty SANDSTONE		

October 16, 2010

Page 1 of 1

Figure 7-3 Core log of MW10 at Beaufort West Service Station

## 7.1.2 Percussion Drilling

Several percussion boreholes were drilled during the course of the most recent investigations with MW9, MW11 and MW12 being installed on Beaufort West Service Station. A further 3 wells were installed by SRK at the BKB and up to 9 wells were installed at Marren Motors by ERM, however information pertaining to these wells was not available. In conversation with the driller who installed the wells at BKB and Marren it was ascertained that no water strikes were intercepted in any of the borings down to 30m and that the wells were very low yielding. The scope of the current study includes data from Beaufort West Service Station, and Figure 7-4 to Figure 7-6 displays the logs of MW9, MW11 and MW12. In general the logs display less detail than that of the core logs however dominant lithologies are still readily discernable. An overburden layer of between 5-7m in thickness covers the site indicating that the bedrock topography may have a slight slope towards the south since MW9 which on the northern portion of the site had an overburden layer of 5m whereas MW11 and MW12 on the southern portion of the site had an overburden of 7m. Alternating layers of mudstone and siltstone were dominant in the geological profile although silty sandstones began to appear at depths beyond 20m below ground level. Water strikes were encountered in MW12 at 15m bgl and in MW9 and MW11 at approximately 20m bgl. These depths are agreeable with fracture zones identified in the core log of MW10. Whilst more fractures may be present in these holes as was observed in MW10, the above mentioned zones at 15m bgl and 20m bgl were the only points at which significant water strikes were encountered in the abovementioned percussion holes. The water strike at 15m bgl in MW12 accompanied a strong hydrocarbon odour and drill cuttings from this depth were observed to be coated in free phase LNAPL.

Well <u>MW9</u>		Location <u>Beaufort West</u>	
Driller <u>WT Drilling</u>	Drilling Method <u>Rotary Air Percussion</u>	Northing <u>-3581215.9</u>	
Logged By <u>W. v Bijon</u>	Borehole Dia. (mm) <u>165</u>	Easting <u>-39192.5</u>	
Checked By <u>S. Mohr</u>	Surface Elev. (m amsl) <u>843.5</u>		
Installation Date <u>15 Feb 2009</u>			

DEPTH (m)	DESCRIPTION	STRATA	SOIL	REMARKS
	Brown, medium-to-coarse sand, rounded pebbles	OVERBURDEN		
	Maroon	MUDSTONE		Moderately weathered
	Grey-green	SILTSTONE		Moderately weathered
	Maroon	MUDSTONE		
10	Grey-green	SILTSTONE		
	Maroon	MUDSTONE		
	Grey-green	SILTSTONE		Weathered fragments at 18m
20	Maroon	MUDSTONE		Water strike at 20m, hydrocarbon odour
	Grey-green	SILTSTONE		
	Maroon	MUDSTONE		
	Grey-green	SILTSTONE		
	Maroon	MUDSTONE		
30	Grey-green	SILTSTONE		

October 18, 2010 Page 1 of 1

Figure 7-4 Percussion Drill Log of MW9 at Beaufort West Service Station

Well <u>MW11</u>		Location <u>Beaufort West</u>	
Driller <u>WT Drilling</u>	Drilling Method <u>Rotary Air Percussion</u>	Northing <u>-3581253.0</u>	
Logged By <u>W. v Biljon</u>	Borehole Dia. (mm) <u>165</u>	Easting <u>-39155.3</u>	
Checked By <u>S. Mohr</u>	Surface Elev. (m amsl) <u>844.0</u>		
Installation Date <u>15 Feb 2009</u>			

DEPTH (m)	DESCRIPTION	STRATA	SOIL	REMARKS
	Brown silty sand & rounded pebbles	OVERBURDEN		
	Green	SILTSTONE		Moderately weathered
10	Maroon	MUDSTONE		
	Grey-green	SILTSTONE		
	Maroon	MUDSTONE		
	Grey-green	SILTSTONE		Water strike between 21-22m
20				
	Maroon	MUDSTONE		
30				

October 18, 2010 Page 1 of 1

Figure 7-5 Percussion Drill Log of MW11 at Beaufort West Service Station

Well <i>MW12</i>		Location <i>Beaufort West</i>		
Driller <i>WT Drilling</i>		Drilling Method <i>Rotary Air Percussion</i>		
Logged By <i>W. v Eiljon</i>		Northing <i>-3581248.3</i>		
Checked By <i>S. Mohr</i>		Borehole Dia. (mm) <i>165</i> Easting <i>-39198.1</i>		
Installation Date <i>15 Feb 2009</i>		Surface Elev. (m amsl) <i>843.4</i>		
DEPTH (m)	DESCRIPTION	STRATA	SOIL	REMARKS
	<i>Clayey sand with rounded pebbles</i>	<i>OVERBURDEN</i>		
	<i>Gray-green</i>	<i>SILTSTONE</i>		
	<i>Marocn</i>	<i>MUDSTONE</i>		<i>Weathered</i>
10	<i>Marocn</i>	<i>MUDSTONE</i>		
	<i>Grey-green</i>	<i>SILTSTONE</i>		<i>Strong hydrocarbon odour at 15m, NAPL in drill cuttings</i>
	<i>Marocn</i>	<i>MUDSTONE</i>		
20	<i>Grey-green</i>	<i>SILTSTONE</i>		
	<i>Marocn</i>	<i>MUDSTONE</i>		
30				
October 16, 2010		Page 1 of 1		

Figure 7-6 Percussion Drill of MW12 at Beaufort West Service Station

## ***7.2 Electrical Conductivity Profiling***

Down-hole electrical conductivity (EC) profiling was conducted on selected wells in the study area. EC profiling can provide insight into the location of flow zones in the well profile since sudden changes in EC values usually represent a change in the water chemistry which may be associated with a flow zone which has been reached and is altering the water chemistry at the specified depth relative to the water in the well bore above and below this depth. The flow zones are most commonly associated with fractures and as a result, a down-hole profile of the electrical conductivity can yield useful information regarding the vertical distribution of fractures in a borehole. It must be noted however that another instance where significant EC variations may be observed is where significant variations in geology occur with the resultant EC change being due to host rock – groundwater interaction.

In addition to this, studies have been conducted which have shown that electrical conductivities of groundwater can be significantly affected by microbial degradation of LNAPL, especially in more aged contamination cases where the process of aerobic degradation results in an increase in reduced species and an increase in the amount of dissolved ions, thereby increasing the EC (Cassidy et al 1998). Therefore, EC profiling can also be used as a down-hole tool to assess whether potentially contaminated fractures are present (usually represented by increases in EC from the ambient conditions). Whilst this does present a relatively inexpensive tool to characterise potentially contaminated flow horizons, the results must be supported by analytical groundwater data since differing (or elevated) EC values may also be a result of the intersection a separate fracture network with differing host rock – groundwater interaction regimes.



**Figure 7-7 Boreholes and monitoring wells which were used for ambient flow electrical conductivity (EC) profiling**

## 7.2.1 Ambient EC Profiling

Several wells have been installed as part of the current study and by the IGS in the recent past and as a result, geological information regarding lithology, water strikes and fractures was available to compare with the EC profiling completed during the site visits. Figure 7-7 displays the boreholes and monitoring wells which profiled by means of ambient flow electrical conductivity profiling. For reasons of conformity, the following sections will refer to the depths of fractures and flow zones in meters below ground level, followed by the elevation of the feature above a common datum (mean sea level) in parentheses. All figures represent the depths in meter above mean sea level in order to provide an easier vertical measurement scale for cross correlating fracture / flow zone depths across boreholes.

Figure 7-8 displays the logs of core hole MW3 (located at Donkin Motors), PW5 (which has been impacted since 2002) and the core hole MW4 which was drilled in Bird Street in a rough line between PW5 and MW3. MW3 was drilled in October 2008 and the log of MW3 indicates a bedding plane parallel fracture to be present at 15.3m bgl (828m amsl) followed by a fractured zone also being present to 17m bgl (826m amsl). The zone between 15m to 17m was so weathered that it caused the core hole to collapse at this point several days later. The fracture at 15.3m was observed to have a distinct hydrocarbon odour when it was removed during drilling. The EC profile only extended to 17m due to the collapse, but a distinct increase in EC values is observed at the 15.3m fracture and is considered to be related to hydrocarbon affected waters flowing through this fracture. EC logging of PW5 (conducted by M. Gomo, IGS) indicated a significant EC increase at approximately 25m bgl ( $\pm 818$ m amsl) and this is interpreted to be due to a contaminated flow zone at this depth. During core drilling, MW4 was found to have a bedding plane fracture at 13m bgl (828m amsl) and a weathered fracture zone from 24m to 25m ( $\pm 818$ m amsl). EC profiling confirmed the flow zone located at 828m, which is comparable in elevation to the fracture found in MW3. The remainder of MW4 could not be logged due to the hole collapsing at approximately 17m bgl. It is not unreasonable to infer that these flow zones in MW3 and MW4 at 828m amsl are connected, or the flow zones in MW4 and PW5 at 816m amsl, since they exist at comparable depths and are within 50m of each other.

Figure 7-9 displays MW5 which was drilled by the IGS on the property to the south of PW12. MW5 was drilled by means of core drilling and when viewing the simplified log it can be seen that the profile is dominated by alternating layers of siltstone and mudstone. Two noteworthy bedding plane parallel fractures were detected at a depth of 18.5m bgl (824.5m amsl) and 28m bgl (815m amsl). As mentioned in Section 5, acoustic televiewer profiling of



MW5 was conducted and confirmed the bedding plane fractures as 824m amsl and 818m amsl. The EC profiling conducted on MW5 also confirmed in particular the presence of the flow zone at 818m amsl.

Figure 7-10 displays logs of MW7 (percussion hole) and MW8 (core hole) which were drilled in a property off Bird Street. These wells were drilled within two meters of each other in order to compare the differences in geological description between the two drill methods. EC profiling of these holes found potential flow zones in both holes at 24m bgl (818m amsl) and 38m (804m amsl). What is most interesting to note is that MW8 drilled straight down a vertical fracture which extended from approximately 4.5m down to 40m where the core hole ended. This vertical joint/fracture was observed in the core log as well as in the acoustic televiewer log of the core hole. This is an extremely rare and fortunate occurrence as it is very rare to drill almost completely down vertical fracture. This fracture also indicates that transport of fluids from shallow levels to deeper levels may be possible via these long vertical fractures. With regards to the penetrations of NAPL, the hydraulic head of the NAPL as it migrates down the unsaturated zone and encounters such a fracture is high, and would result in significant penetration into the aquifer.

Figure 7-11 displays logs of MW9 and MW10 which were drilled by air percussion and core drilling respectively at Beaufort West Service Station. A water strike was encountered in MW9 at approximately 20m bgl (824m amsl) and whilst the EC logging displayed a momentary decrease at this point, a significant increase was observed at 24.5m bgl (818m amsl) and significant decrease was observed at 29m bgl (815m amsl). Flow zones may therefore be present at 824m, 818m and 815m amsl in MW9. Bedding plane fractures were encountered in MW10 at 15m bgl (829m amsl), 19m bgl (825m amsl) and 21m bgl (823m amsl). EC profiling detected increases in values at the 829m and 825m fractures with stabilisation of EC values from the 823m fracture to the bottom of core hole at 30m bgl (814m amsl).

Figure 7-12 displays the logs of MW11 and MW12 which were both drilled by percussion. MW11 encountered a water strike at 21.5m bgl (823m amsl), with EC profiling detecting an increase in EC values at this point, confirming the presence of a flow zone. A water strike was encountered in MW12 at approximately 16m bgl (829m amsl), however EC profiling did not yield any data regarding possible flow zones since the EC values remained relatively stable

throughout the entire profile. This shows that although EC profiling is invaluable to determine flow zones, it is also possible to miss fractures

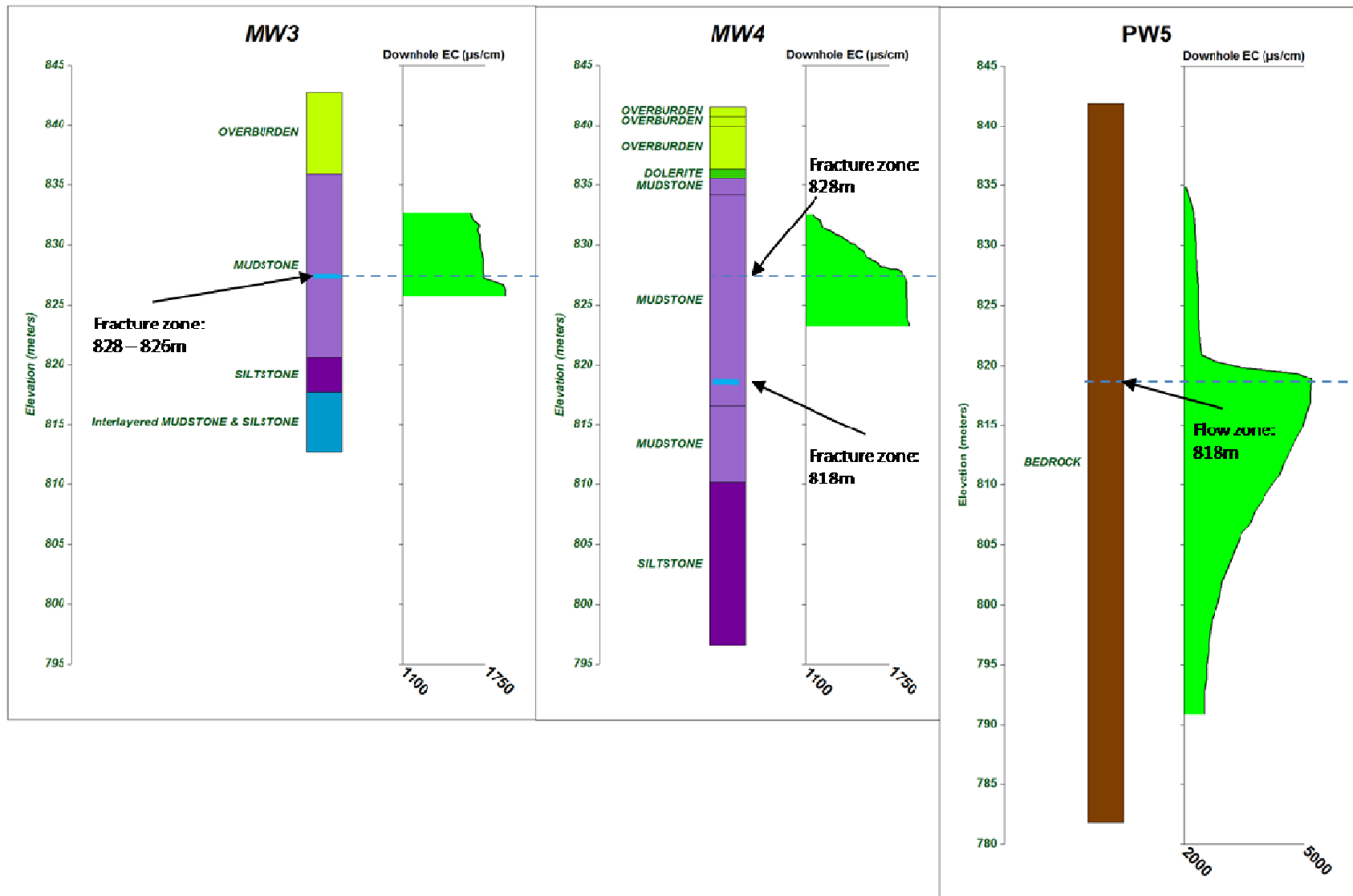


Figure 7-8: EC and basic geology log for MW3, MW4 and PW5 (MW4 & PW5 data courtesy of M. Gomo, IGS)

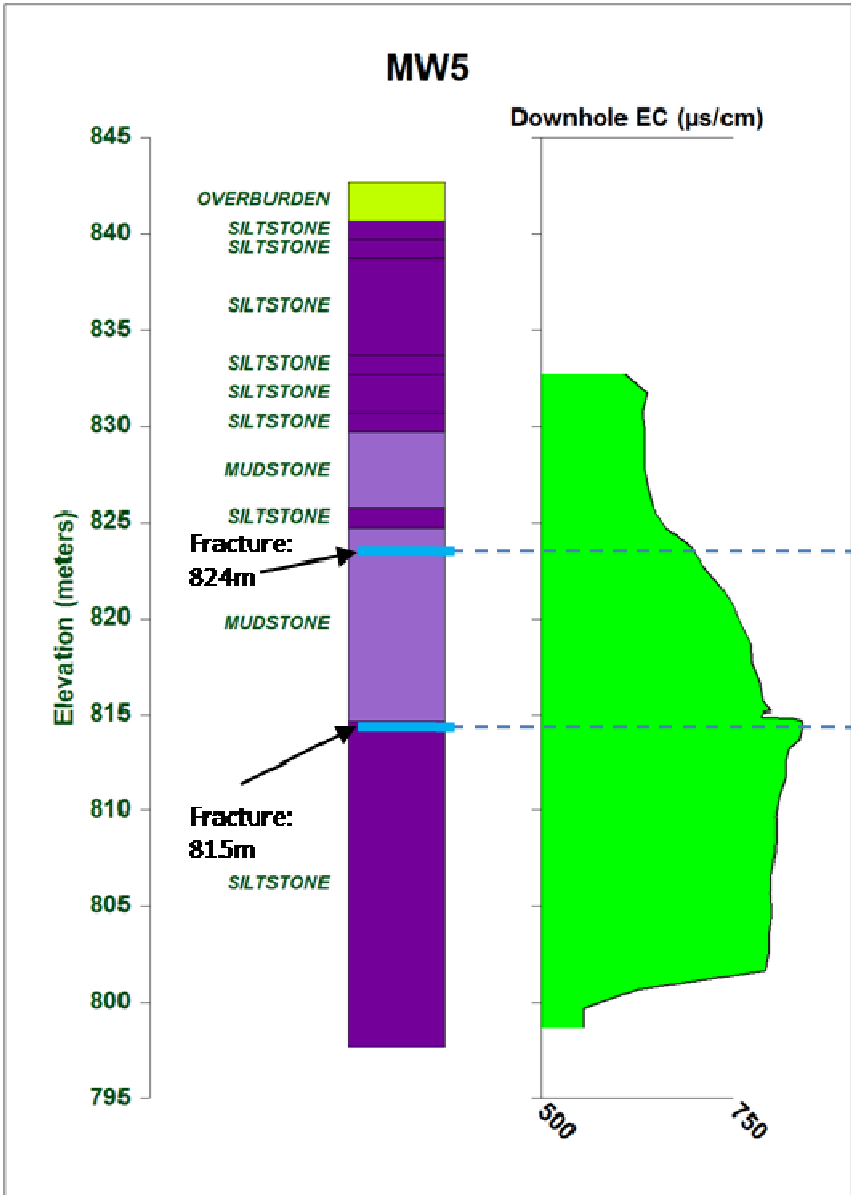


Figure 7-9: EC log and basic geology of MW5 and MW6

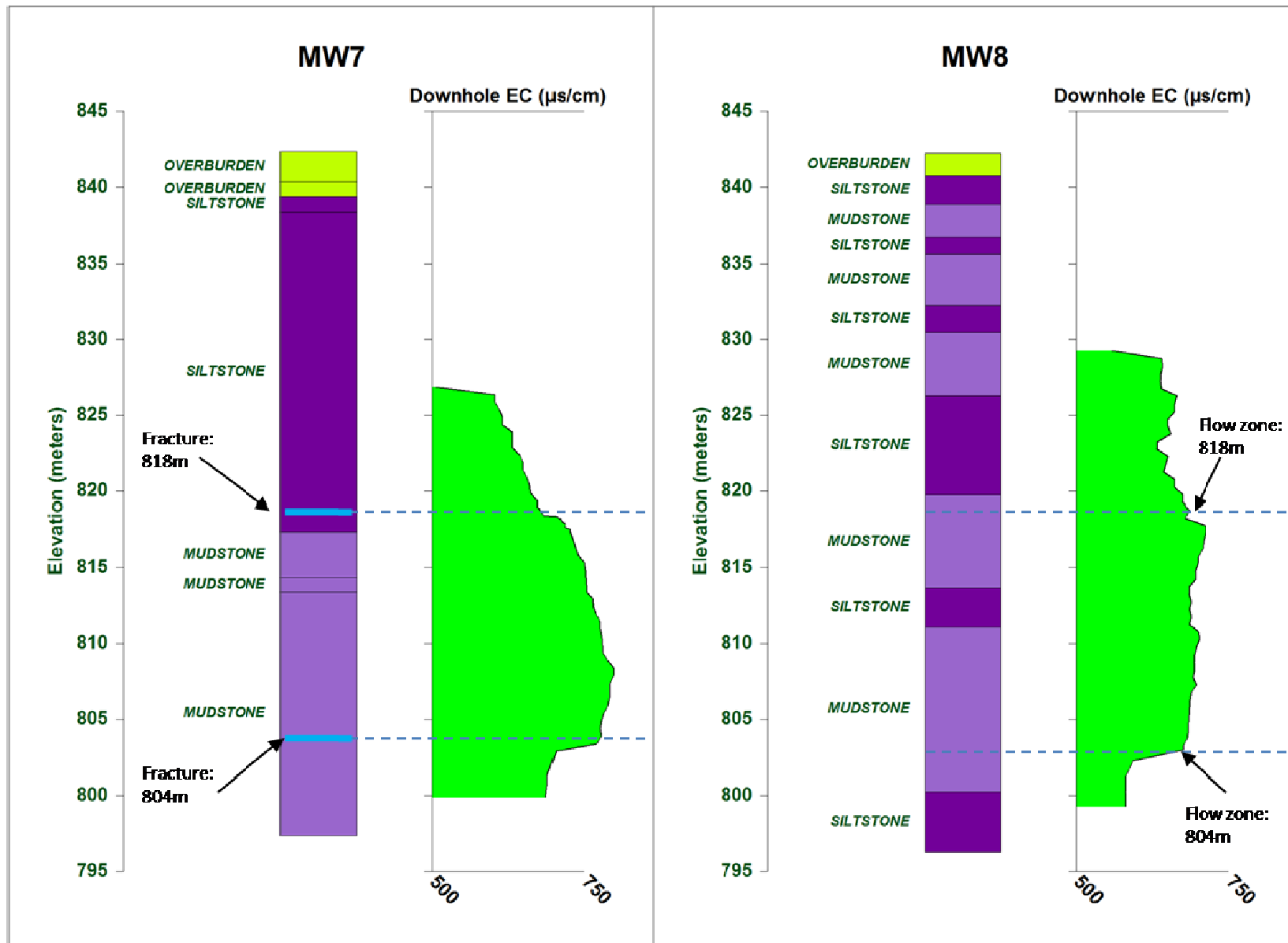


Figure 7-10: EC log and basic geology of MW7 (percussion) and MW8 (core hole)

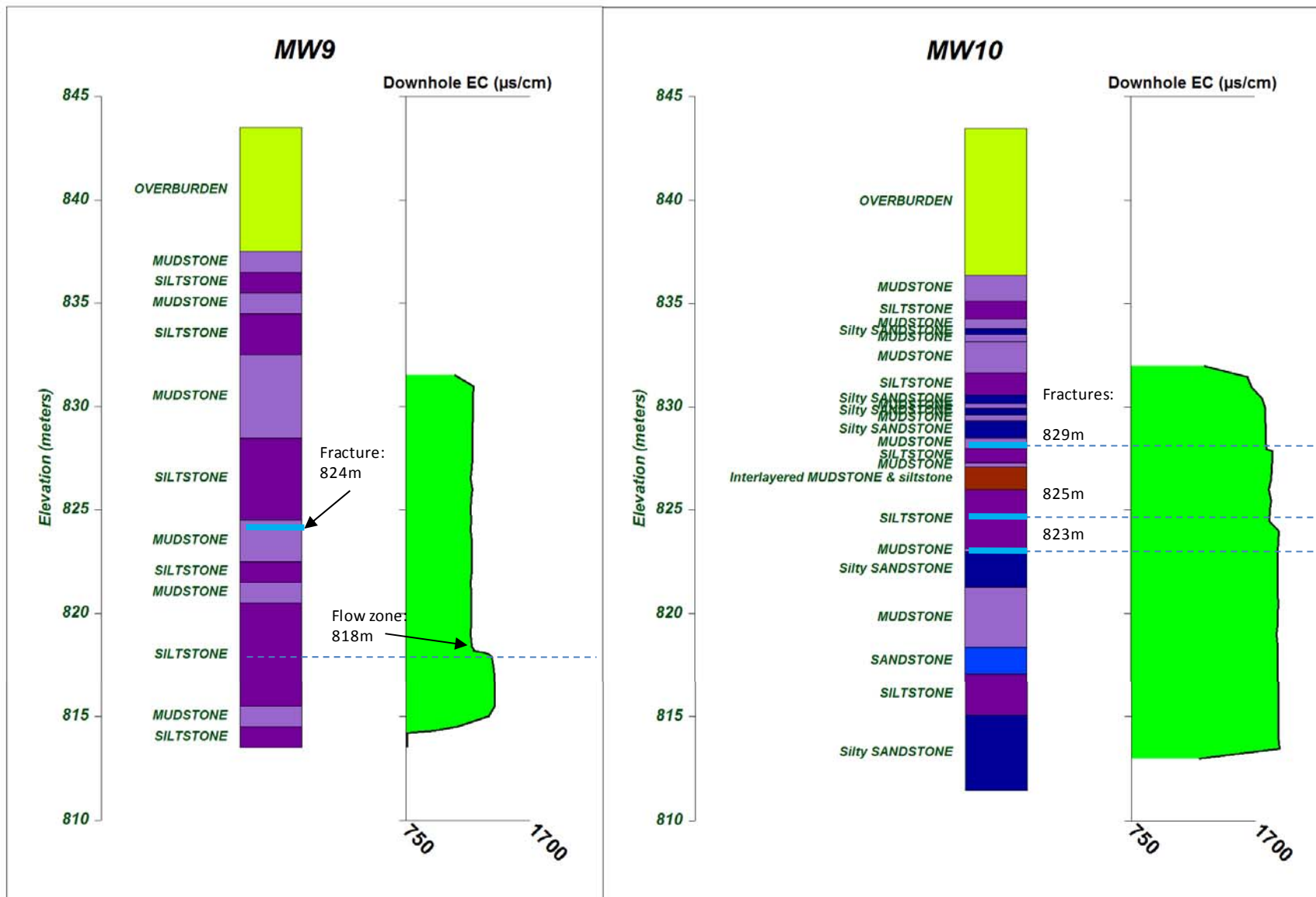


Figure 7-11: EC Log and basic geology of MW9 and MW10

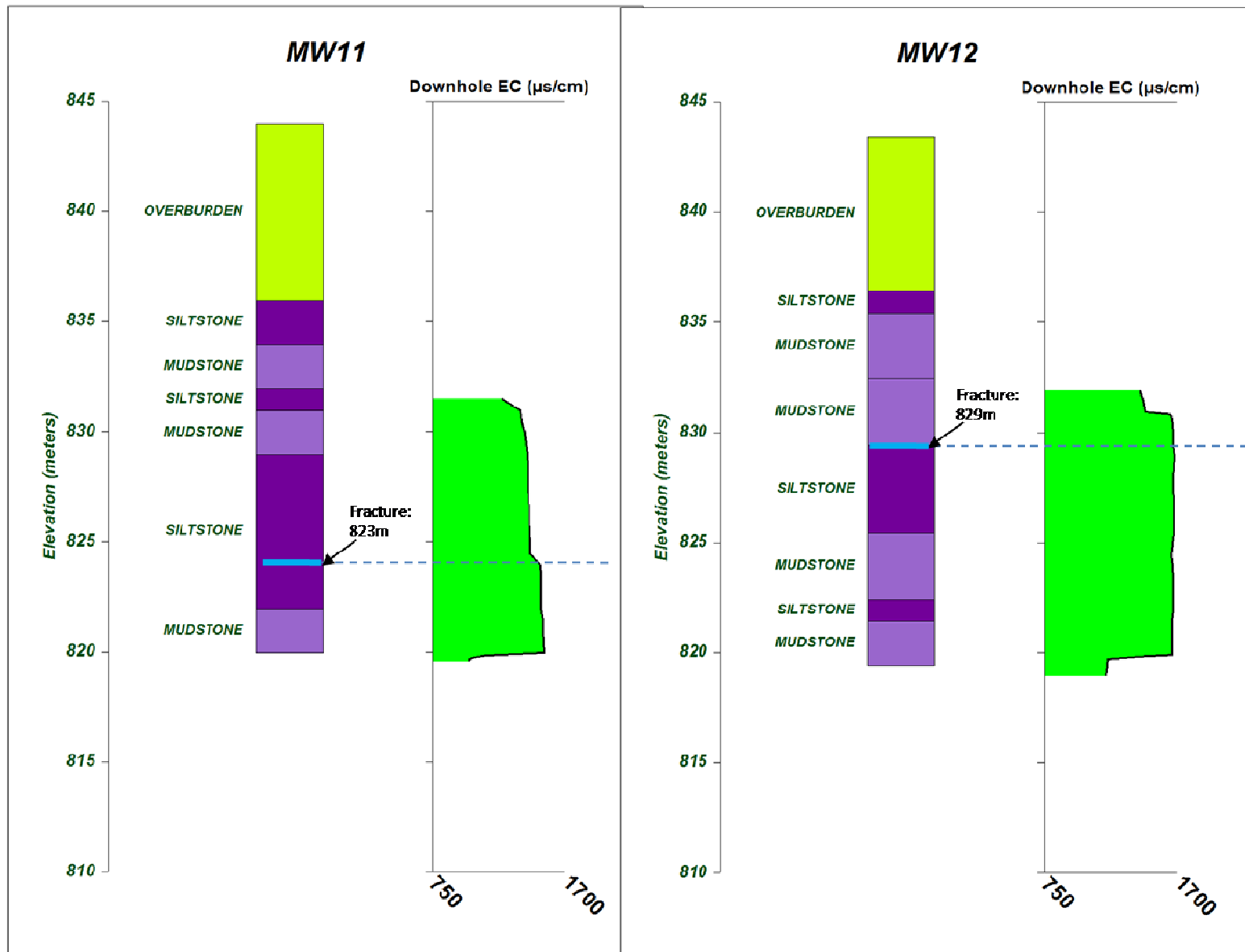


Figure 7-12: EC log and basic geology of MW11 and MW12

## 7.2.2 Electrical Conductivity Profiles of Private Boreholes

Several private boreholes, including the school boreholes were EC profiled in order to identify possible flow zones. Electrical conductivity profiling was performed on PW6, PW12 and PW49 which are located either within, or in close proximity to the main source zones. Figure 7-13 displays the profiles of PW6, PW12 and PW49. When viewing the profile of PW49, an increase in EC values was observed at approximately 21m bgl (821m amsl), indicating a possible flow zone in this section. EC increases in PW12 signifying potential flow zones were identified at 21m bgl (821m amsl), 24m bgl (818m amsl) and 38m depth indicating a possible flow zone at this point. The EC profile of PW6 displayed significant EC increases at 21m bgl (821m amsl) and 24m (818m amsl) which are considered to be related to possible flow zones. Figure 7-14 displays the EC profiles of PW16, PW20 with PW16 being impacted by the dissolved phase hydrocarbon plume. PW16's profile did not yield noticeable variations until 48m bgl (794m amsl) where a slight increase in EC was detected, followed by a more significant increase at 59m bgl (783m amsl). PW20 displayed a rather erratic EC profile however possible flow zone was detected at 48m bgl (790m amsl).

Figure 7-15 displays the EC profiles of NB1, MS02 and HS2 with MS02 known to be contaminated at trace levels and the recent sampling finding traces in HS2 as well. The EC profile of NB1 displays a possible flow zone at 22.5m bgl (819m amsl) followed by a significant flow zone at 35.8m bgl (807m amsl). Another possible flow zone may be present at 70m bgl (774m amsl). MS02's profile shows drops in EC values at 23.4m bgl (817m amsl) and 34m bgl (807m amsl) signifying possible flow zones at these depths however a significant increase in EC was observed at approximately 54m bgl (786m amsl) where EC values jumped from 1500 $\mu$ S/cm to approximately 3300  $\mu$ S/cm and this is interpreted to represent a significant flow zone. Both NB1 and MS02 display possible flow zones at the 807m and 817-819m elevations, which raises the possibility that extensive bedding plane parallel fractures may be present at these elevations. HS2 yielded high EC values in excess of 5000  $\mu$ S/cm which decreased steadily down to a depth of 40m at which the EC probe could go no further, possibly due to the downhole piping, and so the well could not be fully profiled.



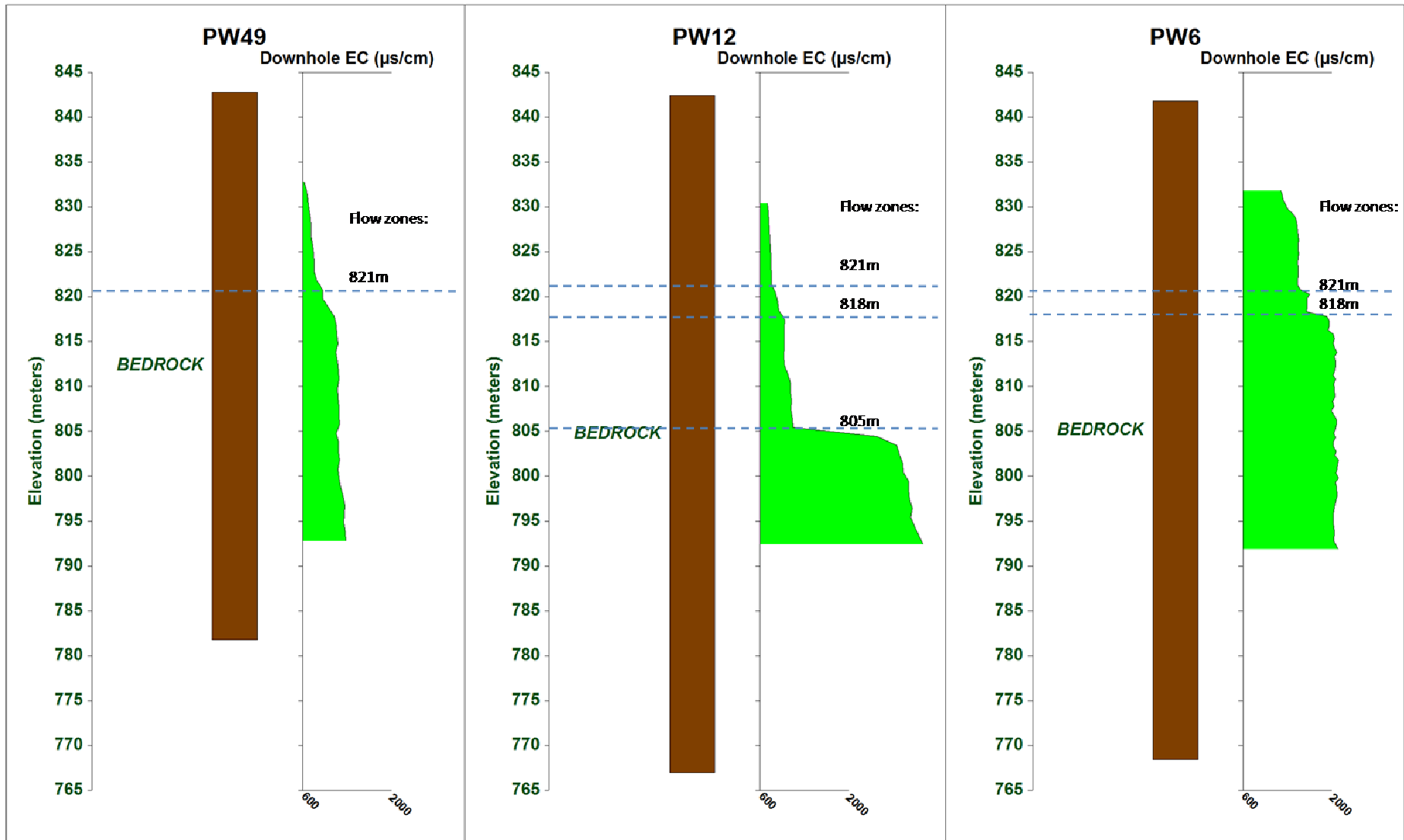


Figure 7-13: Electrical conductivity profiles of PW6, PW12 and PW49.

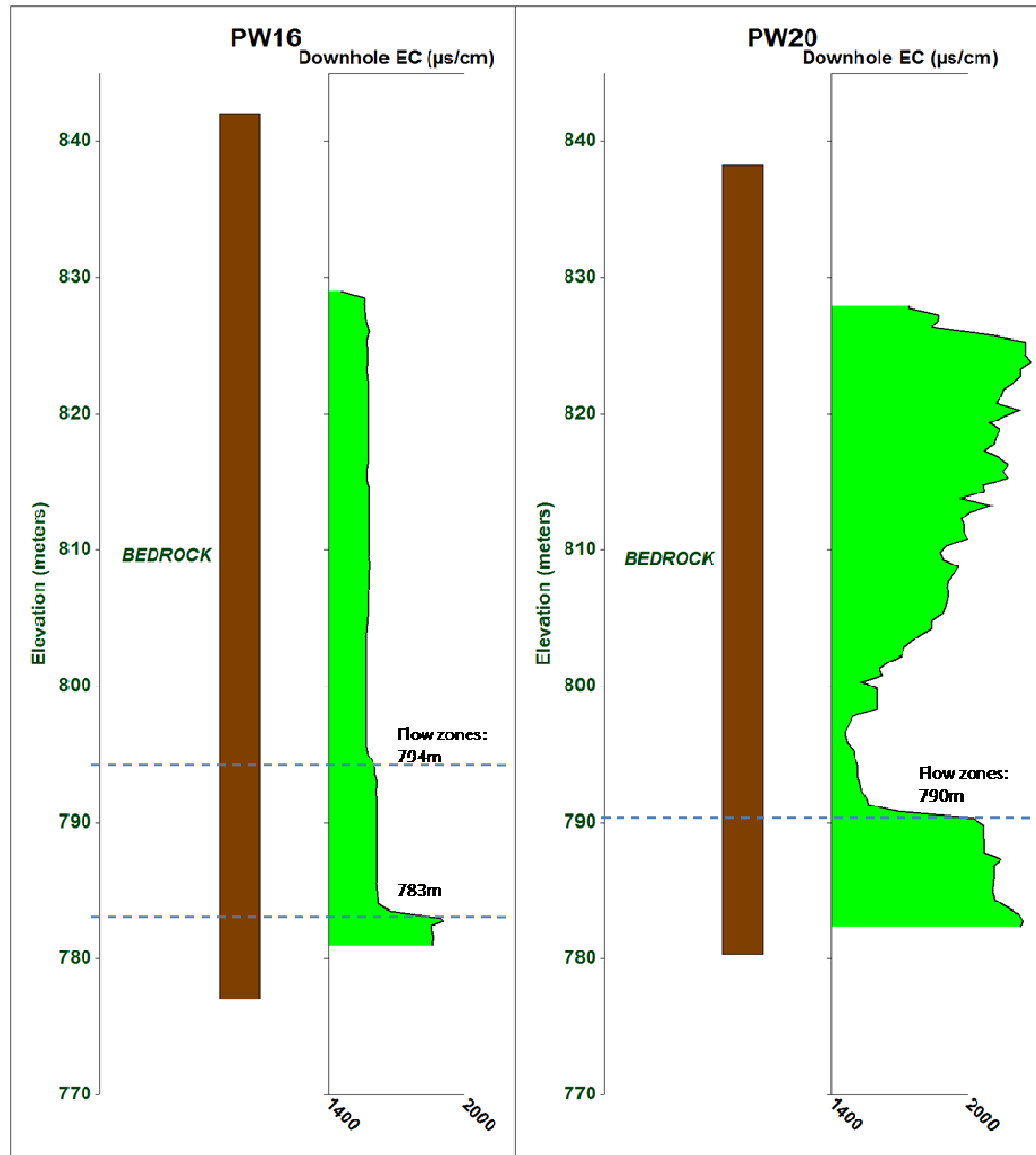


Figure 7-14: EC profiles of private wells PW16, PW20 and PW35

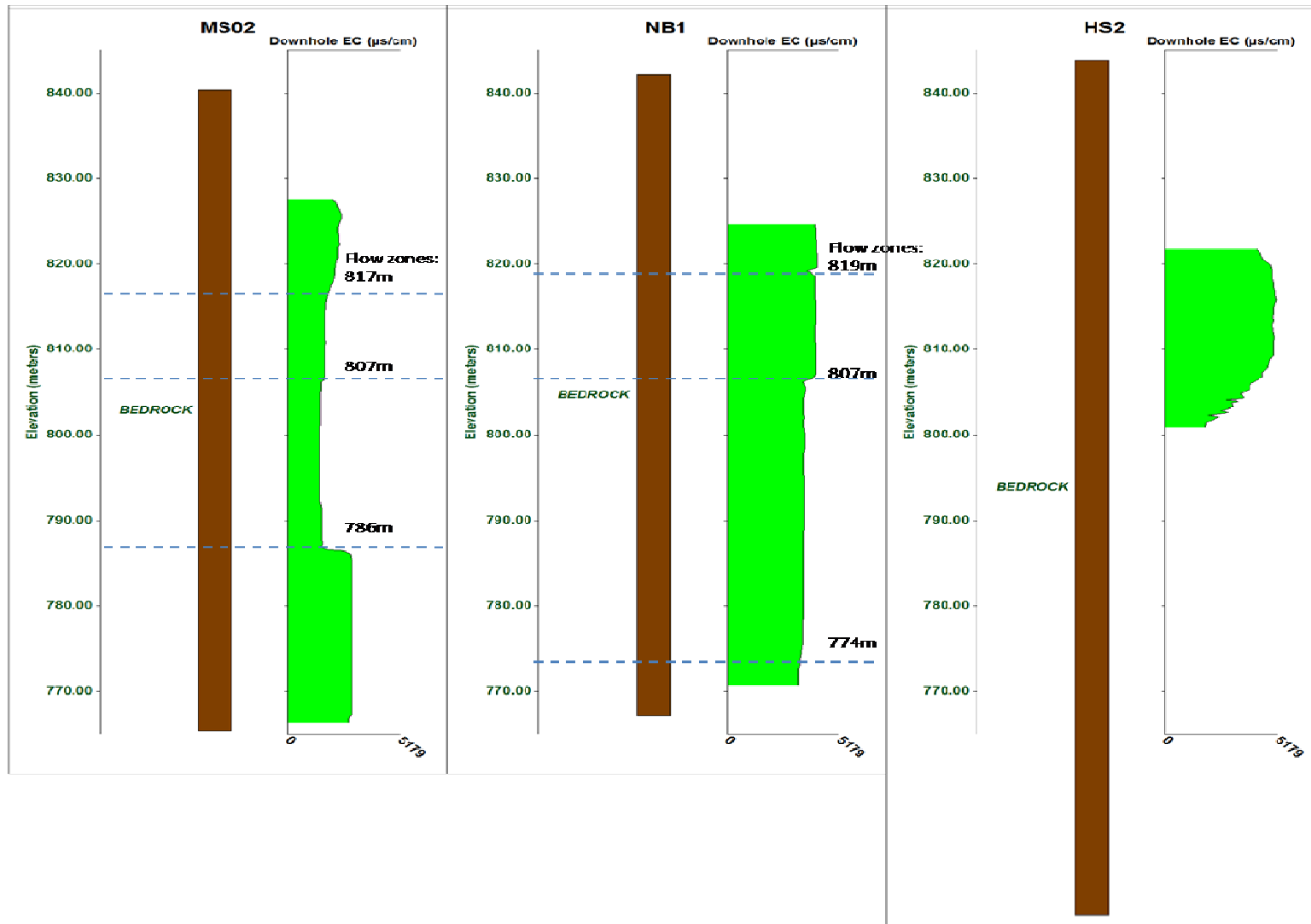


Figure 7-15: EC profiles of NB1 (primary school), MS02 (municipal well) and HS2 (high school)



Figure 7-16 Borehole which were used for fluid flowing electrical conductivity profiling

### 7.2.3 Fluid EC Profiling (FEC Profiling)

Fluid electrical conductivity (FEC) logging provides a relatively simple and inexpensive way to characterise a borehole with regards to the positions of major fractures, the hydraulic properties of the various flow zones and the intra well flow conditions which may be present in the well under ambient conditions. The method essentially involves analyzing the time evolution of fluid electrical conductivities in a borehole under pumped and ambient conditions (Doughty & Tsang, 2004). The premise of the method is that the entire borehole column of water has its electrical conductivity raised by adding salt into the borehole. This results in a significant contrast in salinity (and consequently EC) between the water in the borehole and the water in the neighbouring formation. At depths where fracture zones are present, one will observe significant decreases in EC values in the FEC profile where water with a lower EC (relative to the borehole water column) enters into the well whilst pumping at low abstraction rates. In brief, by significantly altering the salinity of the well bore water and maintaining a constant pumping rate, the sequence of FEC profiles depicts the dynamic flow and transport response which is dependent upon the hydraulic properties of the formation (Doughty & Tsang, 2004).

It must be noted that it is important to not raise the salinity of the water by such an amount that significant density contrasts between the differing waters occurs. As mentioned above, the final data output of the method is a series of time discrete electrical conductivity vs. depth profiles for the selected borehole. Significant decreases in EC are depicted visually in the figures by profile “move out” to the right of the diagram. Flow conditions within the well with regards to upward or downward flow can be quantified by assessing the direction in which successive EC profiles propagate along the well from an identified inflow point. Figure 7-16 displays the boreholes which were used for FEC profiling. It must be noted that “FEC profiling” is used as a general term to describe the method, however in the strictest sense the term fluid electrical conductivity (FEC) profiling refers to profiling under ambient (non pumped) flow conditions whilst flowing fluid electrical conductivity (FFEC) profiling refers to profiling pumped flow conditions. It must also be noted that “ambient” flow conditions is a broad term to indicate that the borehole under observation was not being pumped, however due to the high density boreholes in the area, others boreholes in the area may have been pumping at the time resulting in the ambient flow conditions of the observation borehole being influenced by pumping from neighbouring boreholes.

At this juncture it must be noted that points of investigation within the study area (as indicated in Figure Figure 7-16) has become progressively more focused on the areas directly to the east of Beaufort West Service Station between Bird Street and De Villiers Street as these were the areas which had become most significantly impacted by the contaminant groundwater plume. The level of impact was determined based upon the observed contaminant concentrations (in relation to risk based screening levels) and the groundwater usage type and magnitude in the area. FEC and FFEC profiling was conducted on selected boreholes in order to identify the significant flow zones and to determine intra-wellbore flow conditions within the boreholes. The fieldwork was carried out by students from the University of the Western Cape (UWC) in conjunction with the consultancy under which this study was conducted. Salt was added to the borehole being tested in order to increase the electrical conductivity of the water in the borehole, this was accomplished by raising and lowering a permeable salt filled pouch up and down borehole. The well was then pumped at low rates (<0.4 L/s) with the pump positioned approximately 2m below the water level. Whilst pumping, a YSI™ multi-probe which measured depth, electrical conductivity, oxidation-reduction potential and temperature was continuously raised and lowered from the water level to the borehole bottom taking measurements every 2 seconds. The probe was lowered relatively slowly, taking between 8 and 10 minutes to travel from the water level to the borehole bottom. Profiling would continue on a borehole for between 4 and 7 hours. This profiling was also conducted on selected boreholes when no pump was running in order to determine intra well flow under ambient conditions.

Figure 7-17 depicts the Flowing FEC profile of PW9 which had a measured rest water level of 10.4m bgl. The light blue contours indicate early time profiles whilst the darker contours represent late time contours. Points of inflow (viz. water bearing fractures) are indicated on the FFEC profile as green dashed lines. When viewing the Flowing FEC (FFEC) profile, significant flow zones (indicated by move out to the right) were identified at depths of 13m bgl (829.m amsl), 23m bgl (820m amsl), 25m bgl (818m amsl), 48m bgl (795m amsl) and 53m bgl (789m amsl). The most significant flow zone was identified at the 48m fracture. From the FFEC profile it can be seen that during pumping there was a large amount of dilution above the 48m fracture as time progressed. This indicates that water is entering at the 48m fracture and moving up the well, progressively diluting the high salinity water in the borehole. On a quantitative basis it can be inferred from FFEC profile, that under pumped conditions PW9 sources the majority of its water from the 48m fracture.

Figure 7-18 depicts the results of the profiling from PW17 which had a measured rest water level of 9.59m bgl. When viewing the FFEC profile diagram, flow zones were identified at 11m bgl (831m amsl), 20m bgl (822m amsl), 24m bgl (818m amsl), 27m bgl (816m amsl) and 48m bgl (794m amsl), with the most significant flow zone being observed at the 794m fracture, followed by the 831m fracture. The depths of these fractures are comparable to those in PW9, especially with regards to the major flow zone found at the 794m-795m elevations. The light blue profiles indicate early time whilst the darker profiles indicate late time. FFEC profiles indicate that under pumping conditions the bulk of the water is supplied by the 794m fracture, followed by the 831m fracture. The propagation of the profile lines above the 48m fracture as time progresses indicates upward flow in the well under pumped conditions. Based upon the relative move out of the profiles, the fractures at 816m and 818m do not contribute significantly to inflow, however the slightly stronger move out of the profiles at the 822m fracture, coupled with the strong dilution of the water in the well bore above the 822m fracture would suggest that this fracture is also a relatively strong flow zone with upward flow occurring at this point. The 831m fracture is characterised by a strong move out of the profiles with time and indicates a strong flow zone to be present under pumped conditions.

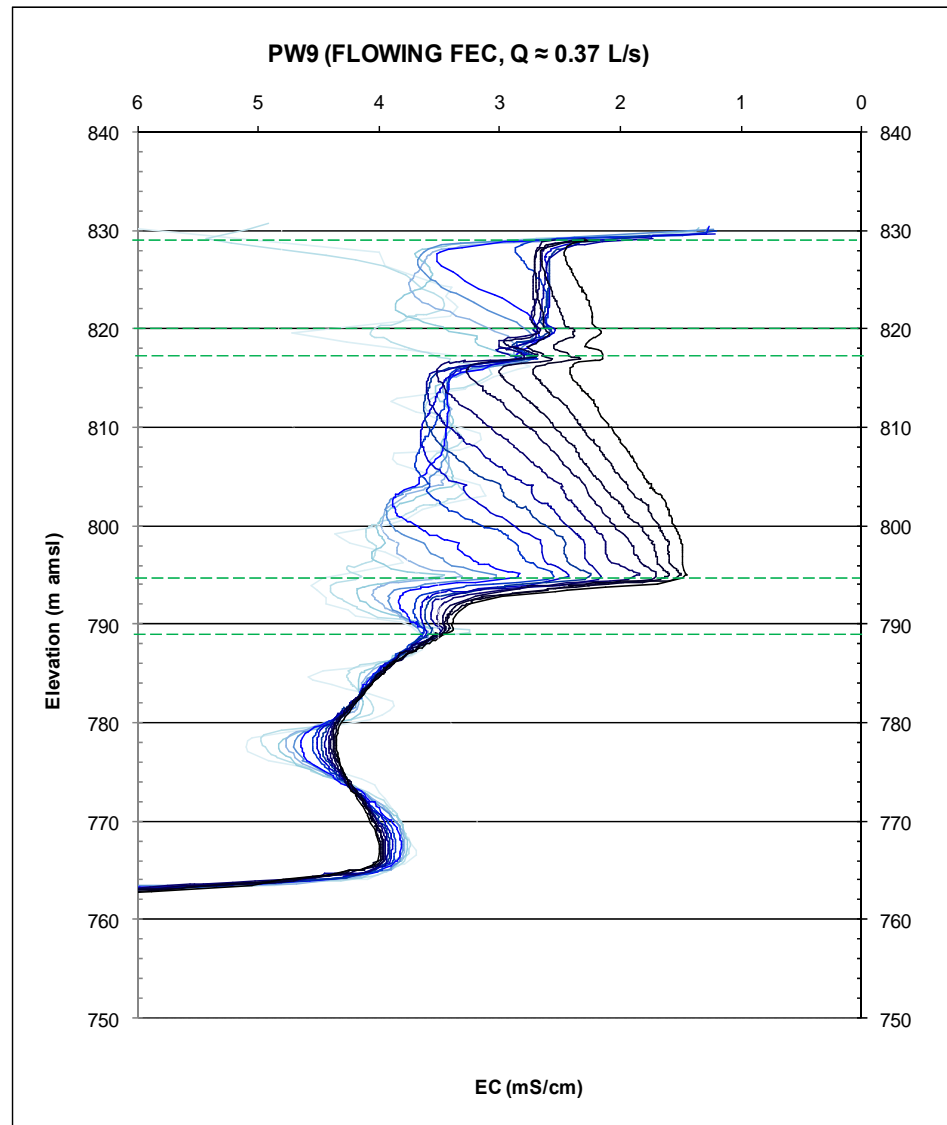
When viewing the ambient FEC profiles of PW17 a significantly different flow regime is observed over the 2.5 hour observation period. The black profile on the right of the figure indicates initial conditions prior to NaCl addition. From the ambient profile it can be seen that a large amount of dilution occurs at the 831m fracture, with EC conditions returning to near initial conditions within the first 50 minutes of observation. This is interpreted to be due to inflow from the 831m fracture. At the end of the 2.5 hour observation period the EC profile has returned to near initial conditions from the 831m fracture down to the 816m fracture. This progressive downhole dilution indicated by the downward propagation of the profiles would suggest downward flow is occurring in the borehole under ambient conditions with water entering the well at the 831m fracture and exiting at the 794m fracture. A small move out can be seen at the 822m fracture and suggests this fracture is also a point of inflow whilst no significant signatures can be observed at the 818m and 816m fractures under ambient conditions. Below 794m the EC profiles are constant indicating no significant intra well flow is occurring below this depth. It must be noted that although ambient conditions in this context implies that no pumping in the borehole is occurring, the apparent ambient conditions may be a result of pumping in a borehole that is connected along a fracture set to the borehole being profiled. In PW17's case it may be that a neighbouring borehole which is connected to the same 794m fracture is being pumped, thereby inducing a hydraulic head difference in PW17 and causing downward flow in the borehole. Irrespective of the cause of the apparent

ambient conditions, the most pertinent observation remains that when PW17 is not being pumped, flow conditions in the well may be such that downward flow from relatively shallow fractures to relatively deep fractures takes place.

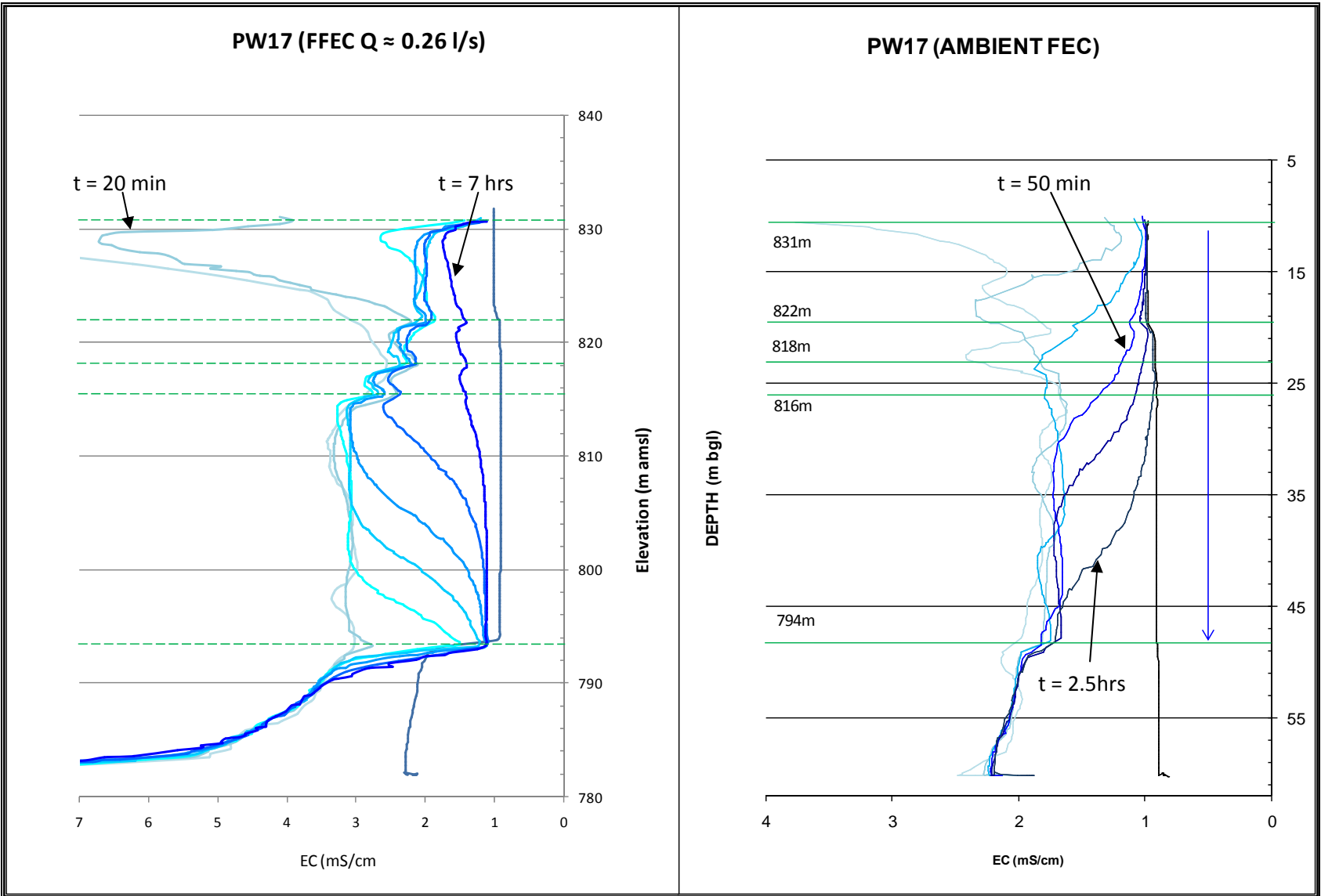
It must be noted that since the ambient EC conditions have been altered in the borehole, one must consider the effects of concentration gradients and diffusion of the NaCl enriched water towards less enriched areas further down the borehole. Whilst this phenomenon may be occurring, diffusion is a relatively slow process and it would not be expected to account for the amount of propagation observed across the 50m saturated profile. Diffusion would also have the effect of lowering the EC in areas of high concentration, and raising it in areas of low concentrations in an attempted to achieve equilibrium, where in the profile it can be seen that the uniform tendency is to move back towards initial conditions. Downward movement of supersaturated saline waters is known to occur, but in this case the EC concentrations are generally below 3mS/cm, which is less than EC values observed in formation waters in NB1 and HS2 which ranged from 3.5-5mS/cm.

Figure 7-19 displays the profile results of PW18 which has a rest water level of 9.51m bgl. Two significant flow zones were identified on the FFEC profile, the first being at 11m bgl (830m amsl) and the second being at 24m bgl (818.5m amsl). When viewing the FFEC profile it can be seen that the 818.5m fracture constitutes the major flow zone. Under pumped conditions the propagation of the contours indicates flow to take place up the well, with dilution of the water column occurring in an upward direction above the 818.5m fracture. The uniformity of the contours below 818.5m suggests that no significant flow intra well flow appears to occur below this fracture. Figure 7-20 depicts the profile results of PW16 which had a measured water level of 9.55m. The FFEC profile of PW16 identified two flow zones at 16m bgl (826m amsl) and 27m bgl (815m amsl). The 826m fracture is considered to be the more dominant of the two flow zones due to a greater move out in the FFEC profiles with time.





**Figure 7-17: Flowing FEC Profile of PW9.**



**Figure 7-18: Flowing FEC and Ambient FEC Profiles of PW17**

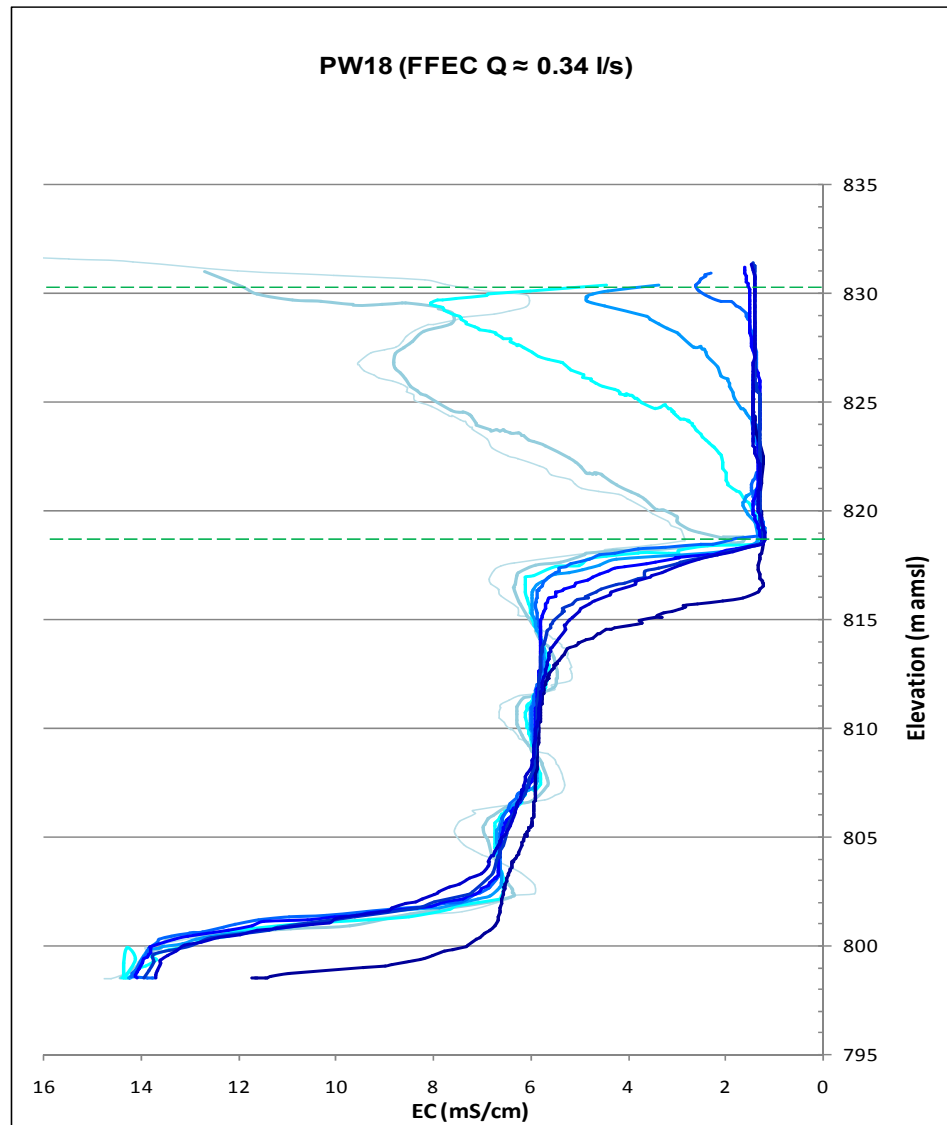


**Figure 7-19: Flowing FEC Profile of PW18**

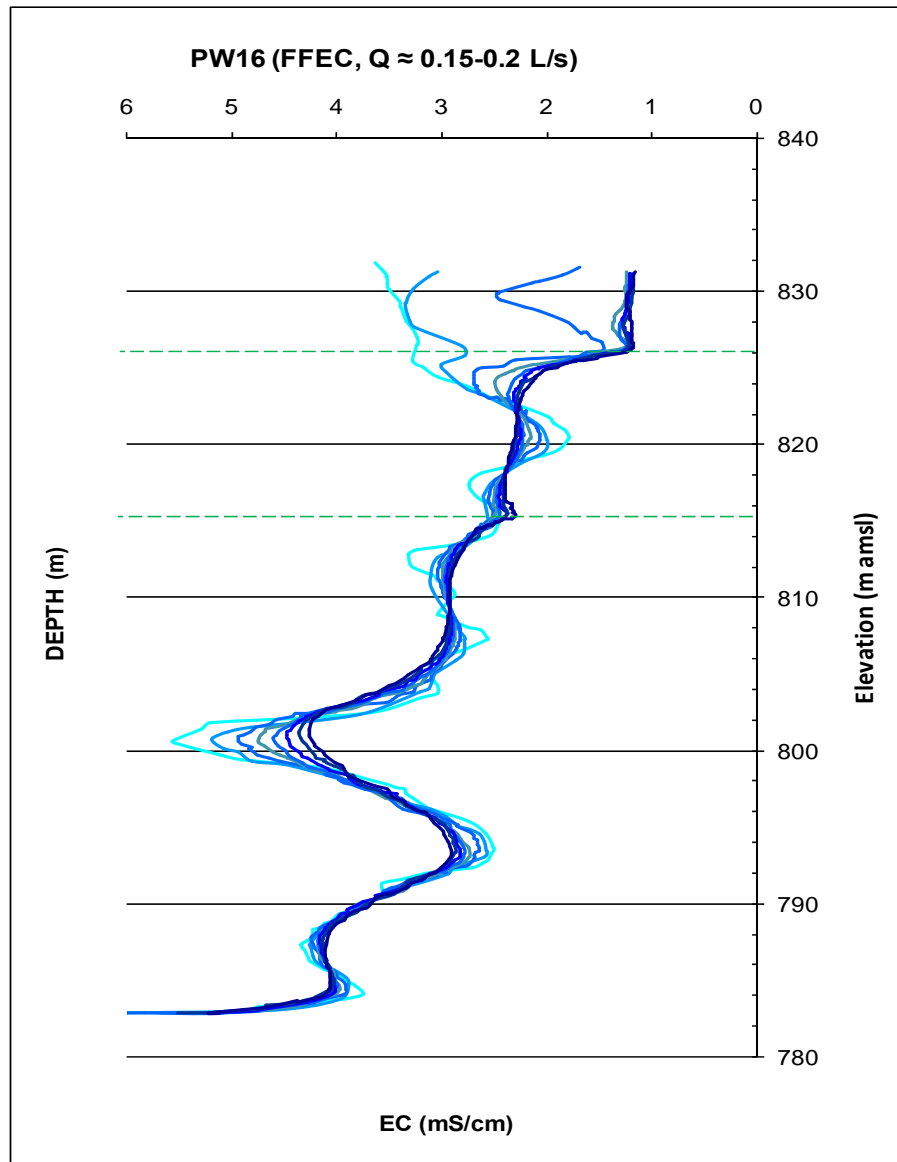


**Figure 7-20: Flowing FEC Profile of PW16.**

### 7.3 Physical Characterisation Summary

Whilst core drilling did identify one vertical joint fracture, the majority of the flow zones which were encountered by the various methods are interpreted to be bedding plane parallel fractures, which is consistent with the published literature’s viewpoint that bedding plane parallel fractures form the predominant flow pathways in Karoo aquifers (Botha et al, 1998). The combination of percussion drilling, core logging, ambient downhole EC profiling, FFEC and FEC profiling have yielded significant information regarding the distribution and occurrence of significant flow pathways in the aquifer within the study area. Table 7-1 to Table 7-3 provide a summary of the identified flow zones within each of the monitoring wells and boreholes which were investigated. As in Section 5, no one method provided all of the information, but rather a combination of methods provided the information. Monitoring wells and boreholes which are located in the south of the study area towards Donkin Motors are indicated by green labels whilst monitoring wells and boreholes located to the north of the study area in the vicinity of Beaufort West Service Station and the to the east are indicated by blue labels. The municipal supply borehole and school boreholes to the east of the Kuils River are indicated by orange labels.

**Table 7-1 Flow zone locations in monitoring wells which were installed within the study area.**

Approximate Depth (m bgl)	Elevation (amsl)	MW3	MW4	MW5	MW7	MW8	MW9	MW10	MW11	MW12
20	820 - 830							829		829
		826 - 828	828					825		
				824			824	823	823	
30	810 - 820		818		818	818	818			
				815			815			
40	800 - 810				804	804				
50	790 - 800									
60	780 - 790									

Note - The lower portions of the table are coloured in grey since none of the monitoring wells exceeded a depth of 40m

**Table 7-2 Flow zone locations in private boreholes in Bird Street and De Villiers Street**

Approximate Depth (m bgl)	Elevation (amsl)	PW5	PW6	PW9	PW12	PW16	PW17	PW18	PW20	PW49
20	820 - 830			829.5			831	830		
						826				
			821	820	821		822			821
30	810 - 820	818	818	818	818		818	818		
						815	816			
40	800 - 810									
					805					
50	790 - 800			795		794	794			
									790	
				789						
60	780 - 790									
						783				

**Table 7-3 Flow zone locations in the municipal supply borehole and school boreholes**

Approximate Depth (m bgl)	Elevation (amsl)	MS02	NB1	HS2
20	820 - 830			
30	810 - 820		819	
		817	818	
40	800 - 810			
		807	807	
50	790 - 800			
60	780 - 790			
		786		

When viewing the tables, several trends become apparent with regards to the fracture network distributions in the investigated boreholes and monitoring wells. In almost all the monitoring wells the first major flow zone occurs between 823m-828m amsl, which is essentially within the first 20m of the geological profile. In a similar fashion the majority of private boreholes also display the first major flow zones within the first 20m of the geological profile. From the tables it can be seen that the highest frequency of flow zones occurs within the first 30m of the profile. When viewing the elevation interval of 810m-820m amsl, the majority of boreholes and monitoring wells were found to have a flow zone at approximately 818m amsl (between 23m-25m below ground level). This 818m amsl flow zone is particularly prevalent in the northern areas (blue labels). The FFEC profiling quantitatively suggested that particular boreholes (PW9, PW16 and PW17) the strongest yielding fractures were located at elevations of 794-795m amsl, which equates to approximately 50m below ground level. This observation and that of the high frequency of flow zones within the first 30m is

also consistent with literature data of the Beaufort West which area which indicated that the highest frequency of fractures is usually found within the first 30m of the geological profile (viz. the weathered zone) whilst the strongest yielding fractures are generally found at depths between 50m-60m below ground level (Campbell, 1980).

## **8 Aquifer Parameter Estimation**

Aquifer parameter estimation encompasses a potentially large body of data pertaining to the aquifer under observation and seeks to describe the nature of groundwater flow within the aquifer and how the flow is affected by various sources (such as recharge) and sinks (such as groundwater abstraction). Aquifer parameter estimation can range from taking simple groundwater level measurements to provide groundwater gradient and flow direction to extensive pumping tests and tracer tests to determine transmissivities and effective porosities. In order for a successful contaminant transport model to be developed, a robust flow model must first be constructed on which the transport model can be based. Within the current study, aquifer parameter estimation took the form of constant rate discharge tests and associated recovery tests, LNAPL recovery tests, and water level measurements and gradient calculations.

### ***8.1 Water Level Measurements***

Whilst monitoring of organic and inorganic groundwater parameters has been occurring on a biannual basis since 2002, a biannual schedule is generally not considered sufficient to provide meaningful insight with regards to groundwater level measurements and the various factors which affect the groundwater levels. Water level measurements have however been recorded for NB1 by the Nico Brummer staff and monthly rainfall data for Beaufort West is available from the SA Weather Bureau. Figure 8-1 displays the measured water levels of NB1 against monthly rainfall totals for the Beaufort West area over the period from July 2007 to December 2008. It must be noted that whilst monthly water level measurements were made at NB1, some of the measurements were made whilst the pump was engaged and these measurements have not been included in order to avoid a misrepresentation of rest water level data. From Figure 8-1 it can be seen that the water levels respond fairly rapidly to rainfall, with water level rises occurring in months of comparatively high rainfall, and water level decreases occurring in months of comparatively low rainfall. This would suggest that firstly, direct recharge to the aquifer is occurring, most likely through vertical joints and fractures within the weathered zone and secondly, the aquifer storativity values are low since the water level responses track the rainfall (and by extension recharge to the aquifer) very closely.



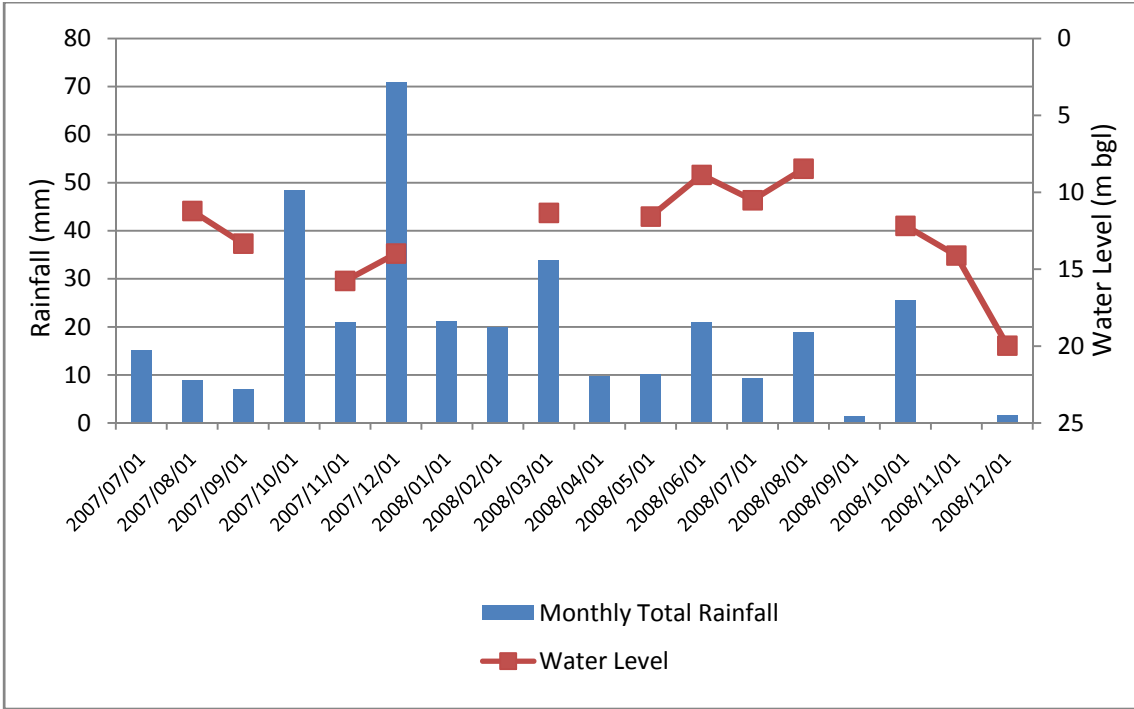


**Figure 8-1 Monthly rainfall data and water level measurements from NB1**

Water level measurements were used in conjunction with DGPS survey data to calculate groundwater gradients for the study area. PW58, PW8 and PW80 were selected and their water levels (in m amsl) were contoured using the “linear interpolation with triangulation” method. Based upon the contoured data which is present in Figure 8-2, a groundwater flow direction towards the south east was inferred, with a calculated gradient of 0.001. This flow direction and gradient is consistent with the topography and slope across the study area. The abovementioned wells were selected primarily due to their locations, being outside the main impacted zones where groundwater abstraction is high and groundwater level, gradients and flow directions are constantly varying. The distance between the wells ranges from 800m to 1.2km and the calculated gradient data is intended to provide a quasi regional scale groundwater gradient and flow direction which minimises the effect of local variations caused by the abstraction in the impacted zones. The observed contaminant plume migration direction has been indicated in Figure 8-2 by red arrows, and can be observed to be migrating cross gradient to the regional setting. This is interpreted to be due to the abstraction in the residential areas which significantly alters groundwater flow directions in the areas from Donkin Street to Brand Street.

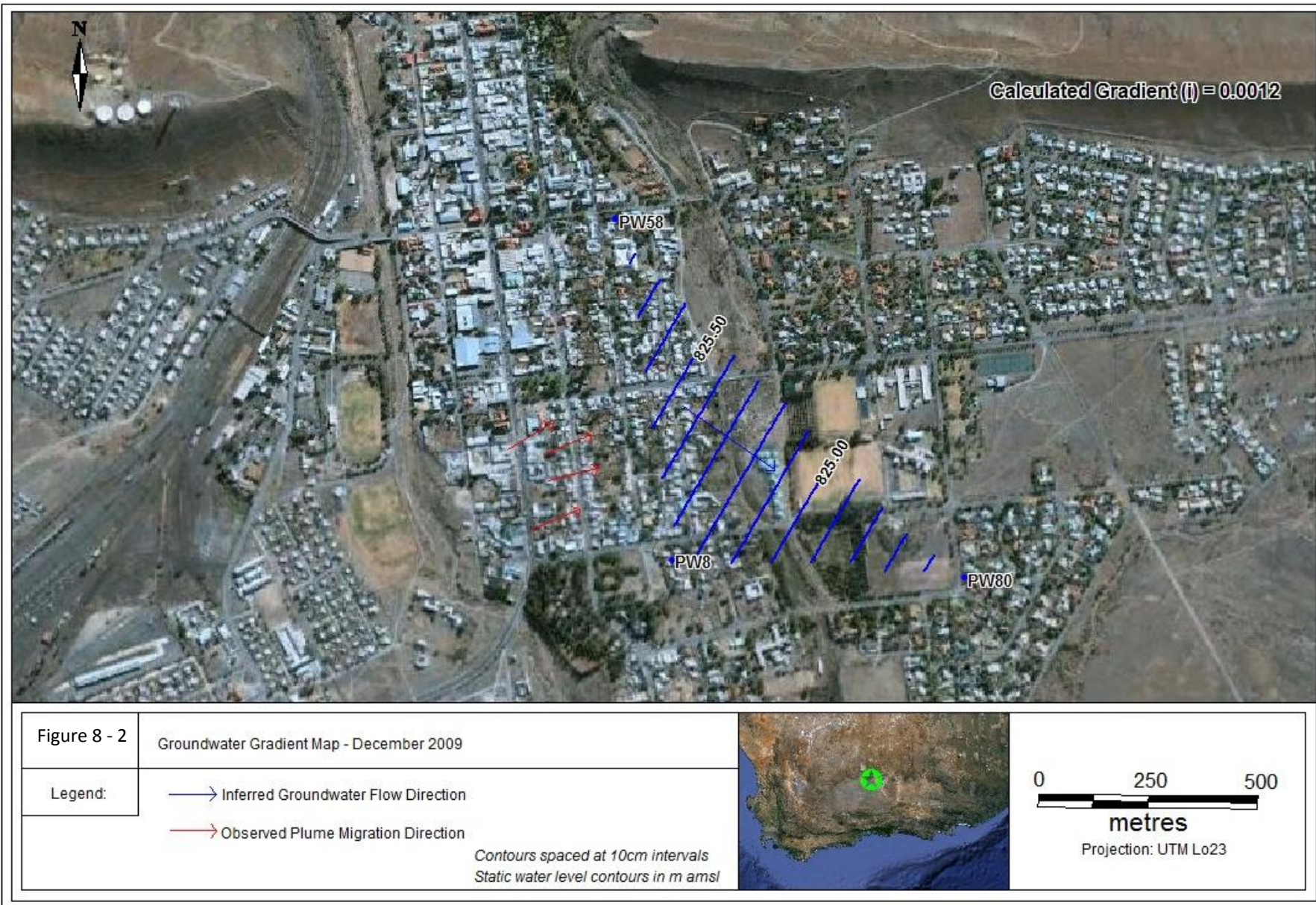


Figure 8-2 Static water level gradient map

## ***8.2 Constant Rate Discharge Tests***

Pumping tests are considered to be one of the most important field experiments that can be conducted on an aquifer in order to determine aquifer parameters. They are considered to be the only method which can simultaneously deliver information regarding the borehole being pumped, as well as the surrounding aquifer (Van Tonder et al, 2001). The premise of a pump test is to abstract water from a well whilst measuring the discharge from the well and the drawdown of the water level in the well. The two major objectives of pumping tests are aquifer parameter estimation and sustainable yield calculations. The first of these objectives is more pertinent to groundwater contamination situations to determine spreading of contaminants, however in situations where remedial systems may abstract large volumes of water the sustainable yield factors must also be considered. In general, the drawdown data from the abstraction well is inputted into an aquifer parameter analysis program such as FC-Programme and aquifer characteristics such as transmissivity, fracture distribution and no-flow boundary conditions can be determined.

In addition to this, several assumptions are made when analysing data from pump tests in a confined or semi-confined aquifer, these are:

- The aquifer is confined.
- The aquifer has a seemingly infinite areal extent.
- The aquifer is homogenous, isotropic and uniform over the area influenced by the test.
- Prior to the pump test the piezometric across the area influenced by the test is horizontal.
- The aquifer is pumped at a constant discharge rate.
- The well is fully penetrating with regards to the aquifer.

(Kruseman & De Ridder, 1999)

It is important to note that for the majority of pump tests not all of these assumptions hold true. For the most part however, the real world conditions will approximate the majority of these assumptions provided the pump test is conducted properly and in order to analyze the data these conditions must be assumed. During the course of this study two separate pump test site visits were conducted. The first visit occurred in March 2009, when a 72 hour constant rate discharge test was conducted on the primary school borehole NB1, with HS2, MS02, PW20, and PW35 being used as observation boreholes. Figure 8.3 displays the locations of the abovementioned boreholes. A second visit was conducted in December 2009, when several constant rate discharge tests were carried out on PW12, PW49, PW2, PW17 and MW12.





Figure 8-3: Site layout of boreholes and monitoring wells used in constant rate discharge test.

### **8.2.1 Nico Brummer Pump Test – March 2009**

Two boreholes are present at Nico Brummer primary school (NB1 & NB2) with the stronger of the two boreholes (NB1 - based upon anecdotal information from the school) being chosen to be the pumping well due to its proximity to boreholes which are known to be affected (MS02 and PW35). The stronger of the two boreholes (HS2) at the high school was chosen to be an observation borehole along with PW20 which is located on the western side of the Kuils River. PW35 and MS02 which are both affected by dissolved phase hydrocarbons were also chosen as observation boreholes in order to determine whether they may possibly be in hydraulic connectivity with the wells at the schools.

In theory, the following conditions should be present for a “perfect scenario” pump test to occur:

- The water level in the abstraction borehole should be at its rest level prior to the test beginning. A preferred rest time of three weeks is usually required if the borehole is subject to a large amount of pumping (Kruseman & De Ridder, 1999).
- The water levels in the observation wells should be at the rest water level prior to the test commencement. The three week rest period is also required at these wells.
- No pumping should occur nearby which could influence the drawdown in the abstraction well or the observations.

Whilst these conditions are desirable, the circumstances under which the pumping test occurred did not allow for these conditions to be met. In order for the test to proceed it was necessary to rest the boreholes at the schools for as long as possible prior to the pump test beginning. The olive groves at the schools are under a very strict irrigation schedule and compromises had to be reached with the schools so that as little disruption to the schedules would take place. The primary school agreed to rest NB1 and NB2 for three days prior to the test commencing in order to allow the water levels to reset. The high school could not however rest HS2 until the day before the pump test due to the fact that HS2 would not be pumped at all during the three days that NB1 was to be pumped. Despite this, previous pump tests investigations conducted within the town have shown that water levels generally reset within 24 hours, and so the one day rest period was considered sufficient. Another complicating factor was that the test had to be conducted under the influence of pumping within the residential areas of the town.

When viewing the pump test data, it became apparent that the nature of the data would not allow for a conventional constant rate drawdown analysis due to several factors which will be discussed below. The data does however yield valuable qualitative information regarding the connectivity of the boreholes in the pump test, as well as the nature of the aquifer. What follows is qualitative time series description of the pump test. Figure 8-4 depicts the drawdown data for the entire pump test. The dark blue line represents the water level fluctuation of NB1 whilst the yellow line represents the water level fluctuation in HS2. The pink line represents the water level fluctuations in the municipal well MS02, whilst the turquoise line represents the water level fluctuations in PW20. PW35 is represented by the purple line. Figure 8-4 to Figure 8-8 display in more detail the information contained in Figure 8-4 and should be viewed with reference to the following discussion.

Figure 8-5 depicts the initial phase of the pump test with NB1 being switched on at 15:30 Monday 16 March. The commencement of pumping in NB1 (at a rate of approximately 1.3 l/s) is marked with a significant drop in NB1's water level of approximately 15m (See dotted area 1 in Figure 8-5). At the same time that pumping commenced in NB1, a discernable water level drop of just over 1m can be observed in HS2. No discernable drop was observed in any of the other observation wells when NB1 was engaged however MS02's water level, which at the time had been rising, displayed a pause in its water level rise and may signify a weak link between NB1 and MS02. Another smaller drop in water level is seen in NB1 at about 17:30 (see dotted area 2). This was due to ground staff at the school changing the valves on the irrigation system – up until 17:30 the discharge had been routed to an irrigation system which restricted flow somewhat. After 17:30 the borehole water was routed to a storage dam with the pump being unrestricted at this point and pumping at its maximum rate of  $\pm 2.5$  l/s. From about 17:30 though to 21:30 a general increase in water levels is seen in all wells despite the pumping of NB1 and after 21:30 this increase becomes slightly more pronounced in NB1 and HS2. It is inferred that most residential pumping would have ceased from about 21:30 onwards and so the general increase in water levels may be related to the aquifer's water levels recovering through the night on a wider scale, with the drawdown effect of NB1 being masked over by this more widespread increase in water levels as water is released from storage in the matrix (GPT, 2009) and as recharge occurs from neighbouring recharge boundaries (i.e. the Beaufort West Sill). At 07:00 a sudden increase in water level of about 7m is seen in NB1, with a slight increase in HS2. This is inferred to be due to ground staff at the primary school altering the flow in some manner.

Figure 8-6 displays the next phase of the pump test, with the sudden increase in NB1 at 07:00 dropping back down before increasing very sharply up to near the rest water level (see dotted area 3). This is interpreted to have been caused by the pump being disengaged for some unknown reason at

9:15. At 10:00 the pump was re-engaged with the water level dropping approximately 10m. The disengagement and re-engagement in pumping in NB1 is reflected in HS2 by a slight increase followed by another drop. A very slight flattening of the drawdown curve in MS02 is also seen at this point. Another trend that can be seen in HS2, MS02, PW20 and PW35 is that from 07:00 the water levels all show a general trend to start decreasing. This is interpreted to be due residents in the area beginning to pump their boreholes again. NB1 is observed to behave rather erratically until 16:45 and this is interpreted to again be due to ground staff at the primary school altering flow by routing the pumped water to various irrigation systems. At 16:45 the water level drops again as the pumped water is routed into the storage dam for the night and the abstraction is regulated to approximately 2.5 l/s. Again no effect is seen in any of the observation wells when this smaller drop occurs. From 21:30 onwards the water levels are again seen to rise in all wells despite the pumping of NB1 and this is inferred to be due to the cessation of pumping in the residential areas. When viewing Figure 8-6 it can be seen that HS2, MS02 and PW20 appear to mimic each other relatively closely, whilst PW35 does not appear to do so to the same degree, although it does mimic the general water level fluctuations, but to a lesser degree (GPT, 2009).

Figure 8-7 displays the passage of time from Tuesday night through to Wednesday morning. Water levels remain relatively constant with the water level in NB1 having been at 36m below ground level for most of the night. From 06:00 onwards a decrease begins to take place in most of the boreholes, possibly due to residents beginning to pump. From approximately 08:30 until 12:00 a set of repetitive water fluctuations occur in NB1 (see dotted area 4). This may again have been due to water routing relating to the irrigation at the school, but it cannot be stated for certain.

Figure 8-8 displays the final phase of the pump test. From the time that the series of water level fluctuations were observed until 15:30 the water level in NB1 was observed to have behaved rather erratically for unknown reasons. At 15:30 the period of 72 hours had been completed and the pump was disengaged. This was followed by an almost instantaneous recovery back to near-rest water levels (see dotted area 5). Shortly after 15:30, HS2's pump was engaged due to a miscommunication between the high school's management and the field personnel. It was disengaged approximately 40 minutes later in order to retrieve the level logger however the effects of the 40 minute pumping period provide useful information. It can be seen that as soon as HS2 began pumping there was a water level response in NB1 with the water level dropping nearly 2m. As soon as HS2 was disengaged the water level in NB1 recovered. A slight rise in MS02 followed by a small drop could be related NB1 being disengaged followed by HS2 being engaged. Once the level logger was removed from HS2, the pump in HS2 was engaged and was pumped until 21:00. The response in NB1 can be observed with NB1's



water level being drawn down until 21:00 at which point the water level began to recover due to HS2's pump being disengaged. HS2 was re-engaged at 06:00 on Thursday morning and the response in NB1 is significant, with almost 10m of drawdown occurring due to HS2's pumping (Although HS1 may have also been pumping at this time). MS02 also depicts a very slight decrease from 06:00 which may be a response to HS2.

The water level of PW20 was plotted on a different set of axes in

Figure 8-9. The axes was set such that PW20's water level fluctuations appeared much more pronounced in order to observe any potential small scale influences which the pump test may be having on PW20. When viewing the diagram it can be seen that PW20's water level is affected more by the general daily variations observed across the area, with no significant affect being observed from the pumping of NB1. In the same manner, MS02's axes were altered in Figure 8-10, which displays the water level data of NB1 and MS02 after the pump test completion. As previously mentioned HS02 was pumped from 16:00 until 21:30, and the drawdown and subsequent recovery response in NB1 and MS02 is evident. HS02 was reengaged at 06:00 the following day (Thursday) and the drawdown response in NB1 and MS02 is clearly evident.

As mentioned previously, the data from the pump test was not inputted into an aquifer analysis program due to factors such as the discharge rates being varied during the test, the fact that the pump was disengaged halfway through the pump test. Another factor which was not optimal was the relatively low pumping rate of 2.5 l/s, however this could not be changed as this was maximum pumping rate of the borehole installed in NB1. Despite these shortcomings, several important factors have been realised through the pump test: Firstly the test clearly shows that a strong hydraulic link exists between NB1 and HS2, with a drawdown being observed in HS2 shortly after NB1 began to pump. It must be noted, that HS2 pumps at a much higher rate ( $\pm 6$  l/s) when compared to NB1 (2.5 l/s) and the effect on NB1 due to pumping HS2 is more pronounced than when pumping takes place the other way round. Water levels in NB1 dropped to approximately 36m below ground level, which is where a major fracture is known to exist (807m amsl fracture as indicated in Table 8-3). Whilst no significant drawdown effects were observed in PW20 and PW35 due to the pumping of NB1, it is not possible to conclude whether a link does or does not exist between NB1 and the set of PW20 and PW35. Since NB1 was not pumped constantly and definitely did not dewater the fracture at 36 m significantly, it is possible that the pressure gradient was insufficient to show an effect which would supersede the general water level fluctuations which were observed.

The water level data of MS02 indicates that a weak link between this well and NB1 may be possible whilst the data from recovery period indicates that HS2 is in hydraulic connectivity with NB1 and

MS02. This is considered to be fairly significant as MS02 has been identified as being affected by dissolved phase hydrocarbons although care must be taken not to equate the propagation of the pressure gradient (which can be induced relatively quickly) between the two boreholes with particle transport between the two wells. When viewing water level variations in PW20, PW35, MS02 and even NB1 and HS2, it can be seen that all the wells appear to be affected by general water level drop during the day and a water level rise during the night. This is attributed to the groundwater pumping by residents in the surrounding residential areas. Upon closer inspection of the data, it was observed that variations were as much as 2m, and indicates that the general abstraction in the residential areas can have a significant impact on the water levels in the study area. It is not to say that all these boreholes are sharing the same set of fractures, as there could be sets of boreholes that are associated. It is likely that different fracture sets overlap in certain areas. As residents close to contaminated areas pump their boreholes, they cause contaminants to migrate and if the dissolved phase comes close to another fracture set that is pumped strongly, it is likely to flow along weak links and migrate to the next set of fractures (GPT, 2009).

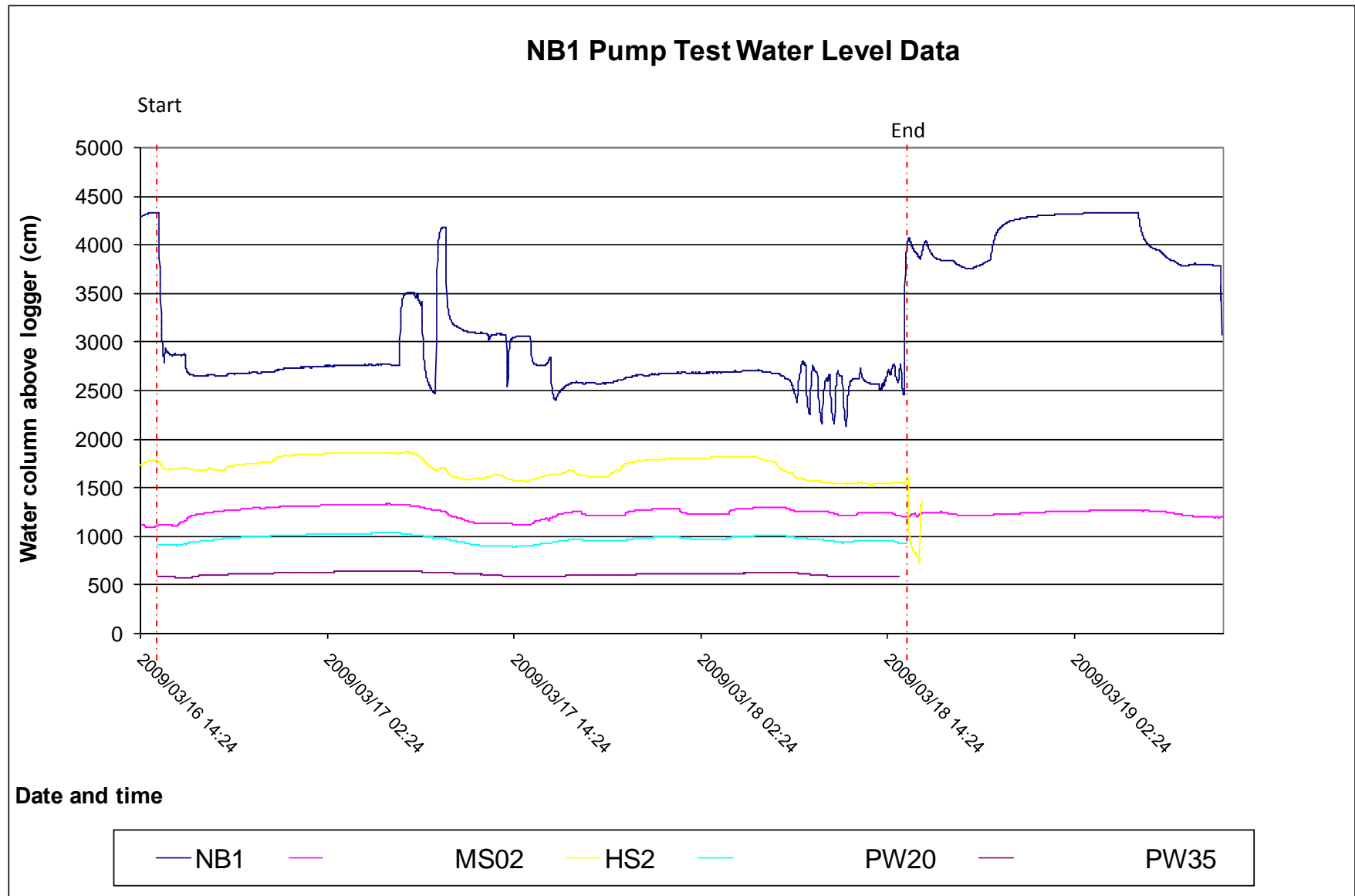


Figure 8-4: Pump test data for the entire 72 hours

### Water level data: Monday 14:00 - Tuesday 07:00

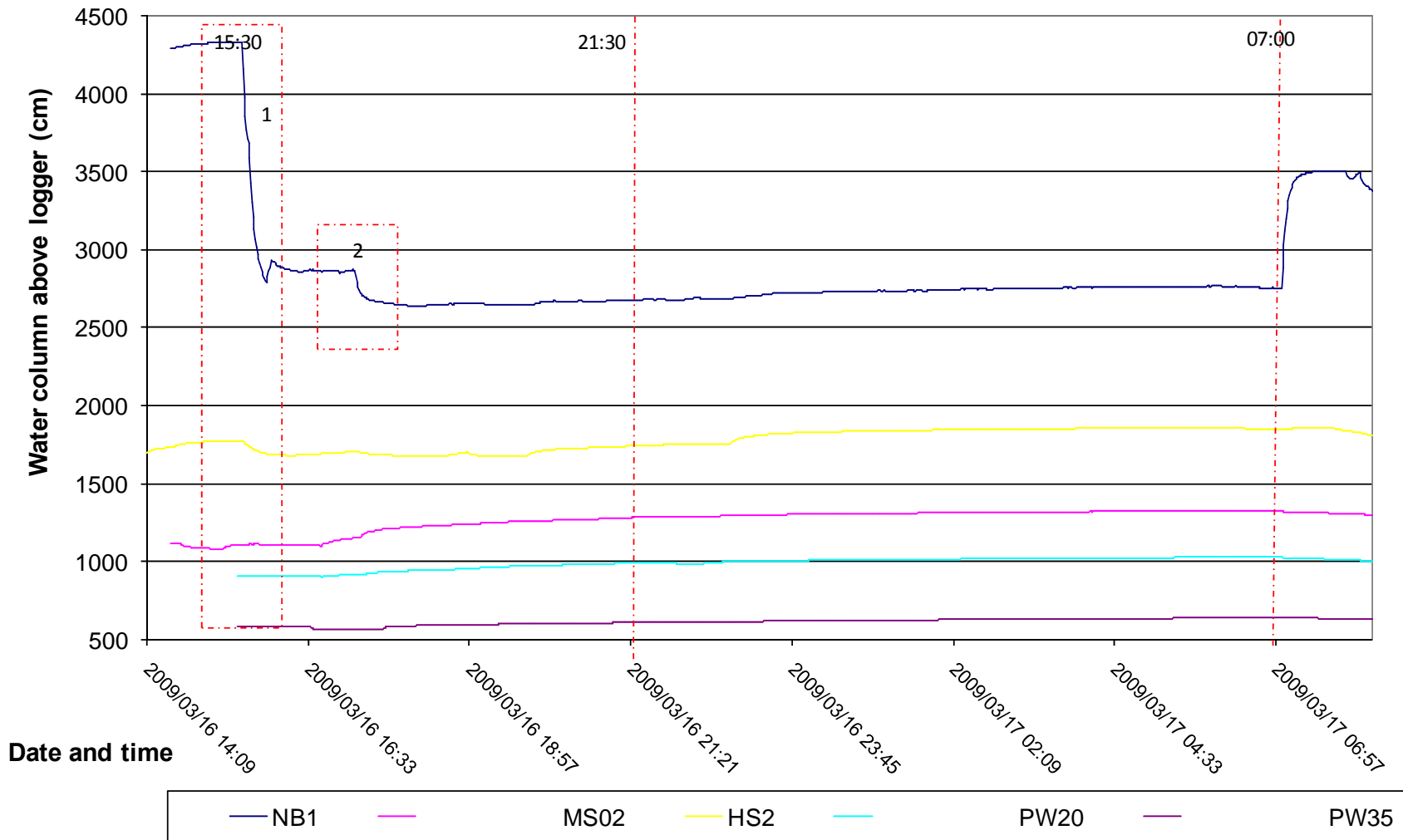


Figure 8-5: Drawdown data from Monday 14:00 to Tuesday 14:00.

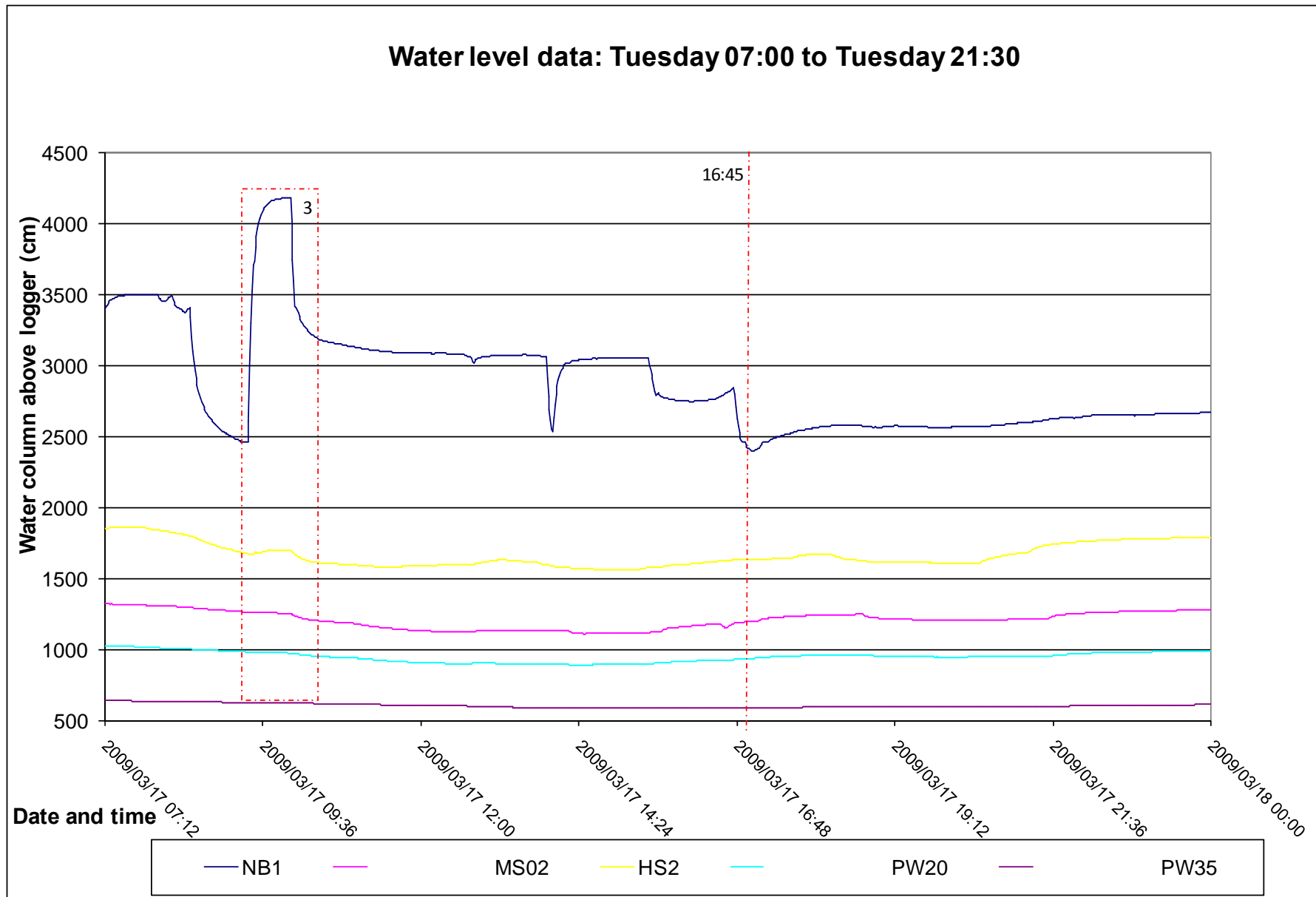


Figure 8-6: Drawdown data from Tuesday 07:00 until Tuesday 21:30

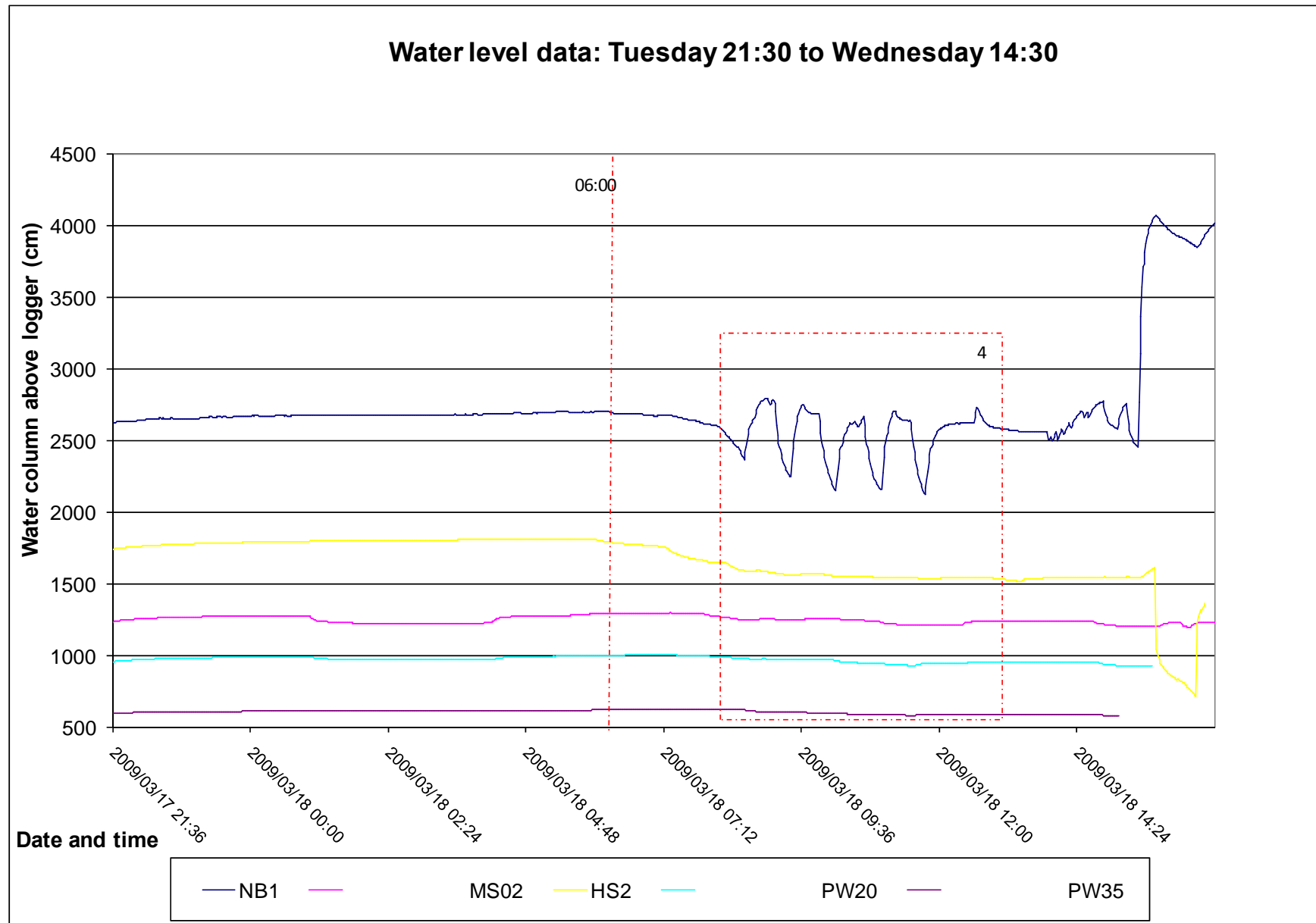


Figure 8-7: Drawdown data from Tuesday 21:30 until Wednesday 14:00

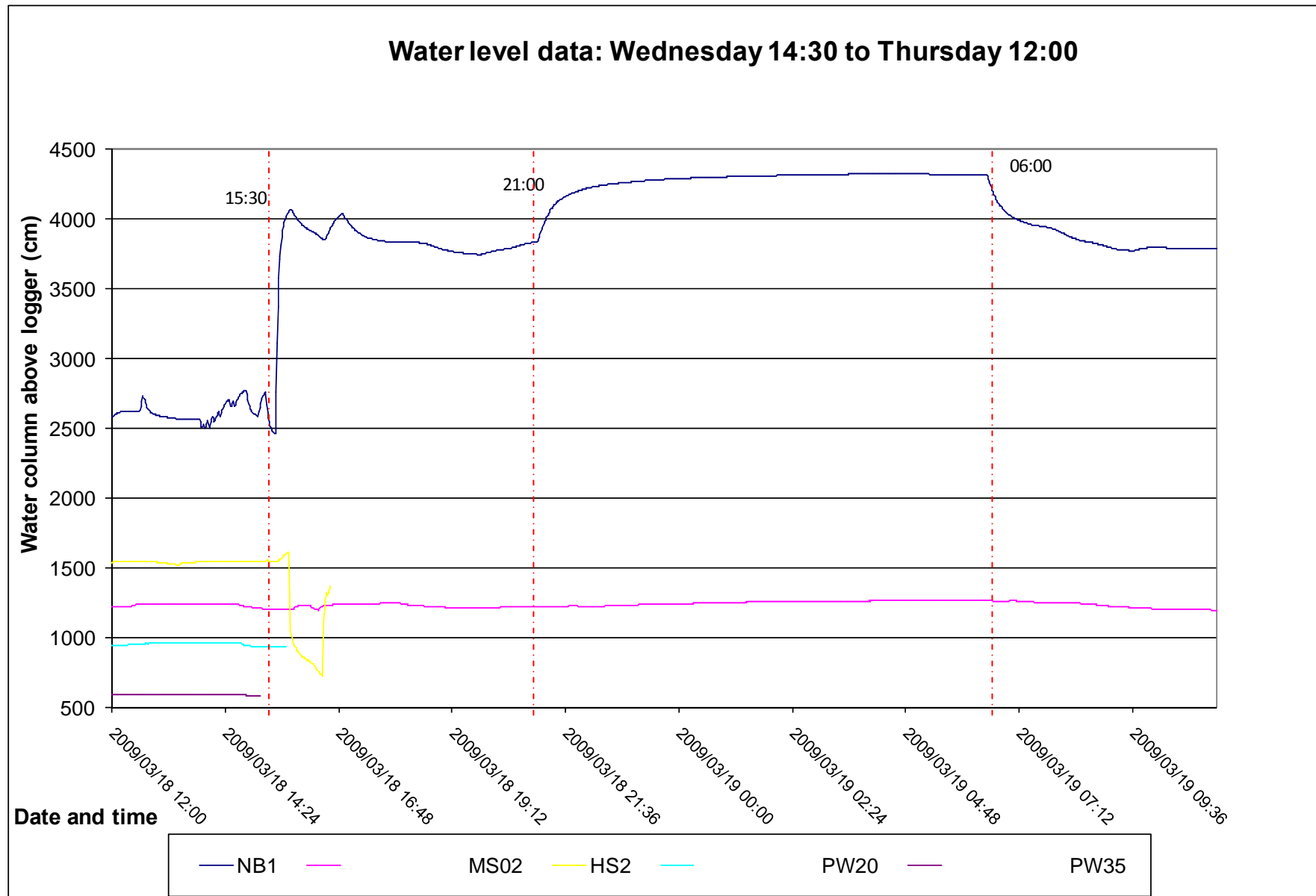


Figure 8-8: Drawdown data from Wednesday 14:30 until Thursday 12:00

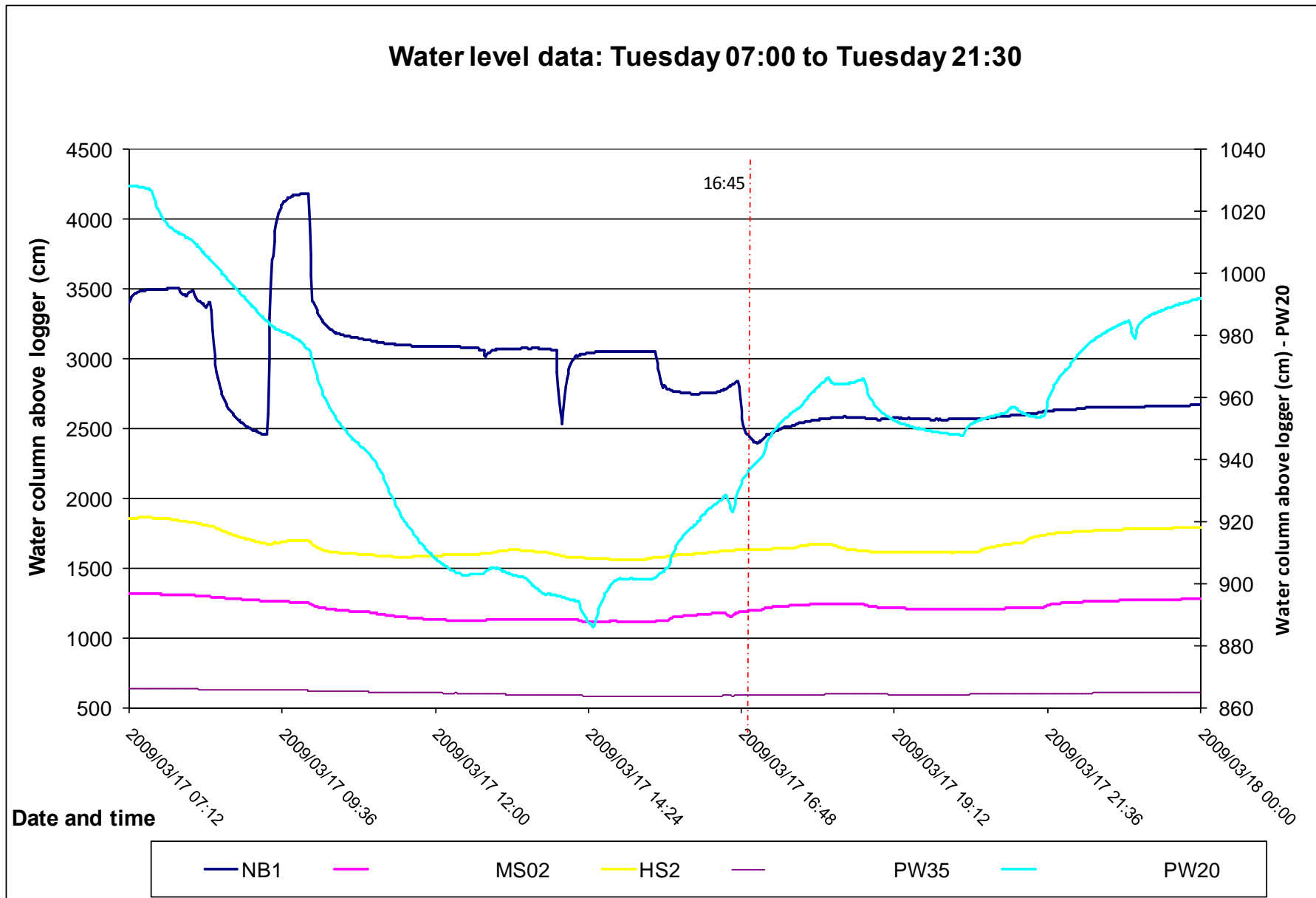


Figure 8-9. Water level data plotted on different scale axes. PW20 is plotted on the axis on the right.



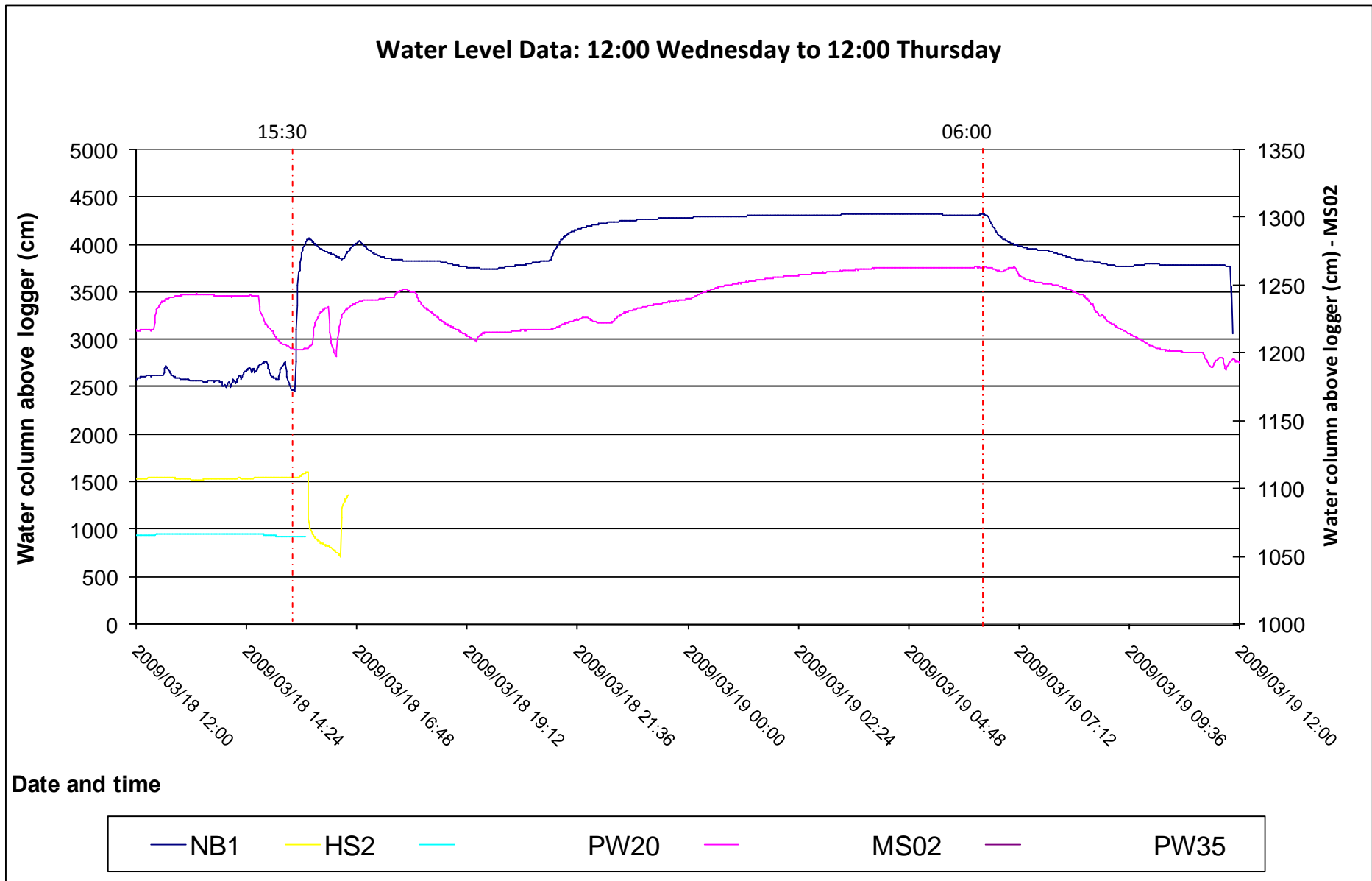


Figure 8-10 Water level data of MS02 and NB1 after pump test completion whilst HS2 was pumping

## 8.2.2 PW12 Constant Rate Discharge Test

PW12 has previously contained significant thicknesses of LNAPL (up to 7m) and due to its proximity to several of the stations was earmarked to be a potential recovery / pump and treat well. The initial water level in PW12 was measured to be 12.75m below ground level. PW17, PW9, PW16 and PW49 were The initial test located the pump at 28m depth however after commencing the test at a discharge rate of 2 l/s the water level was drawn down to the pump intake in less than 10 minutes. The pump was then lowered to a depth of 50m and the water level was allowed to reset overnight. The test was recommenced the following day and the draw down and recovery curves are displayed in Figure 8-11.

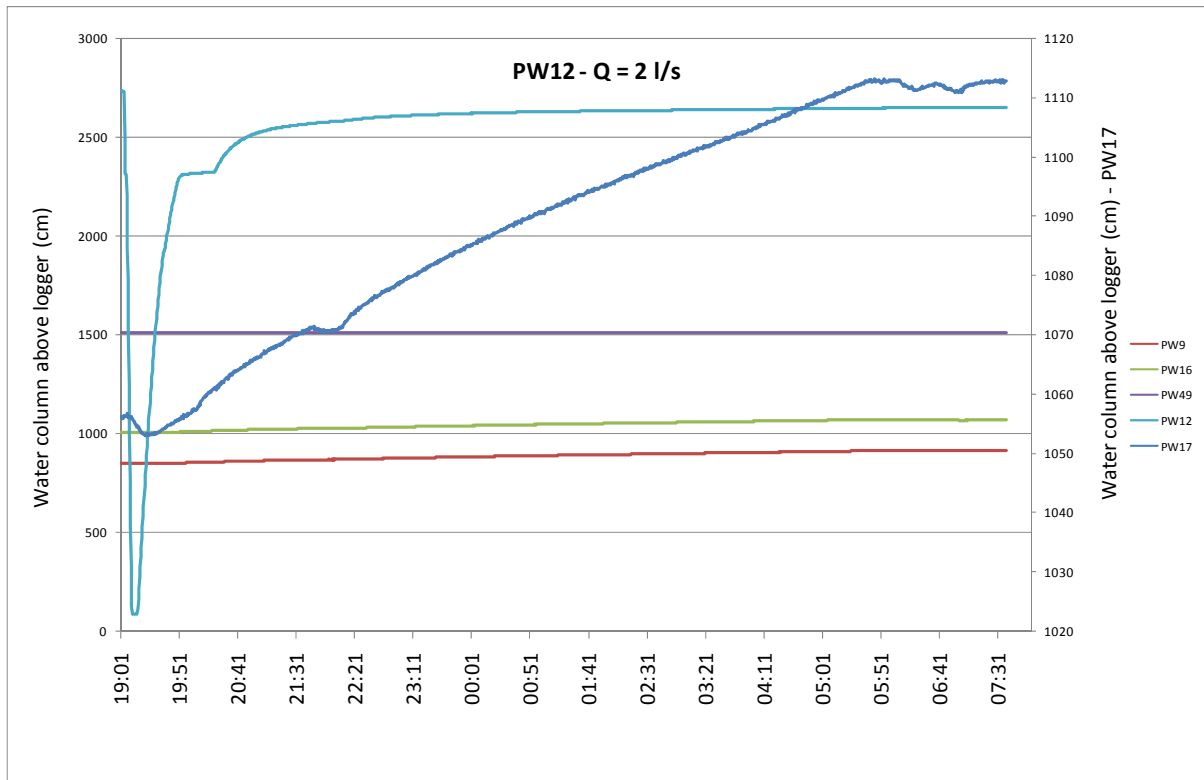


Figure 8-11: Drawdown - recovery curve of PW12.

The second pump test conducted on PW12 was carried out at pumping rate of 2 l/s and as with initial test the drawdown in the well was rapid with the water level being drawn down to depth of nearly 50m bgl in less than 15 minutes. This rapid drawdown resulted in the data not being suitable to conduct a sustainable yield calculation on the drawdown data using the Cooper Jacob method in FC Programme. However the recovery water level data was plotted against the derivate of time in FC Programme as displayed in Figure 8-12 and a transmissivity of 0.7 m<sup>2</sup>/day was calculated. A

flattening of the recovery curve was observed between 20:00 and 20:20 and this is interpreted to be due to the rising water level recharging a low yielding fracture which was dewatered at approximately 17m bgl (825m amsl) during the drawdown test. Despite the rapid drawdown and short abstraction period, a small drawdown response in the middle of a general water level recovery was observed in PW17 during the pumping of PW12. PW17's drawdown curve is displayed in Figure 8-12 on separate set of axes to display the response. No significant effect was measured in the remaining observation boreholes in part due to the short duration of pumping.

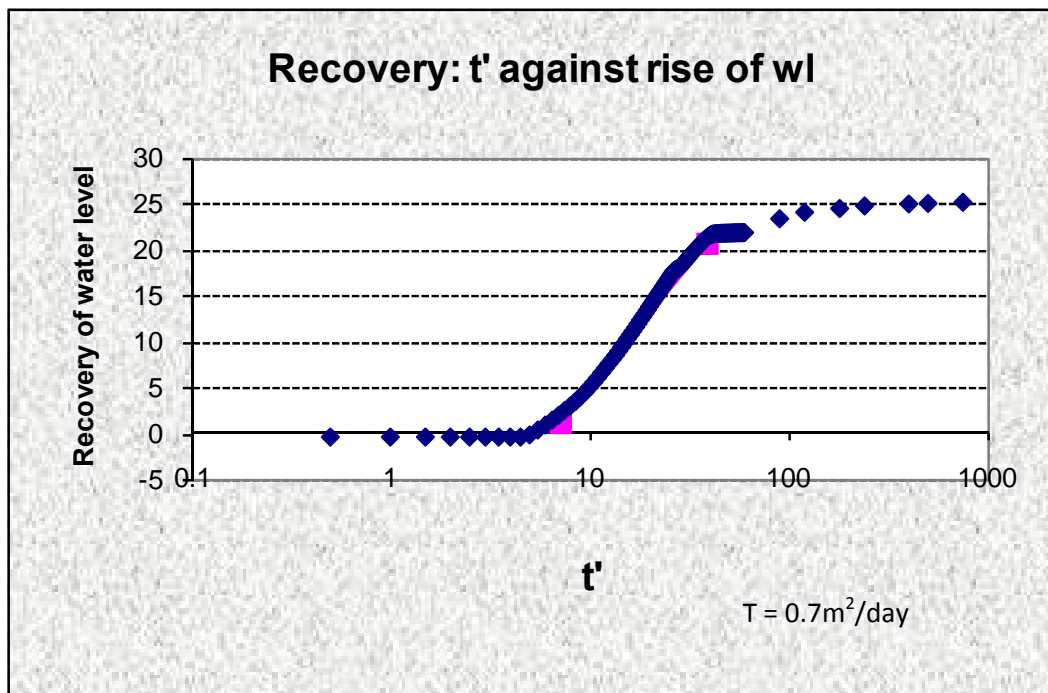
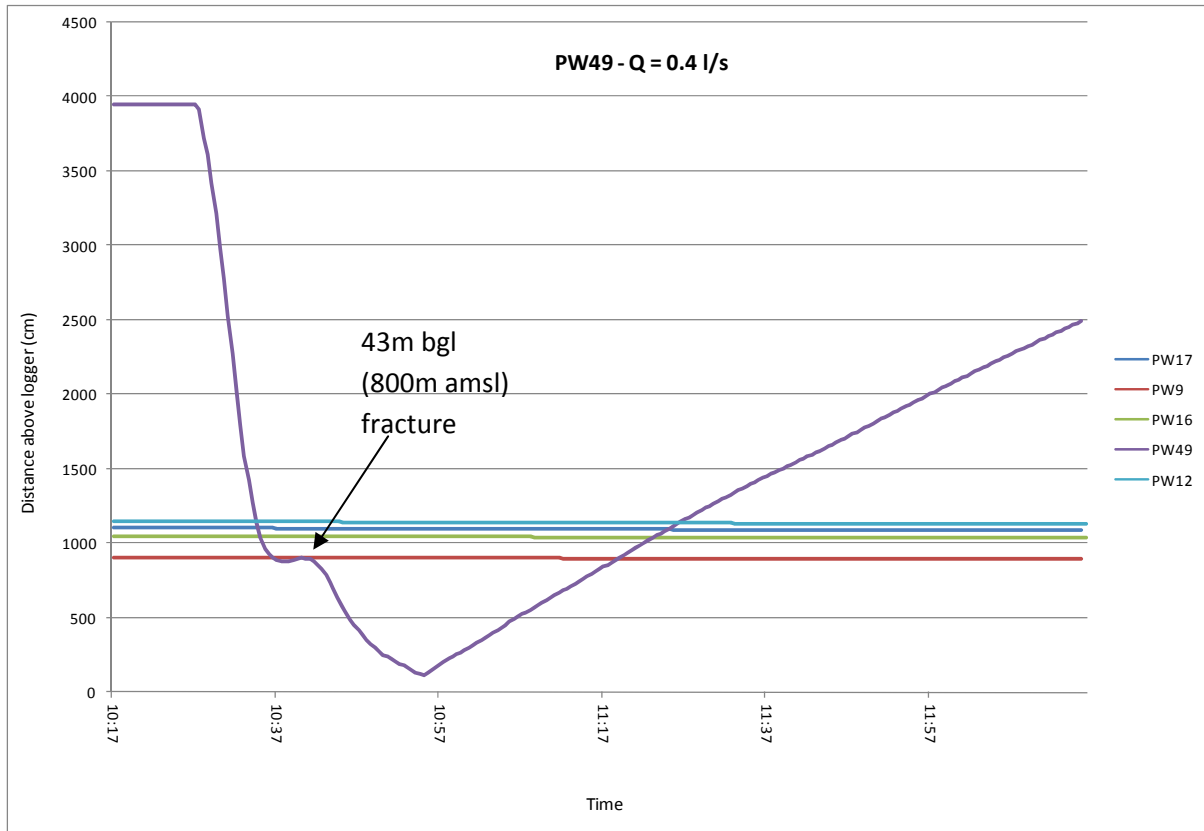


Figure 8-12: PW12 water level recovery data used to calculate transmissivity in FC Programme

### 8.2.3 PW49 Constant Rate Discharge Test – December 2009

PW49 is one of the wells in which passive recovery of NAPL has been taking place and was also earmarked to be a potential pumping/recovery well within the identified source zone area. PW49 was measured to have a 16cm of NAPL present with a corrected water level of 12.8m below ground level. PW12, PW17, PW16, and PW17 were used as observation boreholes. The well was measured to be 61m deep and the submersible pump was placed at a depth of 50m below ground level, thereby giving an available drawdown of 37m. In light of the rapid drawdown observed in PW12, the constant discharge test was conducted at a discharge rate of 0.4 l/s and the drawdown-recovery data is

displayed in Figure 8-13. It must be noted that the recovery curve was cut short due to logistical and time constraints however the recovery data is still considered to be acceptable.



**Figure 8-13: Drawdown & recovery data from PW49 constant rate discharge test**

From the drawdown curve it can be observed that despite the relatively low pumping rates (0.4 l/s), the drawdown in PW49 was rapid with the water level being drawn down to just above the pump intake within 25 minutes. A flattening of the drawdown curve was observed at approximately 43m bgl (800m amsl) which is interpreted to be a water bearing fracture. The fracture at 43m depth was dewatered within approximately 5 minutes of the water level reaching the fracture position at which point the water level continued to fall to the point where the pump was disengaged. Whilst the drawdown data was not considered to be fit for aquifer parameter estimation, the recovery water level data was plotted against the time derivative in Figure 8-14 to calculate a transmissivity of  $0.2\text{m}^2/\text{day}$ . Due to the short duration of the pumping test and low yield of the borehole no response was observed in the observation wells.

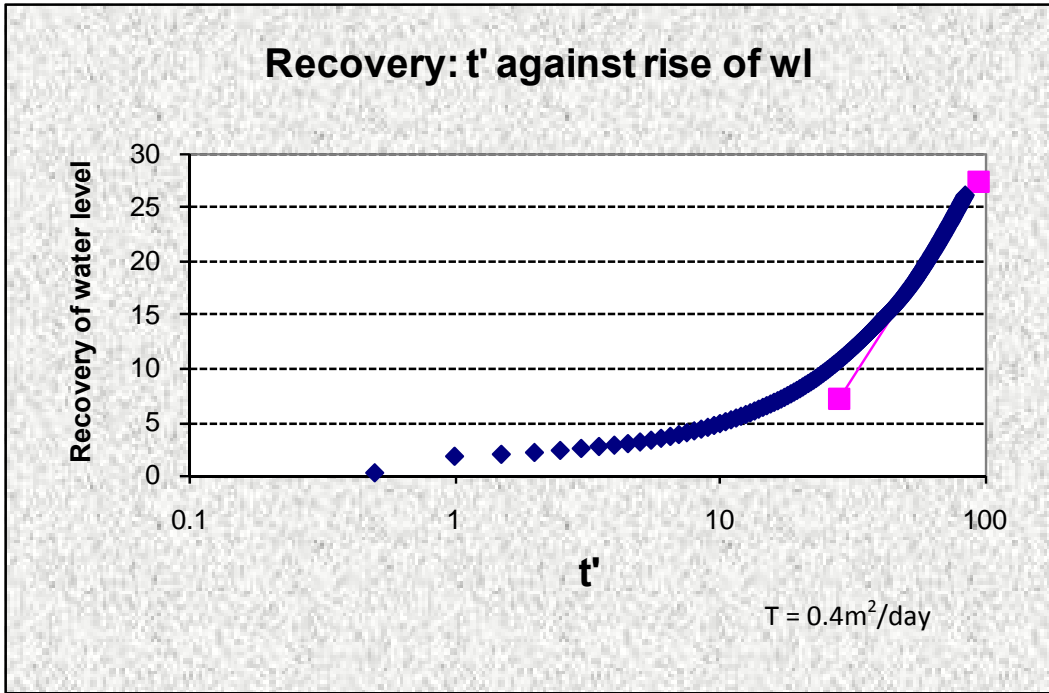


Figure 8-14: PW49 water level recovery data used to calculate transmissivity in FC Programme

## 8.2.4 PW2 Constant Rate Discharge Test – December 2009

PW2 which has been part of the pump and treat system related to Donkin Motors was tested to ascertain whether pumping could occur at higher rates than what was previously conducted. The water level in PW2 was measured to be 13.02m below ground level, the depth of the well was measured to be 72m, the submersible pump was positioned at a depth of 50m below ground level and the discharge rate was set to 0.3 l/s. PW6, PW5, RW1 and PW12 were used as observation boreholes for the pump test. The drawdown and recovery data for PW2 is displayed in Figure 8-15 below.

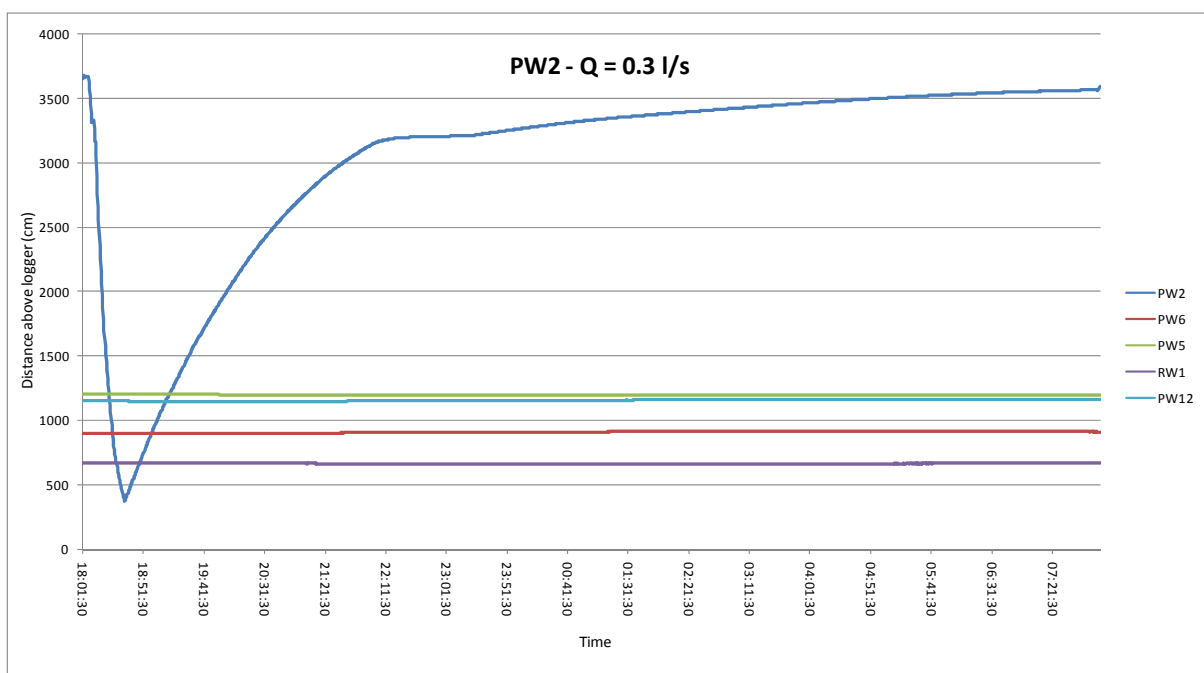
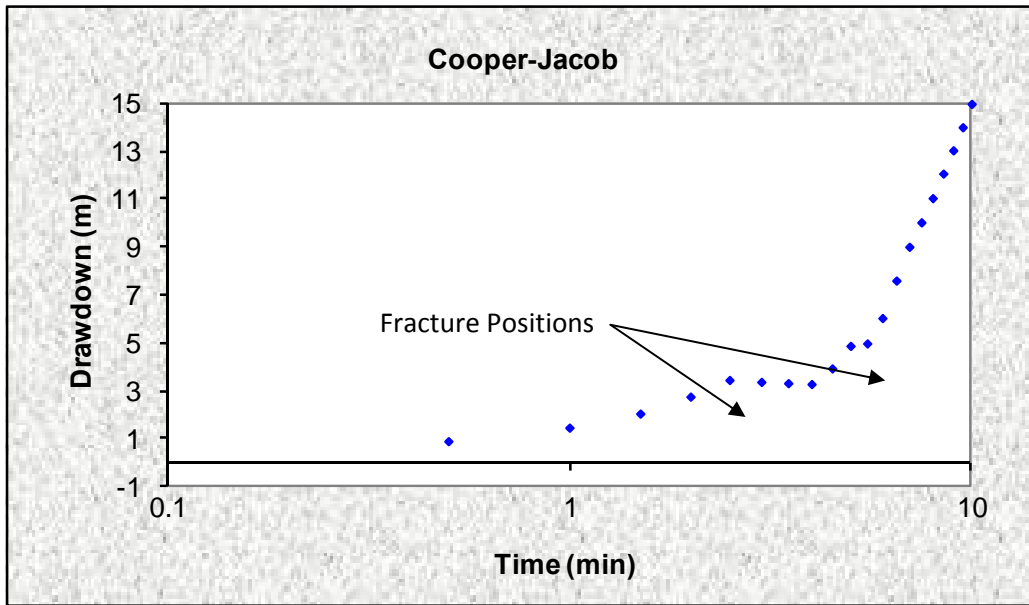


Figure 8-15: Drawdown & recovery data from PW2 constant rate discharge test

Pumping at a rate of 0.3 l/s resulted in a rapid drawdown of the water level in PW2. Figure 8-16, which displays the early stages of the drawdown versus log time plot showed dewatering of a fracture at 16m bgl (826m amsl which is a comparable depth with the fracture zone found in MW4, 80m to the north west of PW2) and another fracture at 18m bgl however these were dewatered within 5 minutes of the test commencement. Following the dewatering of these fractures the water level dropped steadily to just above the pump intake at 50m within 30 minutes at which point the pump was disengaged. Due to the rapid drawdown, the Cooper Jacob method was not employed to calculate aquifer parameters, but rather the recovery data was deemed more trustworthy to deliver aquifer parameters.



**Figure 8-16: Early time data on the Drawdown vs Log (t) for PW2**

Recovery water level data of PW2 was inputted into the FC Programme, plotting water level recovery against the derivative of time. Based upon this value a transmissivity value of 0.2 m<sup>2</sup>/day was calculated for PW2.

## 8.2.5 PW17 Constant Rate Discharge Test – December 2009

PW17, which is one of the more significantly impacted wells within the study area has been shown to potentially be located on one the main fractures sets which transports dissolved phase contamination from the northern source zones towards the vicinity of De Villiers Street and Bird Street. The currently installed pump was used to conduct an 8 hour pump test and the drawdown data of PW17 and the neighbouring observation wells (PW16, PW9, PW12 and PW49) is displayed in Figure 8-17.

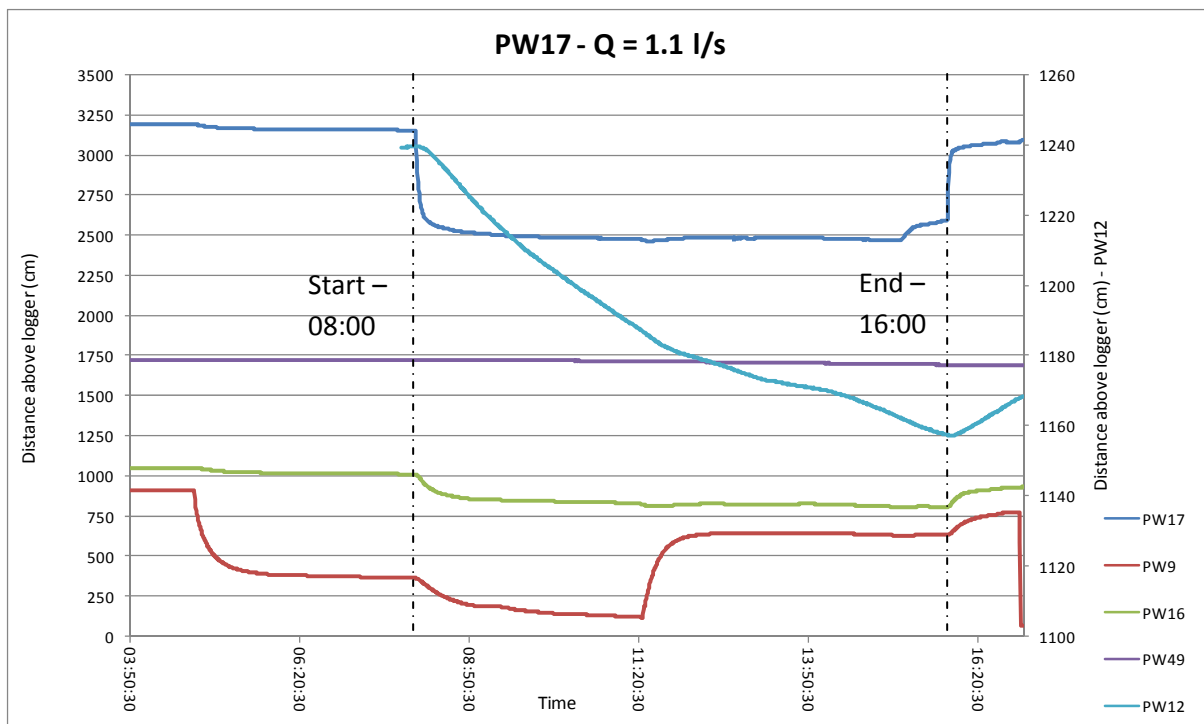


**Figure 8-17: Drawdown & recovery data from PW17 constant rate discharge test**

PW17 was pumped at a constant rate of 1.1 l/s with the pump test beginning at 08:00. The measured rest water level in PW17 was found to be 16.02m below ground level and the well is known to be 60m deep. The main water bearing fracture is considered to be at 48m bgl which provides an available drawdown of 32m. With reference to the diagram above it can be seen that a relatively rapid drawdown occurred in which the water level dropped 7m to a depth of 23m, at which point the drawdown curve flattened out and the water level remained at 23m for the duration of the pump test. (The slight recovery at the end of the test is due to the dam overflowing into the hole when it became full.) A response to the pumping of PW17 can be observed in PW16 which displayed drawdown of 2m. The owner of PW9 by mistake switched on PW9's pump just before 05:00 and the drawdown



curve of PW9 can also be observed in Figure 8-17. When PW17 was engaged at 08:00 a drawdown response in PW9 can be observed. PW9's pump was switched off at approximately 11:30 and the water then recovered to a level where it was in equilibrium with the pumping of PW17. A small response in PW17 can also be seen in Figure 8-17 when PW9 was turned off.

The overall observed drawdown in PW9 in response to PW17's pumping was found to 2.5m. In both PW16 and PW9 the response to the pumping in PW17 was almost immediate. Recovery also starts immediately in PW16 and PW9 when PW17 was turned off. What is of interest is that the pumping of PW9 only invoked a very minor drawdown response in PW17 and PW16. Whilst the pumping rate of PW9 is unknown, it was sufficient to induce a pressure differential in the well which caused comparable drawdown to that of PW17 (approximately 7m). PW12's water level was plotted on a separate axis to exaggerate the small water level fluctuations. From Figure 8-17 it can be seen that PW12 began to decrease almost instantly, as a response to PW17's pumping. A slight flattening of PW12's drawdown curve at 11:00 indicates that the water level also responded to PW9 being turned off. Over the course of the 8 hour pump test PW12's water level dropped by 80cm, and began to rise as soon as PW17 was disengaged.

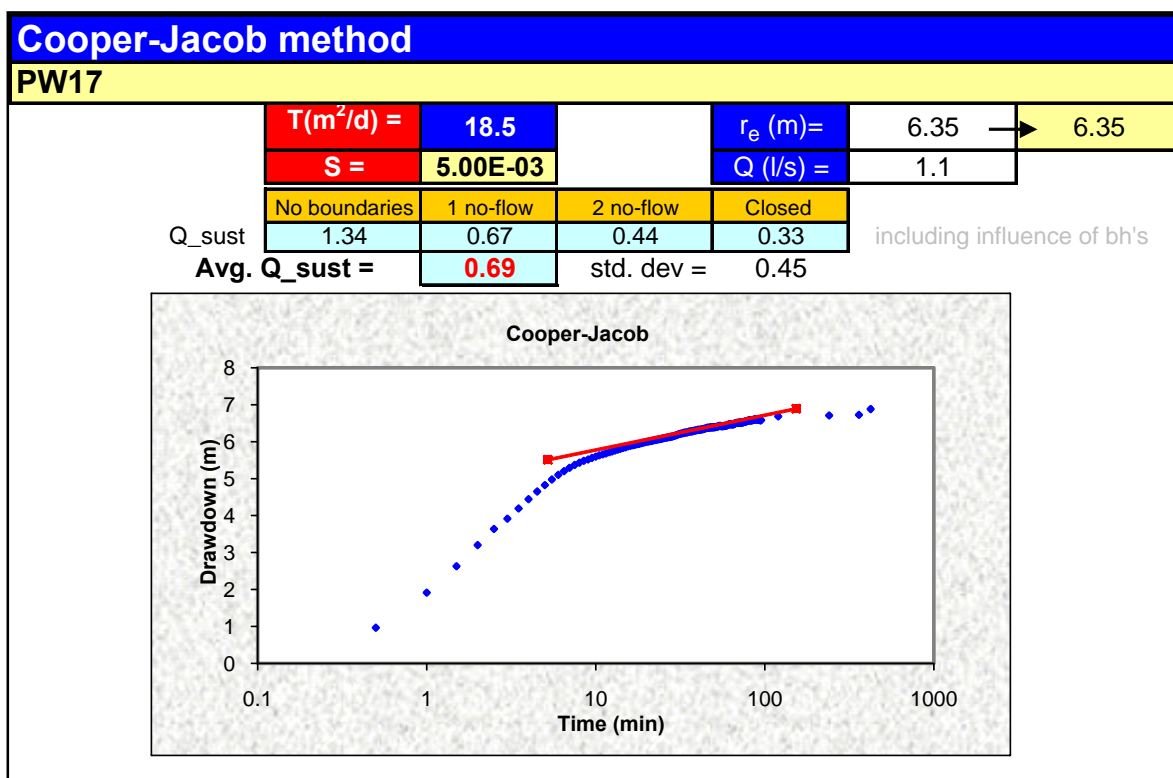


Figure 8-18: Sustainable yield Cooper Jacob method for PW17

The drawdown data from PW17 was inputted into the FC Programme and the Cooper Jacob method was used to calculate a transmissivity value and sustainable yield value for PW17. A transmissivity of approximately  $18.5 \text{ m}^2/\text{day}$  and an average sustainable yield of  $0.69 \text{ l/s}$  was calculated by the Cooper Jacob method. Whilst the drawdown data for PW17 was of good quality, the one shortcoming was that in order for a pump test to deliver truly robust data, the aquifer needs to be stressed (pumped at a rate beyond its capacity) during the test. Usually this means that the main water bearing fracture must be reached and dewatered during the test and the sustainable yield calculations are based upon the transmissivity of the main water bearing fracture. In the case of PW17 the main fractures zone is at approximately  $48\text{m}$  and so was not reached at the given pumping rate of  $1.1 \text{ l/s}$  which only induced a drawdown to a depth of  $23\text{m}$  below ground level. In light of this, the true transmissivity of the borehole is considered to be underestimated by the current data. The recovery water level vs  $t'$  was plotted in Figure 8-19, with a calculated transmissivity of  $20.8\text{m}^2/\text{day}$ , which is comparable, to the pump test drawdown data.

Figure 8-20 displays the logarithm of drawdown vs the logarithm of time (Theis plot) and from the diagram certain flow regimes can be identified based upon the gradient of the tangent lines which have been inserted. The blue tangent has a slope of 1 and indicates early time well bore storage for the first two minutes. From 2 minutes to 6 minutes, linear flow (indicated by the green line with slope = 0.5) which signifies flow from the fracture systems is dominant. From 6 minutes to approximately 50 minutes, bi-linear flow (indicated by red line with slope = 0.25) which signifies flow from the fracture and matrix system is dominant. A flattening of the log-log curve 1 to 1.5 log cycles after the well bore storage flow regime is indicative of potential radial flow conditions (GHR 611 Lecture Notes), and whilst this is observed on the plot after 50 minutes of pumping (yellow horizontal line), this is considered a relatively short time period with which to induce radial flow, in addition to this, the drawdown derivative plots do not indicate radial flow conditions at this point as no flattening of the  $s'$  curve was observed. Moreover, Figure 8-21, displays the fourth root of time vs drawdown diagnostic plot, with the straight line indicating bi-linear flow conditions to be the dominant flow regime.

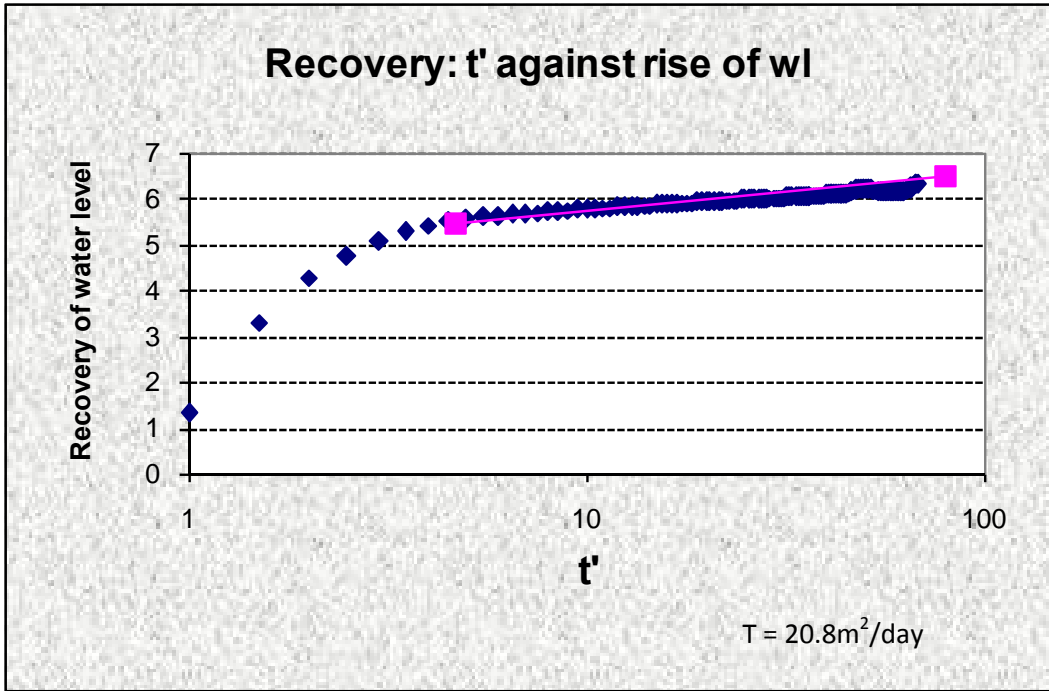


Figure 8-19 Recovery of water level vs  $t'$

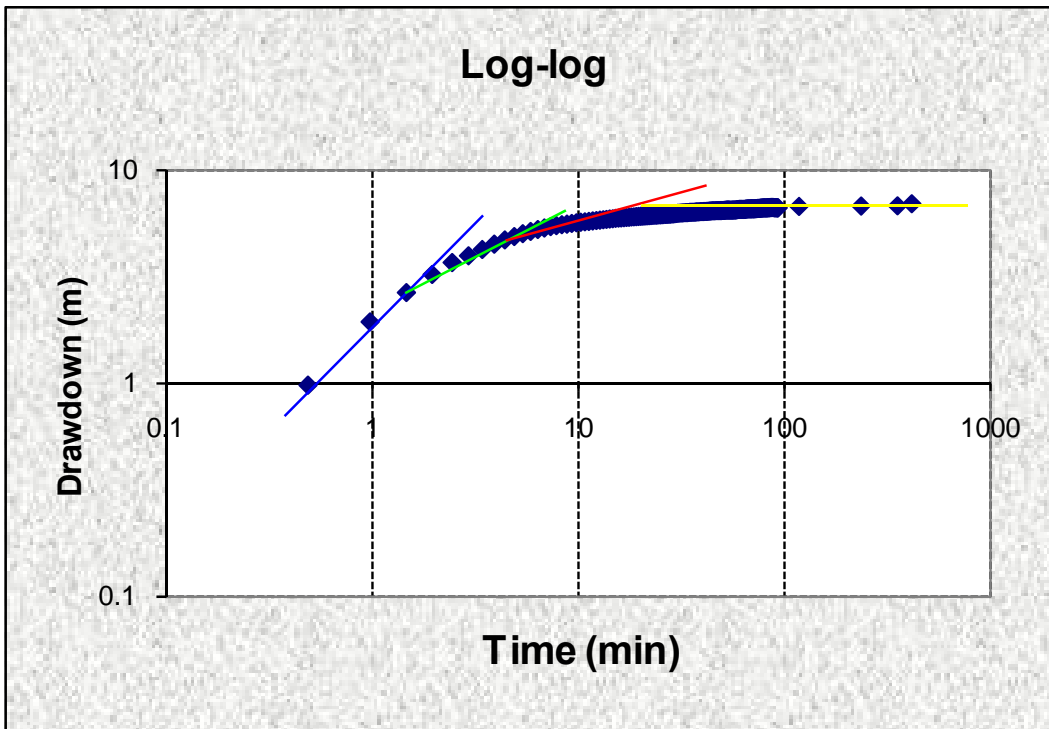


Figure 8-20 Theis (log-log) plot of drawdown vs time.

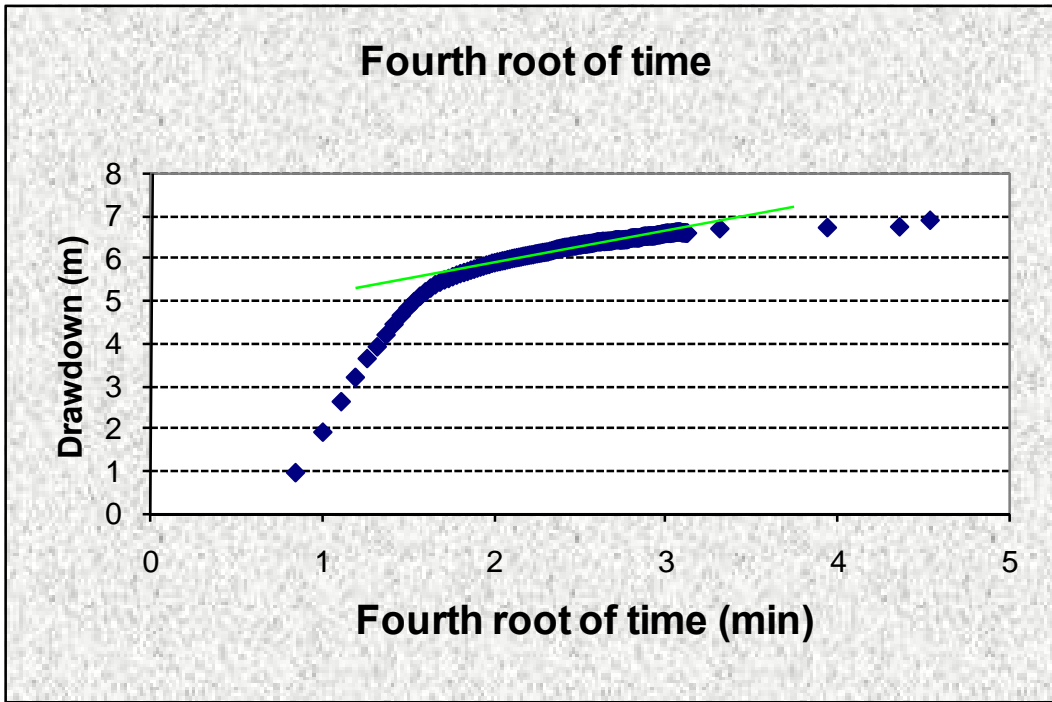
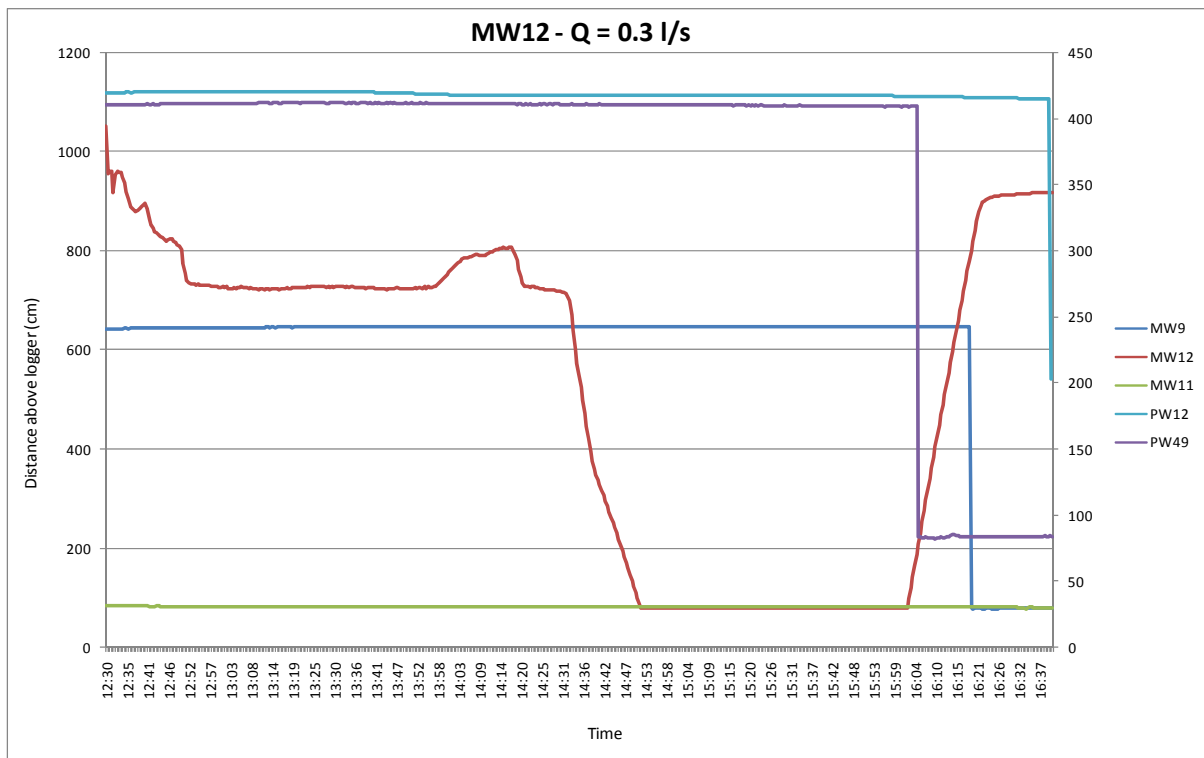


Figure 8-21 Fourth root of time vs drawdown for PW17

## 8.2.6 MW12 Pump Test –December 2009

MW12 was previously identified as being one the monitoring wells on the Total Beaufort West forecourt which had significant amounts of NAPL present. MW12 is 24m deep and had a measured water level of 13.47m below ground level at the time the test was commenced. The pump intake was located at 23m below ground level and the discharge rate was set to 0.3 l/s. MW9, MW11, PW12 and PW49 were used as observation boreholes.



**Figure 8-22: Drawdown & recovery data from MW12 constant discharge test**

The constant discharge test in MW12 lasted for approximately two and half hours in which time the well was completely dewatered at a pumping rate of 0.3 l/s. From the drawdown curve the water level can be observed to drop from the rest water level to a constant level at approximately 16.5m bgl (829m amsl). The small fluctuations during the first twenty minutes of the test were due to valve adjustments in order to maintain a discharge rate of 0.3 l/s. The hump in the drawdown curve at approximately 14:10 was thought to be due to some form a mechanical blockage at the pump intake which was eventually cleared at approximately 14:20. The flattening of the drawdown curve at 16.5m below ground level is interpreted to be a fracture position and diagnostic derivative plots of the drawdown data confirm the presence of a fracture at this position as displayed in Figure 8-23. Once this fracture was dewatered the water level was observed to fall to the level of the pump intake within

20 minutes. It must be noted that whilst no detectable NAPL layer was present in MW12 at the beginning of the test, approximately 400 litres of NAPL was pumped from MW12 into the onsite separator during the pump test. This is a good example of how NAPL within fracture networks can be mobilised towards a well once the potentiometric surface drops below a certain threshold level, allowing the NAPL to penetrate deeper and mobilise along bedding plane fracture pathways. Due to the safety concerns of having a large amount of product in the separator, instruction was given to the site management to lodge a maintenance call to have the separators cleaned urgently.

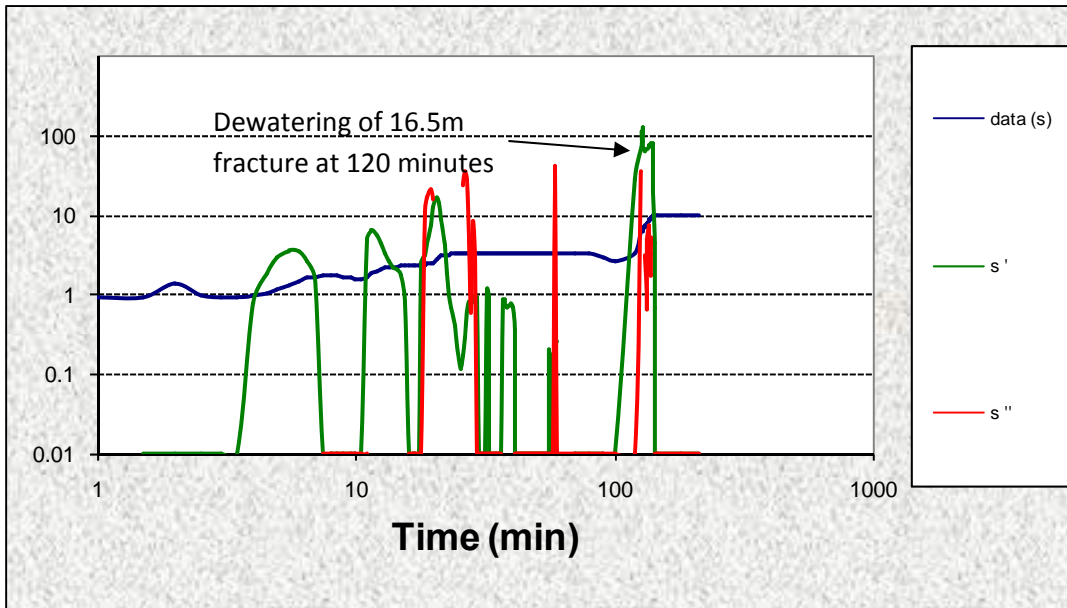
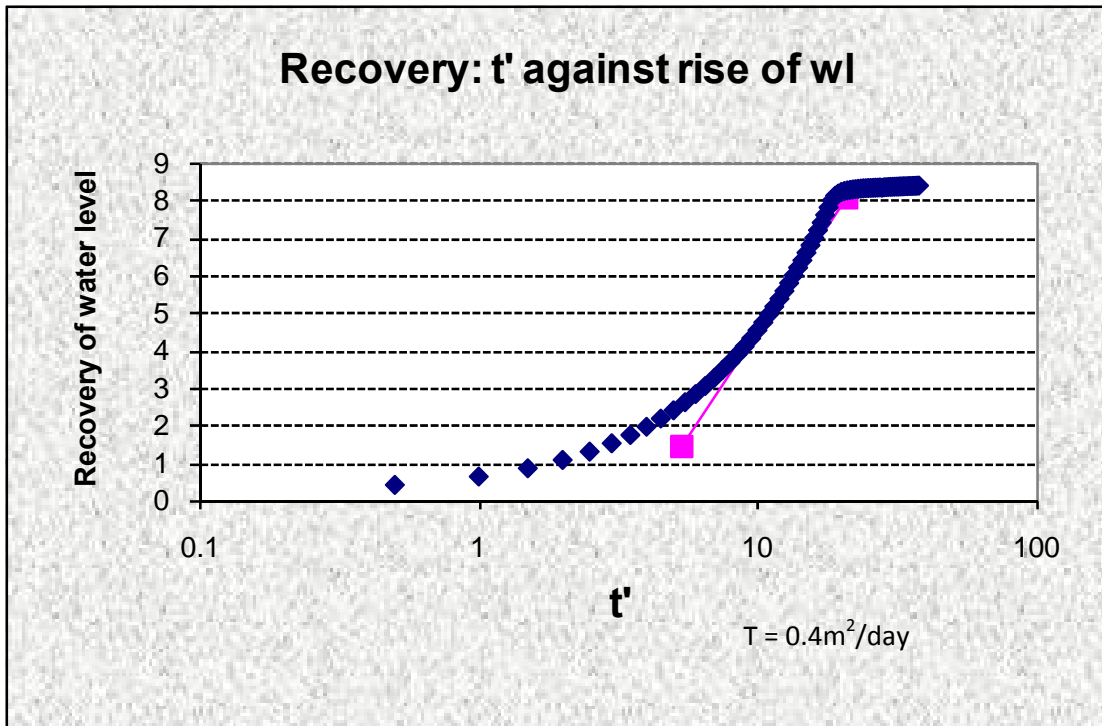


Figure 8-23 Drawdown derivative plot of MW12



**Figure 8-24: Sustainable yield Cooper Jacob method for MW12**

The recovery data was inputted in the FC Programme a transmissivity value of 0.4 m<sup>2</sup>/day was calculated, which is consistent with other affected boreholes in the nearby area such as PW12 and PW49

### ***8.3 Non Aqueous Phase Liquid Recover Tests***

LNAPL recovery tests, otherwise known as “baildown” tests are a common method by which the effective conductivity of free-phase hydrocarbons are assessed under prevailing hydraulic conditions. These tests have particular relevance in hydrocarbon contamination investigations where measures of hydrocarbon fluid mobility and recoverability are required in order to assess the feasibility and effectiveness of various forms of product removal techniques for site remediation. Baildown test in their most basic format entail the removal of a volume of product from a monitoring well or borehole (assumed to be an instantaneous removal as with slug-out tests), followed by measuring the recovery of the NAPL column within the well. This data is often inputted directly into hydraulic conductivity estimation models such as the Bouwer & Rice model and is analysed as if it were a simple slug test, which is incorrect.

As hydrocarbons are removed from a well during a slug test, the removal affects both the hydrocarbons and the groundwater in the vicinity of the well (Huntley, 2000). Consider the following equation:

$$Z_p = Z_w + \rho_r (Z_o - Z_w) \quad \text{Eq 9.1}$$

Where  $Z_p$  is the potentiometric surface elevation,  $Z_o$  is the oil/air interface elevation,  $Z_w$  is the oil/water interface elevation and  $\rho_r$  is the relative density of the LNAPL. According to Eq 9.1, as LNAPL enters the well (subsequent to the initial NAPL removal), the oil water interface will decline to maintain the potentiometric surface. In the scenario where the potentiometric surface resets very quickly, a modification to the Bouwer & Rice method can be employed where by the calculated transmissivity is multiplied by  $1/(1-\rho_r)$  in order to arrive at a LNAPL transmissivity (Huntley, 2000). In certain low permeability environments, or situations where a well is not fully screened, the potentiometric surface will not recover quickly, but will vary during the LNAPL recovery. In this case a variant of the Cooper Jacob method known as the Jacob Lohman method (1952) must be employed where the inverse of LNAPL flow into the well ( $1/Q$ ) is plotted against the logarithm of time ( $\log t$ ) as a straight line and a slope can be used to calculate transmissivity by

$$T = \frac{2.3}{4\pi s \Delta\left(\frac{1}{Q}\right)} \quad \text{Eq 9.2}$$

Where  $s$  is the LNAPL drawdown (assumed constant), and  $\Delta\left(\frac{1}{Q}\right)$  is the change in  $(1/Q)$  per log cycle of time. A further variation on the Cooper Jacob equation is when LNAPL drawdown is varying throughout the test (along with a varying potentiometric surface). In this case  $s/Q$  is plotted against time, which compensates somewhat for the varying drawdown, and the LNAPL transmissivity can be calculated as

$$T = \frac{2.3}{4\pi \Delta\left(\frac{s}{Q}\right)} \quad \text{Eq 9.3}$$

Where  $\Delta\left(\frac{s}{Q}\right)$  is the change in  $(s/Q)$  per log cycle (Huntley, 2000).

Two boreholes, namely PW12 and PW49 were targeted for LNAPL recovery since these wells had previously been observed to have significant free phase thicknesses (4m in PW49 and 7m in PW12). The first recovery test was performed on PW12, which on 17 March 2009 had a NAPL column of 7.46m. During the recovery from PW12 the NAPL level was reduced from 7.46m to 4.33m, with approximately 160L of green LNAPL which is considered to be unleaded fuel, being removed from the borehole. From the LNAPL recovery data displayed in Figure 8-25, it can be seen that the



potentiometric surface took over 100 minutes to stabilise, whilst the LNAPL drawdown varied significantly over the observation period.

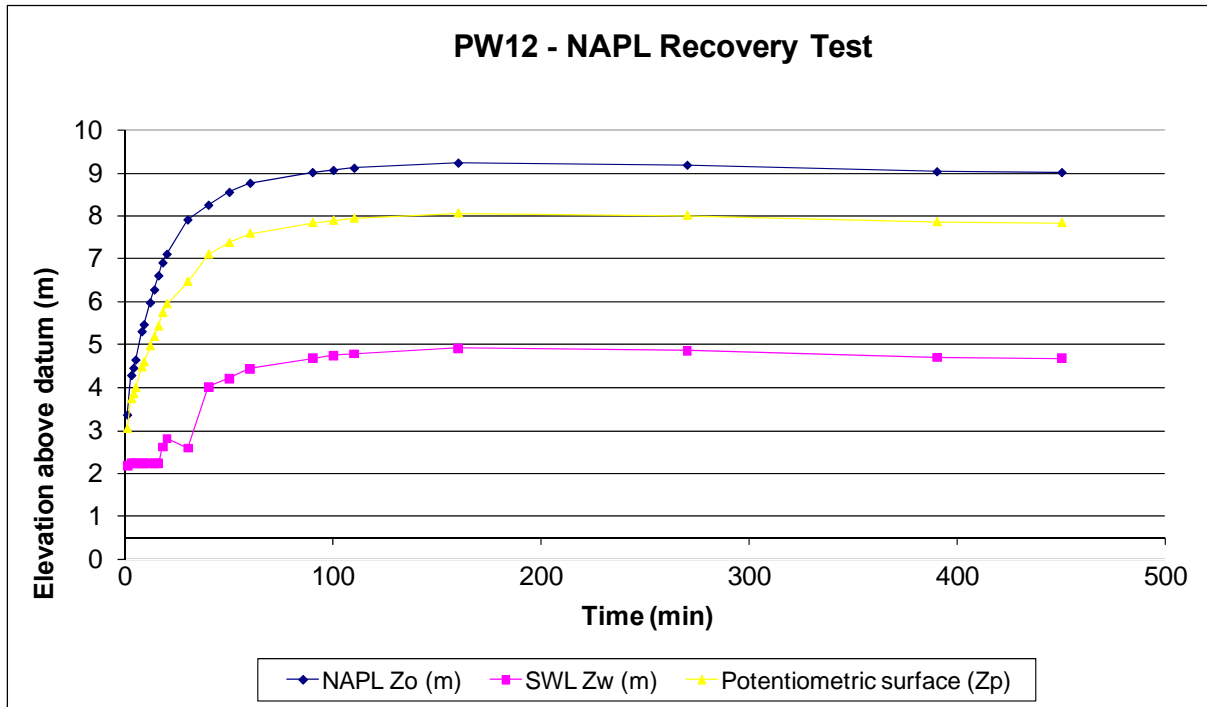
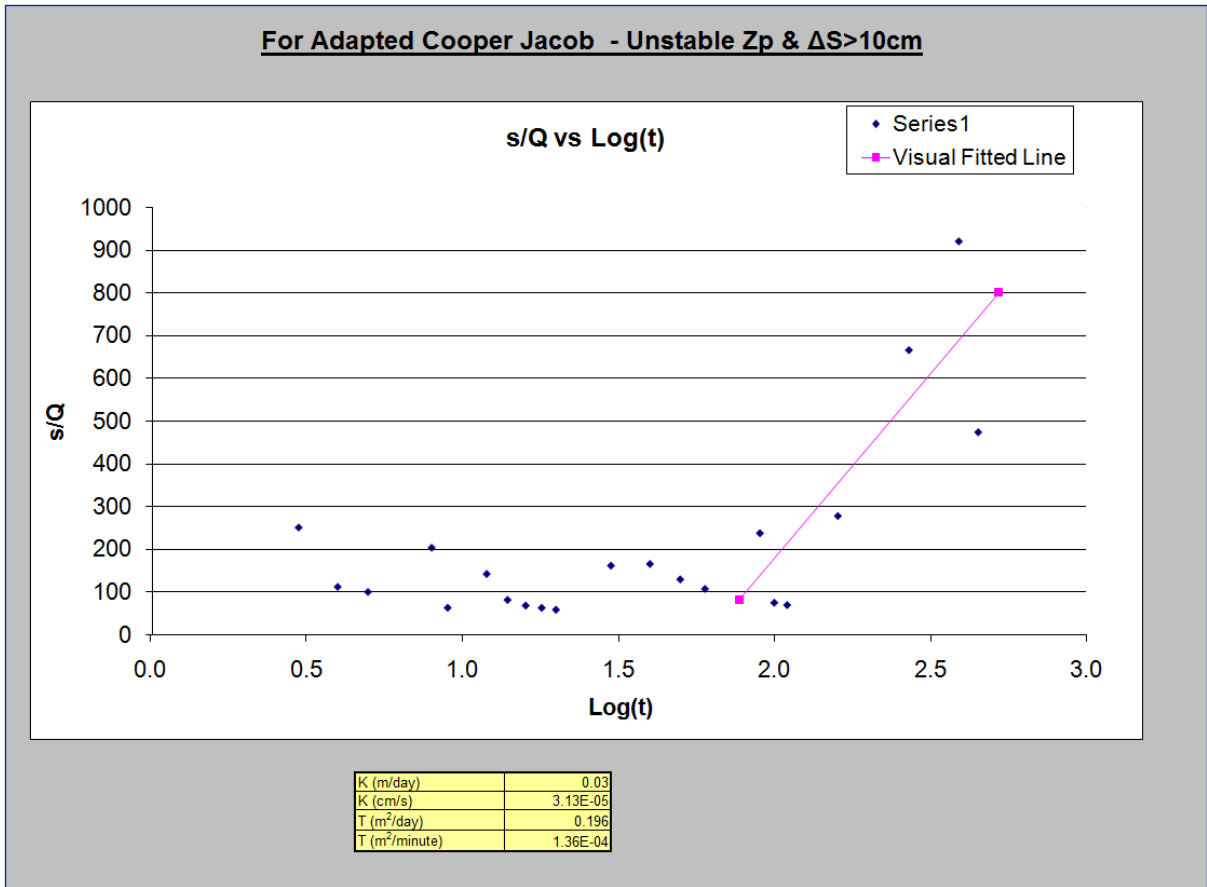


Figure 8-25 LNAPL recovery data for PW12

For this reason the modified Cooper Jacob equation displayed in Eq. 9.3 was used to fit the data and the  $s/Q$  vs time graph is displayed in Figure 8-26 along with the fitted line on the late time data points. The LNAPL transmissivity for PW12 was calculated to be  $1.3 \times 10^{-4} \text{m}^2/\text{minute}$ , which is considered to be a low value.



**Figure 8-26** s/Q vs Log t plot for PW12

The second LNAPL recovery test was conducted on PW49, with the LNAPL thickness being reduced from 1.09m to 0.11m and approximately 23L of green LNAPL being removed from the borehole. The recovery data is displayed in Figure 8-27. From the figure it can be seen that the potentiometric surface stabilised after approximately 70 minutes, whilst significant LNAPL drawdown was observed during the initial stages of the test. For these reason, as with PW12, the adapted Cooper Jacob method was used to estimate transmissivity as is displayed in Figure 8-28. Based upon the data, a LNAPL transmissivity of  $1.8 \times 10^{-4} \text{m}^2/\text{minute}$  was calculated.

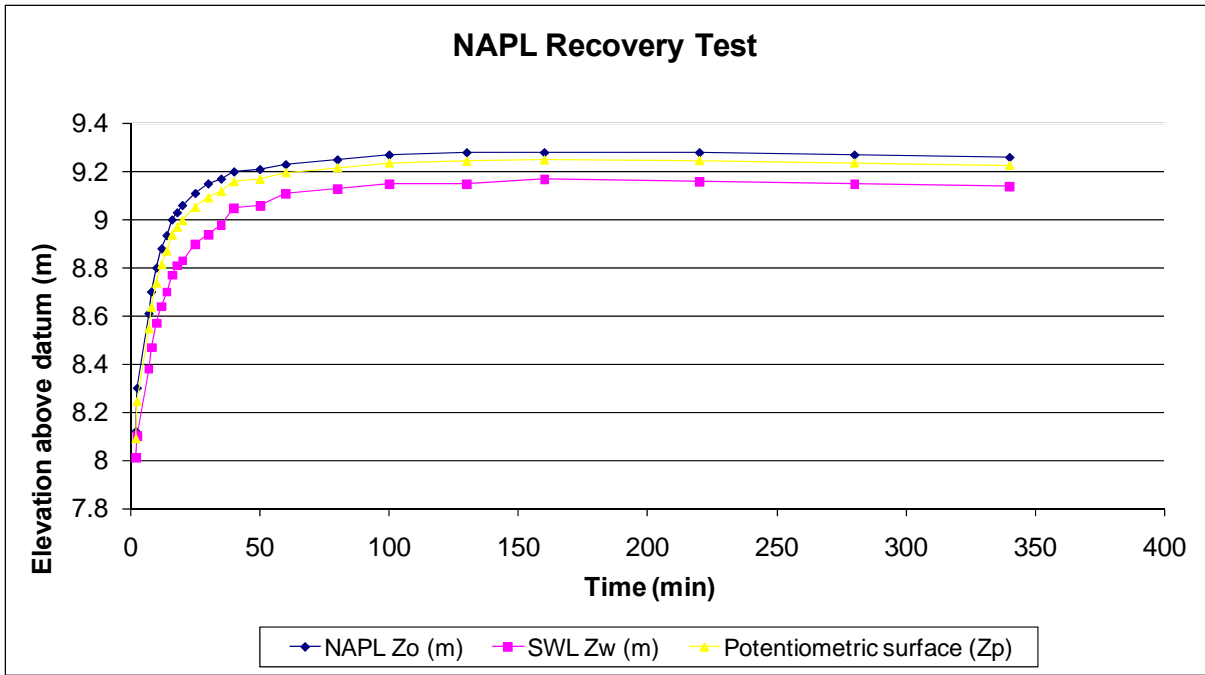


Figure 8-27 LNAPL recovery data for PW49

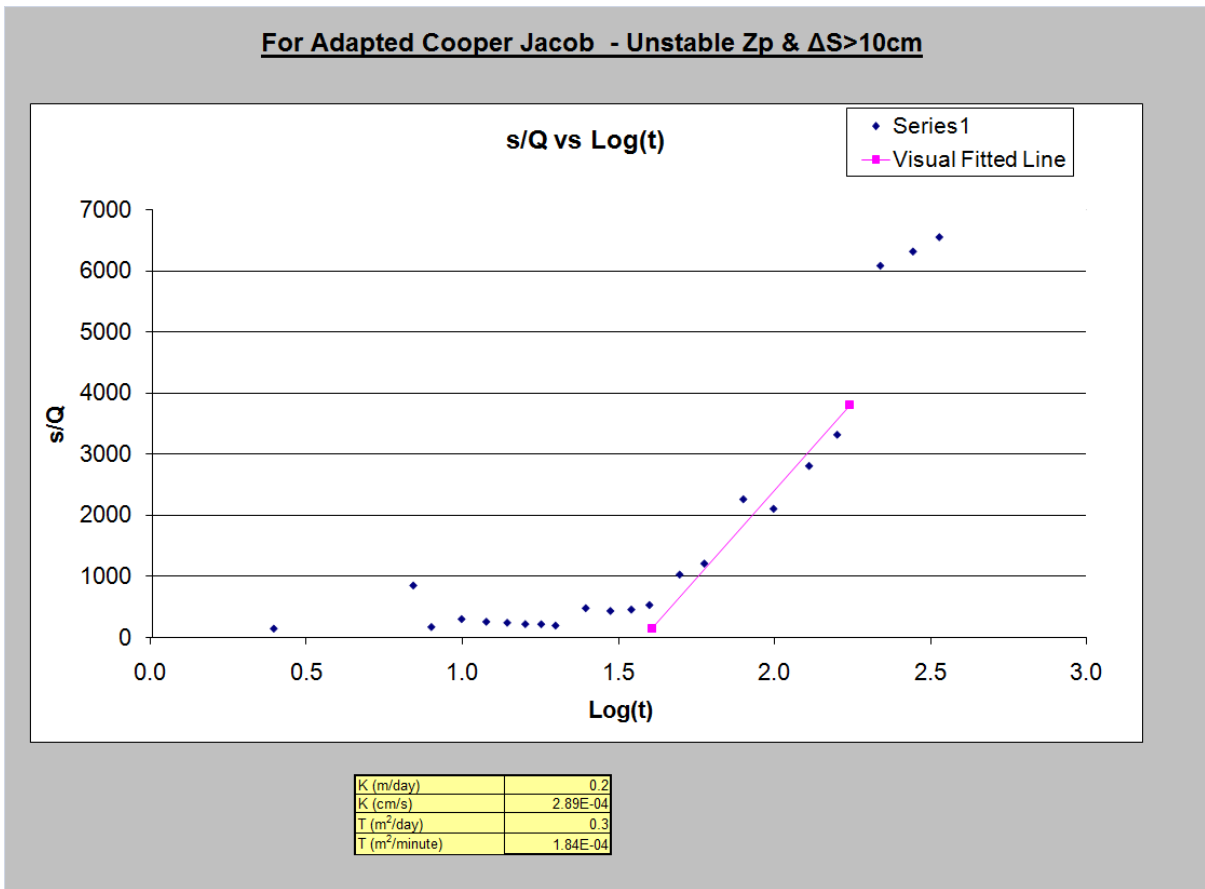


Figure 8-28 s/Q vs Log t plot for PW49

It is important to note however, that the equations and approaches for baildown tests were developed for porous primary aquifer settings and not for fractured rock settings. In porous aquifers the removal of LNAPL from the borehole will induce LNAPL flow into the borehole along its screened section from the adjacent formation in order to re-establish head equilibrium between the borehole and the formation. In a fractured setting this may not occur since flow of LNAPL into the borehole may be more controlled by potentiometric conditions and LNAPL entry pressure regimes within the fractures surrounding the borehole, than by LNAPL column thickness variation inside the borehole. Figure 8-29 and Figure 8-30 display the LNAPL thickness over time for the two respective boreholes, and apart from initial variations, virtually no recovery can be seen on the late time portions of the graphs. The interpretation from the modified slug test methods is therefore not considered to produce reliable measures of transmissivity since the slug test methods assume a porous medium conceptual model whilst the current scenario relates to fracture rock. It must be noted though, that the recoverability of LNAPL under pumped conditions may be significantly different as this will alter the potentiometric conditions and LNAPL entry pressure regimes in the fractures connected to the borehole. This scenario was noted in the pump test of MW12, where no apparent LNAPL was present prior to the test (and so no baildown test would be conducted) and yet during the pumping of MW12, approximately 400L of LNAPL was removed.

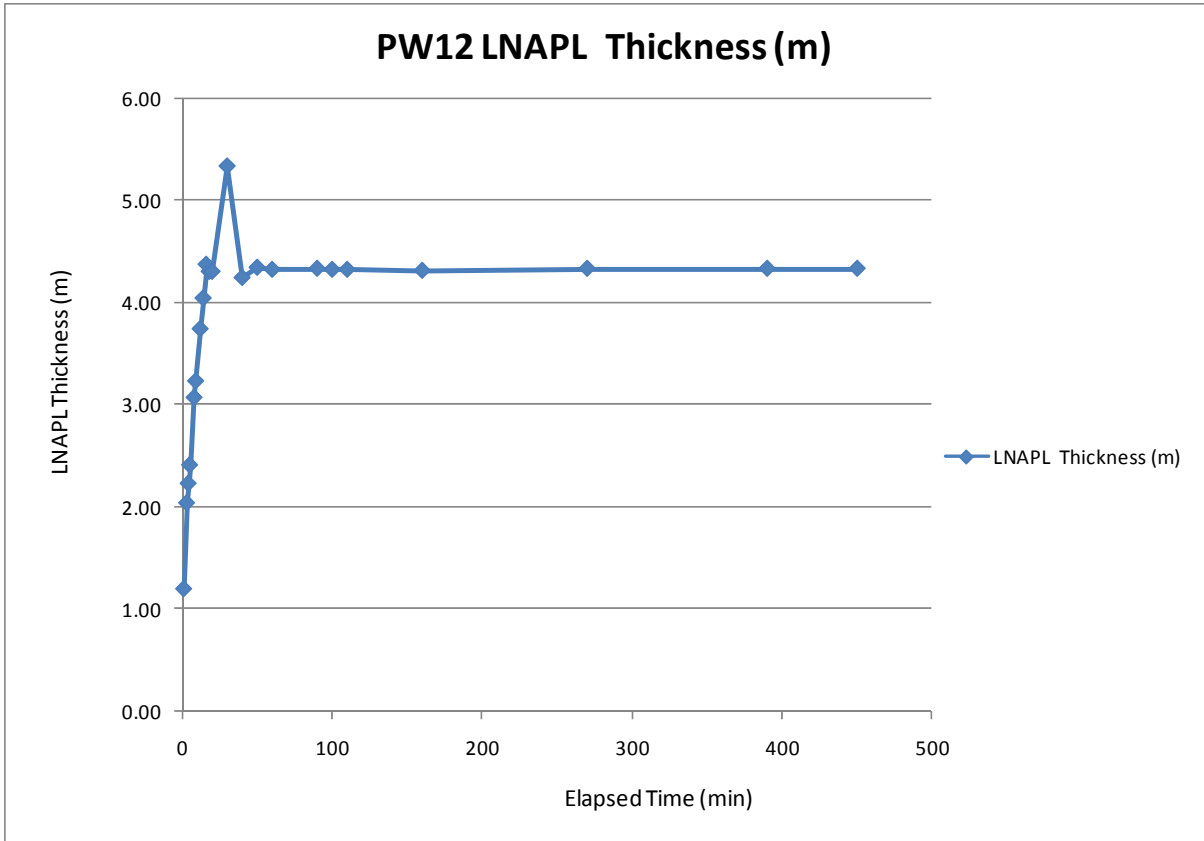


Figure 8-29 PW12 LNAPL thickness vs time

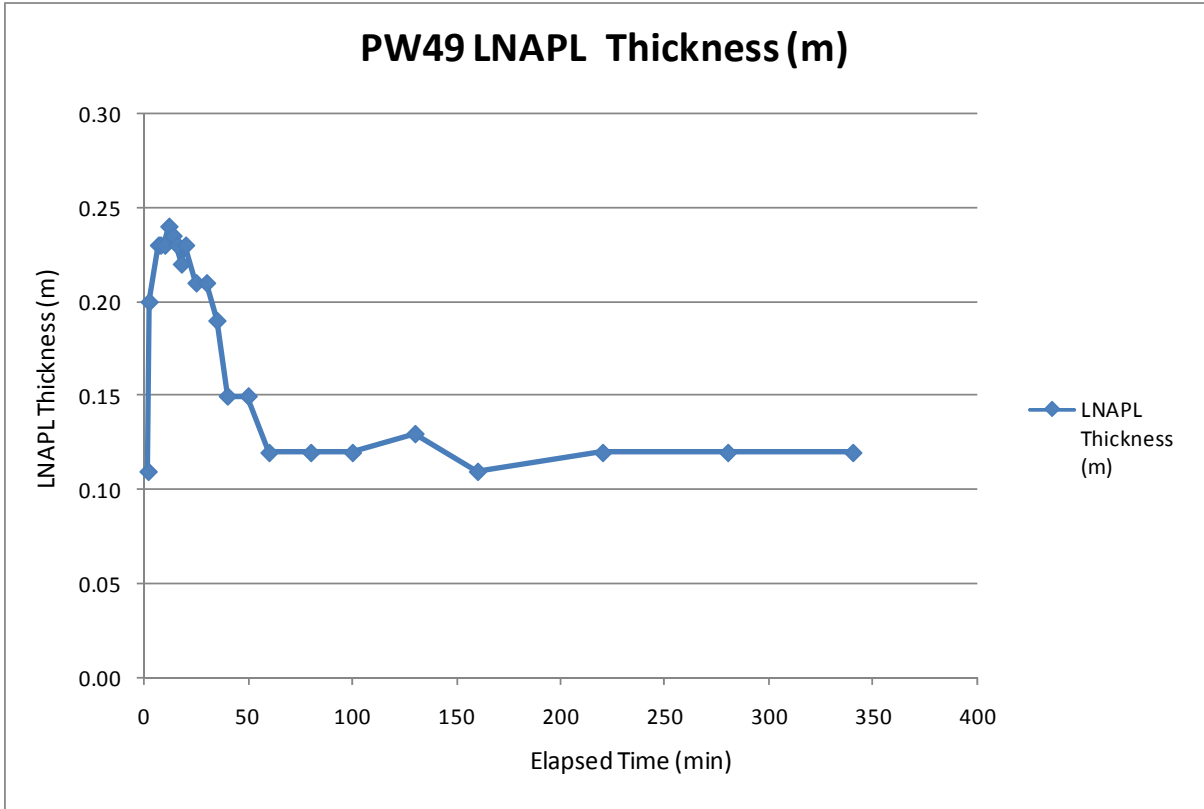


Figure 8-30 PW49 LNAPL thickness vs time

## 8.4 Aquifer Parameter Estimation Summary

The various aquifer parameter estimation methods have yielded important quantitative data (displayed in Table 8-1) and qualitative data regarding the nature of the aquifer. Natural groundwater gradients across the study are relatively flat, with an inferred groundwater flow direction towards the south east. Recharge by means of rainfall is considered to occur, with water levels in the aquifer responding rapidly to rainfall. Pump test data also indicates significant water level variations due to abstraction in the area with daily variations of up to 2.5m across the study area, with water level falling during daytime hours (period of highest abstraction) and recovering through the night (rest period) . The rapid response to rainfall and abstraction suggest that storativity values are low. Pump test and recovery data indicate low transmissivity values, particularly in the vicinity of the source zones, with high transmissivity values being observed further to the east in the residential areas.

**8-1 Aquifer parameter estimation summary**

Well ID	Parameter	Unit	Value	Method
PW12	T	m <sup>2</sup> /day	0.7	Cooper Jacob - Recovery vs t'
PW49	T	m <sup>2</sup> /day	0.2	Cooper Jacob - Recovery vs t'
PW2	T	m <sup>2</sup> /day	0.2	Cooper Jacob - Recovery vs t'
PW17	T	m <sup>2</sup> /day	18.5	Cooper Jacob
PW17	T	m <sup>2</sup> /day	20.8	Cooper Jacob - Recovery vs t'
PW17	S	-	5x10 <sup>-3</sup>	Cooper Jacob
MW12	T	m <sup>2</sup> /day	0.4	Cooper Jacob - Recovery vs t'
PW12	LNAPL Effective Conductivity - not considered dependable			
PW49	LNAPL Effective Conductivity - not considered dependable			

## 9 Chemical Characterisation

Chemical characterisation forms one of the cornerstones of a contaminant hydrogeological investigation. A firm understanding of the nature, severity and distribution of contaminants within an aquifer is required in order to correctly assess the potential remedial steps which may need to be taken in order to address potential contaminant related impacts. Whilst many LNAPL contaminant investigations focus purely on the LNAPL related organic compounds, it is also critical to assess the inorganic water chemistry of the aquifer as key interactions between the organic and inorganic components may occur. As a result, an understanding of the interactions and processes involved is critical in order to correctly identify the compounds and parameters which play the greatest role in the fate and transport of contaminants through the aquifer.

### 9.1 *Solute Forming Processes*

Karoo aquifers' geochemistry are strongly influenced by the incumbent geological setting with regards to sedimentary facies and associated weathering processes (Woodford & Chavelier, 2002) and various solute forming processes have significant effects on the water quality of the abovementioned aquifers. Physical weathering of the incumbent geology is one of the major solute forming processes, weathering of dolerite intrusions and of sedimentary rocks being the dominant processes. The weathering sequence of Karoo geology is described by Tordiffe (1978). With reference to dolerite, the minerals that form dolerite are susceptible to weathering, calcium, magnesium and sodium being the dominant cations which are released into solution. The weathering of the dolerite is not considered to provide significant anion contributions, with sedimentary rocks being dominant in this respect. Mudstones within the Karoo stratigraphy have high concentrations of calcite and pyrite, whilst sandstones are rich in potassium feldspars and sodium plagioclase. Calcite is often present in abundance in the sandstones as it often forms the intergranular cement.

Reduction oxidation (redox) processes are also able to induce the dissolution of various oxides, sulphates and nitrogen compounds. The redox sequence of organic matter follows a well documented sequence as described below:

- O<sub>2</sub> reduction
- Denitrification of NO<sub>2</sub> from NH<sub>4</sub>
- Mn(IV) reduction to Mn(II)

- NO<sub>3</sub> reduction
- Fe(III) oxide reduction to Fe(II)
- Reduction of organic matter
- SO<sub>4</sub> reduction
- CH<sub>4</sub> fermentation

(IGS GHR612, Course Notes, 2010)

## 9.2 Inorganic Sampling

Groundwater sampling for major cation and anion analyses was conducted during the March 2009 site visit. Where present, boreholes were sampled by means of the currently installed pump. The boreholes were purged for at least 30 minutes prior to sampling, with the purge water being passed through a flow cell in order to ascertain when field parameters such as EC, pH, Temperature, TDS and ORP had stabilised. Once the field parameters had stabilised a sample was collected with the prevailing field parameter being recorded at the time of sampling. Samples were decanted into clean plastic containers for major cation/anion analysis, whilst dissolved metals samples (Fe(II) and Mn(II)) were filtered through a 45µm filter, stored in a clean plastic container and preserved with hydrochloric acid. In instances where no pump was installed (i.e. petrol station forecourt monitoring wells) a grab sampled was collected using a bailer. Samples were dispatched to UIS Inorganic Laboratory in Centurion, Pretoria for analysis. A total of twenty one (21) samples were collected for inorganic analysis and the results are displayed in Table 9-1 and Table 9-2, and graphically on the Piper Diagram in Figure 9-1. Based upon the results reported in Appendix A, P alkalinity (expressed as mg/l CaCO<sub>3</sub>) was below detection limits in all samples. The result being that M alkalinity is represented by bicarbonate in solution, and has been reflected in the tables as such.

**Table 9-1 Field measurements and inorganic chemistry data from samples collected in March 2009 (Total M Alkalinity expressed as mg/l HCO<sub>3</sub>)**

		Unit	HS2	MW11	MW2	MW9	NB1	PW1	PW13	PW15	PW16	PW17	PW18
Field Parameters	EC	µS/cm	1786	1239	1886	1160	1647	459	1278	808	1360	952	1114
	ORP	mV	52	-62	26	-27	389	-24	144	134	-140	169	-160
	pH		7.24	7.27	7.16	7.79	7.34	6.8	7.2	7.21	7.26	7.25	7.16
Cations	Ca	mg/l	146	96	136	75.8	131	33.5	90.7	84	84.5	82.9	79.1
	Mg		42.6	43	53	34	43.1	11.5	36	32.3	36.6	30.9	33.8
	Na		180	102	202	107	162	44.8	124	109	136	103	101
	K		4.09	2	14.3	3.94	6.05	5.82	3.77	3.55	4.13	2.16	3.16
Anions	Cl	mg/l	197	66.7	168	93.4	164	25.8	92.3	77.8	80.8	102	64.2
	HCO <sub>3</sub>		380	498	471	403	379	131	367	375	490	421	506.8
	SO <sub>4</sub>		343	43.5	277	37.7	309	63.7	166	117	73.4	42.3	5.84
	NO <sub>3</sub>		21.21	0.42	74.5	<0.03	27.33	6.81	21.6	8.36	<0.03	<0.03	<0.03
Metals	Fe (II)	mg/l	<0.05	0.36	<0.05	0.24	<0.05	0.438	<0.05	<0.05	0.273	1.39	1.21
	Mn(II)		<0.05	4.78	0.474	5.12	<0.05	0.415	<0.05	0.484	4.54	3.48	6.16



**Table 9-2 Field measurements and inorganic chemistry data from samples collected in March 2009 (Total M Alkalinity expressed as mg/l HCO<sub>3</sub>)**

		Unit	PW2	PW21	PW4	PW50	PW57	PW6	PW8	PW9	RW1	RW2
Field Parameters	EC	μS/cm	1302	1161	870	1282	1328	1420	1322	1219	1523	11.2
	ORP	mV	-173	-105	57	151	370	-125	340	350	55	-104
	pH		7.27	7.3	7.26	7.48	7.57	7.26	7.46	7.47	7.22	7.44
Cations	Ca	mg/l	82.5	92.7	91.4	102	111	101	102	104	109	81.1
	Mg		30	37.4	25.8	36	41	45.1	36.8	28	54.1	10.9
	Na		121	125	121	111	97.4	143	122	111	133	163
	K		3.84	1.35	1.8	14	4.15	3.75	4.29	3.33	8.9	1.86
Anions	Cl		86.5	84.8	108	102	111	118	114	99.6	135	113
	HCO <sub>3</sub>		499	514	340	307	312	502	414	403	624	1268
	SO <sub>4</sub>		25.9	30.1	144	174	212	80.7	135	93.4	1.53	1015
	NO <sub>3</sub>		<0.03	<0.03	9.37	24.64	45.72	<0.03	7.98	2.51	<0.03	<0.03
Metals	Fe		0.432	0.16	<0.05	<0.05	<0.05	0.442	0.07	0.09	3.79	1.86
	Mn		2.18	2.69	0.129	<0.05	<0.05	3.26	0.06	1.76	4.36	11.2

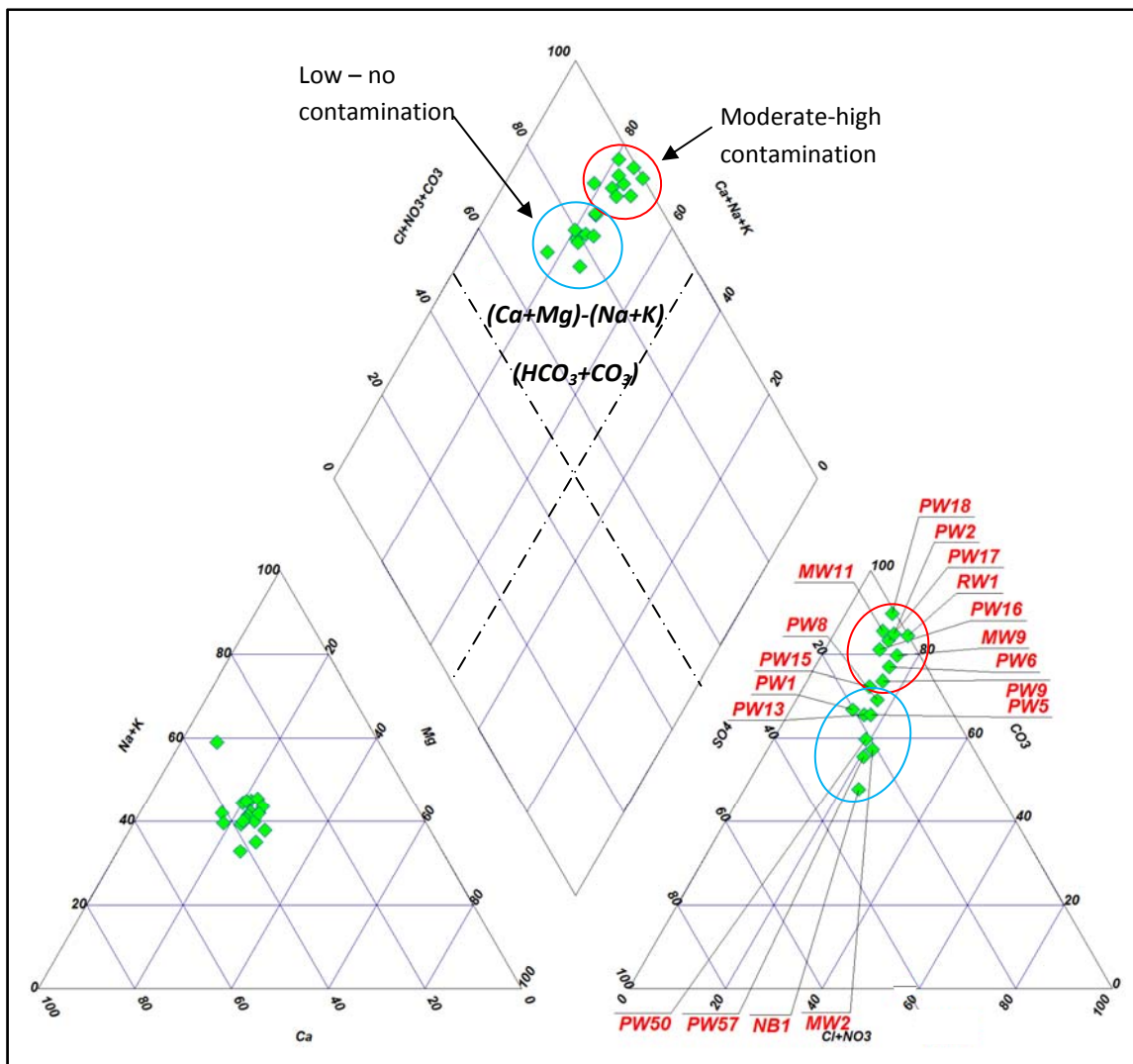


**Figure 9-1 Piper diagram of major cation/anion chemistry of sampled wells (Total M Alkalinity plotted as CO<sub>3</sub> on diagram)**

All of the samples fall within the same general facies, being (Ca+Mg)-(Na+K)-(CO<sub>3</sub>-HCO<sub>3</sub>). As mentioned previously, the calcium and magnesium ions are considered to be from plagioclase weathering of the intrusive dolerites. The carbonate/bicarbonate anion dominance is considered to signify recent recharge of the aquifer. When viewing the anion section of the diagram, an evolution from the CO<sub>3</sub>-HCO<sub>3</sub> end member towards the SO<sub>4</sub> can be observed. This could signify boreholes which intersect deeper fracture networks with water which have had greater residence times, and generally have higher SO<sub>4</sub> concentrations. It must be noted that a boreholes which were more significantly impacted by hydrocarbons tended to plot closer to the CO<sub>3</sub>-HCO<sub>3</sub> end member (viz. being SO<sub>4</sub> poor), whilst those that were less (or not) impacted tended back towards the SO<sub>4</sub> end member. When viewing the result tables another trend that becomes apparent where the presence of Fe(II) and Mn(II) is usually accompanied by low/non detect concentrations of NO<sub>3</sub> and SO<sub>4</sub> and low to negative ORP values. This will be discussed further in Section 9.4.

### **9.2.1 Recharge Calculation – The Chloride Method**

Groundwater monitoring within the study area extends back to 2002. As a result a relatively large data exists with regards to the inorganic chemistry of the area. A total of 81 chloride values are present for the study area for the time period 2002-2010, with a geometric mean of 104mg/l. The average chloride content of rainwater in inland South Africa is 2mg/l. Following the “chloride method” this would translate into an annual recharge of 1.9%, which is consistent with previous data from the area and the general recharge average for fractured rock aquifers in inland South Africa, which is approximately 2%. Based upon this recharge value, the overall study area size (approximately 750,000m<sup>2</sup>), and the mean annual rainfall (300mm), an annual rainfall recharge of 4,500m<sup>3</sup> of water to the aquifer has been calculated.

### **9.3 Organic Sampling**

A large body of organic analytical data is present for parts of the study as monitoring has been occurring since 2002. The most recent general trends in dissolved phase concentrations of hydrocarbon carbons is discussed in Section 6. During the course of this study three sampling events were undertaken in March, July and December of 2009. The March 2009 sampling was aimed at assessing new potential source zones, as well as identifying new boreholes which had been impacted by the seemingly expanding hydrocarbon contaminant plume. The sampling event in July 2009

focused on a sub set of boreholes which had been characterised by means of the FEC profiling discussed in Section 8, whilst the December 2009 sampling focused primarily on boreholes which were considered to be near the plume edges.

Where present, boreholes were sampled by means of the currently installed pump with the boreholes being purged for at least 30 minutes prior to sampling. The resultant dissolved phase concentration would thus be a flow weighted average concentration, and not specific to any one fracture zone which intersects the borehole (Puls, 1996). In selected cases the boreholes were sampled by low flow techniques using a pneumatically driven bladder pump. As with the inorganic sampling, field parameters such as EC, pH, ORP and temperature were recorded at the time of sampling. Samples transferred directly from the pump outlets to amber VOA vials and 500ml cryosilicate amber glass bottles. Samples were kept cool (<4°C) from the time of sampling until they were delivered to laboratory and analysed within 7 days of being sampled. All water samples were analysed for the BTEX range of compounds, as well as PAH, GRO and DRO compounds. UIS Organic Laboratory, a SANAS accredited laboratory in Centurion, Pretoria was contracted to analyse the samples.

### **9.3.1 March 2009 Sampling Event**

Sampling in March 2009 focused on the newly drilled monitoring wells at Beaufort West Service Station (MW9-MW12), along with private residence boreholes in the eastern portion of the study area (MW20, 21, 31, 50) and the boreholes at the two schools to the east of the Kuils River (NB1, NB2, HS1, HS2). The results are displayed in Table 9-3 and graphically in Figure 9-2. From the results it can be seen that elevated dissolved phase concentrations are present in the vicinity of Beaufort West Service Station, with benzene concentrations ranging from 2.646mg/l in MW11 up to 40.395mg/l MW10. Both MW10 and MW12 contained free phase LNAPL (45cm and 60cm respectively), and the concentrations observed in the water below in these wells would suggest that the observed product is from a recent release since the concentrations are comparable to the maximum solubility of benzene in water from fresh petrol ( $\pm 32$ mg/l). Detectable concentrations of MTBE and TAME were also observed in these monitoring wells. When viewing the compositional makeup of the detected analytes in MW10 to MW12 (See Figure 9-2) it can be seen that the relative compositions are similar, suggesting a common source.

Detectable concentrations of hydrocarbon compounds were observed in PW21 and PW50, with benzene being compositionally dominant in both of these wells. TAME, MTBE and subordinate BTEX compounds were also detected in PW21 whilst only TAME was observed in addition benzene in PW50. No detectable concentrations were detected in the school boreholes NB1, NB2 and HS1, whilst trace concentrations of benzene (0.003mg/l) and TAME (0.02mg/l) were observed in HS2, which is currently abstracting the largest volumes of groundwater in the study area. When viewing Figure 9-2 it can be seen that although total dissolved phase concentrations decrease as one moves eastwards away from the source zones, there is a relative enrichment in benzene and TAME, which are more readily dissolved from the parent fuel and are mobile than other compounds. As distance increase further, to HS2 for example, TAME has become the dominant compound rather than benzene. This is due to benzene being more readily attenuated than TAME due to TAME's lower organic based carbon partitioning co-efficient (Martensson et al, 2006)

**Table 9-3 Dissolved phase hydrocarbon concentrations from boreholes and monitoring wells sampled during March 2009**

	Benzene	Toluene	Ethylbenzene	Xylenes	MTBE	TAME	Naphthalene	1,2,4 TMB	1,3,5 TMB	TPH C8-10	TPH C10-12	TPH C12-16	TPH C16-35
Tier 1 Risk Based Screening Level for Ingestion of Groundwater (mg/l)													
Sample ID	0.0017	1.6	0.78	16	-	-	0.16	-	-	>sol	>sol	>sol	>sol
PW50	0.382	0.012	BDL	0.005	BDL	0.12	BDL	BDL	BDL	BDL	BDL	BDL	BDL
MW11	2.646	1.086	0.572	1.301	BDL	0.17	0.03	0.345	0.082	BDL	BDL	BDL	BDL
HS2	0.003	BDL	BDL	BDL	BDL	0.02	BDL	BDL	BDL	BDL	BDL	BDL	BDL
HS1	BDL	BDL	BDL	BDL	BDL	BDL	BDL	BDL	BDL	BDL	BDL	BDL	BDL
NB1	BDL	BDL	BDL	BDL	BDL	BDL	BDL	BDL	BDL	BDL	BDL	BDL	BDL
NB2	BDL	BDL	BDL	BDL	BDL	BDL	BDL	BDL	BDL	BDL	BDL	BDL	BDL
PW31	BDL	BDL	BDL	BDL	BDL	BDL	BDL	BDL	BDL	BDL	BDL	BDL	BDL
PW21	2.777	0	0.38	0.14	0.11	0.41	0.048	BDL	0.01	BDL	BDL	BDL	BDL
MW9	8.881	16.065	3.561	8.016	BDL	0.13	0.07	0.956	0.2	BDL	BDL	BDL	BDL
MW10	40.395	60.916	5.545	16.739	0.88	1.94	0.07	1.169	0.278	BDL	BDL	BDL	BDL
MW12	31.925	56.867	4.839	14.637	0.29	1	0.09	1.373	0.318	BDL	BDL	BDL	BDL
PW20	BDL	BDL	BDL	BDL	BDL	BDL	BDL	BDL	BDL	BDL	BDL	BDL	BDL

Notes:

All results reported in mg/l

TAME – Tert-Amyl-Methyl-Ether

>sol RBSL exceeds compound solubility limit

BDL Below Detection Limit

MTBE Methyl-Tert-Butyl-Ether



Figure 9-2 BTEX Compositions from March 2009 Sampling

### **9.3.2 July 2009 Sampling Event**

The July 2009 groundwater sampling event took place on the 13<sup>th</sup> to the 16<sup>th</sup>, and 28<sup>th</sup> and 29<sup>th</sup> of July. The primary objective of the sampling event was to verify the status of key boreholes (such as HS2), to provide data for new wells which were identified during the March 2009 hydrocensus, and to perform depth discrete low flow sampling on boreholes where flow zones were identified during the FEC profiling which occurred from 29 June to 3 July 2009.

#### **9.3.2.1 Conventional Sampling**

Conventional sampling (viz. sampling as per the methods described in previous sections) for dissolved phase hydrocarbons was conducted on selected boreholes and monitoring wells in the study area. The results are summarised in Table 9-4 with a graphic representation of the data in Figure 9-3 (Included in the figure are representative sample compositions from wells which were sampled by means of depth discrete low flow sampling). From the data it can be seen that no detectable concentrations were observed in several wells, including HS2. With reference to Table 9-4, the majority of the samples with detectable concentrations were dominated by benzene and TAME in varying concentrations, with TAME becoming progressively more compositionally dominant towards the east away from the source zones. MW5 is observed to differ compositionally from the majority samples, having a more varied range across the BTEX compound spectrum. When comparing the compositional variation of the abovementioned samples to samples from boreholes which are strongly connected to the source zones (i.e. PW12, PW49) one observes the relative increased concentrations as well as the more complete compositional makeup of petrol related compounds. Trace concentrations of benzene were also observed in PW69 to the north of the study area. The progressive relative enrichment of benzene and TAME away from the source zones is related to their increased mobility when compared to other compounds such as toluene and ethylbenzene. Of interest is the migration of the plume in an eastward direction, which is interpreted to be largely due to the abstraction in the residential areas, but also in a southerly direction, which is consistent with regional groundwater flow.



**Table 9-4 Conventional sampling results from the July 2009 sampling event**

	Benzene	Toluene	Ethyl- benzene	Xylenes	Naph- thalene	TAME	1,2,4 TMB	1,3,5 TMB	MTBE
Sample ID	Tier 1 Risk Based Screening Level for Ingestion of Groundwater (mg/l)								
	0.0017	1.6	0.78	16	0.16	-	-	-	-
HS2	BDL	BDL	BDL	BDL	BDL	BDL	BDL	BDL	BDL
MW2	BDL	BDL	BDL	BDL	BDL	BDL	BDL	BDL	BDL
Mw4	0.165	BDL	0.001	BDL	BDL	0.0055	BDL	BDL	BDL
MW5	0.0229	0.0012	0.0226	0.0148	0.00165	0.0052	0.0072	0.0015	BDL
PW13	BDL	BDL	BDL	BDL	BDL	BDL	BDL	BDL	BDL
PW15	0.01123	BDL	BDL	BDL	BDL	0.0274	BDL	BDL	BDL
Pw69	0.0038	BDL	BDL	BDL	BDL	0.0019	BDL	BDL	BDL
PW20	BDL	BDL	BDL	BDL	BDL	BDL	BDL	BDL	BDL
PW22	0.5229	0.0033	BDL	0.0099	BDL	0.0555	BDL	BDL	BDL
PW27	BDL	BDL	BDL	BDL	BDL	BDL	BDL	BDL	BDL
PW4	BDL	BDL	BDL	BDL	BDL	0.0046	BDL	BDL	BDL
PW50	BDL	BDL	BDL	BDL	BDL	BDL	BDL	BDL	BDL
PW7	0.2239	BDL	0.0016	BDL	BDL	0.1692	BDL	BDL	BDL
PW8	BDL	BDL	BDL	BDL	BDL	0.0091	BDL	BDL	BDL
PW78	0.00703	BDL	BDL	BDL	BDL	0.0039	BDL	BDL	BDL

Notes:

All results reported in mg/l

TAME – Tert-Amyl-Methyl-Ether

BDL Below Detection Limit

MTBE Methyl-Tert-Butyl-Ether





Figure 9-3 BTEX, TMB, TAME Compositions from July 2009 Sampling

### **9.3.2.2 Low Flow Sampling**

Based upon the results of the FEC logging, identified flow zones within each of the selected boreholes were sampled. This was accomplished by lowering a pneumatically driven bladder pump to the depth of the flow zone in the well beginning with the deepest flow zone, purging the delivery line of water which entered the pump whilst it was being lowered to the specified depth and collecting the sample. Average flow rates during sampling ranged from 100ml – 200ml per minute. Once the sample was collected the pump was raised to the next identified flow zone, the delivery line was again purged of all water in the line to ensure a depth representative sample and the sample was collected. Chemically resistant Teflon bladders and LDPE tubing was used in all cases to minimise the possibility of cross contamination of samples. Bladders pumps were decontaminated between borehole sampling events and new tubing was used on each borehole.



**Photo 9-1 Low flow bladder pump sampling of PW9**





**Photo 9-2 Water was sampled at a rate of 100-200ml per minute.**

Figure 9-4 and Figure 9-5 display the FFEC profiles along with the sampling locations for boreholes PW9, PW16, PW17 and PW18, whilst the results for these wells and other wells which were sampled by this technique are summarised in Table 9-5 and Table 9-6.

Sampling of PW17 detected elevated hydrocarbon concentrations at all points which were sampled, however a progressive dilution of dissolved phase concentrations is observed moving down the well from the shallower fractures towards the deeper fractures. Ambient FEC profiling of PW17 indicated downward flow from the shallow fractures (20 -24m bgl / 822 – 818m amsl) downwards towards the fracture located at 48m below ground level (794m amsl), at which point flow exited the borehole via this fracture. Sample results from PW9, which is 60m from PW17 indicated the most contaminated sample to be from sample PW9.4, which is situated at the 794m amsl fracture indicating that in PW9, the greatest contaminant mass is entering at a deep level. The potential interplay between PW17 and PW9 could be that contaminant mass is entering PW17 at shallow depths, moving down the borehole, exiting at a deeper fracture and migrating along this fracture where it is intersected at PW9. An idealised conceptualisation of this is displayed in Figure 9-7.

Sampling of PW16 indicated a steady dilution down the borehole and would suggest the majority of contaminant mass enters the borehole at shallow depths. Sampling of PW18 also detected the highest concentrations at shallow levels with concentrations decreasing with depth towards the main fracture identified in PW18 25m bgl (818m amsl). Sampling of PW12 also indicated decreasing concentration with depth although. PW6 although displaying considerably lower concentrations when compared to the abovementioned wells, displayed increasing concentrations with depth, suggesting that the main contaminant bearing fracture could be located a deeper levels (>35m bgl) in the borehole.

Figure 9-6 depicts a 3-dimensional visualisation of the depth discrete sampling for selected wells in the study area with benzene concentrations plotted as coloured rings around the borehole. When viewing the diagram is clear that the most elevated concentrations are observed in PW49 and PW12 which are closest to the source zones. Although PW9 and PW18 are closer to PW12 and PW49, PW17 displays the most elevated concentrations to the east of the source zones, and the current data from previous section confirms a hydraulic connection between PW17 and PW12 with fracture zones being observed to be comparable depths in the shallow zones of both boreholes (represented by dotted lines between boreholes in Figure 9-6). PW17 appears to be distributing the contaminant plume to deeper fracture networks within the aquifer, and is also hydraulically connected to wells nearby such as PW9 and PW16. It could well be that abstraction of PW17 rapidly mobilises contaminants from the source zones, towards PW17, where after the plume is “distributed” to other wells which hydraulically connected to PW17 in the nearby area.

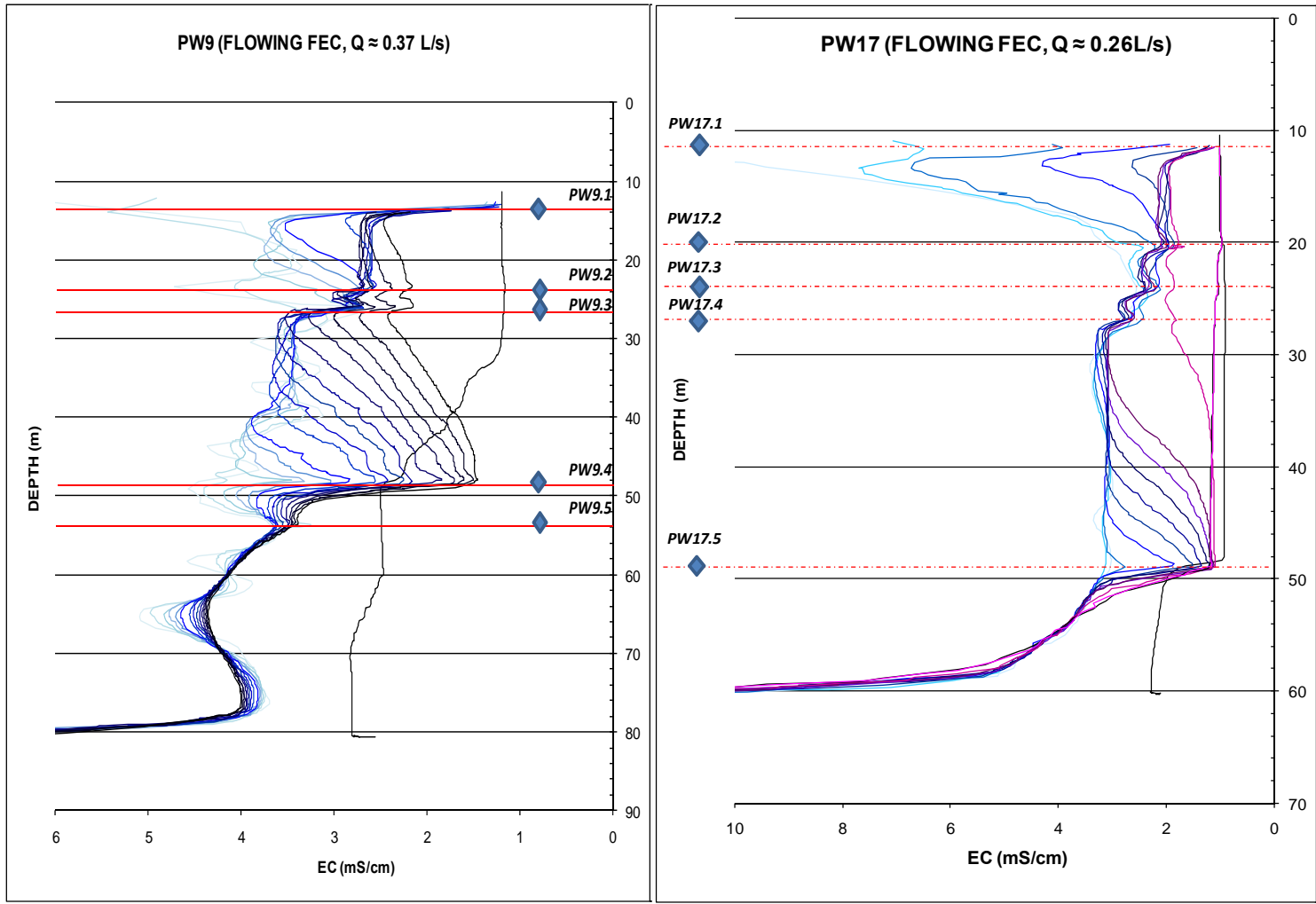


Figure 9-4 FFEC profiles and sampling points for PW9 & PW17

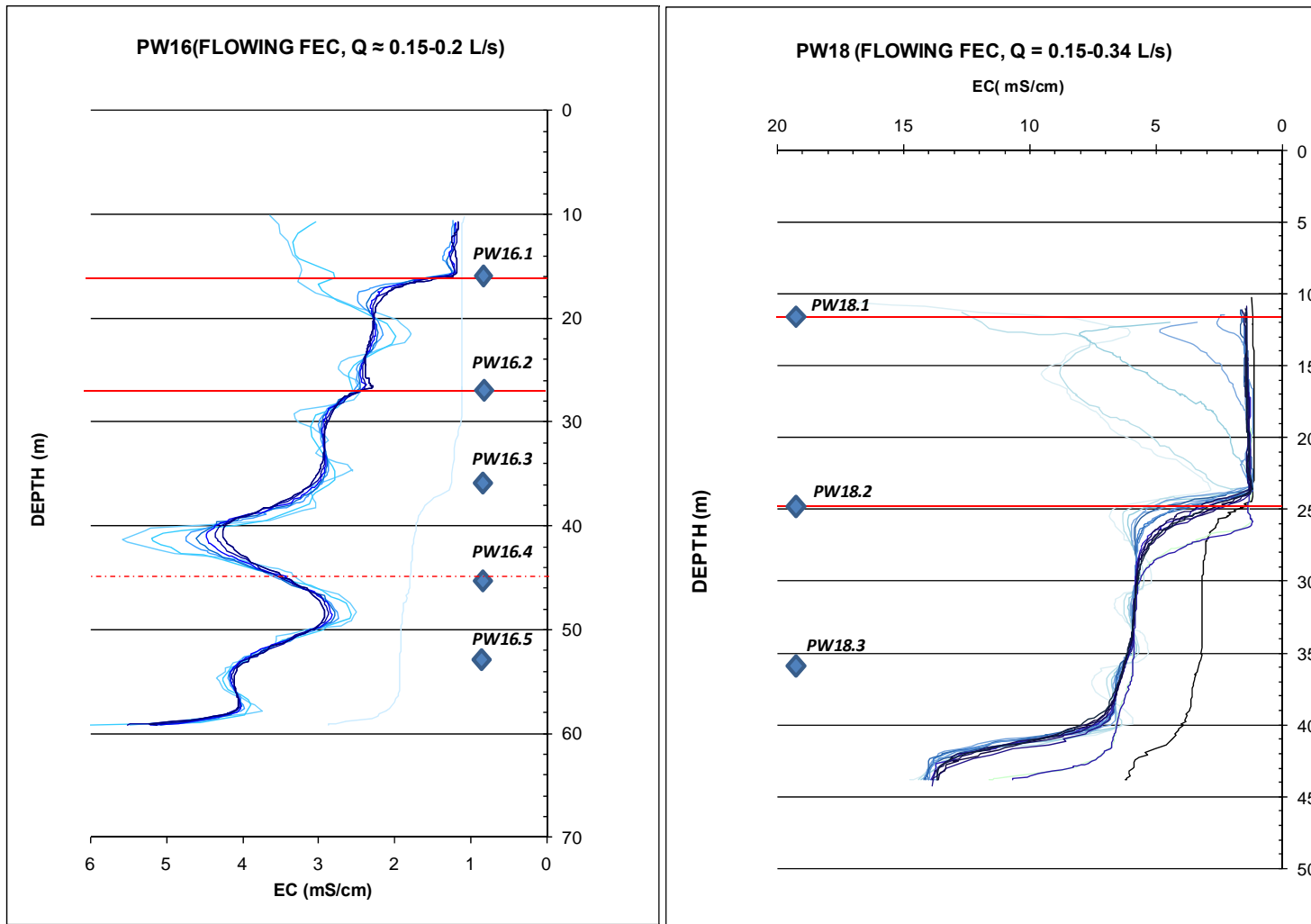


Figure 9-5 FFEC profiles and sampling points for PW16 & PW18

**Table 9-5 Depth discrete low flow results for PW12, PW16, PW17 and PW18**

Sample ID	Depth (mbgl)	Benzene	Toluene	Ethyl-benzene	Xylenes	Naphthalene	TAME	1,2,4 TMB	1,3,5 TMB	MTBE
		Tier 1 Risk Based Screening Level for Ingestion of Groundwater								
		0.0017	1.6	0.78	16	0.16	-	-	-	-
PW12.1	15	16.211	30.863	1.660	3.297	0.109	0.547	0.480	0.183	BDL
PW12.2	24	12.279	16.502	1.161	2.419	0.042	0.507	0.297	0.081	BDL
PW12.3	38	11.554	8.388	0.717	1.587	0.017	0.775	0.179	0.042	BDL
PW16.1	16	5.056	0.007	0.475	0.526	0.015	0.443	0.112	0.014	BDL
PW16.2	27	3.717	BDL	0.361	0.328	0.012	0.346	0.082	0.008	BDL
PW16.3	36	3.868	BDL	0.222	0.125	0.007	0.335	0.029	BDL	BDL
PW16.4	46	2.795	BDL	0.107	0.093	0.000	0.274	0.008	BDL	BDL
PW16.5	58	2.128	BDL	0.060	0.046	0.000	0.414	BDL	BDL	BDL
PW17.1	11	15.448	9.366	0.499	1.201	BDL	0.950	0.025	BDL	BDL
PW17.2	20	14.265	12.860	1.392	2.897	0.054	0.689	0.380	0.094	BDL
PW17.3	24	12.383	11.081	1.288	2.668	0.050	0.605	0.334	0.077	BDL
PW17.4	27	12.341	9.117	1.014	2.153	0.037	0.641	0.234	0.048	BDL
PW17.5	48.5	11.454	5.744	0.522	1.314	0.008	0.674	0.070	0.012	BDL
PW18.1	11	7.9701	0.3038	0.9872	0.6937	0.0342	0.3923	0.1933	0.0138	BDL
PW18.2	24	5.1879	0.0746	0.5984	0.2851	0.0112	0.4142	0.0732	0.0079	BDL
PW18.3	36	5.0608	0.085	0.3276	0.1370	0.0038	0.3027	0.0032	0.0069	BDL
PW21.1	17	0.0099	BDL	BDL	BDL	BDL	0.3615	BDL	BDL	BDL
PW21.2	21	0.002	BDL	BDL	BDL	BDL	0.5146	BDL	BDL	BDL

Notes:

All results reported in mg/l

TAME – Tert-Amyl-Methyl-Ether

BDL Below Detection Limit

MTBE Methyl-Tert-Butyl-Ether

**Table 9-6 Depth discrete low flow results for PW6, PW9 and PW49**

Sample ID	Depth (mbgl)	Benzene	Toluene	Ethyl-benzene	Xylenes	Naphthalene	TAME	1,2,4 TMB	1,3,5 TMB	MTBE
		Tier 1 Risk Based Screening Level for Ingestion of Groundwater								
		0.0017	1.6	0.78	16	0.16	-	-	-	-
PW6.1	12.5	0.2279	BDL	BDL	0.0001	0	0.0234	0	BDL	BDL
PW6.2	21	0.4354	BDL	BDL	0.0097	0.0015	0.0353	0.0032	BDL	BDL
PW6.3	24	0.5926	BDL	BDL	0.0069	0.0009	0.0428	0.0043	BDL	BDL
PW6.4	34.5	0.8622	BDL	BDL	0.0021	BDL	0.064	0.0021	BDL	BDL
MW7	25	1.236	0.0081	BDL	0.0946	0.0392	1.7808	0.0036	BDL	BDL
PW9	13	1.534	0.0427	0.2207	0.3318	0.0155	0.1503	0.1172	0.0258	BDL
PW9	23.5	1.4947	0.0654	0.2677	0.4002	0.0161	0.2037	0.1359	0.0267	BDL
PW9	26	1.3327	0.0723	0.2214	0.3409	0.0103	0.171	0.0944	0.0296	BDL
PW9	47.5	2.0753	0.274	0.2505	0.4627	0.0126	0.214	0.1186	0.0253	BDL
PW9	53	1.5687	0.1369	0.1107	0.2914	0.0037	0.2007	0.0483	0.0148	BDL
PW49.1	20	20.5199	43.142	1.8696	3.7598	0.0932	0.7359	0.4677	0.1697	BDL
PW49.2	24	24.1716	33.677	1.8424	3.8157	0.0599	1.0691	0.4521	0.1376	BDL
PW49.3	30	21.886	30.767	1.6009	3.3106	0.0722	1.0709	0.4145	0.1278	BDL

Notes:

All results reported in mg/l

TAME – Tert-Amyl-Methyl-Ether

BDL Below Detection Limit

MTBE Methyl-Tert-Butyl-Ether



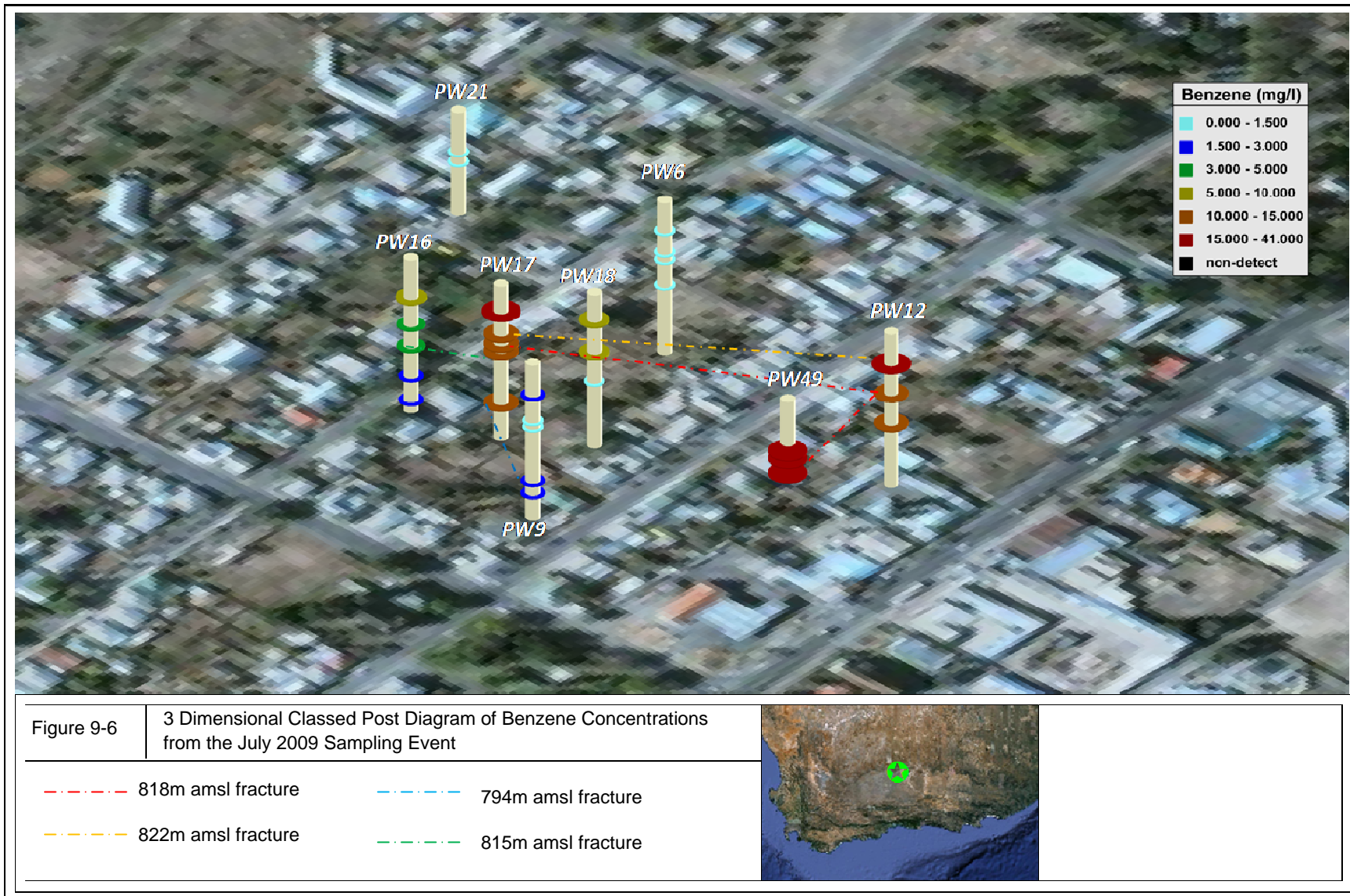


Figure 9-6 3 Dimensional Classed Post Diagram of Benzene Concentrations from July 2009 Sampling Event

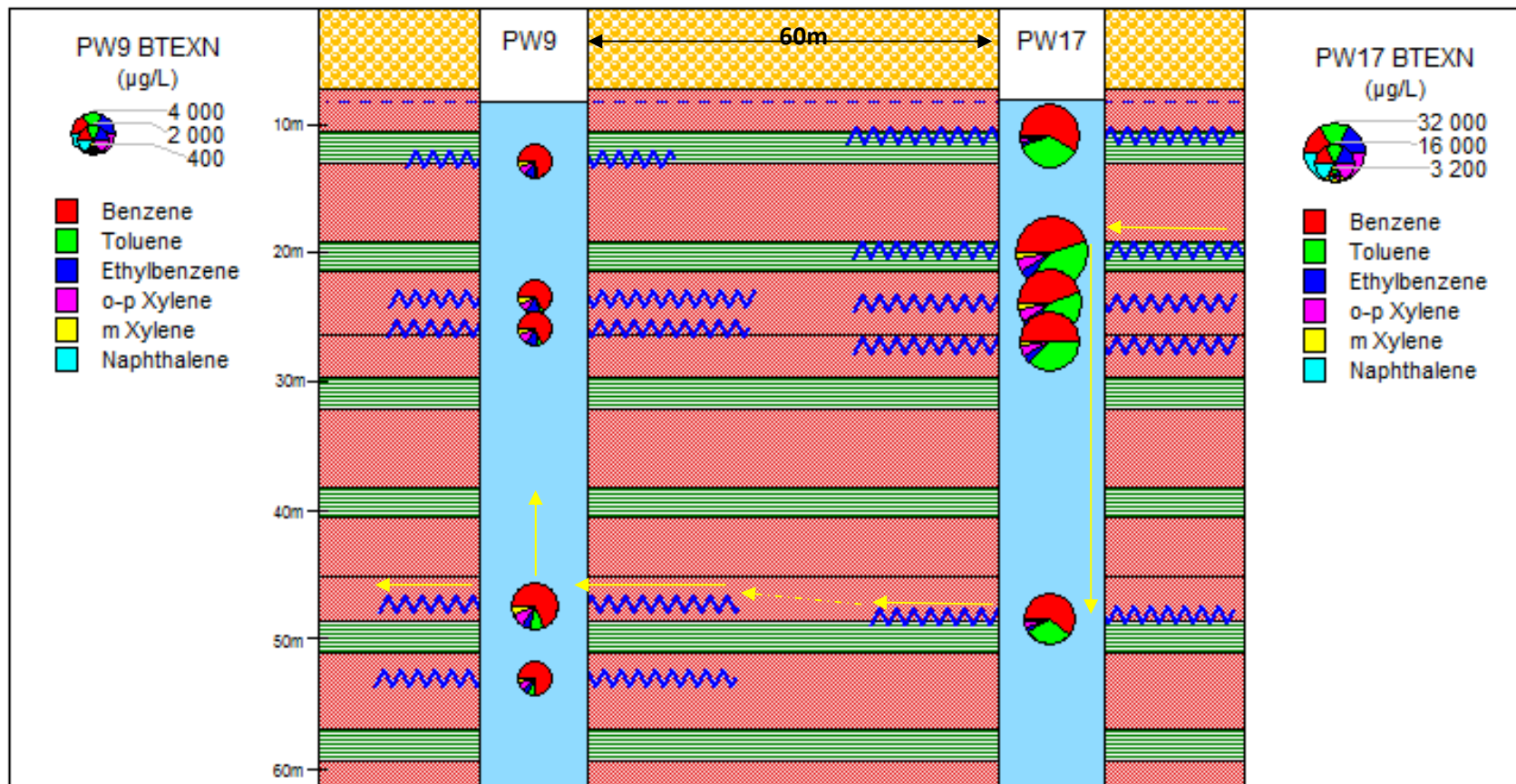


Figure 9-7 An idealised conceptualisation of contaminant transfer between PW17 and PW9

### 9.3.3 December 2009 Sampling

The December 2009 sampling event took place on the 3<sup>rd</sup> of December in order to monitor the contaminant status of selected private wells, key boreholes such as H2, NB1 and NB2, and monitoring wells at Beaufort West Service Station and Donkin Motors. The results are summarised in Table 9-7 and are displayed graphically in Figure 9-8. In the northern portion of the study area PW17 and MW9 yielded the most elevated hydrocarbon concentrations with benzene concentrations of 3.002mg/l and 2.686mg/l respectively. RW1 at Donkin Motors yielded the most elevated concentrations in the southern portion of the study area and compositional variations can be seen between RW1, RW2 and MW9 at Beaufort West Service Station. The sample from PW17 was a pumped sample using the borehole's installed pump, and the contaminant concentrations are much lower when compared to the July 2009 low flow sampling results. This may be due to contaminant mass fluctuations in the aquifer, but is also attributed to the fact that the pumped sample will provide a flow weighted average contaminant concentration for the borehole since the fractures with the highest transmissivity (viz. those that supply the most water to the borehole) are not necessarily the fractures which contain the greatest contaminant mass and so a dilution of contaminants occurs. This dilution is considered to have not occurred to such an extent with the low flow sampling which was aimed at sampling under ambient conditions. Another potential cause for a decrease in concentrations is that the installed pumps may experience cavitations within the impellers of the pump, and the increase flow rate at the pump outlet may volatilise BTEX compounds, whilst the bladder pumps abstract water at near laminar flow rates, thus reducing volatilisation.

When viewing Figure 9-8, a fairly widespread, low concentration TAME plume is observed across much of the area extending eastwards from De Villiers Street across the Kuils River, with H2 and NB1 both yielding trace concentrations of TAME. The diagram again displays the tendency of TAME to form large widespread plumes due to its high degree of solubility and low affinity for attenuation.

**Table 9-7 Dissolved phase hydrocarbon concentrations from boreholes and monitoring wells sampled during December 2009**

	Benzene	Toluene	Ethyl- benzene	Xylenes	MTBE	Naph- thalene	1,2,4 TMB	1,3,5 TMB	TAME
Sample ID	Tier 1 Risk Based Screening Level for Ingestion of Groundwater								
	0.0017	1.6	0.78	16	0.16	-	-	-	-
HS2	BDL	BDL	BDL	BDL	BDL	BDL	BDL	BDL	0.02
MS02	BDL	BDL	BDL	BDL	BDL	BDL	BDL	BDL	BDL
MW9	2.686	0.136	0.215	1.113	BDL	0.062	0.201	0.062	BDL
NB1	BDL	BDL	BDL	BDL	BDL	BDL	BDL	BDL	0.02
NB2	BDL	BDL	BDL	BDL	BDL	BDL	BDL	BDL	0.00
PW13	BDL	BDL	BDL	BDL	BDL	BDL	BDL	BDL	0.04
PW16	BDL	BDL	BDL	BDL	BDL	BDL	BDL	BDL	0.10
PW17	3.002	0.007	0.23	0.127	BDL	0.022	0.063	BDL	0.15
PW18	BDL	BDL	BDL	BDL	BDL	BDL	BDL	BDL	0.02
PW20	BDL	BDL	BDL	BDL	BDL	BDL	BDL	BDL	BDL
PW22	BDL	BDL	BDL	BDL	BDL	0.031	BDL	BDL	BDL
PW30	BDL	BDL	BDL	BDL	0.049	0.137	BDL	BDL	BDL
PW50	BDL	BDL	BDL	BDL	BDL	BDL	BDL	BDL	BDL
PW57	BDL	BDL	BDL	BDL	BDL	BDL	BDL	BDL	BDL
PW60	BDL	BDL	BDL	BDL	BDL	BDL	BDL	BDL	BDL
PW7	BDL	BDL	BDL	BDL	BDL	0.129	BDL	BDL	BDL
Pw78	BDL	BDL	BDL	BDL	BDL	0.015	BDL	BDL	BDL
PW8	BDL	BDL	BDL	BDL	BDL	0.068	BDL	BDL	BDL
PW9	0.134	BDL	BDL	0.002	BDL	0.115	0.002	BDL	0.005
RW1	3.288	BDL	1.751	0.452	BDL	BDL	0.165	0.152	0.028
RW2	0.037	BDL	0.125	0.158	BDL	BDL	0.067	BDL	BDL

Notes:

All results reported in mg/l

TAME – Tert-Amyl-Methyl-Ether

BDL Below Detection Limit

MTBE Methyl-Tert-Butyl-Ether






Figure 9-8	BTEX, TMB, TAME Compositions from December 2009 Sampling		UTM Projection Lo 23

Figure 9-8 BTEX, TMB, TAME Compositions from December 2009 Sampling

#### **9.4 Monitored Natural Attenuation**

Biodegradation or natural attenuation of hydrocarbon plumes is well documented and is currently a popular remedial approach. The natural attenuation of a contaminant within an aquifer is dependant upon several factors, these include:

- The source and concentration of contaminant;
  - The chemistry and toxicity of the contaminant;
  - The solubility, transport, adsorption, dispersion and volatility of the contaminant compounds;
  - The chemistry, physics and microbiology of the groundwater;
  - The hydrogeology and hydrology of the contaminated site;
  - The environmental conditions, nutrient sources and presence of electron acceptors;
  - The biodegradability of contaminants, and the presence of a competent biodegrading population of microorganisms.
- (Farhadian et al, 2007)

In situ biodegradation can be inferred through microbial activity in groundwater by changes in the inorganic chemistry of the groundwater. Petroleum hydrocarbon compounds such as benzene present a source of carbon for the incumbent microbial population within the aquifer, which utilizes electron acceptors during the biodegradation process. Different electron acceptors offer different energy yields and micro organisms utilizing electron acceptors with higher energy yields can often out-compete other micro organisms, with the highest energy yielding electron acceptors being preferentially utilized. The hierarchy of energy yields follows the redox sequence with oxygen offering the highest energy yield for microbial metabolism. Nitrate, manganese oxides and iron oxides (forming Mn(II) and Fe(II) respectively when reduced) and sulphate follow in terms of decreasing energy yield (Stumm & Morgan, 1996). A wide range of bacteria are able to biodegrade various hydrocarbon compounds, with *Rhodococcus* and *Pseudomonas* being two of the more common bacterial groups involved in biodegradation (Farhadian et al, 2007)

It is thus possible to assess whether biodegradation is taking place at a site by monitoring the concentrations of the electron acceptors (viz. dissolved oxygen, nitrates and sulphates) and the products of reduction (for manganese and iron). Previous work done in Beaufort West has shown that microbial degradation is occurring with the inorganic signature of groundwater that is affected by hydrocarbons (which are undergoing degradation) being characterised by negative oxidation reduction potential values (oxygen depletion), lowered sulphate and nitrate concentrations and elevated Mn(II) and Fe(II) concentrations (Van Biljon et al, 2006). Table 9-8 summarises the parameters and analytes from the March 2009 sampling event which are relevant for the assessment of natural attenuation.

**Table 9-8 Monitored natural attenuation parameters and analytes**

Sample ID	Benzene	ORP	NO3	SO4	Mn(II)	Fe(II)
H2S	BDL	52	21.21	343	0	0
MW2	BDL	26	74.5	277	0.474	0
NB1	BDL	389	27.33	309	0	0
PW13	BDL	144	21.6	166	0	0
PW4	BDL	57	9.37	144	0.129	0
PW50	BDL	151	24.64	174	0	0
PW57	BDL	370	45.72	212	0	0
PW8	BDL	340	7.98	135	0.06	0.07
PW21	0.0099	-105	0	30.1	2.69	0.16
PW15	0.0229	134	8.36	117	0.484	0
PW1	0.073	-24	6.81	63.7	0.415	0.438
PW9	0.134	350	2.51	93.4	1.76	0.09
PW6	0.8622	-125	0	80.7	3.26	0.442
MW9	2.8	-27	0	37.7	5.12	0.24
RW1	3.288	55	0	1.53	4.36	3.79
PW16	5.056	-140	0	73.4	4.54	0.273
PW18	7.9701	-160	0	5.84	6.16	1.21
PW17	15.448	169	0	42.3	3.48	1.39
MW11	LNAPL	-62	0.42	43.5	4.78	0.36
PW2	LNAPL	-173	0	25.9	2.18	0.432

Notes:

BDL Below Detection Limit

LNAPL Free Phase LNAPL present

Analytes reported in mg/l

ORP reported in mV

With reference to Table 9-8, it can be observed that boreholes and monitoring wells which are not impacted by hydrocarbon contamination (benzene is used as a proxy for overall contamination in the table) generally tend to have appreciable concentrations of NO<sub>3</sub> and SO<sub>4</sub>, positive ORP values and low to no detectable concentrations of Fe(II) and Mn(II). Boreholes which are impacted by hydrocarbon contamination tend to have depleted concentrations of SO<sub>4</sub> and NO<sub>3</sub>, negative ORP values and comparatively elevated concentrations of Fe(II) and Mn(II). When assessing natural attenuation it is important to establish what the naturally occurring background concentrations within the aquifer are so that comparisons can be made with regards to the potential alteration of the groundwater chemistry caused by natural attenuation within the plume. PW57, which is considered to be upgradient of the known contaminant plume and is not known to be impacted, was selected to represent the prevailing background concentrations. Figure 9-9 displays relevant compositions as radial diagrams, with PW57's as the background composition being outlined on the radial diagrams in yellow.





Figure 9-9 Radial Diagrams Displaying ORP, Fe(II), Mn(II), SO<sub>4</sub> & NO<sub>3</sub>



UTM Projection

Lo 23

Figure 9-9 Radial Diagrams Displaying ORP, Fe(II), Mn(II), SO<sub>4</sub> & NO<sub>3</sub>



From Figure 9-9 it be seen that boreholes which are outside of the plume (PW57, PW50, NB1, PW13) show similar signatures, with positive ORP values, appreciable concentrations of  $\text{SO}_4$  and  $\text{NO}_3$  and low concentrations of Mn(II) and Fe(II). Sample collected from within the extents of the known contaminant plume (in March 2009) yielded the reduced  $\text{SO}_4$  and  $\text{NO}_3$  concentrations along with elevated Fe(II) and Mn(II). Samples collected from the area with the highest contamination concentrations (PW17, MW11, and MW9) were completely depleted of  $\text{NO}_3$ . RW1 which is located at Donkin Motors yielded no detectable  $\text{NO}_3$  and yielded the most elevated Fe (II) concentrations and the lowest  $\text{SO}_4$  concentrations by an order of magnitude. The reduction of Fe(II) and depletion of  $\text{SO}_4$  are considered to occur at late stages of the redox sequence and near complete depletion of  $\text{SO}_4$  would suggest that the natural attenuation processes in the vicinity of RW1 are well established, which is agreeable with the observation that the releases and associated plume in the vicinity of RW1 are considered to be older than those observed further north. The inorganic chemistry does therefore suggest that natural process are occurring which play a role in attenuating the plume. A major complicating factor in assessing the efficacy of natural attenuation within the study zone is the fact that multiple releases appear to have occurred from several sources, with the resultant fresh pulses of contaminants through aquifer masking the attenuating effects which were a result of the original microbial degradation. Whilst natural biodegradation may be effective in attenuating the plume in the distal parts, the efficacy of natural attenuation within the areas near the source zones is considered to be low due to the continual contaminant mass source loading which appears to be occurring. Further future monitoring (and the cessation of future hydrocarbon releases) may provide a better quantification of the rates of degradation within the aquifer.

## **10 Site Conceptual Model**

Based upon the information contained in the previous sections, a site conceptual model has been developed. Further to the development of the conceptual model, the basic requirements for constructing a numerical groundwater model have been reviewed and compared to the current data set and conceptual understanding of the site. In conclusion this section assesses the feasibility of a groundwater fate and transport model in light of the current conceptual understanding.

Often the subsurface environment is too complex to describe in its entirety. A conceptual model can be thought of as an organised, but simplified mental picture of a hydrogeological environment. The model attempts to explain the movement/behaviour of fluids and contaminants occupying an aquifer within a set of imprecise, but reasonable bounds. The conceptual model aims to provide a basis for planning further studies and to explain the hydrogeological conditions in a clear and understandable way (Le Grand & Rosen, 2000). This process is iterative, and the model is constantly updated as new information becomes available. The conceptual site model for the study area has been organised into three sub sections dealing with the physical characteristics, the flow and transport characteristics, and the chemical characteristics.

### **10.1.1 Physical Characteristics**

The aquifer underlying the study area is considered to be a typical Karoo fractured rock, dual porosity aquifer. The geological medium consists of alternating layers of mudstone and silts stone, with occasional sandstone layers being present. Based upon outcrop data and geological maps, the bedding dip angles within the study are approximately horizontal. The main transport flow paths are considered to be bedding plane parallel fractures, with the bedrock matrix providing the bulk storage component of the aquifer. From core logs it was observed that vertical and sub-vertical jointing is present, particularly within the first 15m-20m of the bedrock profiles and is considered to be a significant recharge pathway for the aquifer based upon the rapid rise in water levels observed after rainfall events.

The first 30m of the geological profile within the study was observed to have the highest frequency of fractures with core logs displaying in excess of 30 discrete (but not all water bearing) fractures within the first 25m of the geologic profile, whilst the most transmissive zones were found to be located at depths usually greater than 50m below ground level (approximately 795m amsl). A relatively shallow flow zone, which appeared to be laterally extensive across much of the study area, was found between 818m-820m amsl and is considered to be significant flow horizon across the study area. Relatively

poor fracture development appears to be present in the areas to the west of Bird Street, with the majority of the monitoring wells drilled at the filling stations along Donkin Street having virtually no significant yield in comparison to borehole located further to the east where water yields were found to increase.

### **10.1.2 Flow and Transport**

Beginning at a “quasi regional scale”, groundwater flow is inferred to be towards the south east, with a very flat gradient of 0.001. General topographic gradients for the area are comparable and would suggest that Bayesian interpolation of water levels from topography would provide reasonable approximations at a regional scale. Water levels within the study area respond rapidly to rainfall recharge and to groundwater abstraction suggesting that aquifer storativity values are low. Whilst an S value of  $5 \times 10^{-3}$  was yielded from the pump test on MW17, mean S values within the Beaufort West area are in the range of  $10^{-4}$  to  $10^{-5}$ . The rapid water level response to rainfall events also suggests direct recharge to the aquifer along vertical and sub vertical joints within the weathered profile. Recharge in the area is estimated to be approximately 2% of annual rainfall, which translates to an annual rainfall recharge to the aquifer of approximately  $4500\text{m}^3$  per annum. Daily abstraction rates within the study area are considered to be between  $400\text{m}^3$ - $900\text{m}^3$  per day.

Water level measurements indicate that water levels may drop (as a response to abstraction) during a single day by up to 2.5m, but recover during the night, whilst seasonal variations indicate the water levels to vary between approximately 10m below ground level in the wet season, to 20m below ground level in the dry season. In light of this, and considering the estimated recharge and abstraction rates, it is considered likely that recharge to the aquifer is occurring from the north, most likely across, or along the Beaufort West Sill.

On a more local study area scale, flow is considered to occur primarily along bedding plane parallel fractures. Transmissivity values range of  $0.4\text{m}^2$  per day to  $20\text{m}^2$ /day, with T values being low along the western section of the study area and increasing as one moves eastwards into the residential areas. Two dominant flow zones appear to be present across much of the study area, a shallow flow zone with many fractures being observed between 815m-830m amsl, and in particular between 818m-820m amsl, and a second deeper zone at 795m amsl, which is considered to be more transmissive and potentially semi confined.

The local Kuils and Gamka rivers do not appear to be “no flow” boundaries, but are most likely intermittent recharge points during times of heavy rainfall. It must be noted, however that flow events in the rivers are infrequent and the overall effect of the rivers on the general hydrology of the area is considered to be minimal. The residential area to the east of Donkin Street is considered to equate to a well field, with over 80 private wells being present, and being used on a daily basis. The pumping in this area between Bird Street and Brand Street is considered to have a significant effect on groundwater gradients and flow. The exact effect that the private boreholes have on flow in the area will be difficult to quantify, as the abstraction takes place in an uncontrolled and unmonitored fashion. The boreholes themselves are considered to be vertical “macro-fractures” connecting shallow, unconfined fractures systems to deeper, potentially semi confined fractures systems. Vertical downward flow within the residential boreholes is considered to have been observed, with the vertical head gradient in one borehole possibly being the result of abstraction in another well which is connected to the same deeper fracture system, but possibly not the shallower fracture system.

Free phase LNAPL movement in the source zones is considered to be controlled by the governing potentiometric conditions and LNAPL entry pressure regimes within the fractures surrounding the borehole, with LNAPL appearing and disappearing in boreholes in a pulse like manner. Based upon the conceptual understanding of LNAPL movement in fractured rock aquifers, it is highly likely that due to the water level variations observed across the study area, LNAPL may be entrapped as immobile discontinuous bodies in fractures at significant depths beneath the water level.

### **10.1.3 Chemical Characteristics**

With respect to the general water chemistry of the study area, a dominant (Ca+Mg)-(Na+K)-(CO<sub>3</sub>-HCO<sub>3</sub>) composition is observed across the study area, which is consistent with previous studies in the area and the (CO<sub>3</sub>-HCO<sub>3</sub>) dominance would suggest recent meteoric recharge to the aquifer. A slight evolution towards SO<sub>4</sub> end member is observed in less contaminated wells as a result of sulphate depletion in wells which have been impacted by hydrocarbon contaminants.

Multiple source zones are considered to be present, with multiple releases having occurred to date. The source zones can be considered to have a “southern zone” in the vicinity of Donkin Motors and a “northern zone” in the vicinity of Beaufort West Service Station and Marren Motors. The southern zone is considered to be the older of the releases, with no evidence of a recent release being present, whilst the northern zone is considered to have had more recent releases. Free phase LNAPL has been observed on both source zones, with old, degraded LNAPL being observed in the southern zones, and fresh green unleaded petrol being observed in the northern zone, with apparent LNAPL thicknesses in

the wells having reached 7m in PW12 (within northern zone). The dissolved phase compositions and concentrations in the two source zones are considered to be distinct from each other, further substantiating the assertion of multiple source zones. It is unclear to what degree a potential comingling of contaminant plumes may have occurred. Whilst significantly elevated dissolved phase concentrations (approaching maximum compound solubilities) has been observed, particularly within the northern zone, the dissolved phase concentrations have been observed to fluctuate significantly over the course of 2009.

Dissolved phase hydrocarbon concentrations, and in particular benzene are observed to have exceeded the RBCA Tier 1 RBSLs for ingestion of groundwater at almost all observation points where the plume was detected. Whilst no further risk assessment is being conducted within the scope of this study, the exceedences are mentioned to illustrate that unacceptable levels of contamination are present within the aquifer. Monitoring data suggests that the contaminant plumes is migrating in an East-North-East direction, which is cross gradient to regional groundwater flow and is most likely the result of the abstraction in the residential areas to the east of the source zones. Low flow sampling data suggests that the bulk of the dissolved phase contaminant mass is migrating from the source zones to the residential areas along the shallow fractures zones between 815m-830m amsl, and then in some instances, migrating vertically down the boreholes and exiting the boreholes into the deeper fracture systems. Benzene has been detected 400m to 900m away from the source zones on the eastern side of the Kuils River, and considering benzene's relatively high capacity for attenuation under aerobic conditions (which prevail in the distal areas of the plume), would suggest relatively rapid advective flow towards the east in order for the plume to migrate to such distance. At present TAME is the most widespread compound observed across the study area, which is consistent with its high mobility and low affinity for attenuation.

Natural attenuation of the observed contaminant plumes is considered to be occurring by means of microbial degradation, with secondary lines of evidence being present in affected areas in the form of negative ORP values, depleted sulphate and nitrate concentrations, and elevated concentrations of Fe(II) and Mn(II). Whilst the biodegradation is considered to be occurring, it may only be effectively attenuating the distal regions of the plume and is considered to be having little effect in the proximal areas near the source zones due to the presence of free phase LNAPL and subsequent contaminant mass loading into the aquifer.

## 11 Conclusion

The concluding chapter of this thesis seeks to recap the requirements for a model and to compare these requirements to the acquired, citing potential data gaps and further data requirements, and then to assess the feasibility of a model in light of the conceptual understanding of the site and the model objectives cited in Section 1.

### *11.1 A Review of Data Requirements for a Model*

In order for a numerical flow and transport model to be robust and provide dependable data, the most crucial step is the development of the site conceptual model which will represent the relevant flow and transport phenomena. The construction of a robust groundwater flow model, which can acceptably model and predict the groundwater flow conditions and responses in the groundwater system under study is considered a vital precursor to constructing a viable contaminant transport model. As mentioned in Section 1, the basic requirements which need to be constrained in order to construct a successful flow model have been given below along with a review of the data obtained specific to the requirement:

*The aquifer type and geometry with respect to hydraulic barriers and zones of preferential flow* - The conceptual model supplies sufficient information regarding the aquifer type as being a fractured, dual porosity aquifer. The geometry with regards to the location of preferential flow zone viz. major fracture zones is reasonably well defined in that two major flow zones, a shallower, potentially less transmissive flow zone and a deeper, potentially more transmissive flow zone have been identified.

*The model boundary conditions* – Model boundary conditions for the study area could be readily defined at the scale of the entire town and then be extrapolated to the smaller study area. The inclined sill to the north of the town would be the most obvious choice for a boundary in this direction and could be assigned as a Neumann or constant flux boundary as groundwater is considered to leak across (or along) the sill from the north to recharge the aquifer in the town. As discussed previously, the rivers in the town are not considered to be hydraulic boundaries, and boundaries to the west, south and east could most likely be assigned as Dirichlet or constant head boundaries provided they are positioned a sufficient distance to not be affected by abstraction in the town.

*The governing aquifer parameters such as transmissivity and storativity* – Aquifer tests in this study and other studies has provided data regarding transmissivity and storativity. Whilst storativity values are considered to be low across the entire study area, the transmissivity values are considered to vary significantly across the study area, with low T values being observed in the source zones, and higher T values being observed to the east of the source zone.

*The initial conditions within the aquifer and field observations to calibrate the flow model -*

Difficulties would begin to arise in trying to constrain the initial conditions and to calibrate the model with observed data since the available field data yielded from pump tests is significantly affected by various external factors (such as 3<sup>rd</sup> party abstraction during the test periods), and the prospects of performing successful pump tests in the affected areas are not good due to the high amount of “uncontrolled” abstraction taking place which would affect the observation data.

*Relevant groundwater sources (such as recharge) and sinks (such as abstraction)* – Estimates have been given on potential meteoric recharge to the aquifer and for potential abstraction rates for the town as whole. From a conceptual standpoint the recharge effect of the rivers has been discounted as these are seen as transient features with flow being extremely infrequent.

Following onto this, the contaminant transport model transport would require the input of data pertaining to contaminant sources and sinks, along with the various transport parameters in order to model the plume migration. Considering the abovementioned requirements, the current conceptual model and the available data therein, it is evident that the conceptual model could provide some of the information required, but not all of the required data. At a very local scale the nature and geometry of the aquifer is relatively well constrained, with preferential fracture flow zones having been identified at discrete depths within the study area. Boundary conditions could be loosely constrained given the available recharge and abstraction information and some estimation of transmissivities and storativity could be made.

A key step in creating a model is selecting the type of numerical model, such as finite element or finite difference, and defining the approximation of the natural system to the model domain. Often the aim of a model is to reduce the complexity of the natural system by means of a set of reasonable, but

well founded assumptions however this case the conceptual model has shown that the model geometry and flow conditions are complex, and would not likely be best approximated by a simple one layer model, but would need to be accommodated in a more complex model which could take into account the discrete preferential pathways and specific flow conditions. Challenges to creating a successful and meaningful model would arise as the model would need to account for the affects of the abstraction in the residential areas, which would not be practicable given the uncontrolled nature of the abstraction in the residential areas. With regards to the transport model, the constantly varying source concentrations would create considerable problems since the concentration initial conditions in the source zones are required to be constant (or at least behave in some form of predictable fashion), which is not being observed in reality due to presence of the LNAPL and potential future releases.

## ***11.2 Concluding remarks***

Significant challenges exist with regards to creating a successful model. Whilst a significant amount of fieldwork and site characterisation has been conducted in the study area by various parties, the resulting picture that is being created is one of increasing complexity. Whilst it is theoretically possible to further constrain the requirements for the model, some of the required actions would be extreme, such as needing to control all abstraction within the study area in order to provide a predictable flow environment. But perhaps a more overarching challenge lies at the very core why groundwater models are constructed. Groundwater models are generally constructed as decision making and management tools, with the model being designed to provide answers to specific questions regarding the modelled system. The question that one needs therefore to ask is: “What would we actually want to model, given the reality of the situation and what questions would we want to have answered?”

Within the context of the current study, as mentioned in Section 1, the primary contaminant management approach has been one of hydraulic containment in order to retract the contaminant plumes back towards the source zones and away from the residences. In light of this approach, the key question that has been asked is: “Is it feasible to employ hydraulic containment within the identified source zones and if so, what would the effects of source pumping at different rates and locations have on the observed contaminant plume in light of the observed groundwater abstraction within the town?”



Whilst this is a common question which is answered by a model, the conceptual site model has shown that fracture development in the source areas is poor, with all boreholes drilled in the source zones being very low yielding with no significant water bearing fractures being present. As a result, the potential for hydraulic containment within the source zones is poor since there would not be sufficient abstraction to induce plume containment back towards the source areas in light of the high level of abstraction in the residential areas to the east.

Another question following this could be “If hydraulic containment cannot be achieved in the source zones, what would be the effect of attempting hydraulic containment in the residential properties to the east at PW17 for instance?” Whilst this could potentially be modelled, the potential of inducing large scale contaminant migration from the current source zones, and effectively increasing the size of the source zone is not considered a feasible option, and would not prevent further release from entering the residential areas to the east.

In light of this, it is the Author’s opinion that whilst it may be possible, with additional investigation, to construct a flow model for the study area, the conceptual understanding of the site would appear to negate the use of a model with regards to lack of meaningful value it could add to the remediation decision management process.

At present the current strategy in Beaufort West appears to be focused on three objectives:

- The small scale LNAPL source removal where it is evident, either by passive skimming and very low abstraction rate pump and treat systems;
- The treatment of abstracted water at the most significantly impacted boreholes in the residential areas for garden irrigation usage and;
- The potential exploitation of deeper, hydraulic disconnected groundwater resources for water supply.

Whilst this is a somewhat symptomatic treatment approach, it is currently the most feasible since the potential residence time of contaminants in Karoo aquifers is considerable, and the potential for future releases from the source zones remains a possibility.

## 12 References

- API, 2004. API Interactive LNAPL Guide Version 2.04, American Petroleum Institute, USA
- Botha, J.F., Verwey, J.P., Van der Voot, I., Vivier, J.J.P., Buys, J., Colliston and Loock, J.C., 1998. Karoo Aquifers: Their Geology, Geometry and Physical Properties. Water Research Commission, South Africa.
- Bear, J., Beljin, M.S. and Ross, R.R., 1992. Fundamentals of Groundwater Modelling, Ground Water Issue, United States Environmental Protection Agency Publication: EPA/540/S-92/005, USA
- Belluomini, S., Owen, B. And Woodling, J., 1995. Groundwater Modelling for Hydrogeologic Characterisation – Guidance Manual for Groundwater Investigations, State of California Environmental Protection Agency, USA
- Burgers, C.L., and Rosewarne, P.N., 2009. BKB Trading Centre: Environmental Contamination Assessment: Beaufort West, Western Cape. SRK Consultancy Report 400790/1
- Campbell, G.D.M., 1980. Beaufort West groundwater investigation, 1975 – 77; unpublished Technical Report GH 3155, Department of Water Affairs. South Africa
- Cassidy, D. P. D., Werkema, D. Jr., Sauck W, Atekwana, E, Rossbach, S and Duris, J, 1998. The Effects of LNAPL Biodegradation Products on Electrical Conductivity Measurements. USA
- Davis, A.R. Jr., 1983. Depositional systems: A Genetic Approach to Sedimentary Geology. Prentice Hall Inc., Englewood Cliffs, New Jersey, USA
- Dobson, R., Schroth, M.H. and Zeyer, J., 2007. Effect of water-table fluctuation on dissolution and biodegradation of a multi-component, light nonaqueous-phase liquid. Journal of Contaminant Hydrology 94 (2007) 235–248, USA
- Doughty, C. and Tsang, C., 2004. Signatures in Flowing Fluid Electrical Conductivity Logs. Journal of Hydrology 310 (02005) pp157-180
- Ellis, P., 2000, MTBE and BTEX Plume Behaviour. Unpublished Internal Paper, Delaware Department of Natural Resources and Environmental Control
- Enslin, J.F., 1961. Groundwater Abstraction Report for the Beaufort West Municipality; Unpublished Consulting Report; Beaufort West Municipality, South Africa

- Farhadian, M., Vachelard, C., Duchez, D. and Larroche, C., 2008. In Situ Bioremediation of Monoaromatic Pollutants in Groundwater: A Review. *Bioresource Technology* 99 (2008) 5296–5308
- Gomo, M., 2009. Site Characterisation of LNAPL – Contaminated Fractured - Rock Aquifer. Unpublished Master’s Thesis, Institute for Groundwater Studies, University of the Free State, South Africa.
- Geo Pollution Technologies (GPT). Unpublished Consulting reports 2001 – 2007.
- Hardisty, P.E., Wheeler, H.S., and Parker, T.M., 1998. Monitoring LNAPL in Fractured Media: Assessing Apparent Thickness Data. Proc. API / NGWA Conference on Hydrocarbons and Organic Chemicals in Groundwater, Houston
- Hardisty, P.E., Roher, J. and Dottridge, J., 2004. LNAPL Behavior in Fractured Rock: Implications for Characterization and Remediation. Proc. NGWA Conference on Hydrocarbons and Organic Chemicals in Groundwater, USA
- Huntley, D., 2000. Analytic Determination of Hydrocarbon Transmissivity from Baildown Tests. *Groundwater*, Vol. 38 (1) January –February 2000.
- IGS, 2009. Field investigations to study the fate and transport of light non-aqueous phase liquids (LNAPLs) in groundwater: Deliverable 3: Initial Field Results. Report to the WRC by the Institute for Groundwater Studies, University of Free State.
- Kent, L.E., 1949 Borings Sites Reports. Unpublished Report, Geological Survey, South Africa.
- Kotze, J.C., Pointer, C. and Rosewarne, P.N., 1997. Assessment of the Hydrogeological Potential of the Brandwacht Aquifer Phase 2, Report 227331/2; Unpublished Consulting Report. SRK Consulting, South Africa
- Kotze, J.C. and Gilbert, A.D., 2000. Investigation into Increased Groundwater Supply to Beaufort West Report 227331/4; Unpublished Consulting Report. SRK Consulting, South Africa
- Kruseman, G. P. and de Ridder, N.A., 1999. Analysis and Evaluation of Pumping Test Data. Second Edition. International Institute for Land Reclamation and Improvement. Wageningen. The Netherlands
- Kueper, B.H. and McWhorter, D.B. 1991. The Behaviour of Dense Non Aqueous Phase Liquids in Fractured Clay and Rock. *Groundwater* 29 (5), pp716-728.

- Kurikami, H., Takeuchi, R. and Yabuuchi, S., 2008. Scale Effect and Heterogeneity of Hydraulic Conductivity of Sedimentary Rocks at Horonobe URL site. *Physics and Chemistry of the Earth* 33 (2008) S37–S44
- Legrand, H.E. and Rosen, L., 1998. Systematic Makings of Early Stage Hydrogeologic Conceptual Models. *Groundwater* 38 (6): pp887-893
- Martienssen, M., Fabritius, H., Kukla, S., Balcke, G.U., Hasselwander, E. And Schirmer, M., 2006. Determination of naturally occurring MTBE biodegradation by analysing metabolites and biodegradation by-products. *Journal of Contaminant Hydrology* 87 (2006) pp37–53
- McKelvie, J.R., Lindstrom, J.E., Beller, H.R., Richmond, S.A. and Sherwood Lollar, B., 2005. Analysis of Anaerobic BTX Biodegradation in a Subarctic Aquifer Using Isotopes and Benzylsuccinates. *Journal of Contaminant Hydrology* 81 (2005) pp167– 186
- Pike, C.L., 1948. Borings Sites Report; Unpublished Report, Geological Survey, South Africa.
- Puls, R.W. and Paul, C.J., 1996. Multi-layer sampling in conventional monitoring wells for improved estimation of vertical mass distributions and mass. *Journal of Contaminant Hydrology* 25 pp85-111.
- Rose, R. And Conrad, J., 2008. Aquifer Characterisation and Groundwater Flow Regimes of Karoo Aquifers in Beaufort West, Western Cape Province, Report G2008/07-01; Unpublished Consulting Report. GEOSS Consulting, South Africa
- Schumann, F.W. and Mellet, P. 1959. Geological and Hydrogeological Investigation in the Town of Beaufort West. Unpublished Report, Geological Survey, South Africa.
- Selroos, J., Walker, D.D., Ström, A., Gylling, B. and Follin, S., 2002. Comparison of Alternative modelling Approaches for Groundwater Modelling Flow in Fractured Rock. *Journal of Hydrology* 257 (2002) pp174-188
- Small, M.C. and Weaver, J., 2000. An Updated Conceptual Model for Subsurface Fate and Transport of MTBE and Benzene; Unpublished US EPA Region 9 Internal Paper, USA
- Smit, L., 2009. Personal conversations with Mr Louw Smit – Water and Sanitation Engineer for the Beaufort West Municipality
- Stumm & Morgan, 1996. *Aquatic chemistry: Chemical Equilibria and Rates in Natural Waters*. 3rd Edition. Environmental Science and Technology. A Willey-Interscience publication. John Wiley & Sons. USA

- Tankard, A.J., Jackson, M.P.A., Eriksson, K.A., Hobday, D.K., Hunter, D.R. and Minter, W.L., 1982. *Crustal Evolution of Southern Africa*. Springer-Verlag, New York.
- Tordiffe, E.A.W., 1978. *Aspects of the hydrogeochemistry of the Karoo Sequence in the Great Fish River Basin Eastern Cape Province: With special reference to the groundwater quality*. Unpublished Ph.D. Thesis, University of the Free State, Bloemfontein
- Vandoolaeghe, M.A.C., 1978. *Report on geophysical interpretation of Geohydrological investigation at Beaufort West; unpublished Technical Report 2970, Department of Water Affairs. South Africa*
- Van Biljon W.J. and Swanepoel, T., 2007. *Petroleum Hydrocarbon Groundwater Remediation Technologies – Successes and Failures*. 2007 Groundwater Conference Proceedings, Groundwater Division of the Geological Society of South Africa.
- Van Tonder, G. J., Bardenhagen, I., Riemann, K., Van Bosch, J., Dzanga, P. And Xu, Y., 2001. *Manual on Pumping Test, Analysis in fractured – Rock Aquifers*. Institute of Groundwater Studies, University of the Free State. Bloemfontein.
- Van Tonder, G.J., Kunstmann, H., Xu, Y., 2001. *FC Programme, software developed for DWAF by the Institute of Groundwater Studies*. Institute of Groundwater Studies, University of the Free State, South Africa.
- Vermeulen, D., 2009. *Personal conversations held with Dr Danie Vermeulen of the Institute for Groundwater Studies*
- Verwey, J., Kinzelbach and Van Tonder, G.J., 1995. *Interpretation of pumping test from fractured porous aquifers with a numerical model*. IGS- University of the Orange Free State.
- Woodford, A and Chevallier, L., 2002. *Hydrogeology of the main Karoo Basin: Current Knowledge and Research Needs*. Water Research Commission, Report No TT 179/02, 466 pp

## Appendix A

### DGPS Data

Well ID	Lo	Lat	z (mamsl)	Measuring point	Measured Water Level Dec09	SWL (amsl)
PW85	39044.171	3581261.026	842.527	COVER	-	
129BIRD	38982.094	3581444.744	841.329	PLATE	-	
PW53	38884.984	3581001.503	842.59	COVER	16.63	825.96
PW86	38919.291	3580780.601	843.491	COVER	17.63	825.861
39DEV	38924.126	3581267.119	841.493	PLATE	-	
PW30	38899.27	3581458.103	842.909	PLATE	17.56	825.349
C1	39217.716	3581393.831	843.326	COVER	-	
C10	39218.028	3581384.737	843.424	COVER	-	
C2	39229.18	3581389.617	843.428	COVER	-	
C3	39229.548	3581384.055	843.496	COVER	-	
C4	39220.787	3581350.509	843.5	COVER	-	
C5	39216.339	3581348.636	843.415	COVER	-	
C6	39212.136	3581355.241	843.053	COVER	-	
C7	39211.23	3581362.161	843.034	COVER	-	
C8	39210.359	3581368.73	843.033	COVER	-	
C9	39209.672	3581375.812	843.144	COVER	-	
HS1	38332.364	3581495.382	843.849	COVER	-	
MS02	38658.115	3581042.505	840.32	COLLAR	-	
MW10	39179.859	3581263.424	843.468	COVER	13.99	829.478
MW11	39155.349	3581253.005	843.959	COVER	14.44	829.519
MW12	39198.053	3581248.25	843.423	COVER	12.82	830.603
MW2	39304.092	3581489.186	843.598	COLLAR	-	
MW4	39062.108	3581423.294	841.55	COLLAR	-	
MW5	39173.442	3581406	842.696	COLLAR	-	
MW7	39038.075	3581241.65	842.362	COLLAR	-	
MW8	39033.388	3581240.835	842.265	COLLAR	-	
MW9	39192.544	3581215.901	843.498	COVER	13.83	829.668
NB1	38399.149	3581139.982	842.099	PLATE	-	
NB2	38400.629	3581176.315	841.953	PLATE	-	
PW1	39243.484	3581541.403	843.031	COVER	-	
PW12	39150.278	3581347.761	842.44	COVER	13.99	828.45
PW13	38835.985	3581454.708	840.402	PLATE	-	
PW15	38872.173	3581307.5	840.595	COLLAR	15.58	825.015
PW16	38973.493	3581251.175	842.001	COVER	15.63	826.371
PW17	39013.71	3581262.419	842.237	PLATE	15.76	826.477
PW18	39044.696	3581284.347	842.311	COVER	-	
PW19	38791.201	3581389.169	839.732	PLATE	-	
PW2	39137.435	3581454.867	842.05	COLLAR	13.02	829.03
PW20	38754.302	3581274.954	838.283	PLATE	13.62	824.663
PW21	38907.377	3581344.087	841.61	PLATE	16.37	825.24
PW22	38925.054	3581224.169	841.442	PLATE	-	
PW27	39300.184	3581414.222	842.9	COVER	-	
PW49	39157.078	3581281.866	842.785	COLLAR	12.91	829.875
PW5	39022.653	3581400.823	841.859	COLLAR	12.39	829.469
PW50	38858.845	3581062.022	841.935	COLLAR	16.48	825.455
PW51	38862.273	3580885.875	843.036	BRICKS	17.37	825.666
PW52	38877.655	3580939.284	842.373	PLATE	-	
PW56	38987.732	3580983.683	842.879	HOLE	17.21	825.669
PW57	38951.713	3581008.37	842.523	PLATE	17.02	825.503
PW58	38983.131	3580771.307	844.06	COVER	18.16	825.9
PW59	38504.129	3580857.363	844.797	PLATE	-	
PW6	39014.732	3581354.381	841.819	PLATE	15.07	826.749
PW69	39134.422	3580979.869	844.072	COVER	17.47	826.602
PW7	38885.632	3581428.962	842.75	PLATE	-	
PW70	39094.505	3580828.724	844.447	PLATE	-	
PW75	38465.131	3581061.583	842.497	COLLAR	-	
PW76	38548.374	3581093.062	841.686	PLATE	-	
PW78	38835.15	3581259.61	840.38	COVER	15.32	825.06
PW79	38827.378	3581234.009	840.552	PLATE	14.28	826.272
PW8	38856.706	3581549.296	842.842	COLLAR	17.59	825.252
PW80	38187.129	3581595.237	838.844	PLATE	14.36	824.484
PW81	38108.157	3581656.099	837.707	PLATE	13.66	824.047
PW83	38129.745	3581710.766	837.793	PLATE	13.76	824.033
PW9	39065.628	3581228.698	842.941	COVER	16.47	826.471
RW1	39194.978	3581530.625	842.723	COVER	13.6	829.123
RW2	39202.848	3581473.763	842.916	COVER	13.91	829.006
SH1	39294.451	3581318.112	843.109	COVER	-	
SH2	39291.688	3581305.719	843.182	COVER	-	
SH3	39288.279	3581285.407	843.22	COVER	-	